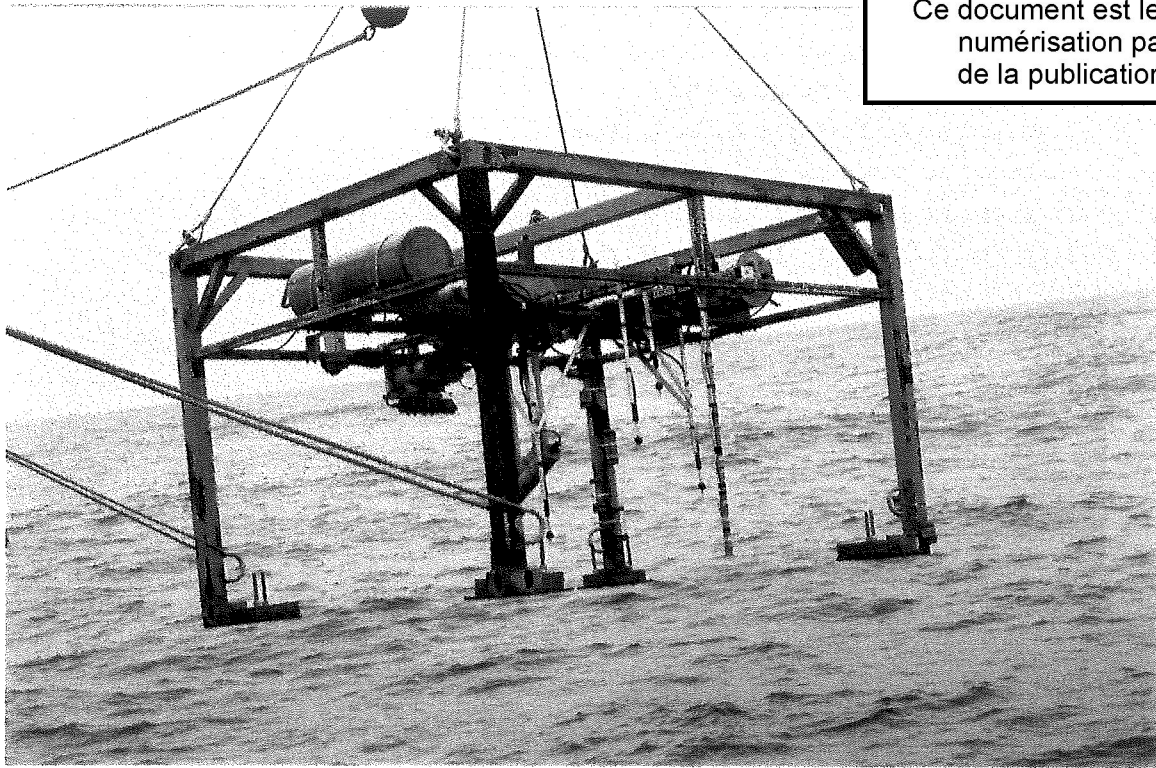


This document was produced
by scanning the original publication.

Ce document est le produit d'une
numérisation par balayage
de la publication originale.



Hydrodynamics and Seabed Stability Observations On Sable Island Bank: A summary of the Data for 1996/1997

Michael Li, Carl Amos and David Heffler

A Technical Report Submitted to
Sable Offshore Energy Inc

Geological Survey of Canada
Open File Report 2997
January 1999



Natural Resources
Canada

Ressources naturelles
Canada

Canada

**Hydrodynamics and Seabed Stability Observations on Sable Island Bank:
A Summary of the Data for 1996/1997**

by

Michael Z. Li, Carl L. Amos,
David E. Heffler

Geological Survey of Canada - Atlantic
Bedford Institute of Oceanography
P.O.Box 1006, Dartmouth, N.S.
B2Y 4A2 Canada

A Technical Report Submitted to
Sable Offshore Energy Project (SOEP)

Geological Survey of Canada
Open File Report 2997

January, 1999

TABLE OF CONTENTS

TITLE PAGE

1. INTRODUCTION	1
2. INSTRUMENTATION	2
3. DATA FROM SI96A DEPLOYMENT	7
3.1 General Description of Deployment	7
3.2 S4 Wave-Current Meter Data	7
3.3 Ralph Data	14
3.3.1 Hydrodynamics and Sediment Suspension	14
3.3.2 Bedform and Bed Elevation Change	19
3.4 Predictions By SEDTRANS92	23
4. DATA FROM SI97A DEPLOYMENT	25
4.1 General Description of Deployment	25
4.2 S4 Wave-Current Meter Data	25
4.3 Ralph Data	25
4.3.1 Hydrodynamics and Sediment Suspension	25
4.3.2 Bedform and Bed Elevation Change	30
4.4 Predictions By SEDTRANS96	34
5. DATA FROM SI97B DEPLOYMENT	34
5.1 General Description of Deployment	34
5.2 S4 Wave-Current Meter Data	35
5.3 Ralph Data	35
5.3.1 Hydrodynamics and Sediment Suspension	35
5.3.2 Bedform and Bed Elevation Change	40
5.4 Predictions By SEDTRANS96	40
6. DATA FROM SI97C DEPLOYMENT	43
6.1 General Description of Deployment	43
6.2 S4 Wave-Current Meter Data	43
6.3 Ralph Data	46
6.3.1 Hydrodynamics and Sediment Suspension	46
6.3.2 Bedform and Bed Elevation Change	50
6.4 Predictions By SEDTRANS96	53
7. PREDICTIONS OF MOBILE LAYER DEPTH DURING STORMS	53
8. SUMMARY	55
Acknowledgements	58
References	59

APPENDICES

- Appendix 1 The burst-averaged wave, current and sediment suspension data for SI96a Ralph deployment
- Appendix 2 Predictions by SEDTRANS96 for SI96a Ralph deployment: (a) bottom boundary layer dynamics parameters; (b) sediment transport parameters
- Appendix 3 The burst-averaged wave, current and sediment suspension data for SI97a Ralph deployment
- Appendix 4 Predictions by SEDTRANS96 for SI97a Ralph deployment: (a) bottom boundary layer dynamics parameters; (b) sediment transport parameters
- Appendix 5 The burst-averaged wave, current and sediment suspension data for SI97b Ralph deployment
- Appendix 6 Predictions by SEDTRANS96 for SI97b Ralph deployment: (a) bottom boundary layer dynamics parameters; (b) sediment transport parameters
- Appendix 7 The burst-averaged wave, current and sediment suspension data for SI97c Ralph deployment
- Appendix 8 Predictions by SEDTRANS96 for SI97c Ralph deployment: (a) bottom boundary layer dynamics parameters; (b) sediment transport parameters

LIST OF FIGURES

Figure 1	Location map showing the study area of Sable Island Bank and sites of instrument deployments	3
Figure 2	Image of the upgraded Ralph	5
Figure 3	S4 wave and current meter with an attached Cyclops	5
Figure 4	Time-series plots of (a) mean current and its direction, (b) mean water depth, and (c) instantaneous current speed for the S4A meter of SI96a deployment	9
Figure 5	Time series plot of the OBS data on the S4A meter of SI96a deployment	10
Figure 6	Time-series plots of (a) mean current and its direction, (b) mean water depth, and (c) instantaneous current speed for the S4B meter of SI96a deployment	11
Figure 7	Time series plot of the OBS data on the S4B meter of SI96a deployment	12
Figure 8	Time series plots of (a) mean water depth h , (b) mean current speed u_{50} , (c) significant wave height H_s , (d) mean wave period T_z , and (e) obs1 reading of SI96a Ralph deployment	15
Figure 9	Time series plots of (a) significant wave height H_s , (b) mean current speed u_{50} , (c) direction of mean current, and (d) maximum instantaneous velocity u_{max} of SI96a Ralph deployment	17
Figure 10	The roll and pitch data of (a) SI96a, (b) SI97a, (c) SI97b, and (d) SI97c Ralph deployments	20
Figure 11	The seabed elevation changes recorded by the ABS sensors in SI96a Ralph deployment	21
Figure 12	Examples of the Imagenex (a) profiler and (b) sonar images collected in SI96a Ralph deployment	22
Figure 13	Time-series plots of (a) mean current and its direction and (b) mean water depth for the S4 meter of SI97a deployment	26
Figure 14	Time series plots of (a) mean water depth h , (b) mean current speed u_{50} , (c) significant wave height H_s , (d) mean wave period T_z , and (e) obs1 reading of SI97a Ralph deployment	28
Figure 15	Time series plots of (a) significant wave height H_s , (b) mean current speed u_{50} , (c) direction of mean current, and (d) maximum instantaneous velocity u_{max} of SI97a Ralph deployment	29
Figure 16	The seabed elevation changes recorded by the ABS sensors in SI97a Ralph deployment	31

Figure 17	Examples of the Imagenex (a) profiler and (b) sonar images collected in SI97a Ralph deployment	32
Figure 18	Time-series plots of (a) mean current and its direction and (b) mean water depth for the S4A meter of SI97b deployment	36
Figure 19	Time-series plots of (a) mean current and its direction and (b) mean water depth for the S4B meter of SI97b deployment	37
Figure 20	Time series plot of the OBS data on the S4B meter of SI97b deployment	38
Figure 21	Time series plots of (a) mean water depth h , (b) mean current speed u_{50} , (c) significant wave height H_s , (d) mean wave period T_z , and (e) obs1 reading of SI97b Ralph deployment	39
Figure 22	Time series plots of (a) significant wave height H_s , (b) mean current speed u_{50} , (c) direction of mean current, and (d) maximum instantaneous velocity u_{max} of SI97b Ralph deployment.	41
Figure 23	The seabed elevation changes recorded by the ABS sensors in SI97b Ralph deployment	42
Figure 24	Time-series plots of (a) mean current and its direction and (b) mean water depth for the S4A meter of SI97c deployment	44
Figure 25	Time-series plots of (a) mean current and its direction and (b) mean water depth for the S4B meter of SI97c deployment	45
Figure 26	Time series plots of (a) mean water depth h , (b) mean current speed u_{50} , (c) significant wave height H_s , (d) mean wave period T_z , and (e) obs2 reading of SI97c Ralph deployment	47
Figure 27	Time series plots of (a) significant wave height H_s , (b) mean current speed u_{50} , (c) direction of mean current, and (d) maximum instantaneous velocity u_{max} of SI97c Ralph deployment	48
Figure 28	The seabed elevation changes recorded by the ABS sensors in SI97c Ralph deployment	51
Figure 29	Examples of the Imagenex (a) profiler and (b) sonar images collected in SI97c Ralph deployment	52
Figure 30	Scatter plot of significant wave height versus the mobile layer depth for storms recorded in all 1996/97 deployments	56

LIST OF TABLES

Table 1	Summary of sites, instrumentation and collected data for the SIB GSCA-MOBIL joint project in 1996 and 1997	4
Table 2	Mean grain size and sorting of sediment trap sample from S4A of SI96A deployment.	13
Table 3	Mean grain size and sorting of sediment trap sample from S4B of SI96A deployment	13
Table 4	Mean grain size and sorting of sediment trap samples from SI96a Ralph deployment	18
Table 5	Estimated bed-elevation changes and bedform parameters in the storms of SI96a Ralph deployment	23
Table 6	Mean grain size and sorting of sediment trap samples from SI97a Ralph deployment	30
Table 7	Estimated bed-elevation changes and bedform parameters in the storms of SI97a Ralph deployment	33
Table 8	Mean grain size and sorting of sediment trap samples from SI97c Ralph deployment	49
Table 9	Estimated bed-elevation changes and bedform parameters in the storms of SI97c Ralph deployment	53
Table 10	Summary of the hydrodynamics parameters and estimated maximum mobile layer depths for the storms recorded in all 1996/97 deployments	54

Hydrodynamics and Seabed Stability Observations on Sable Island Bank: A Summary of the Data for 1996/1997

Michael Z. Li, Carl L. Amos, and David E. Heffler

Geological Survey of Canada - Atlantic
Bedford Institute of Oceanography
P.O.Box 1006, Dartmouth, N.S.
B2Y 4A2 Canada

1. INTRODUCTION

It is well established that storm processes dominate the transport of sediment on Scotian Shelf, and the resulting seabed scouring and migration of large-scale bedforms cause serious problems for offshore installations (Hodgins and Sayao, 1986; Amos and Judge, 1991; Amos et al., 1996; Li et al., 1997). Several bottom boundary layer models have been proposed for the prediction of near-bed velocity profiles and enhanced bed shear stresses under combined waves and currents (e.g., Smith, 1977; Grant and Madsen, 1979, 1986), but their applicability over a wide range of conditions is not tested due to the lack of high quality field data of simultaneously measured waves, currents and seabed responses (Cacchione and Drake, 1990). Bedforms are almost always present on the continental shelf. The development of these bedforms and their interaction with waves and currents strongly control the near-bed velocity profile, sand resuspension and the partition of skin friction from form drag (Wiberg and Nelson, 1992; Vincent et al., 1991; Li, 1994; Li et al., 1996a). There are extensive laboratory and field measurements of wave ripples and these have been used to derive several wave-ripple predictors. Due to the co-existence of waves and current, these wave-ripple predictors are found not applicable under combined-flow conditions (Osborne and Vincent, 1993; Li et al., 1996a). As bed shear stress increases, sediment transport will go through the following distinctive stages: no motion, bedload transport, saltation/suspension and sheet flow transport. The critical shear stresses for the onset of these transport modes need to be properly defined before we can correctly assess sediment transport rates and seabed stability. While these threshold criteria are reasonably defined, solutions and field data are very limited for combined flows (Hammond and Collins, 1977; Amos et al., 1988; Li et al., 1997).

Due to the complexity of the above mentioned processes and problems, the predictions of sediment transport and seabed scouring are poor both for the free stream and around offshore installations on continental shelves. In order to further our understanding on these complex issues, a joint project between GSCA (with funding from the Panel on Energy Research and Development, PERD) and PanCanadian (formerly LASMO Nova Scotia Ltd.) was carried out from 1993 to 1995 to monitor storm wave-current

dynamics and seabed responses on the Scotian Shelf. GSCA's instrumented tripod Ralph and S4 wave-current meters have been deployed at several sites near the Cohasset/Panuke production region to obtain *in situ* wave, current and seabed response data under storm conditions. The field activities and preliminary data analyses of this joint project have been reported in Zevenhuizen and Li (1994), Amos et al. (1994a) and Li et al. (1994, 1996b). Results of advanced analyses of the data collected in this project have been published in several scientific papers (Li et al., 1997; Li and Amos, 1998; Li and Amos, in press^{a,b}). Some of the key accomplishments and insights from this joint project include the following: (1) Storms dominate sediment transport processes on Sable Island Bank; bed shear stress and roughness can be strongly enhanced due to wave-current interaction; (2) Thresholds for bedload, suspension and sheet-flow transport modes are reasonably well established for medium sand; less well for fine sand and coarse sand; (3) Existing wave-ripple predictors do not work in combined flows and a new empirical ripple predictor has been proposed; (4) These advances have been used in the upgrade and calibration of GSCA's numerical sediment transport models for continental shelves (Li and Amos, 1995,1997); and (5) Leading-edge technologies and instrumentation have been developed for offshore sediment transport/seabed stability monitoring studies (Amos et al., 1994b; Heffler, 1996).

As the joint project between GSCA and PanCanadian ended in 1995, the Sable Offshore Energy Project (SOEP) entered the application and engineering design stage. Seabed stability along the gas pipeline routes was one of the most important engineering problems for the development of this natural gas field. GSCA and Mobil Oil Canada Ltd. began in 1995 a joint venture to develop an instrument system to remotely measure 3-dimensional seabed scouring and to evaluate the stability of large-scale bedforms and the depth of mobile layer during storms on Sable Island Bank (SIB). The key sensors added to Ralph were an Imagenex 2-D sector scanning profiler (SSP) for 2-dimensional profiling of the seabed along a line and an Imagenex 3-D sector scanning sonar (SSS) for 3-dimensional imaging of seabed scours. The upgraded Ralph was deployed jointly with S4 wave-current meters at four strategically selected sites on SIB (Fig. 1 and Table 1) in 1996 and 1997 to obtain *in situ* wave, current and seabed response data under storm conditions. This report is a summary of the data sets collected from these deployments.

2. INSTRUMENTATION

The key instrument packages used in this project were the upgraded GSCA multi-sensor platform Ralph (Fig. 2) and the InterOcean S4 wave-current meters with a single Optical Backscatter Sensor (Cyclops) mounted on top (Fig. 3).

Ralph is a computer controlled, autonomous instrumented platform used for measuring near-bed

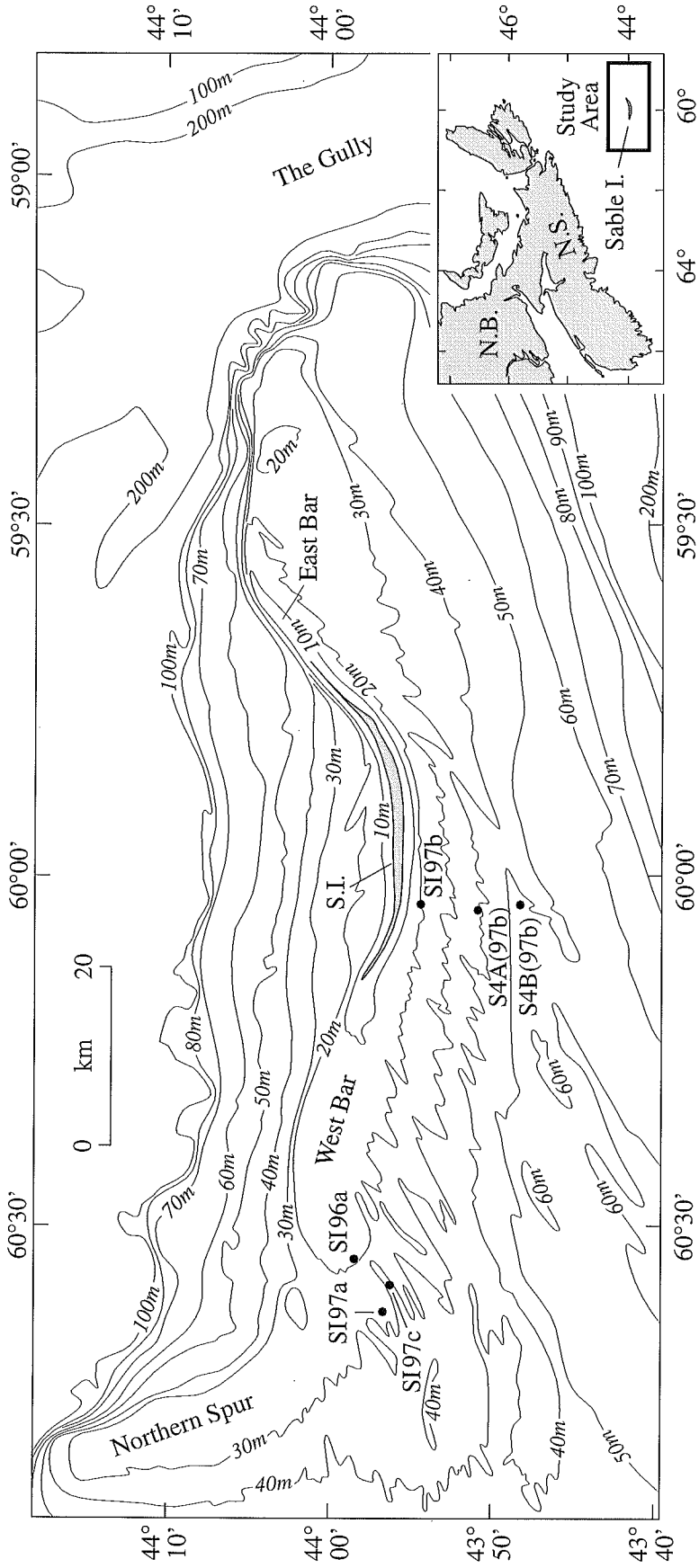


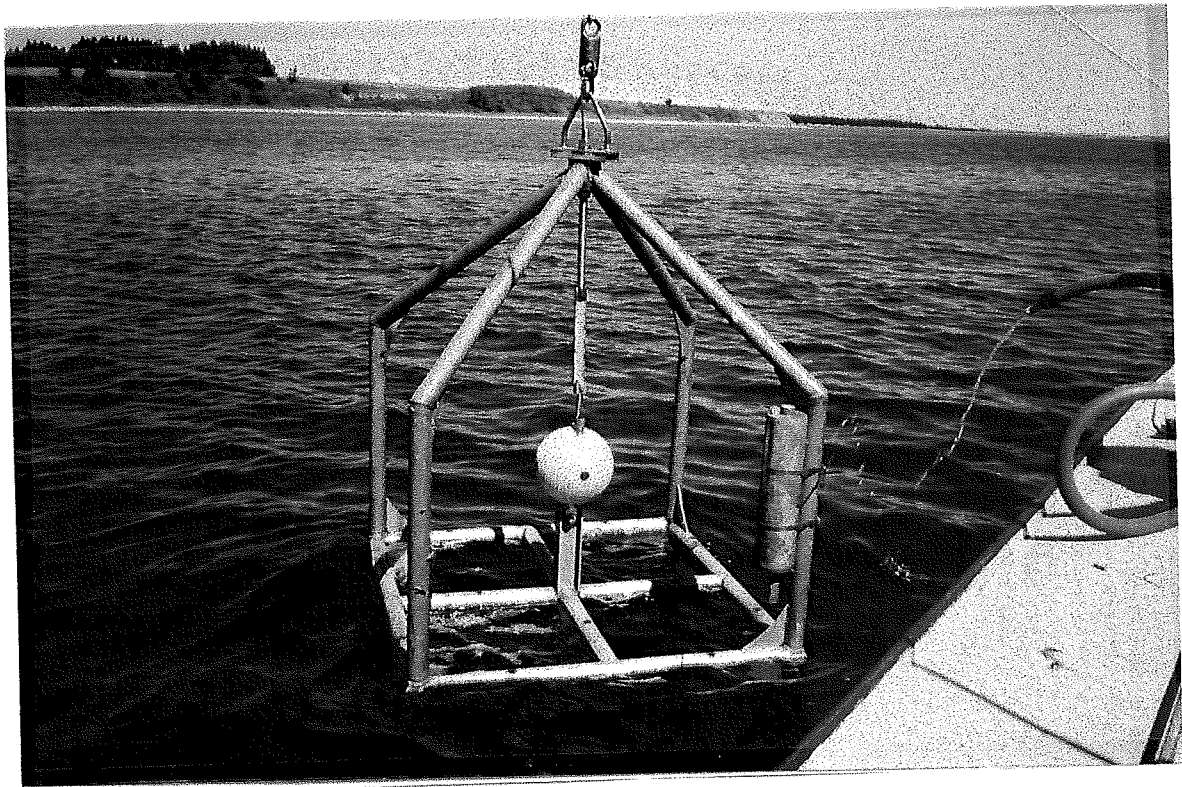
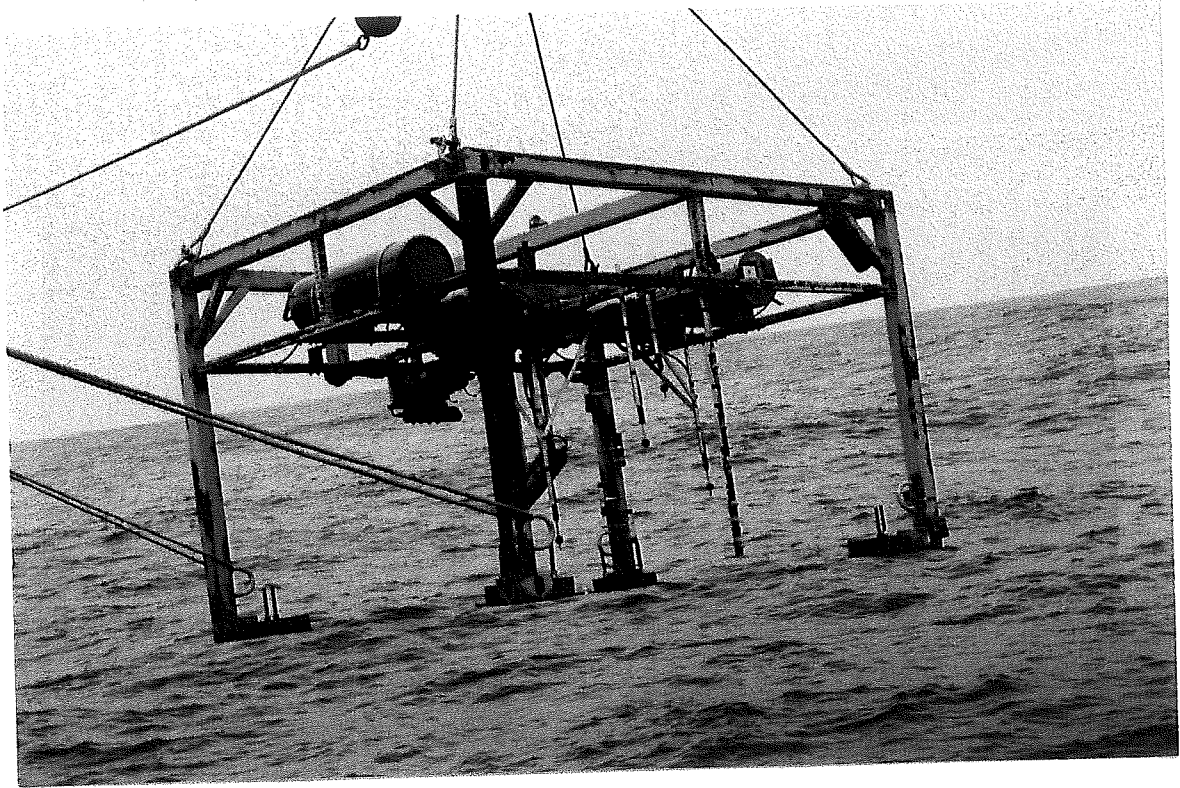
Fig. 1 Location map showing the study area of Sable Island Bank and sites of instrument deployments

Table 1 Summary of sites, instrumentation and collected data for the SIB GSCA-MOBIL joint project in 1996 and 1997.

Site/Date	Instrument/Location	Depth	Sampling Program	Sediment Samples	Data Acquired and Notes
S196a 26/11/96- 06/12/96	Ralph: 43° 58.35'N 60° 33.26'W	20 m	15 min. burst every hour at 5 Hz ABS: 1 min. every hour at 1 Hz Profilor/Scanner: 3 min. every hour 8 mm camera: every 15 min.	5 IKU grabs, D=0.39 mm sediment trap samples	Ralph on crest of sand ridge and recorded 98 bursts of data
	S4A: 43° 57.71'N 60° 33.31'W	24 m	5 min. burst every hour at 1 Hz OBS: every 24 sec. same as above	IKU grab, D = 0.32 mm Sediment trap samples	S4A on upper lee flank of sand ridge and recorded 242 bursts of data
S197a 28/01/97- 24/03/97	S4B: 43° 57.44'N 60° 33.29'W	30 m	same as above	IKU grab, D = 0.28 mm Sediment trap samples	S4B on lower lee flank of sand ridge and recorded 242 bursts of data
	Ralph: 43° 56.45'N 60° 37.77'W	32 m	15 min. burst every 2 hours at 5 Hz ABS: 1 min. every 2 hours Profilor/Sonar: 3 min. every 2 hours Digital camera: every 20 min.	No bottom sediment samples; 3 sediment trap samples recovered	Ralph on crest of sand ridge; Recorded from 28/1 to 19/2/97 for 266 bursts
S197b 09/04/97- 12/04/97	S4: 43° 56.10'N 60° 33.40'W	38 m	5 min. burst every hour at 1 Hz OBS: every 24 sec (?)	No bottom sediment samples	S4 on lower lee flank of sand ridge Recorded 1167 bursts of data
	Ralph: 43° 54.27'N 60° 02.69'W	31 m	15 min. burst every hour at 5 Hz ABS: 1 min. every hour at 1 Hz Profilor/Scanner: 3 min. every hour Digital camera: every 20 min.	IKU grab, D = 0.23 mm	Ralph on crest of sand ridge, recorded data 9/4 to 12/4/97 for 73 bursts
S197c 12/04/97- 29/05/97	S4A: 43° 50.60'N 60° 02.98'W	45 m	5 min. burst every hour at 1 Hz	no bottom sediment sample	Recorded 75 bursts of data
	S4B: 43° 47.98'N 60° 02.69'W	55 m	5 min. burst every hour at 1 Hz OBS: 16 second average	no bottom sediment sample	Recorded 75 bursts of data
S197c 12/04/97- 29/05/97	Ralph: 43° 56.03'N 60° 37.77'W	42 m	15 min. burst every hour at 5 Hz ABS: 1 min. every hour at 1 Hz Profilor/Scanner: 3 min. every hour Digital video every 20 min.	no bottom sediment sample; sediment trap samples collected	Ralph in trough of sand ridge; Recorded data from 12/4 to 29/4/97 for 410 bursts
	S4A: 43° 56.56'N 60° 35.01'W	28 m	3 min. burst every 2 hrs. at 1Hz	no bottom sediment sample sediment trap sample	upper lee flank of sand ridge; recorded 579 bursts of data
	S4B: 43° 56.28'N 60° 35.58'W	31 m	3 min. burst every 2 hrs. at 1Hz OBS: 16 second average	no bottom sediment sample sediment trap sample	at brink point of lee flank; recorded 578 bursts of data

Fig. 2 Image of the upgraded Ralph (top image on next page).

Fig. 3 S4 wave and current meter with an attached Cyclops (bottom image on next page).



wave-current dynamics and monitoring seabed responses in marine environments (Heffler, 1984). The earlier versions of Ralph were successfully deployed several times on the Scotian Shelf and collected useful *in situ* wave, current and seabed response data (Amos et al., 1988; Li et al., 1994, 1996b, 1997). Ralph has recently been significantly upgraded (Heffler, 1996). The Ralph used in this project was mounted on an 3 m x 3 m x 2 m quad frame (see Fig. 2). The key sensors on Ralph included:

- a main case that contains a strain-gauge 300 psi pressure transducer for measuring depth, tide and wave height; a fluxgate compass for measuring the heading of Ralph; and a tilt sensor to record Ralph's roll and pitch. All these sensors are at 150 cm above the seabed and their data are recorded on a Tattletale Model 7 data logger with a 120 Mbyte hard disk.
- 4 Marsh McBirney Electro-Magnetic Current Meters (EMCM) for velocity measurements at heights of 30, 50, 70 and 100 cm above the seabed. The current meters are sampled by a Tattletale Model 5 computer and their data are logged on the hard disk of the Tattletale Model 7 computer in the main case.
- 6 Optical Backscatter Sensors (OBS, Downing, 1983) to measure the concentration of suspended sediment at heights of 10, 30, 50, 70, 100 and 136 cm above the seabed. The OBS are also controlled by the Tattletale Model 5 computer and their data are logged on the hard disk in the main case. An array of sediment catchment traps are mounted at the height of each OBS to catch suspended sediment samples.
- 4 Mesotec (2.2 MHz) Acoustic Backscatter Sensors (ABS) at 130 cm above the bottom to measure seabed elevation (scour) at four positions: 3 ABS aligned normal to the Imagenex profiler at the front of Ralph frame with spacings of 32 and 70 cm and the fourth ABS located at the rear of the frame 175 cm back. The ABS data are recorded on a Tattletale Model 7 data logger with a 540 Mbyte hard disk.
- an Imagenex sector scanning profiler (SSP) at 135 cm above the bed to provide a scan profile across 10 m of seabed for bedform height and scour depth.
- an Imagenex sector scanning sonar (SSS) at the height of 165 cm to provide 270° 2-dimensional scanning images of the seabed of 5 - 40 m diameters for bedform and scour patterns. The data from SSS and SSP both are recorded on a Tattletale Model 7 data logger with a 840 Mbyte hard disk.
- an underwater digital video camera system (DULCE) at 150 cm height, with a 50 W incandescent light at 50 cm height, to monitor sediment transport and bedform development. The camera is mounted vertically to give a 0.9 m x 0.7 m view of the seabed. The digital files from the camera are stored on a PC104 computer with a 1Gbyte hard drive.

Other components on Ralph include a Vemco 27 kHz acoustical relocation pinger and a Vemco VM-10-S acoustical uplink for quick after-deployment check on Ralph operation. Overall, the upgraded Ralph now has 23 sensors, 7 computers and 2.5 Gbyte data storage capacity. More technical details of the upgraded

Ralph can be found in Heffler (1996).

S4 Wave-Current Meters are self-contained, spherical, and commercially available electromagnetic wave-current meters (Fig. 3) from InterOcean Systems Inc. They measure depth, waves, current magnitude and direction. An internal fluxgate compass records the current direction relative to magnetic north. Data are stored internally in solid-state, high-reliability memory (1 Mbyte). The electronics and power supply modules are contained within a compact 25 cm diameter sphere. S4 wave-current meters can be deployed independently on current meter stands, or incorporated on a tripod. In the four deployments described in this report, S4 meters were mounted on a aluminum tubular frame at 50 cm above the bed. A single OBS (Cyclops) was installed at 20 cm height to measure suspended sediment concentration, and a catchment sediment trap was attached to the frame at a height of 20 cm. The sediment trap was made of 5 cm plastic core liner with a 2.45 cm diameter hole punched in the top.

3. DATA FROM SI96A DEPLOYMENT

3.1 General Description of Deployment

Ralph and two S4 wave-current meters were deployed at this site about 32 km to the west of Sable Island in November 1996. Ralph was deployed at 43° 58.35'N, 60° 33.26'W in 20 m water depth (Fig. 1). The first S4 meter (S4A) was deployed at 43° 57.71'N, 60° 33.31'W in 24 m water depth, and the second S4 meter (S4B) was deployed at 43° 57.44'N, 60° 33.29'W in 30 m water depth. These locations were strategically selected to cover different parts of a sand ridge: Ralph was on the crest of a first-order sand ridge, S4A and S4B were respectively on the upper and lower lee flank of the sand ridge.

Surface sediment samples from 5 IKU grab samples show that the bottom sediment at the Ralph site was well sorted (average sorting coefficient 0.45 ϕ) medium sand with an average mean grain size of $D = 0.39$ mm. IKU grabs collected at the S4 deployment sites show that the bottom sediment at these sites was also well sorted medium sand: a mean grain size of $D = 0.32$ mm and sorting coefficient of 0.42 ϕ at S4A; $D = 0.28$ mm and sorting coefficient of 0.35 ϕ at S4B.

3.2 S4 Wave-Current Meter Data

Two S4 wave-current meters were deployed from 26 November to 6 December 1996 in the SI96a expedition. They measured depth (hence waves) and velocity at 50 cm above the seabed. Both meters were programmed to burst sample for 5 minute duration every hour at a frequency of 1 Hz. The single OBS sensor on these S4 meters continuously recorded data of 24 s averages of sediment suspension. Both S4 meters

worked well for the entire deployment duration. Fig. 4 shows the time-series plots of (a) mean current averaged over 30 s and the direction of the mean current, (b) the mean water depth (lower panel) also averaged over 30 s, and (c) the instantaneous current speed (upper panel) for the S4A meter. The time in Fig. 4, as throughout this report, is in GMT. These plots show that the water was about 24 m deep at S4A site and that the tides were clearly semi-diurnal with roughly a 1 m range (Fig. 4b). Fig. 4c shows that two major storms occurred during the early and late parts of the deployment, and two moderate events occurred during the middle part of the data set. The maximum instantaneous velocity, mostly due to wave oscillations, reached about 120 cm/s during the two major storms, while that of the two minor storms also reached about 60 to 80 cm/s. The 30 s averaged current speed in Fig. 4a clearly shows the effect of storms on the mean velocity: the mean current speed was only around 25 cm/s during non-storm periods, but increased to 40 - 50 cm/s during storms. The direction of the peak mean current was mostly to N-NE or S-SW. The suspended sediment concentration (in sensor output voltage) measured by the OBS on S4A meter is plotted in Fig. 5. It shows that the first major storm caused strong sediment resuspension, but the effect of the second major storm during the late stage of the deployment was much less significant. Tidal currents did not seem strong enough to cause sand suspension at S4A site.

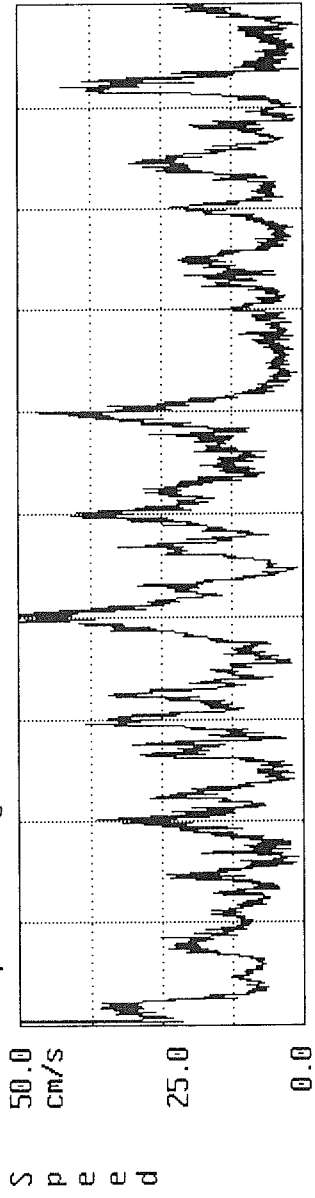
S4B was deployed about 1.2 km southward from S4A on the lower lee flank of the sand ridge. The 30 s average current speed and its direction, mean water depth and instantaneous current speed of the S4B meter were plotted in Figs. 6a, b and c respectively. The mean water depth at S4B was about 30 m and the depth time series again shows semi-diurnal tides with about 1 m range. The instantaneous velocity data in Fig. 6c again demonstrates the passage of the two major storms during the early and late stages of the deployment. Due to the deeper water at the S4B site on the lower lee flank of the sand ridge, however, the maximum instantaneous velocity was smaller than that of S4A site and only reached about 80 cm/s. The peaks of the 30 s averaged mean current (Fig. 6a) reached only about 40 cm/s, 20% smaller than that at the S4A site. But the directions of these peaks were again predominantly to the N-NE or S-SW. The time series of the OBS data at S4B is plotted in Fig. 7. In contrast to S4A, Fig. 7 shows that the second major storm caused stronger sand resuspension than the first one. The strongest suspension peak around 12/04 does not seem to correlate with the peak of wave activity, though other suspension peaks are correlated either with the peaks of wave activity or with the peaks of tidal current.

The sediment traps on the S4 meters collected composite suspended sediment samples at 20 cm above the seabed. Table 2 lists the mean grain size D (mm) and sorting coefficient (ϕ) as a function of height (cm) above the bottom of the trap for the S4A meter. The total length of the sample is 18 cm. Three layers can be seen from the trap: approximately at 0.5-4.5, 5.5-10.5, and 11.5-17.5 cm. Each layer exhibited a fining

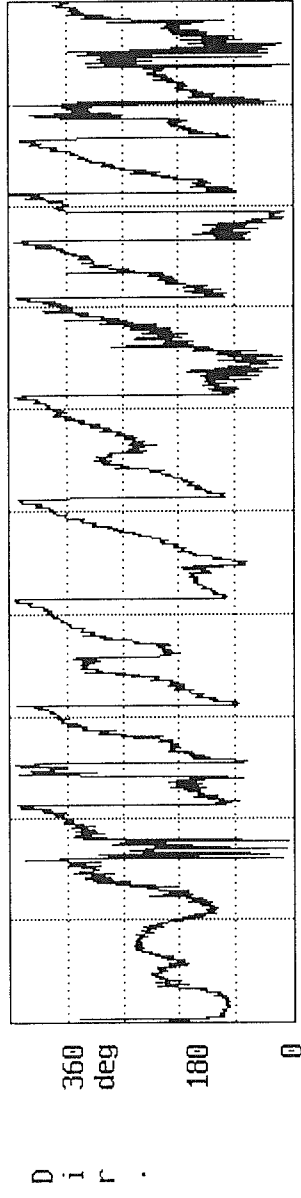
Fig. 4 Time-series plots of (a) mean current and its direction, (b) mean water depth (lower panel), and (c) instantaneous current velocity (upper panel) for the S4A meter of SI96a deployment.



InterOcean Systems, Inc. Model S4 Current Meter #078001668
SABLE ISL96-2 File : SAB96-1.S4B
Xoffset: +0.00 cm/s Yoffset: +0.00 cm/s Mag.Var.: 0 deg
Samples averaged : 30 Mean : 14.42



Mean Direction : 84.0

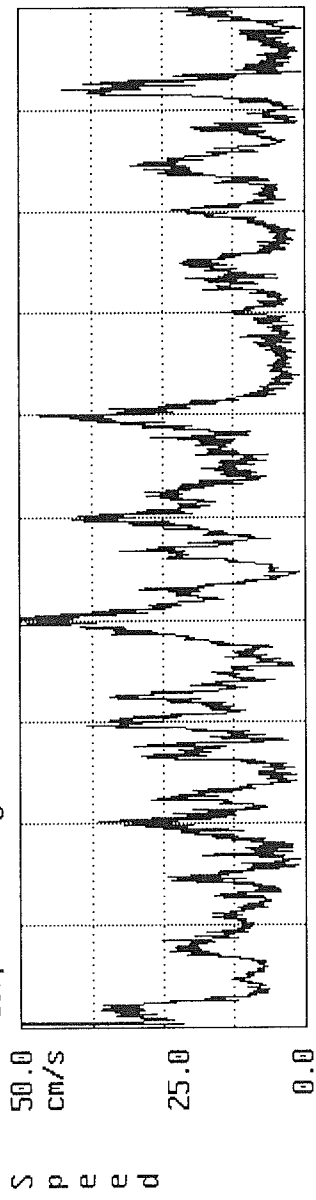


1
11/26/96 10:04:00

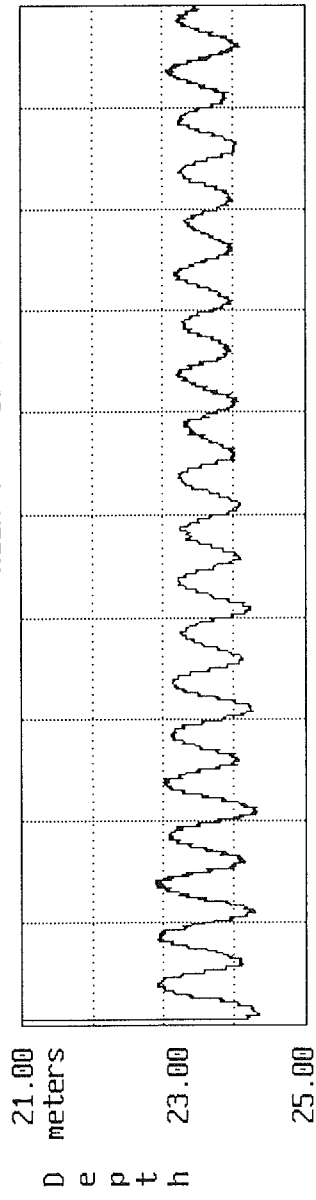
Samples 74399
12/06/96 17:08:58



InterOcean Systems, Inc. Model S4 Current Meter #07801668
SABLE ISL96-2 File : SAB96-1.S4B
Xoffset: +0.00 cm/s Yoffset: +0.00 cm/s Mag.Var.: 0 deg
Samples averaged : 30 Mean : 14.42



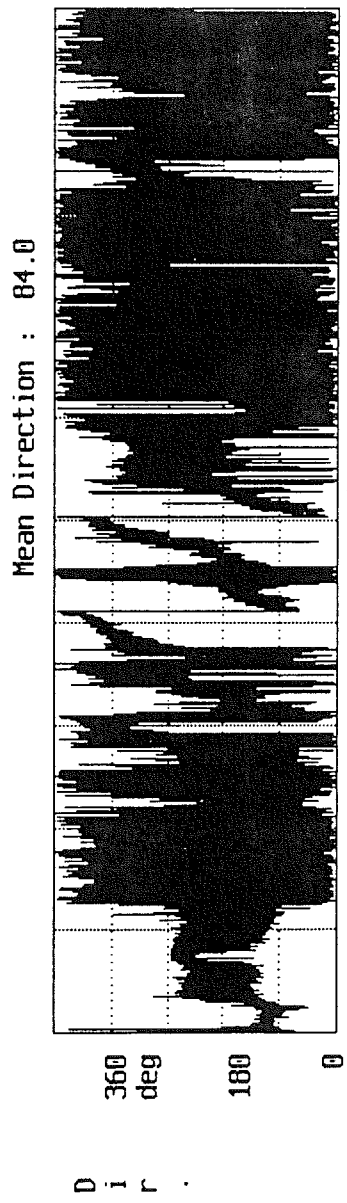
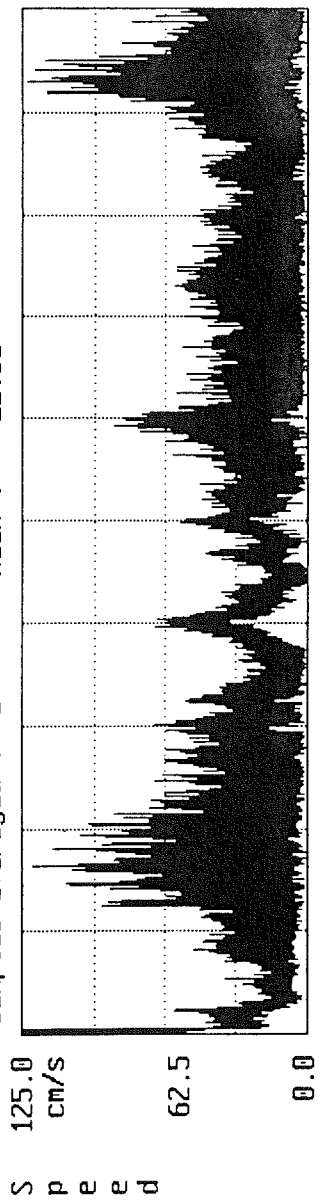
Mean : 23.52



1 11/26/96 10:04:00 Samples 74399
12/06/96 17:08:58



InterOcean Systems, Inc. Model S4 Current Meter #078001668
SABLE ISL96-2 File : SAB96-1.S4B
Xoffset: +0.00 cm/s Yoffset: +0.00 cm/s Mag.Var.: 0 deg
Samples averaged : 1 Mean : 22.51



1 11/26/96 10:04:00 Samples 74399
12/06/96 17:08:58

Fig. 5 Time series plot of the OBS data on the S4A meter of SI96a deployment.

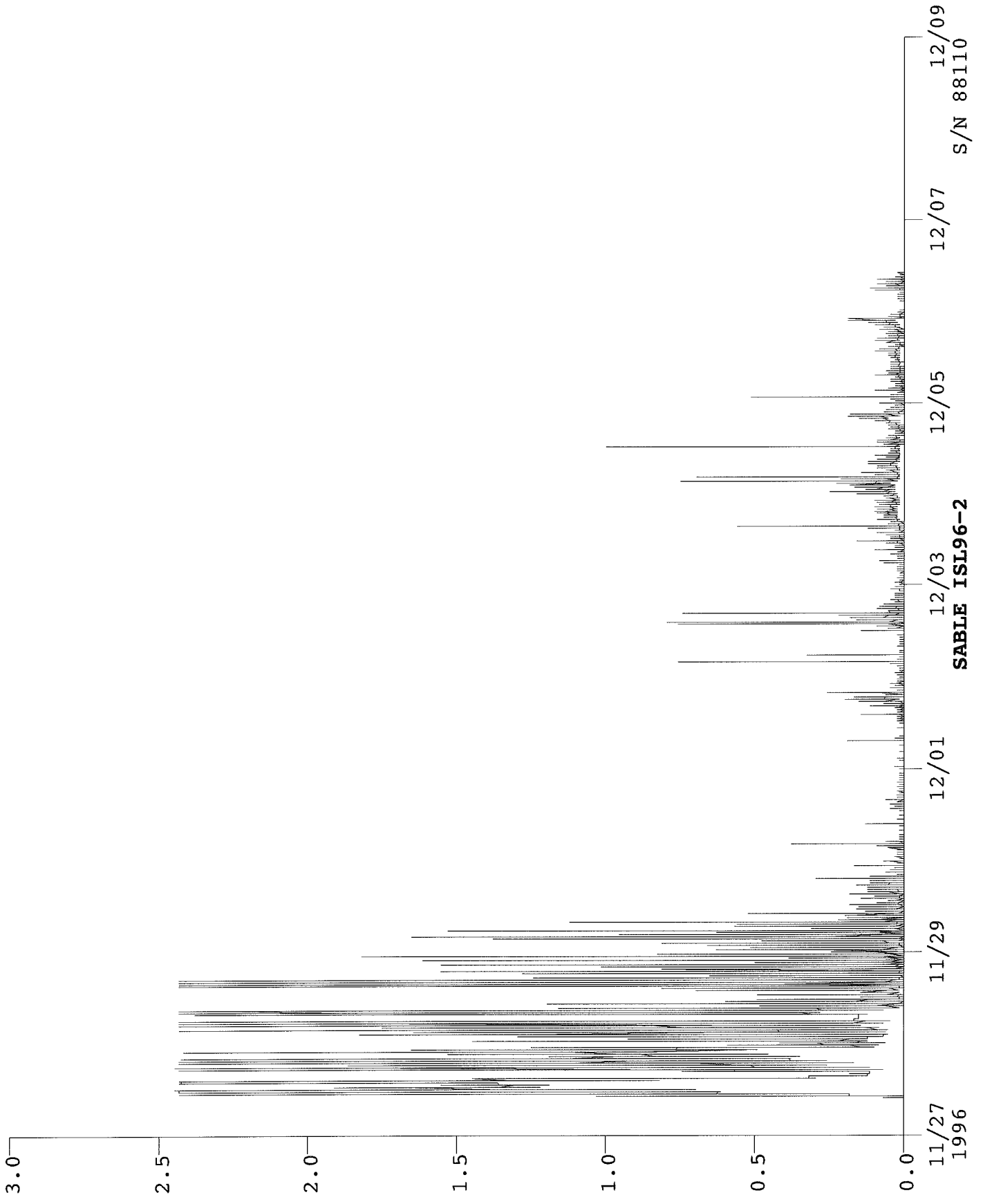
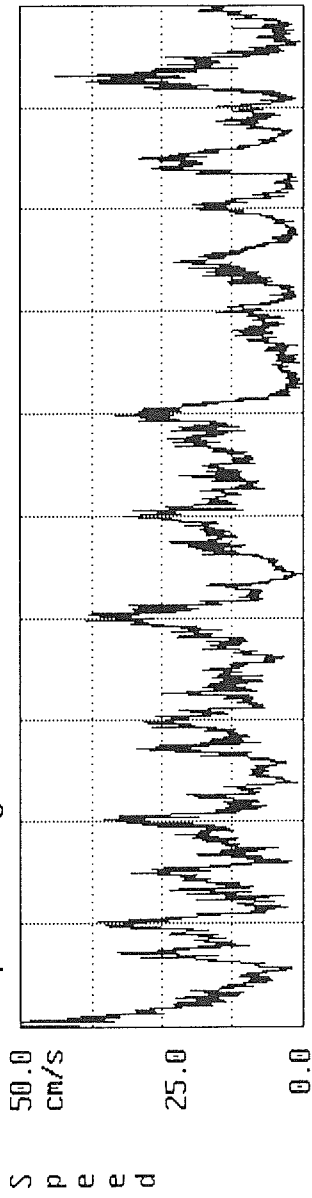


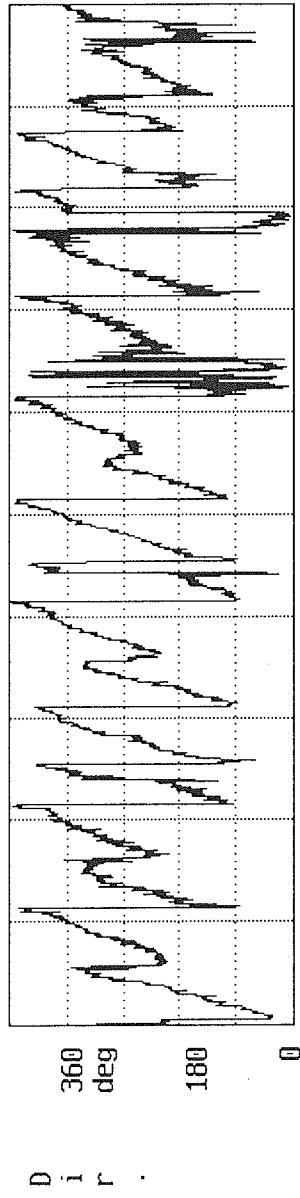
Fig. 6 Time-series plots of (a) mean current and its direction, (b) mean water depth (lower panel), and (c) instantaneous current velocity (upper panel) for the S4B meter of SI96a deployment.



InterOcean Systems, Inc. Model S4 Current Meter #010002196
SABLE ISL96-1 File : SAB96-2.S4B
Xoffset: +0.00 cm/s Yoffset: +0.00 cm/s Mag.Var.: 0 deg
Samples averaged : 30 Mean : 13.04



Mean Direction : 312.8

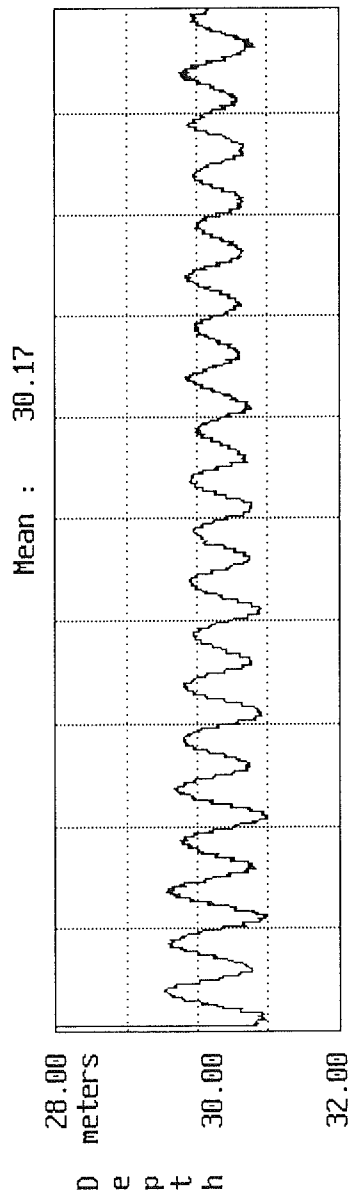
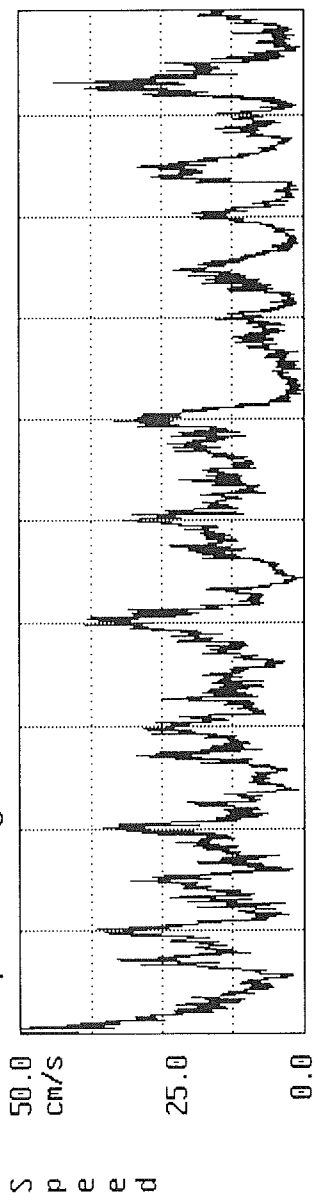


1
11/26/96 10:17:00

Samples 74099
12/06/96 16:21:58



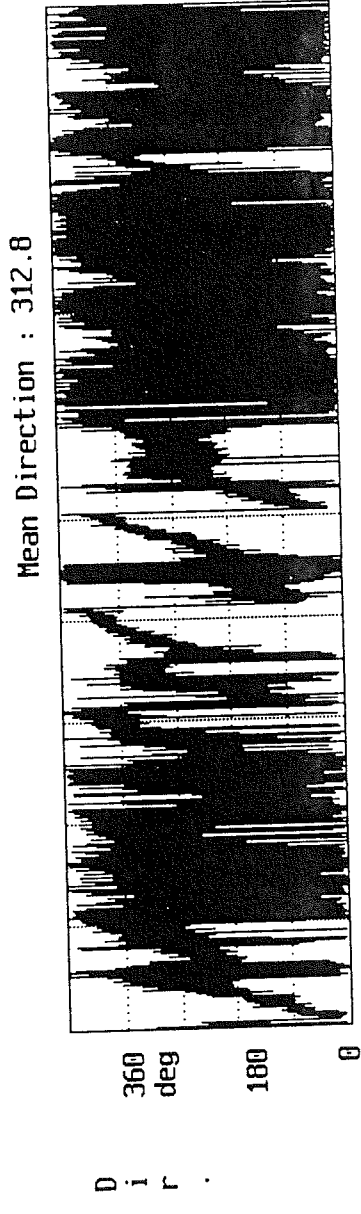
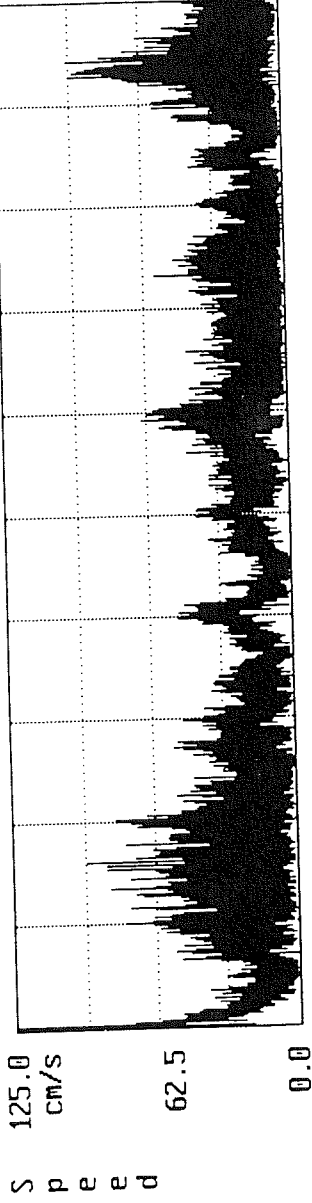
InterOcean Systems, Inc. Model S4 Current Meter #01002196
SABLE ISL96-1 File : SAB96-2.S4B
Xoffset: +0.00 cm/s Yoffset: +0.00 cm/s Mag.Var.: 0 deg
Samples averaged : 30 Mean : 13.04



1 11/26/96 10:17:00 Samples 74099 12/06/96 16:21:58



InterOcean Systems, Inc. Model S4 Current Meter #01002196
SABLE ISL96-1 File : SAB96-2.S4B
Xoffset: +0.00 cm/s Yoffset: +0.00 cm/s Mag.Var.: 0 deg
Samples averaged : 1 Mean : 17.94



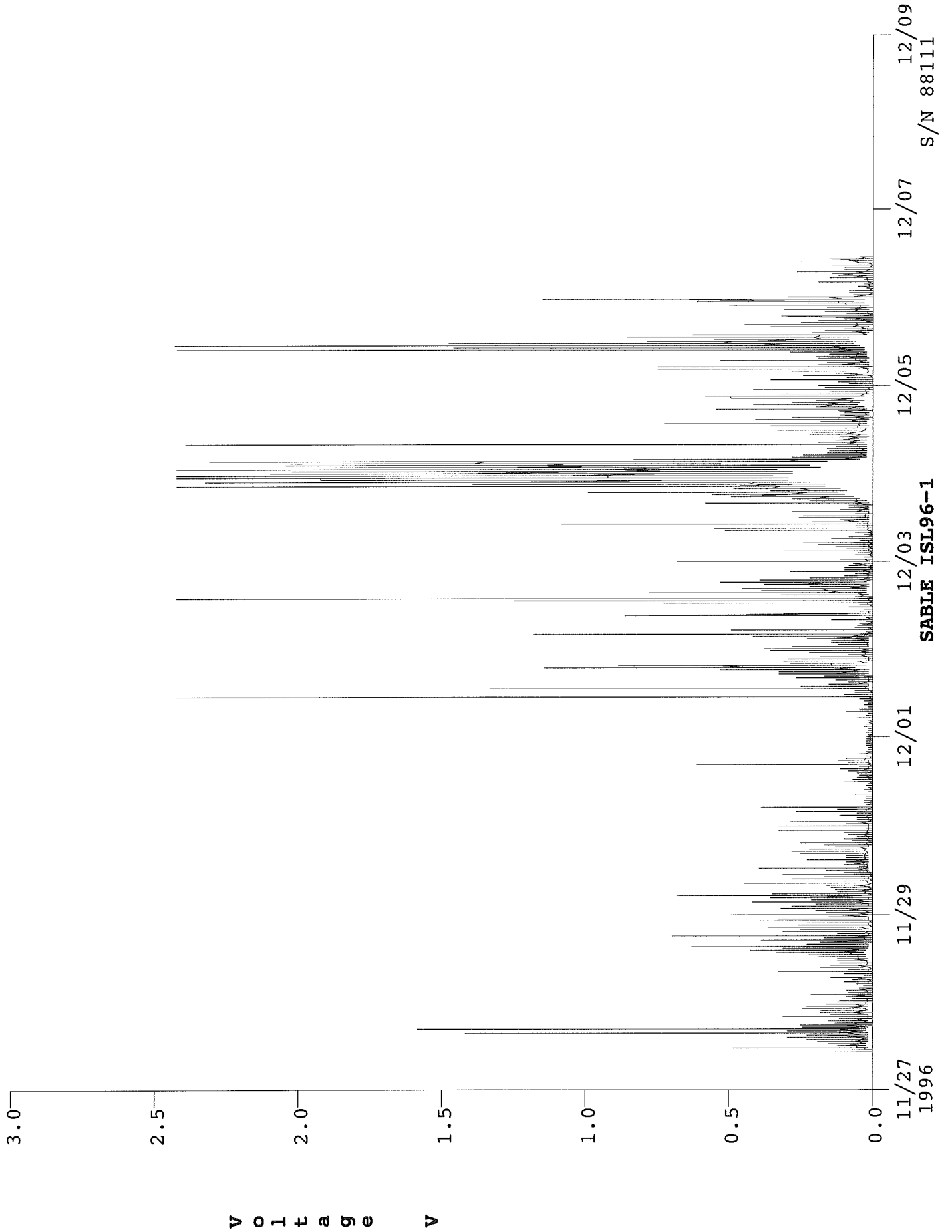
1
11/26/96 10:17:00

Samples

74099
12/06/96 16:21:58

C

Fig. 7 Time series plot of the OBS data on the S4B meter of SI96a deployment.



upward trend and sediment sorting also became better. It is surprising, however, to see that the mean grain size of suspended sand (average of 0.42 mm, ranging from 0.34 to 0.54 mm) was coarser than the mean grain size of the bottom sediment (0.32 mm) at the S4A site. The grain size data for the S4B sediment trap are given in Table 3. The total length was only 11 cm and much shorter than that of S4A. Two layers can be

Table 2 Mean grain size D and sorting of sediment trap sample for S4A of the SI96a deployment. Height is from the bottom of the trap upward. The total length of sample is 18 cm.

Height (cm)	D (mm)	Sorting (phi)
0.5	0.50	0.98
1.5	0.54	1.09
2.5	0.47	0.99
3.5	0.47	0.78
4.5	0.39	0.68
5.5	0.44	0.73
6.5	0.50	0.78
7.5	0.45	0.70
8.5	0.41	0.67
9.5	0.37	0.59
10.5	0.37	0.58
11.5	0.38	0.58
12.5	0.40	0.62
13.5	0.41	0.67
14.5	0.41	0.67
15.5	0.38	0.66
16.5	0.35	0.58
17.5	0.34	0.71

Table 3 Mean grain size D and sorting of sediment trap sample for S4B of the SI96a deployment. Height is from the bottom of the trap upward. The total length of sample is 11 cm.

Height (cm)	D (mm)	Sorting (phi)
0.5	0.28	0.47
1.5	0.28	0.40
2.5	0.28	0.42
3.5	0.21	1.44
4.5	0.04	3.01
5.5	0.15	2.32
6.5	0.23	1.29
7.5	0.27	0.52
8.5	0.28	0.48
9.5	0.29	0.52
10.5	0.27	0.79

clearly defined, approximately from 0.5 to 3.5 cm and then from 6.5 to 10.5 cm. These two layers again show upward fining and better sorting trend and their mean grain size (around 0.24 mm) was roughly equivalent

to that of the bottom sediment at the S4B site. These two layers apparently were correlated with the two major storms at the early and late parts of the deployment (Fig. 6c). The suspended sediment was finer at the middle section of the trap (4.5 and 5.5 cm) and these probably represent the weaker suspensions by the weak events during the middle part of the deployment (Fig. 6c).

3.3 Ralph Data

3.3.1 Hydrodynamics and Sediment Suspension

Ralph was deployed on the crest of a first-order sand ridge (Fig. 1) from 27th to 30th of November, 1996. Ralph was programmed to log pressure, velocity, and OBS data for a 15 minute duration every hour at a frequency of 5 Hz. Corresponding to these data bursts, the four ABS logged data for 1 minute duration at the frequency of 1 Hz for each hour. Similarly, the Imagenex profiler and sonar scanned the seabed for 3 minutes at the beginning of each hour. The DULCE digital camera was not available for the SI96a deployment and the super 8 camera was used to take seabed photographs continuously in 15 minute intervals. Ralph worked well for the entire duration and recorded a total of 98 bursts of good data.

Each burst of the pressure, velocity and OBS data was decoded and processed using the procedures and Matlab programs specifically developed for the preliminary processing of Ralph data (Li, Heffler and Gatchalian, in preparation). In general, the entire Ralph data set was first checked for data quality, sensor drifting and malfunction. Each data burst was then averaged to obtain the mean depth (h), the mean velocities of u_{100} , u_{70} , u_{50} and u_{30} respectively at the heights of 100, 70, 50 and 30 cm above the seabed, the direction of the mean current u_{50} (c_{dir}), and the mean OBS reading (which gives relative suspended sediment concentration) of obs1 to obs6 respectively at the heights of 10, 30, 50, 70, 100 and 136 cm above the seabed. The significant wave height (H_s) was calculated as 4 x the root-mean-square of surface elevation. For each data burst, the mean water depth h was subtracted from the water depth data to derive the instantaneous wave height data which were then analysed to obtain the upward zero-crossing mean wave period (T_z). The current meters measure the instantaneous velocity in the x (90° clockwise from Ralph's heading) and y (parallel with Ralph's heading) directions. The mean values of the x and y components of u_{50} were subtracted from the instantaneous velocity data to derive the instantaneous nearbed wave orbital velocity in these components. Scatter plots of these decomposed wave orbital velocities were used in combination with the wave height data to obtain the wave propagation direction (w_{dir}). The burst-averaged data of h , u_{50} , C_{dir} , H_s , T_z , W_{dir} , and obs1 of SI96a are listed in Appendix 1. The time series of h , u_{50} , H_s , T_z , and obs1 are plotted in Fig. 8.

The depth data in Fig. 8 again show semi-diurnal tides with an approximately 1 m range. The peaks

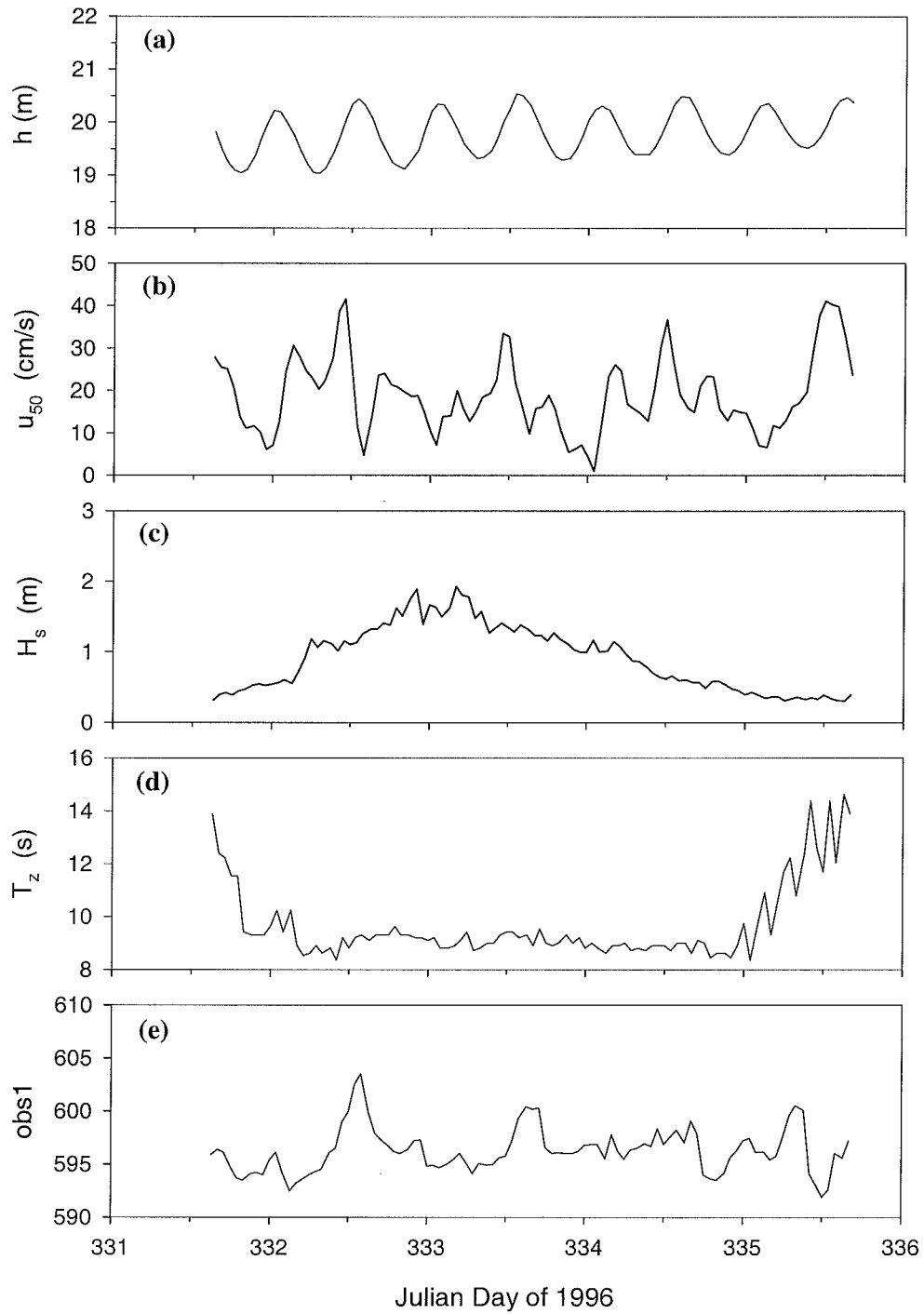


Fig. 8 Time series plots of water depth h , mean velocity u_{50} , significant wave height H_s , mean wave period T_z and obs1 reading of the SI96a Ralph deployment.

of the mean velocity u_{50} ranged from 20 to 40 cm/s. One winter storm occurred during the deployment. If a storm is defined as when $H_s > 0.8$ m, this storm was from Julian day 332 (November 27) hour 05 to Julian day 334 (November 29) hour 08. The peak significant wave height H_s reached about 2 m and the mean wave period was about 9 s (Fig. 8c,d), though periods of swells before and after the storm were much longer (about 14 s). The time series of obs1 data in Fig. 8e shows moderate suspension of sand and the peaks are approximately correlated with the peaks of the mean current. The time series of burst-averaged mean velocity u_{50} , mean-flow direction C_{dir} , and the maximum instantaneous velocity u_{max} are plotted in Fig. 9 for SI96a Ralph data. The peaks of the mean current ranged from 20 to 40 cm/s and they were dominantly to the N, NE or S, SW. The wind-driven currents seemed to have suppressed the tidal current and changed the direction of the peak current to SW during the storm.

Ralph and the two S4 meters were strategically deployed at the crest, upper and lower lee side of a sand ridge so that the flow dynamics across the sand ridge could be evaluated. Comparing Figs. 4a, 6a and 9b indicate that the peaks of u_{50} do not differ significantly from the ridge crest (Ralph location) to the upper (S4A) and lower (S4B) lee flank: the maximum magnitude was around 40 cm/s and were predominantly to the N or NW, though u_{50} at the upper lee flank was slightly higher reaching about 50 cm/s. The maximum instantaneous current speed data plotted in Figs. 4c, 6c and 9d show that the peaks of the maximum instantaneous velocity (predominantly due to wave oscillations) reached about 120 cm/s on the ridge crest (Fig. 9b) and upper lee side (Fig. 4c), but was somehow smaller in the trough (lower lee side) reaching only about 90 cm/s (Fig. 6c). These values are 2 to 3 times higher than the mean current speed u_{50} .

Four sediment traps were attached to Ralph at the following heights: trap1 at 0.3 m, trap2 at 0.5 m, trap3 at 0.7 m and trap4 at 1.0 m. The mean grain size D (mm) and sorting coefficient (ϕ) of these sediment trap samples are listed in Table 4. The height again is upward from the bottom of the sediment trap. The amount of sediment collected by the sediment traps was largest at the lower trap and decreased with the heights above the seabed: trap1 was full with a total length of 16 cm, trap2 had 13 cm length, the length of trap3 was about 4 cm and the highest trap had only 0.8 cm of sand. These obviously indicate that sand resuspension happened predominantly in the lower half meter and that suspension was insignificant at heights beyond 1 m from the seabed. The mean grain size became finer from lower to upper sediment traps: systematically decreasing from 0.45 mm to 0.31 mm. The suspended sediment was moderately sorted and the sorting generally became better except for the upper-most sediment trap. The lower three sediment traps on Ralph all show one layer of suspended sediment deposition which corresponded with the passage of the storm from Julian day 332 to 334 shown in Fig. 9. In each of these 3 layers, grain size was initially finer corresponding with the start of the storm. Grain size reached the maximum roughly at the middle of the

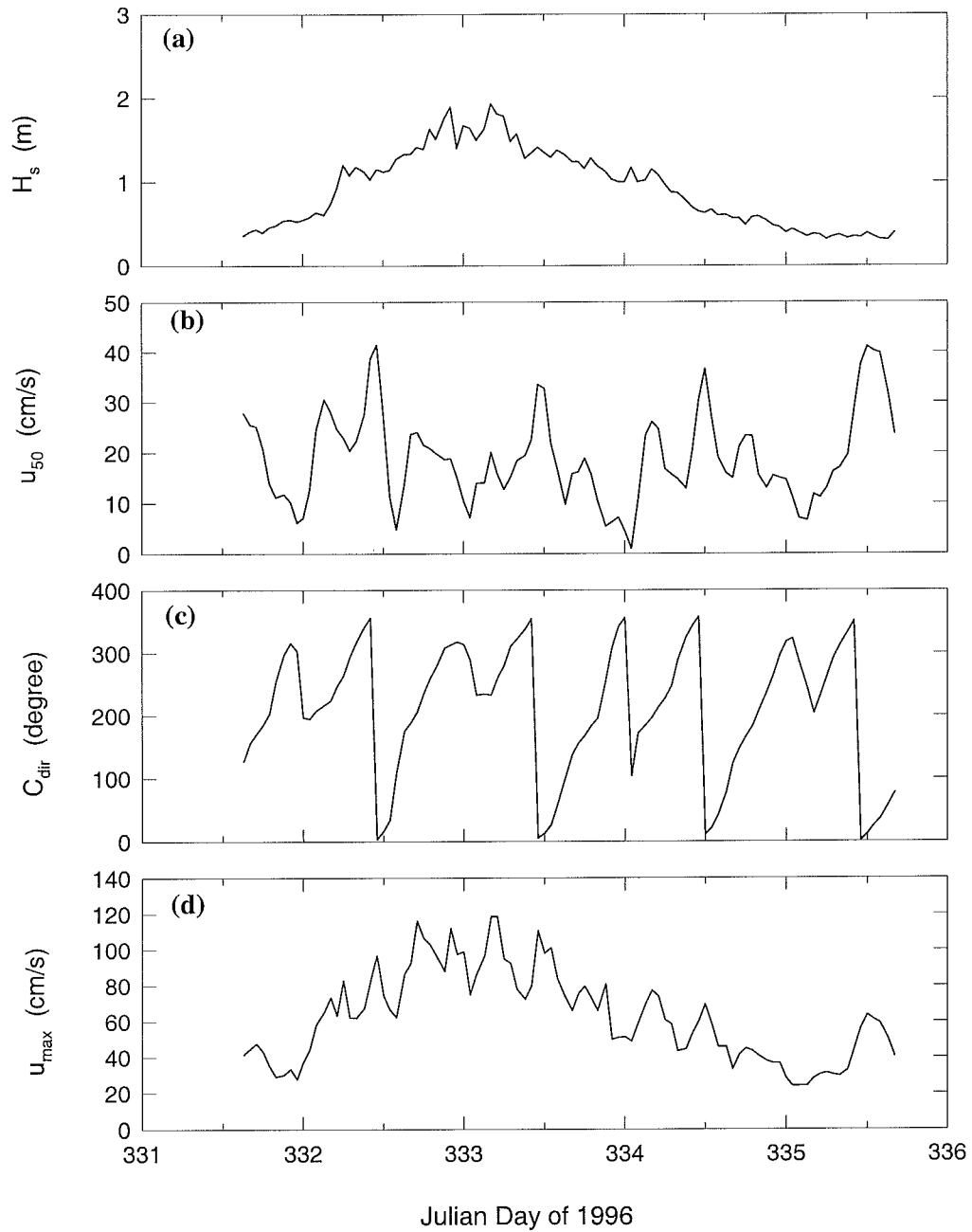


Fig. 9 Time series plots of significant wave height H_s , mean current velocity u_{50} , mean current direction C_{dir} and maximum instantaneous velocity u_{max} (at 50 cm above the seabed) for SI96a Ralph deployment.

Table 4 Mean grain size D and sorting coefficient of SI96a Ralph sediment trap samples.

Sediment trap sample at 0.3 m height; total length 16 cm.

Height (cm)	D (mm)	Sorting (ϕ)
0.5	0.40	0.60
1.5	0.42	0.61
2.5	0.48	0.74
3.5	0.46	0.63
4.5	0.48	0.68
5.5	0.48	0.66
6.5	0.49	0.64
7.5	0.47	0.63
8.5	0.45	0.68
9.5	0.44	0.60
10.5	0.45	0.64
11.5	0.43	0.62
12.5	0.45	0.60
13.5	0.45	0.63
14.5	0.42	0.48
15.5	0.38	0.58
average:	0.45	0.63

Sediment trap sample at 0.5 m height; total length 13 cm.

0.5	0.41	0.51
1.5	0.41	0.53
2.5	0.44	0.58
3.5	0.44	0.64
4.5	0.44	0.64
5.5	0.44	0.65
6.5	0.43	0.63
7.5	0.42	0.61
8.5	0.44	0.64
9.5	0.47	0.68
10.5	0.47	0.66
11.5	0.42	0.57
12.5	0.39	0.60
average:	0.43	0.61

Sediment trap sample at 0.7 m height; total length 4 cm.

height	D(mm)	sorting
0.5	0.37	0.57
1.5	0.40	0.53
2.5	0.41	0.57
3.5	0.39	0.60
average:	0.39	0.57

Sediment trap sample at 1.0 m height; total length 0.8 cm.

0.4	0.31	0.72
-----	------	------

layer (at the peak of the storm) and then decreased again as the storm waned. The mean grain size of the suspended sediment (in trap1 and trap2) was again found to be coarser than that of the surface bottom sediment.

3.3.2 Bedform and Bed Elevation Change

One of the main goals of the joint project between GSCA and Mobil was to estimate the depth of the mobile layer for a storm of a known return interval. The data collected by the Acoustic Backscatter Sensors (ABS) and the Imagenex sector scanning profiler (SSP) and sector scanning sonar (SSS) were analysed to evaluate bedform development, seabed erosion and depth of mobile layer during storms on Sable Island Bank. The roll and pitch data of Ralph were examined first to detect and correct any significant sinking of the Ralph frame due to scouring. Then the bed elevation data recorded by ABS were analyzed to derive the bed level changes due to erosion and/or bedform migration. The seabed profiles and 2-D images collected by the Imagenex SSP and SSS were used to derive for each storm the height and wavelength of the dominant bedforms, and seabed erosion and bedform development processes. Finally, the greater of the maximum bed elevation change and half of the maximum bedform height was estimated as the maximum depth of mobile layer for the storm.

The roll and pitch data of the SI96a Ralph deployment are plotted against the Julian day in Fig. 10a. Except for a few electronic glitches, the roll and pitch of Ralph did not change dramatically for this deployment. The small variations of less than 1° should not cause significant error in Ralph data. The ABS data, plotted in Fig. 11, show that Ralph platform sank about 4 cm into the sand after casting off so that all 4 ABS detected a seabed at about 126 cm from the sensors. As the only storm in this deployment started to build up at hour 05 on day 332 (D332H05), seabed began to rise and reached the maximum level of about 106 cm around D332H20-D333H04, which is roughly the peak of the storm (see Fig. 8). During the remainder of the deployment, seabed elevation stayed around this height and oscillated with an amplitude of about 8 - 10 cm. Since the roll and pitch data did not show significant change, the bed elevation changes shown in Fig. 11 were most likely due to the passing through of bedforms of different scales. The ABS data in Figure 11 clearly show bedforms of three magnitudes: large bedforms of around 20 cm height, medium-scale bedforms of 8 - 10 cm height and the superimposed small ripples of 2 - 4 cm height.

The Imagenex profiler and sonar scanned the seabed for 3 minutes at the beginning of each hour. The profiler was programmed to scan a line of the seabed of about 10 m. An example of the profiler image is shown in Fig. 12a and the vertical height of the image is about 1.3 m. The sonar was supposed to provide 270^o scanning images with a 40 m diameter range. Due to technical problems, the sonar only scanned the

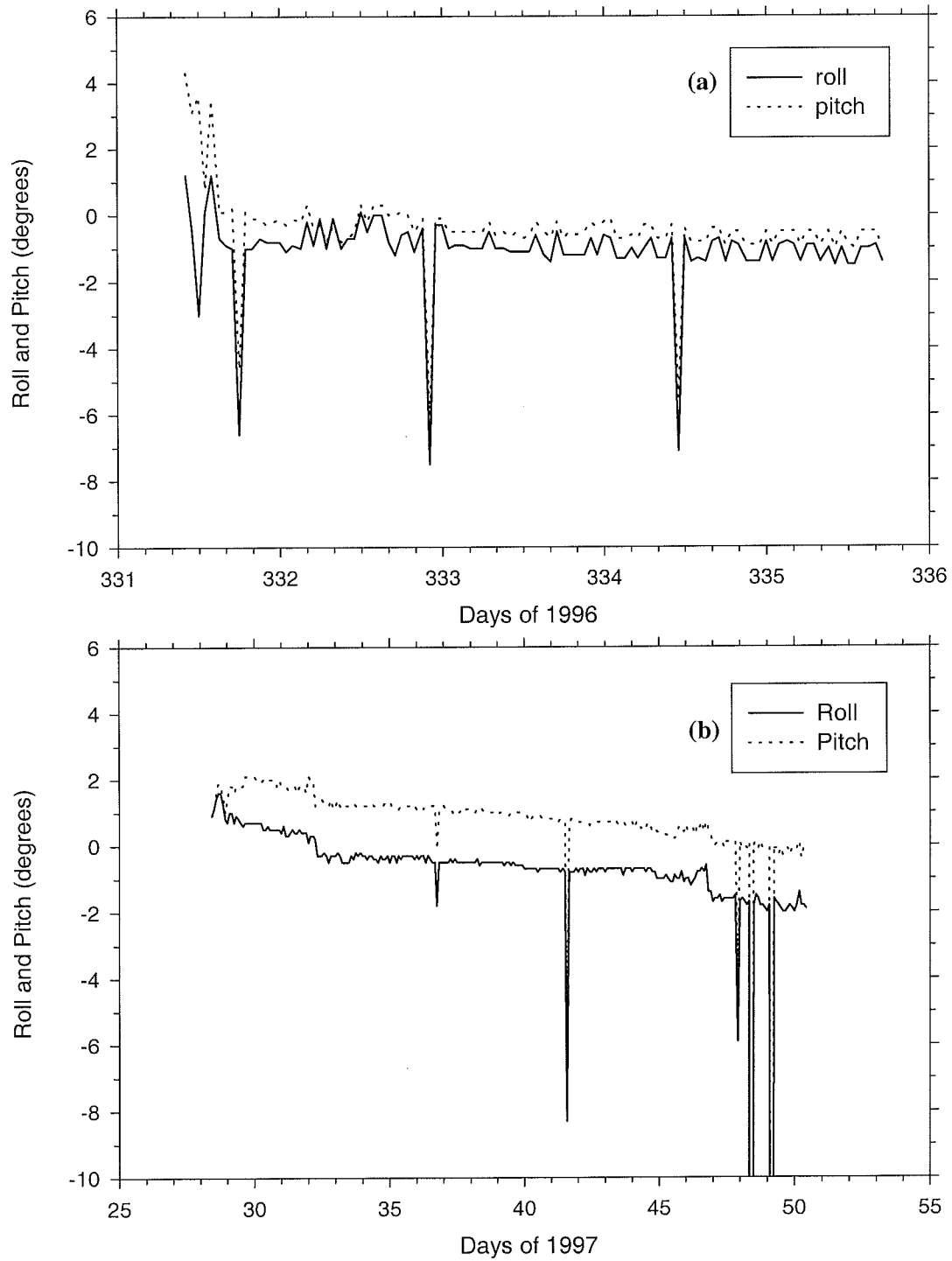


Fig. 10 The roll and pitch data of (a) SI96a and (b) SI97a Ralph deployments.

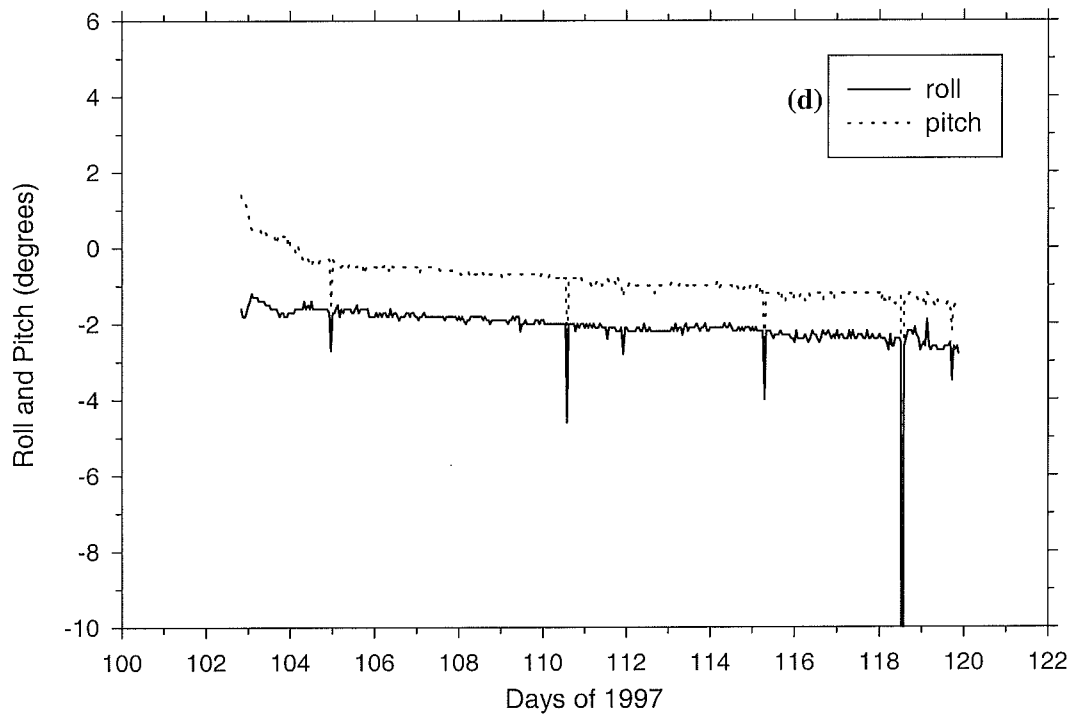
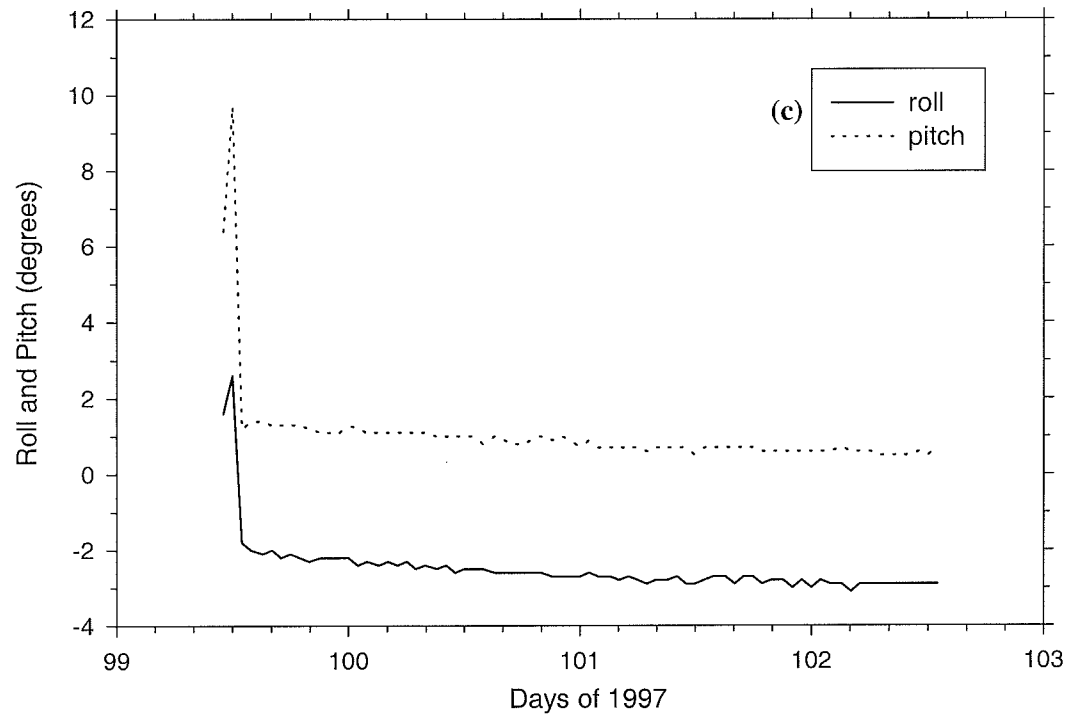


Fig. 10 (continued) The roll and pitch data of (c) SI97b and (d) SI97c Ralph deployments.

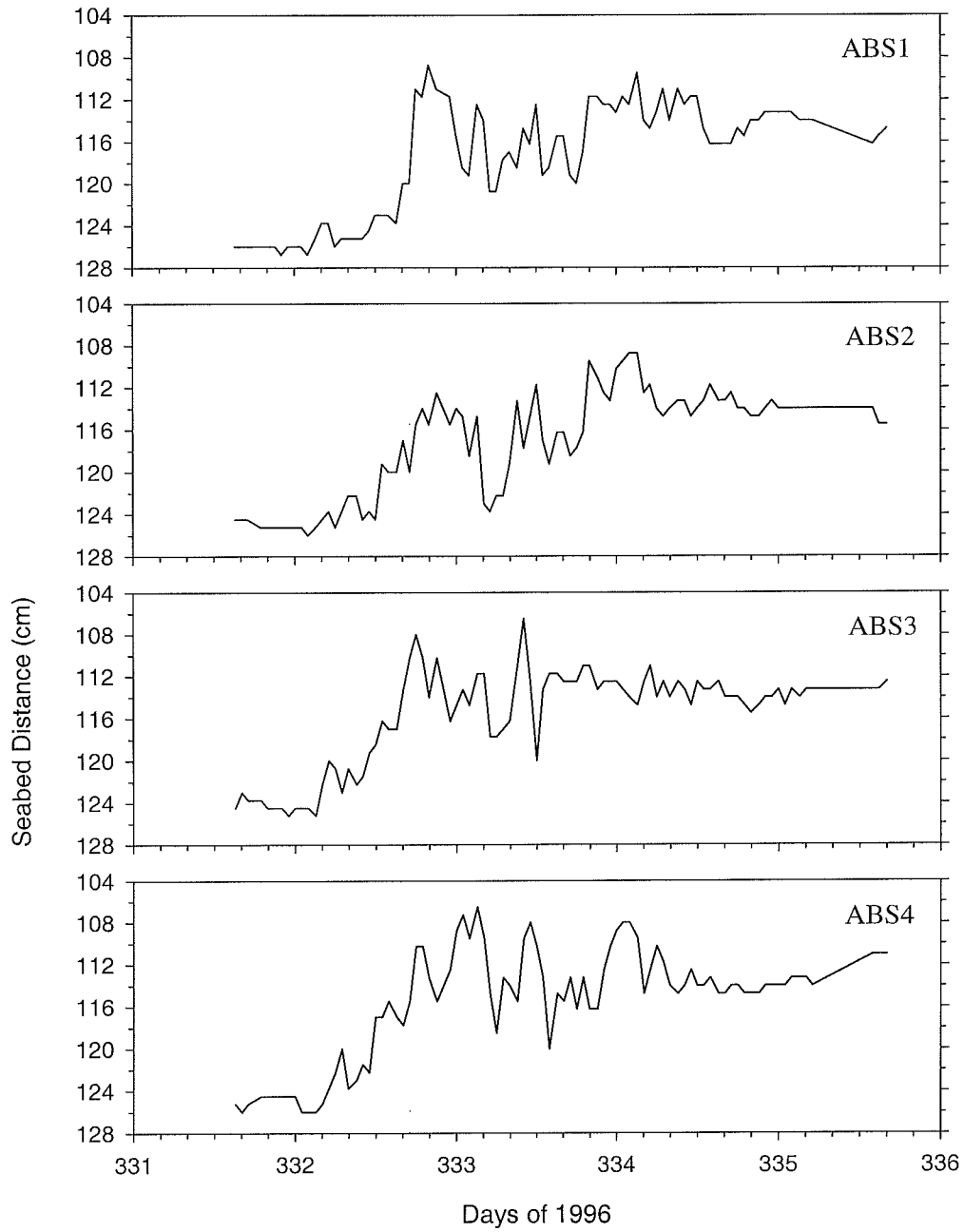


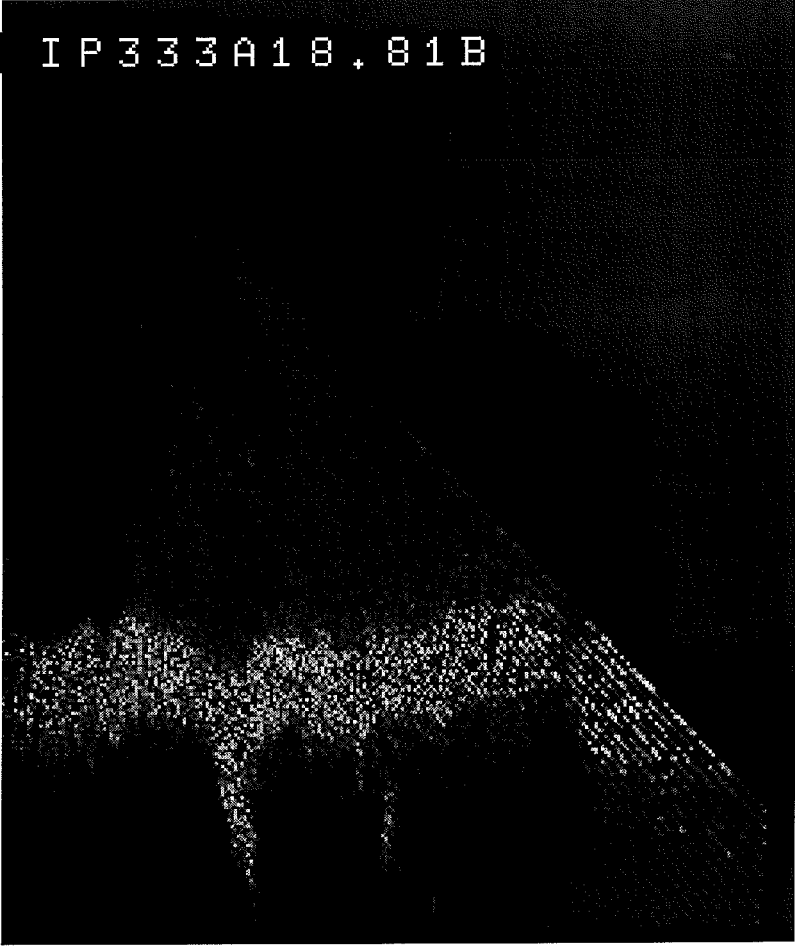
Fig. 11 The seabed elevation changes recorded by ABS sensors in SI96a Ralph deployment.

Fig. 12 Examples of the Imagenex (a) profiler and (b) sonar images collected in SI96a Ralph deployment. The vertical height of the profiler image is 1.3 m and the diameter of the sonar image is 40 meters.

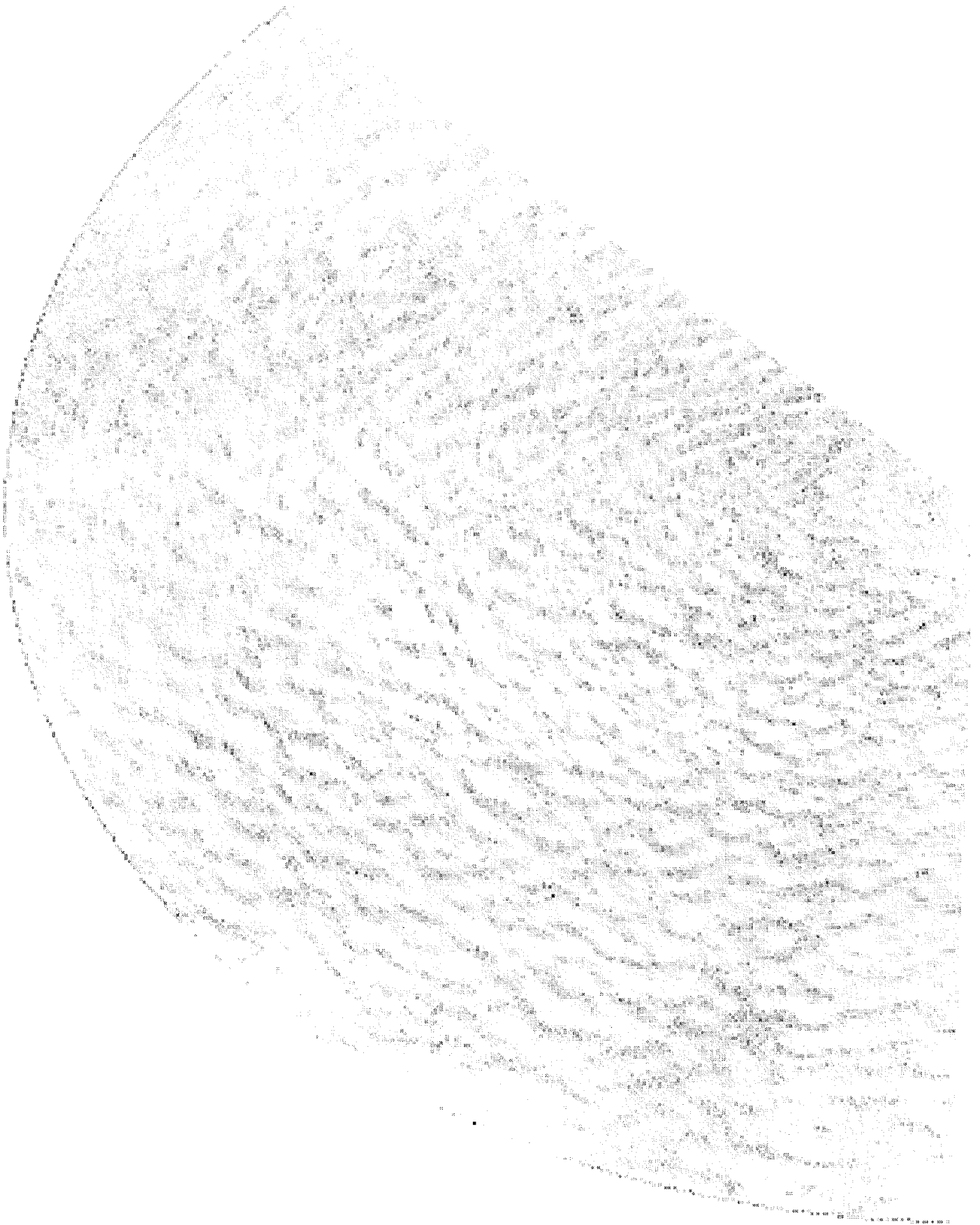
A

11-NOV-1996 18:02:10

IP333A18.81B



B



seabed for 135° in SI96a deployment and an example sonar image is shown in Fig. 12b. The diameter of the sonar image in Fig. 12b is 40 m with the top of the image pointing 70° from the magnetic North. Fig. 12a shows a maximum bedform height of 12 cm, while Fig. 12b depicts combined wave-current ripples with about 0.85 m wavelength oriented 30° from the magnetic North. Linguoid wave-current ripples can also be seen in the middle and lower right portions of the image in Fig. 12b. There was only one storm recorded by Ralph in SI96a deployment. Table 5 lists the significant wave height H_s and the estimated bedform parameters for this storm in SI96a: η_{\max} is the maximum ripple height, λ is the average ripple wavelength, E is the average of the bed elevations at the ripple crest and trough, and E_c is the average of the seabed elevations at ripple crests. Table 5 shows that at the beginning of the storm, bedforms had maximum height

Table 5 Estimated bed-elevation changes and bedform parameters in the storms of SI96a Ralph deployment.

DayHour	H_s (m)	η_{\max} (m)	λ (m)	E (m)	E_c (m)
D332H05	0.9	0.07	0.43	1.13	1.10
D332H13	1.1		0.56		1.02
D333H04	2.0	0.06	0.37	1.12	1.11
D333H08	1.6		0.50		
D333H18	1.2	0.12	0.85	1.00	0.96
D333H21	1.1	0.13		1.03	0.99
D334H04	1.2	0.21	1.09	0.99	0.94
D334H08	0.9	0.18	0.71	1.06	0.97

of 0.07 m and wavelength of 0.43 m, and the bed elevation was 1.13 m from the profiler sensor. As storm built up, ripple height and wavelength were reduced to 0.06 m and 0.37 m respectively at the peak of the storm. As the storm decayed, bedform scales increased and reached the maximum at D334H04: ripple height reached 0.21 m and ripple wavelength reached 1.09 m. The elevation of the seabed (E) also rose to a maximum of 0.99 m to the sensor. The combined ABS data and the data from the Imagenex profiler and sonar suggest that the maximum bedform height during this storm was 0.21 m. If the depth of the mobile layer is taken to be equal to half of the bedform height, then the estimated mobile layer depth was 0.11 m for this storm. However, the maximum bed elevation change during the storm was about 0.14 m.

3.4 Predictions By SEDTRANS92

The application of the GSC sediment transport model SEDTRANS96 is an important aspect in studying bottom boundary layer dynamics and sediment transport on continental shelves (Li and Amos, 1995; Amos, et al., 1996; Li et al., 1997; Li and Amos, 1997). For given inputs of wave, current and seabed conditions, this Fortran 77 numerical model applies the combined wave-current bottom boundary layer theory

to predict wave-enhanced bed shear stresses, velocity profiles, suspended and bedload sediment transport rates and directions. Besides the wave and current data, running SEDTRANS96 also requires sediment mean grain size D , initial ripple height η and ripple wavelength λ , bed slope β , sediment density ρ_s and fluid density ρ . The mean grain size D is 0.39 mm for the SI96a deployment. Based on field measurements of ripple heights and wavelengths over medium sand sediment on SIB by Li and Amos (1998), the initial mean ripple height and wavelength were taken to be 1.4 cm and 12.2 cm, respectively. Bed slope β was assumed to be 0. ρ_s and ρ were taken as 2.65 and 1.025 g/cm³, respectively. These values, together with the wave and current data in Appendix 1, were used in SEDTRANS96 (Li and Amos, 1997) to predict various boundary layer dynamics and sediment transport parameters for the SI96a deployment. The output of bottom boundary dynamics parameters from SEDTRANS96 are listed in Appendix 2a and include:

u_b	-	near-bed maximum wave orbital velocity (m/s)
A_b	-	near-bed wave orbital amplitude (m)
f_{cw}	-	combined wave-current friction factor
u_{*cs}	-	skin friction current shear velocity (cm/s)
u_{*ws}	-	skin friction wave shear velocity (cm/s)
u_{*cws}	-	skin friction combined wave-current shear velocity (cm/s)
u_{*cwe}	-	ripple-enhanced combined wave-current shear velocity (cm/s)
u_{*cwb}	-	bedload-enhanced combined wave-current shear velocity (cm/s)
u_{*c}	-	total current shear velocity (cm/s)
u_{*w}	-	total wave shear velocity (cm/s)
u_{*cw}	-	total combined wave-current shear velocity (cm/s)
δ_{cw}	-	thickness of the wave-current boundary layer (cm)
z_o	-	inner layer bottom roughness (cm)
z_{oc}	-	apparent bottom roughness above the wave boundary layer (cm)

The sediment transport parameters generated by SEDTRANS96 are given in Appendix 2b and these are:

η_p	-	predicted ripple height (cm)
λ_p	-	predicted ripple wavelength (cm)
Q_b	-	mean sediment transport rate of Einstein-Brown bedload method (kg m ⁻¹ s ⁻¹)
Q_{b-dir}	-	direction of mean sediment transport
Q_s	-	mean suspended load sediment transport rate (kg m ⁻¹ s ⁻¹)

Appendix 2b shows that the predicted bedload transport rate reached about 0.005 kg m⁻¹ s⁻¹ during the passage of the storm and was predominantly to the north or northeast. The maximum value of the suspended

load transport was about $0.004 \text{ kg m}^{-1} \text{ s}^{-1}$ which was comparable to the magnitude of the predicted bedload transport.

4. DATA FROM SI97A DEPLOYMENT

4.1 General Description of Deployment

Ralph and a S4 wave-current meter were deployed at the SI97a site about 37 km to the west of Sable Island (Fig. 1) from 27 January to 24 March of 1997. Ralph was deployed at $43^{\circ} 56.45' \text{N}$, $60^{\circ} 37.77' \text{W}$ in 32 m water depth on the crest of a sand ridge (Fig. 1). The S4 meter (S4) was deployed at $43^{\circ} 56.10' \text{N}$, $60^{\circ} 33.40' \text{W}$ in 38 m water depth on the lower lee flank of the sand ridge. The S4 site is not shown in Fig. 1 because of its closeness to Ralph SI97a site.

No bottom sediment sample was collected at these Ralph and S4 deployment sites. However, the sediment trap samples on Ralph (see description in 4.3.1) show that the bottom sediment was probably moderately sorted medium sand. The composite sediment collected in the lowest trap (0.3 m above the seabed) had a mean grain size of 0.40 mm and a sorting coefficient of 0.95ϕ . These were taken as the characteristics of the bottom sediment at the Ralph deployment site.

4.2 S4 Wave-Current Meter Data

The S4 wave-current meter was again programmed to burst sample for 5 minute duration every hour at a frequency of 1 Hz. Good data were recorded from 27 January to 17 March 1997 for a total of 1167 data bursts. Fig. 13 shows the time-series plots of mean current averaged over 60 s, the direction of the mean current, and the mean water depth averaged over 120 s. The water depth plot showed semi-diurnal tides and the occurrences of 3 neap and spring tides. Tide range reached about 1.5 - 2 m during the spring tides and was only about 1 m for neap tides. The peak mean current speeds were around 40 cm/s.

Sediment trap data from the two S4 meters were not available.

4.3 Ralph Data

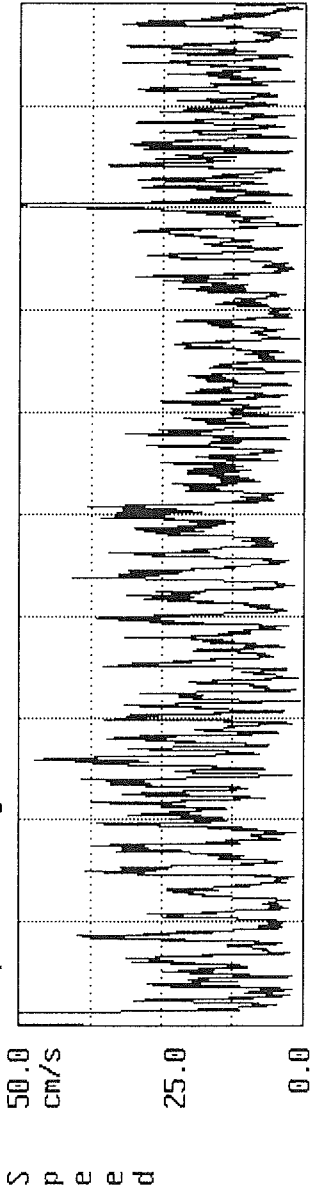
4.3.1 Hydrodynamics and Sediment Suspension

Ralph was deployed on the crest of a sand ridge from 28 January to 24 March of 1997. The pressure, velocity, and OBS data were logged for a 15 minute duration every 2 hours at a frequency of 5 Hz. Corresponding to these data bursts, the four ABS logged data for 1 minute duration at the frequency of 1 Hz

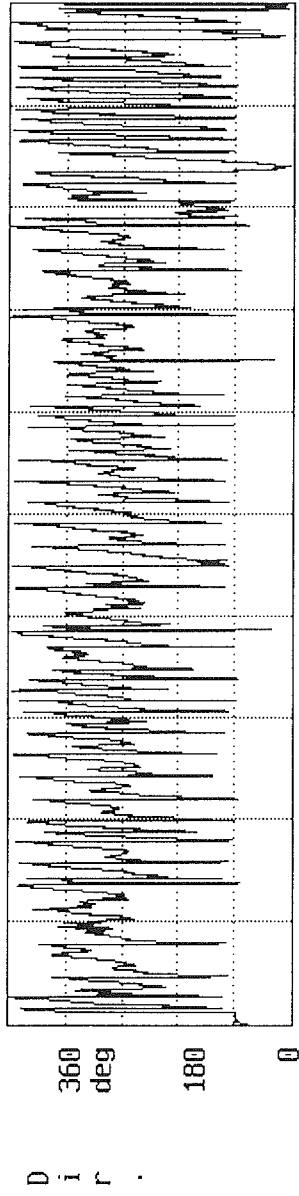
Fig. 13 Time-series plots of (a) mean current and its direction, and (b) mean water depth (lower panel), for the S4 meter of SI97a deployment.



InterOcean Systems, Inc. Model S4 Current Meter #078001668
SABLE-97 File : SAB-97-1.S4B
Xoffset: +0.00 cm/s Yoffset: +0.00 cm/s Mag.Var.: 0 deg
Samples averaged : 60 Mean : 16.49



Mean Direction : 322.0

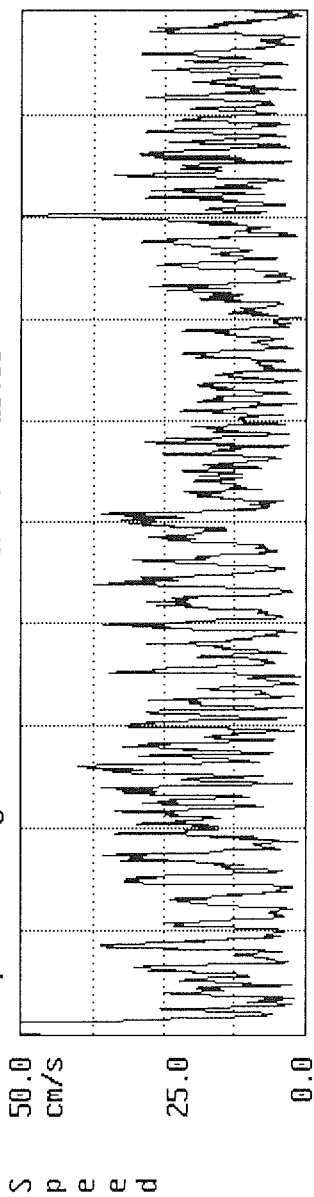


1 1/27/97 23:13:00 Samples 207795 3/17/97 01:14:14

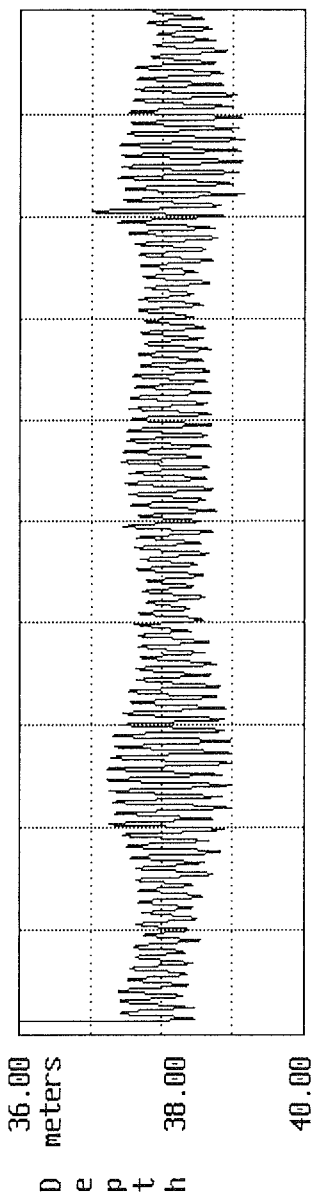
A



InterOcean Systems, Inc. Model S4 Current Meter #07801668
 SABLE-97 File : SAB-97-1.S4B
 Xoffset: +0.00 cm/s Yoffset: +0.00 cm/s Mag.Var.: 0 deg
 Samples averaged : 120 Mean : 16.36



Mean : 37.70



1 1/27/97 23:13:00 Samples 207795 3/17/97 01:14:14

B

every 2 hours. Similarly, the Imagenex profiler and sonar scanned the seabed for 3 minutes at the beginning of each data burst. The super 8 camera was replaced by the DULCE digital camera in this deployment to obtain seabed photographs continuously in 20 minute intervals. Ralph recorded good data from 10:00 GMT on 28th January to 10:00 GMT 19th February for a total of 266 data bursts.

The same procedures and programs as described in section 3.3.1 were used to process the Ralph data collected in this deployment. The burst-averaged data of h , u_{50} , C_{dir} , H_s , T_z , W_{dir} and obs1 of SI97a Ralph deployment are listed in Appendix 3. The time series of h , u_{50} , H_s , T_z , and obs1 are plotted in Fig. 14. Ralph recorded one spring and two neap tides in this deployment (Fig. 14a). The peaks of the mean velocity u_{50} ranged from 20 to 40 cm/s (Fig. 14b). One major storm and four minor events were recorded by Ralph (Figs. 14c and 14d). The peak significant wave height H_s reached about 3 m and the mean wave period was about 13 s for the major storm. The time series plot of obs1 data in Fig. 14e shows gradual drift of the OBS sensor, but some correlation with the peaks of the mean current and significant wave height can be seen.

The time series of burst-averaged mean velocity u_{50} , its direction C_{dir} , and the maximum instantaneous velocity u_{max} are plotted in Fig. 15 for SI97a Ralph data. The peaks of the mean current ranged from 20 to 40 cm/s and they were dominantly to the N, NE or S, SW. The peak values of the maximum instantaneous velocity u_{max} , however, ranged from 80 to 130 cm/s (Fig. 15d). These are again about 3 times higher than that of the mean current speed. The durations, peak values of u_{max} and their directions are listed below for the storms in the SI97a data set:

- storm 1, D028H22 to D030H06, $u_{max} = 80$ cm/s, direction is to 116°
- storm 2, D031H20 to D033H14, $u_{max} = 129$ cm/s, direction is to 359°
- storm 3, D037H00 to D038H12, $u_{max} = 102$ cm/s, direction is to 220°
- storm 4, D041H04 to D041H16, $u_{max} = 115$ cm/s, direction is to 307°
- storm 5, D036H06 to D048H02, $u_{max} = 111$ cm/s, direction is to 200°

Figs. 13 and 15b indicate that the mean current speeds at the ridge crest and lower lee flank were of similar magnitude (20 to 40 cm/s) and they were generally to the N, NE or S, SW. This agrees with what was found in the SI96a data set.

Four sediment traps were attached to Ralph at the following heights above the seabed: trap1 at 0.30 m, trap2 at 0.56 m, trap3 at 1.00 m and trap4 at 1.56 m. The lower three traps collected a small amount of suspended sediment, while the top trap was empty. This suggests that resuspension of sediment did not reach the height of 1.56 m during the storms recorded in the SI97a Ralph deployment in 32 m water depth. The mean grain size D (mm) and sorting coefficient (ϕ) of the sediment samples collected by these traps are listed in Table 6. The mean grain size of these composite samples is coarsest at the lowest sediment trap

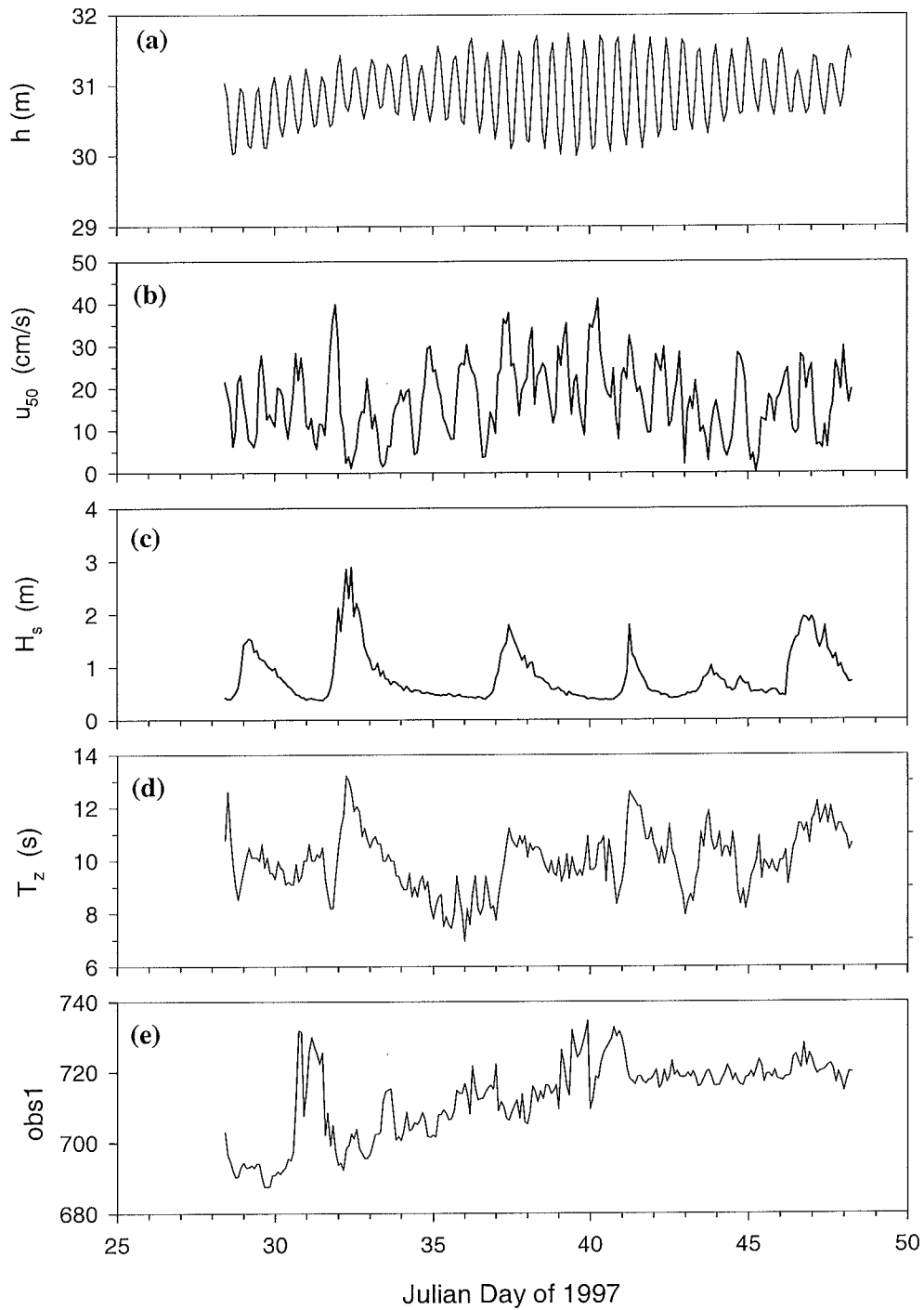


Fig. 14 Time series plots of water depth h , mean velocity u_{50} , significant wave height H_s , mean wave period T_z and obs1 reading for the SI97a Ralph deployment.

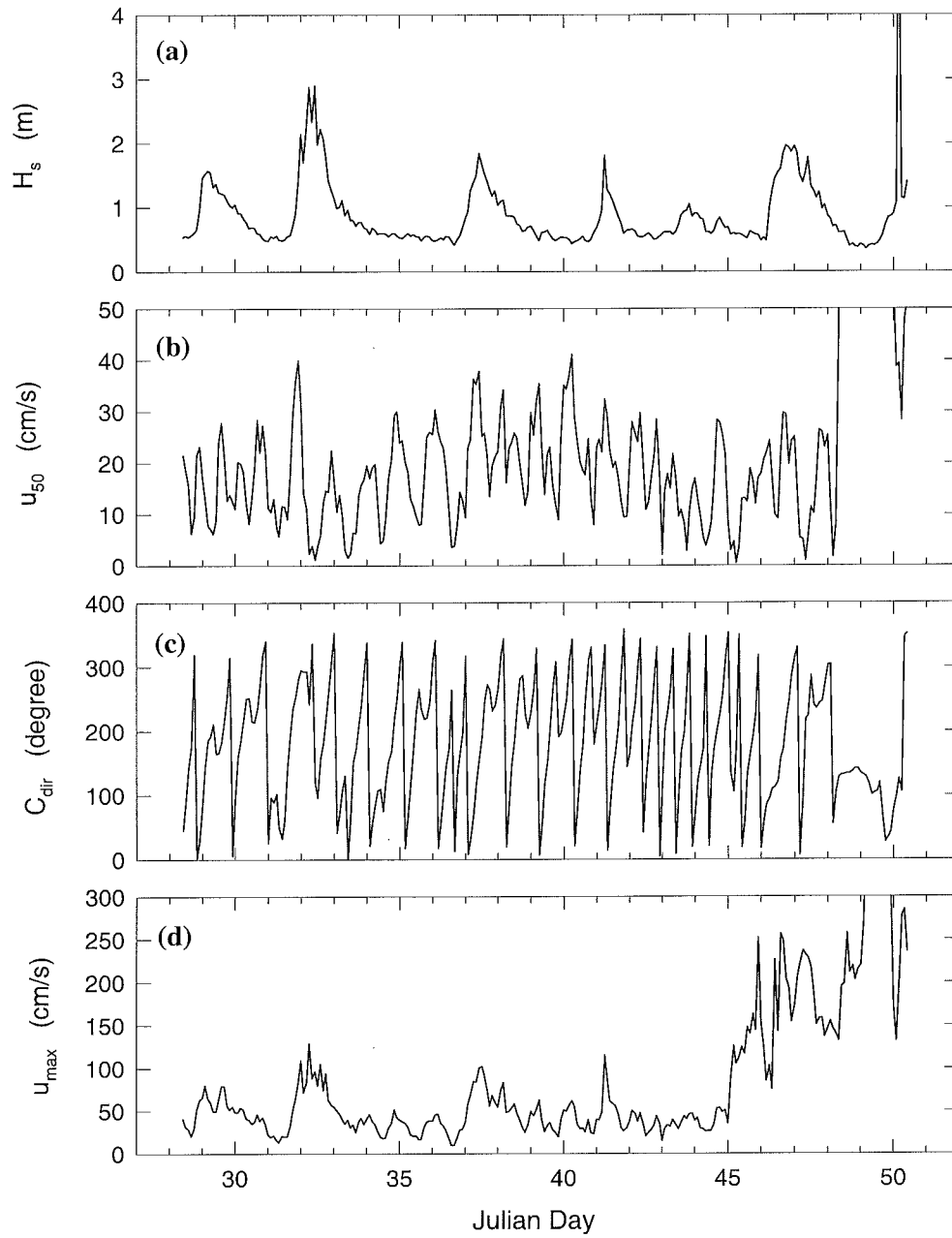


Fig. 15 Time series plots of significant wave height H_s , mean current velocity u_{50} , mean current direction C_{dir} and maximum instantaneous velocity u_{max} (at 50 cm above the seabed) for SI97a Ralph deployment.

Table 6 Mean grain size D and sorting coefficient of SI97a Ralph sediment trap samples.

Trap number	Height (m)	D (mm)	Sorting (ϕ)
trap 1	0.30	0.40	0.95
trap 2	0.56	0.33	0.73
trap 3	1.00	0.23	0.54
trap 4	1.56	no sample	

(D = 0.40 mm, 0.30 m above the seabed) and decreases to 0.33 mm at 0.56 m height and to 0.23 mm at 1.0 m height, suggesting finer suspended sediment at heights further away from the seabed. As the mean grain size of suspended sediment decreased with increasing sediment trap height, the sorting of the suspended sediment improved (see Table 6).

4.3.2 Bedform and Bed Elevation Change

Following the procedures described in section 3.3.2, the roll/pitch data, ABS data and the images recorded by the Imagenex profiler and sonar were analysed to evaluate bedform development, seabed erosion and mobile layer depth during storms for the SI97a Ralph deployment. The roll and pitch data of the SI97a Ralph deployment are plotted against the Julian day in Fig. 10b. As found for the SI96a data, Fig. 10b shows that the roll and pitch of Ralph did not change dramatically during this deployment. There was, however, a gradual decrease of about 2° in both roll and pitch of the Ralph frame. The maximum uncertainty of measured seabed elevation caused by this tilt was less than 5 cm. The ABS data for the SI97a Ralph deployment are plotted in Fig. 16. All 4 ABS sensors show a similar pattern of seabed elevation change: the initial bed was about 130 cm from the ABS sensors (140 cm to ABS1, probably because it was over a bedform trough). The seabed rose 10 to 20 cm during the first storm around Day029 and rose another 20 cm during the second storm at Day032. After a drop of about 10 cm following the decay of the second storm, seabed stayed roughly constant until the onset of the third storm at Day037, which caused a moderate drop of about 15 cm. The seabed experienced another small drop (5 cm) due to storm 4 at Day041. Finally at the end of the deployment, the seabed was raised about 15 cm due to the passage of the fifth storm. Thus the ABS data suggest the following possible maximum bedform heights: 20 cm for storm 1, 23 cm for storm 2, 15 cm for storm 3, about 5 cm for storm 4 and 15 cm for storm 5.

The Imagenex sonar worked perfectly in this deployment providing 270° coverage of the seabed and the profiler also worked well. Example profiler and sonar images are shown in Fig. 17. Again, the height of the profiler image in Fig. 17a is about 130 cm and the diameter of the sonar image in Fig. 17b is 40 m with the top of the image pointing about 350° from magnetic North. Fig. 17a shows a maximum bedform height of 27 cm, while Fig. 17b displays dominant bedforms of about 1.7 m wavelength oriented 100° from the

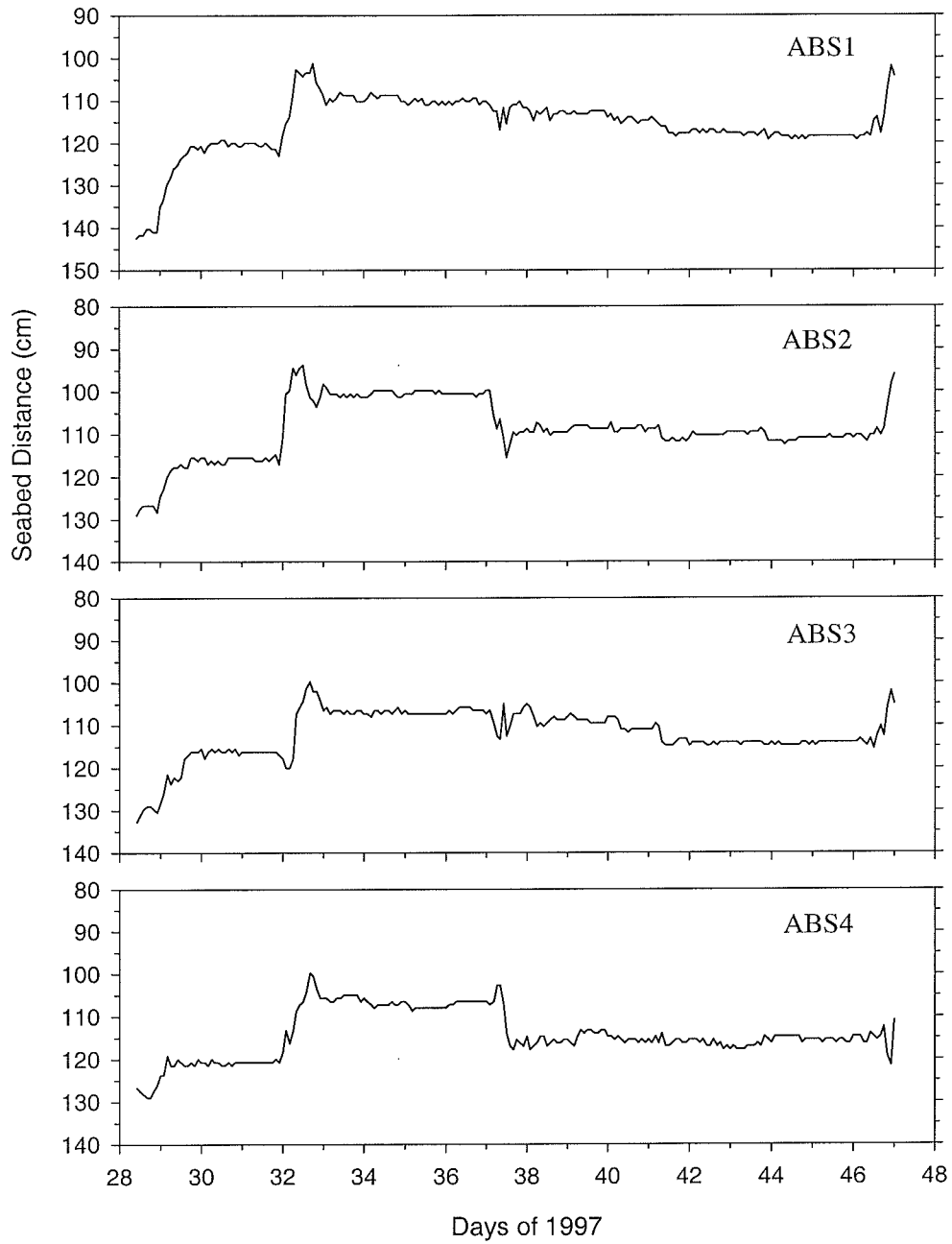


Fig. 16 The seabed elevation changes recorded by ABS sensors in SI97a Ralph deployment.

Fig. 17 Examples of the Imagenex (a) profiler and (b) sonar images collected in SI97a Ralph deployment.

01-FEB-1997 18:04:14

IP032A1B.81B



A

01-FEB-1997 18:01:50 II032A18.81B



magnetic North. Bed elevation changes and bedform parameters derived from the Imagenex profiler and sonar data are listed in Table 7 for each of the 5 storms recorded by Ralph in SI97a deployment. The peak significant wave height in storm 1 was 1.6 m. Large wave ripples developed with a wavelength of 1.8 m. The maximum bedform height was measured at 0.11 m. But the recorded maximum bed elevation change was about 0.11- 0.12 m, thus the estimated maximum mobile layer depth is about 0.11 m. Storm 2 was the strongest of the 5 storms in the deployment. H_s reached as high as 2.9 m (Table 7). The measured maximum bed elevation change was 0.17 m. The maximum bedform height was 0.27 m and bedform wavelength was

Table 7 Estimated bed-elevation changes and bedform parameters in the storms of SI97a Ralph deployment.

DayHour	H_s (m)	η_{\max} (m)	λ (m)	E (m)	E_c (m)
storm 1					
D029H00	1.5	0.06	1.81	1.19	1.16
D029H04	1.6	0.04		1.13	1.11
D029H06	0.8	0.11		1.08	1.04
storm 2					
D031H20	0.9	0.11		1.09	
D032H00	2.1	0.08		1.02	
D032H06	2.9	0.13	1.01	0.97	
D032H10	2.9	0.13	1.60	0.92	
D032H12	2.0	0.16	1.69	0.93	
D032H18	1.8	0.27	1.70	0.96	
D033H04	1.0	0.14	1.76	0.95	
storm 3					
D037H02	0.9	0.10	2.02	0.97	
D037H08	1.5	0.11		0.97	
D037H10	1.8	0.10		0.98	
D037H12	1.7	0.14	1.94	0.99	
D037H18	1.3	0.14		0.99	
D038H10	0.9	0.15		1.00	
storm 4					
D0 41H04	1.0	0.13		1.01	
D0 41H06	1.8	0.12		1.00	
D0 41H10	1.2	0.16		1.03	
storm 5					
D0 46H08	1.3	0.15	0.72	1.03	
D0 46H12	1.5	0.16		1.02	
D0 46H14	1.6	0.24	0.87	0.99	
D0 46H20	2.0	0.16	1.96	0.89	
D0 47H00	2.0	0.22	1.81	0.94	

1.76 m. The estimated maximum mobile layer depth is about 0.17 m. The measured bedform height and wavelength data in Table 7 again show that the largest bedforms developed during the decay of the storm,

not at the peak of the storm. The peak significant wave height of storm 3 reached 1.8 m. The maximum bedform height was 0.15 m and bedform wavelength was at 2.02 m, though bed elevation change was only about 0.03 m. The maximum mobile layer depth is thus estimated to be 0.08 m. Again, the largest bedforms seem to form toward the latter part of the storm. The intensity of storm 4 is similar to that of storm 1 and H_s only reached 1.8 m. The maximum measured ripple height was 0.16 m and the maximum bed elevation change was 0.03 m. Bedform wavelength could not be measured for this storm. The maximum mobile layer depth is estimated at 0.08 m. The last storm of the SI97a deployment was of moderate intensity in which H_s reached about 2 m (Table 7). The maximum measured bedform height and wavelength were 0.24 m and 1.96 m, respectively. The detected maximum bed elevation change was 0.14 m. So the estimated maximum mobile layer depth will be 0.14 m.

4.4 Predictions By SEDTRANS96

The mean grain size D was 0.40 mm at the SI97a site. This value, the mean ripple height of 1.4 cm, mean ripple wavelength of 12.2 cm, bed slope $\beta = 0$, sediment density ρ_s of 2.65 g/cm³, fluid density ρ of 1.025 g/cm³, together with the wave and current data in Appendix 3, were used to run the sediment transport model SEDTRANS96. The model outputs are again divided into two parts: Appendix 4A lists the predicted bottom boundary layer parameters and Appendix 4B gives the predicted ripple height, ripple wavelength, and the magnitude and direction of predicted sediment transport. Definitions of the parameters in Appendices 4A and 4B are the same as that in section 3.4 for SI96a predictions. Appendix 4B shows that using the Einstein-Brown bedload formula, the peak values of the predicted bedload transport rates during storms were about 0.006 kg m⁻¹ s⁻¹ and were to the N, NW or S, SW. The maximum predicted suspended load transport rates were around 0.003 kg m⁻¹ s⁻¹.

5. DATA FROM SI97B DEPLOYMENT

5.1 General Description of Deployment

Ralph and two S4 wave-current meters were deployed at this site about 2.5 km to the south of Sable Island (Fig. 1) from 9 to 12 April of 1997 on the Hudson 97001 cruise. Ralph was deployed at 43° 54.27'N, 60° 02.69'W in 31 m water depth on the crest of a sand ridge. One S4 meter (S4A) was deployed at 43° 50.60'N, 60° 02.98'W in 45 m water depth and the other (S4B) was deployed at 43° 47.98'N, 60° 02.69'W in 55 m water depth. The geomorphological locations of the two S4 meters were not defined.

One IKU grab sample was collected at the Ralph site and it shows that the bottom sediment was

composed of well sorted (sorting coefficient 0.45ϕ) fine sand with mean grain size of 0.23 mm. Bottom sediment samples were not obtained from the two S4 deployment sites.

5.2 S4 Wave-Current Meter Data

The two S4 wave-current meters were again programmed to burst sample for 5 minute duration every hour at a frequency of 1 Hz. A single OBS sensor was also attached to the deeper water S4 meter (S4B) at 20 cm above the seabed to continuously record 16 s averages of suspended sediment concentration. S4A recorded data from hour 9:24 of 9 April to hour 12:29 of 12 April for 75 data bursts. S4B recorded data from 9:28 of 9 April to 12:31 of 12 April also for 75 data bursts. The 30 s average mean velocity, direction of this mean flow, and water depth are plotted in Fig. 18 for S4A meter and in Fig. 19 for S4B meter. The depth and mean velocity data from both S4 meters demonstrate semi-diurnal tide of roughly 1 m range. The peak mean current speeds reached about 25 cm/s at S4A site with directions predominantly to the N, NW or E-SE. At the deeper site (S4B), the peak mean current speeds were generally smaller (around 15 cm/s) and the mean flow were generally to the N, NW or S, SE. The suspended sediment concentration (in sensor output voltage) measured by the OBS on the S4B meter is plotted in Fig. 20. It shows three small suspension events roughly at 10, 11 and 12 April which approximately corresponded with peaks of the mean current speed.

Sediment trap data for the two S4 meters were not available.

5.3 Ralph Data

5.3.1 Hydrodynamics and Sediment Suspension

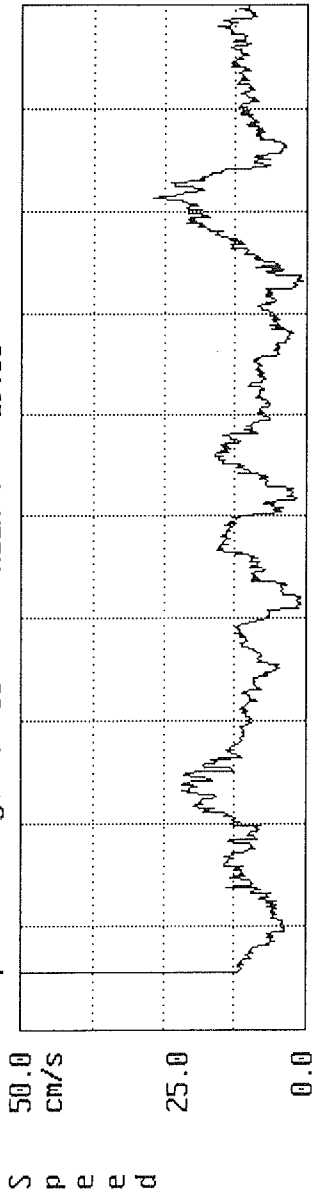
Ralph was deployed on the crest of a sand ridge from 9 to 12 April 1997. The pressure, velocity, and OBS data were logged for a 15 minute duration every hour at a frequency of 5 Hz. Corresponding to each data burst, the four ABS logged data for 1 minute duration at the frequency of 1 Hz every hour. Similarly, the Imagenex profiler and sonar scanned the seabed for 3 minutes at the beginning of each data burst. The DULCE digital camera took a seabed photograph every 20 minutes. Ralph recorded good data from 13:00 GMT on 9 April to 13:00 GMT on 12 April for a total of 73 data bursts.

The Ralph data were processed following the same procedures and programs as described in section 3.3.1. The burst-averaged data of h , u_{50} , C_{dir} , H_s , T_z , W_{dir} and obs1 of the SI97b Ralph deployment are listed in Appendix 5. The time series of h , u_{50} , H_s , T_z , and obs1 are plotted in Fig. 21. Similar to the S4 data in Figs. 18 and 19, the depth data recorded by Ralph show semi-diurnal tidal oscillation of 1 m range (Fig. 21a) and the peak mean current was about 25 cm/s (Fig. 21b). The significant wave height was generally less than

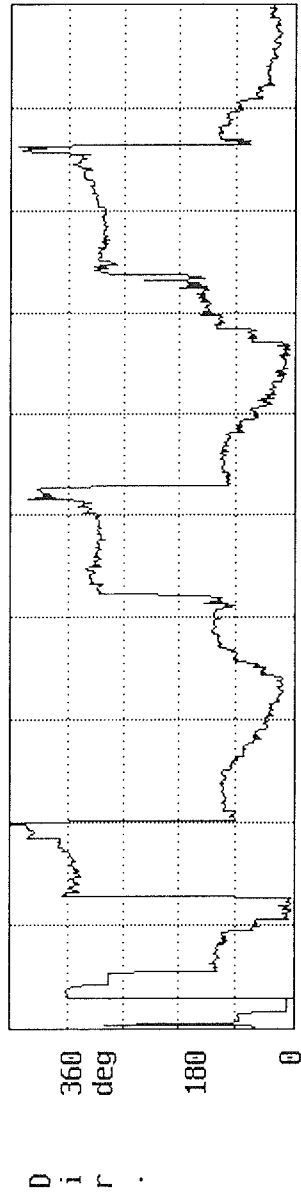
Fig. 18 Time-series plots of (a) mean current and its direction, and (b) mean water depth (lower panel) for the S4A meter of SI97b deployment.



InterOcean Systems, Inc. Model S4 Current Meter #01002196
SABLE ISL97-1 File : S4B97-1.S4B
Xoffset: +0.00 cm/s Yoffset: +0.00 cm/s Mag.Var.: 0 deg
Samples averaged : 30 Mean : 19.08



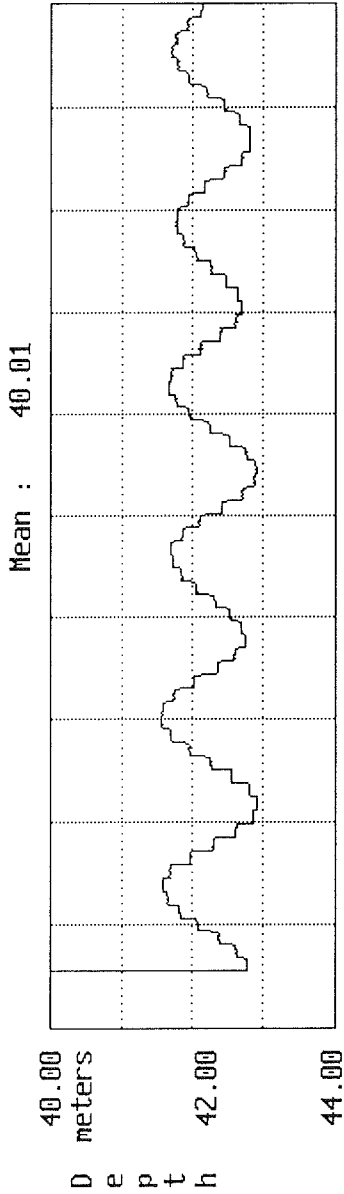
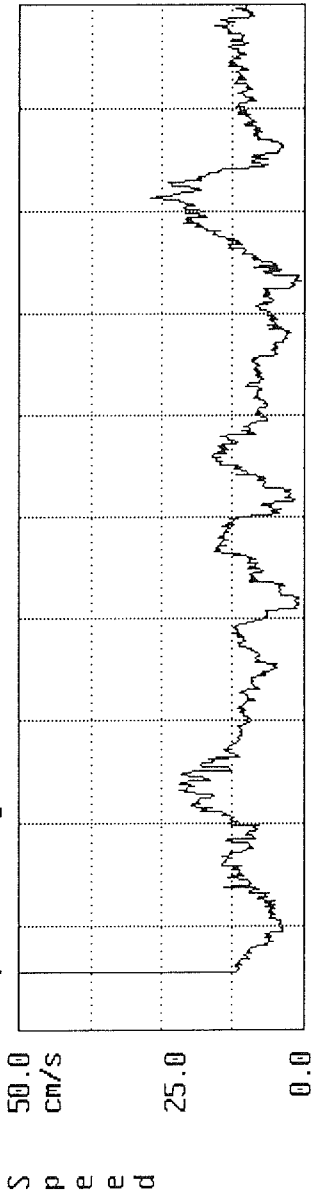
Mean Direction : 11.3



1 4/09/97 09:24:00 Samples 22799 4/12/97 12:28:58



InterOcean Systems, Inc. Model S4 Current Meter #01002196
SABLE ISL97-1 File : S4B97-1.S4B
Xoffset: +0.00 cm/s Yoffset: +0.00 cm/s Mag.Var.: 0 deg
Samples averaged : 30 Mean : 19.08

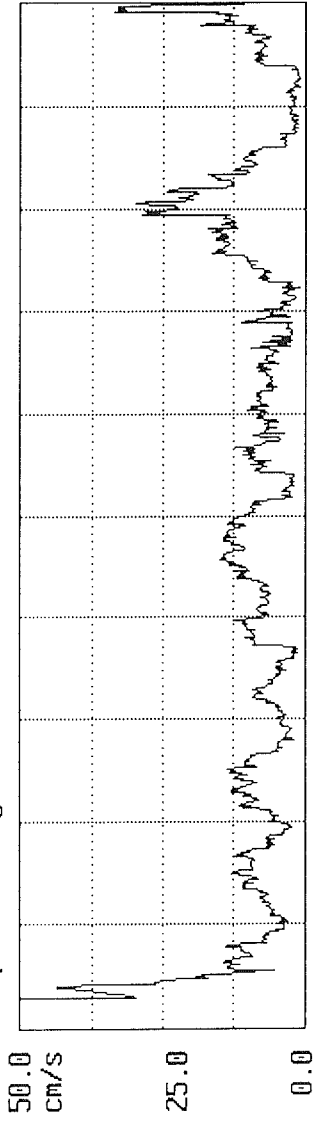


1 4/09/97 09:24:00 Samples 22799 4/12/97 12:28:58

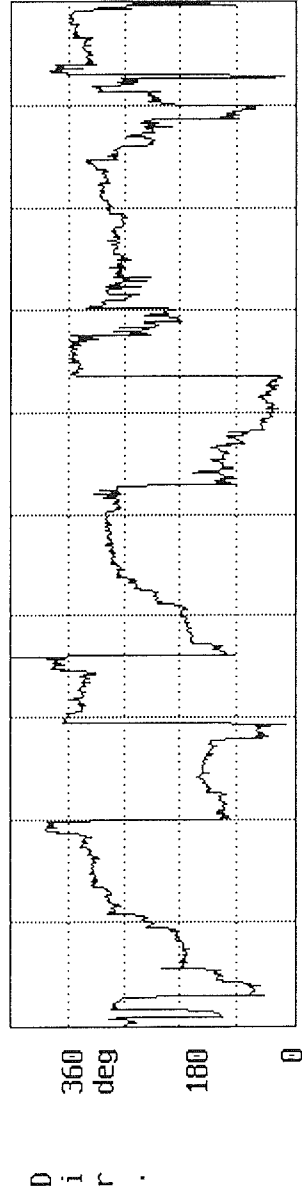
Fig. 19 Time-series plots of (a) mean current and its direction, and (b) mean water depth (lower panel) for the S4B meter of SI97b deployment.



InterOcean Systems, Inc. Model S4 Current Meter #078001668
SABLE ISL97-2 File : SAB97-2.S4B
Xoffset: +0.00 cm/s Yoffset: +0.00 cm/s Mag.Var.: 0 deg
Samples averaged : 30 Mean : 12.35



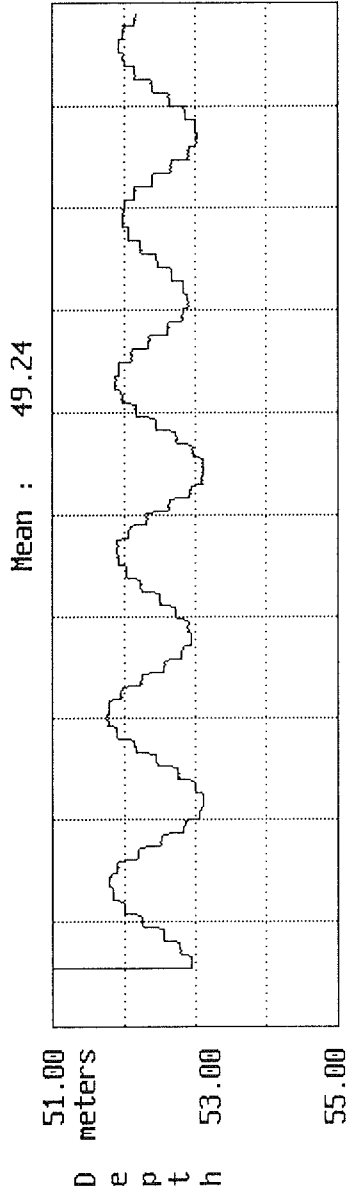
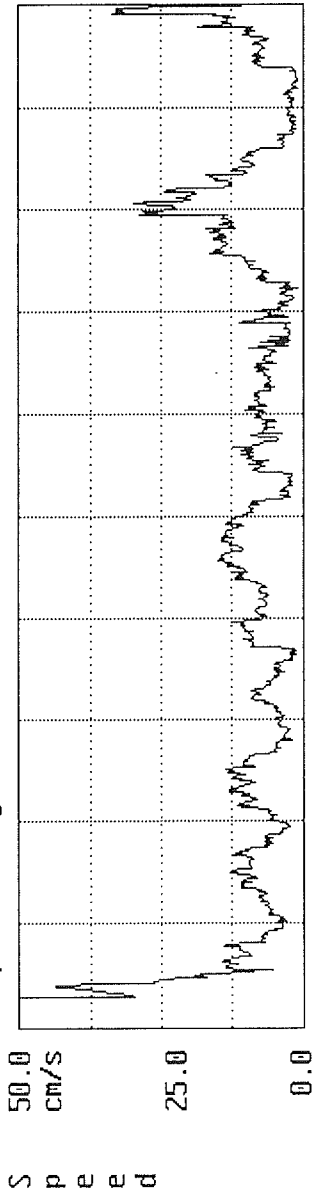
Mean Direction : 286.5



1 4/09/97 09:28:00 Samples 22681 4/12/97 12:31:00

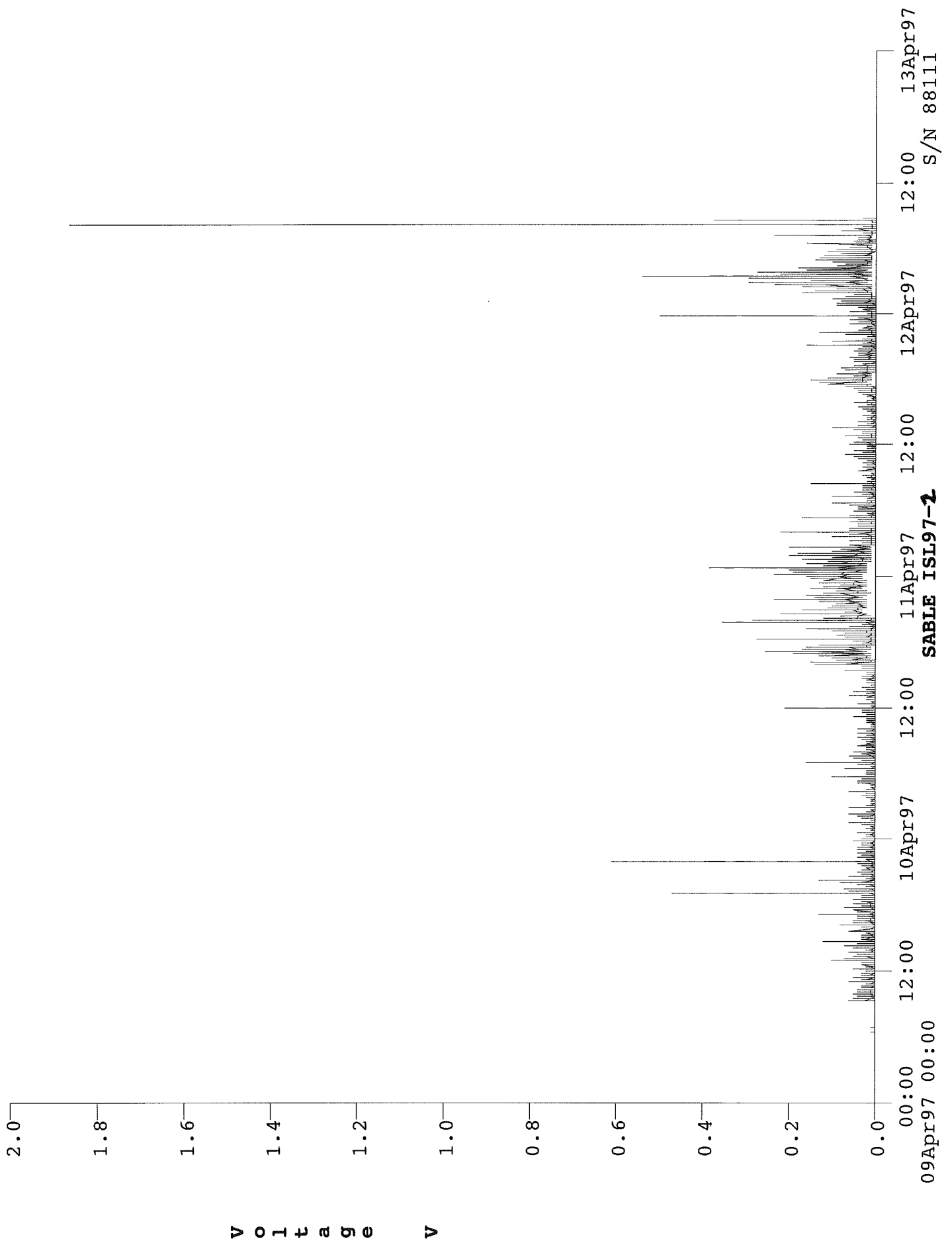


InterOcean Systems, Inc. Model S4 Current Meter #07801668
SABLE ISL97-2 File : SAB97-2.S4B
Xoffset: +0.00 cm/s Yoffset: +0.00 cm/s Mag.Var.: 0 deg
Samples averaged : 30 Mean : 12.35



1 4/09/97 09:28:00 Samples 22681 4/12/97 12:31:00

Fig. 20 Time series plot of the OBS data on the S4B meter of SI97b deployment.



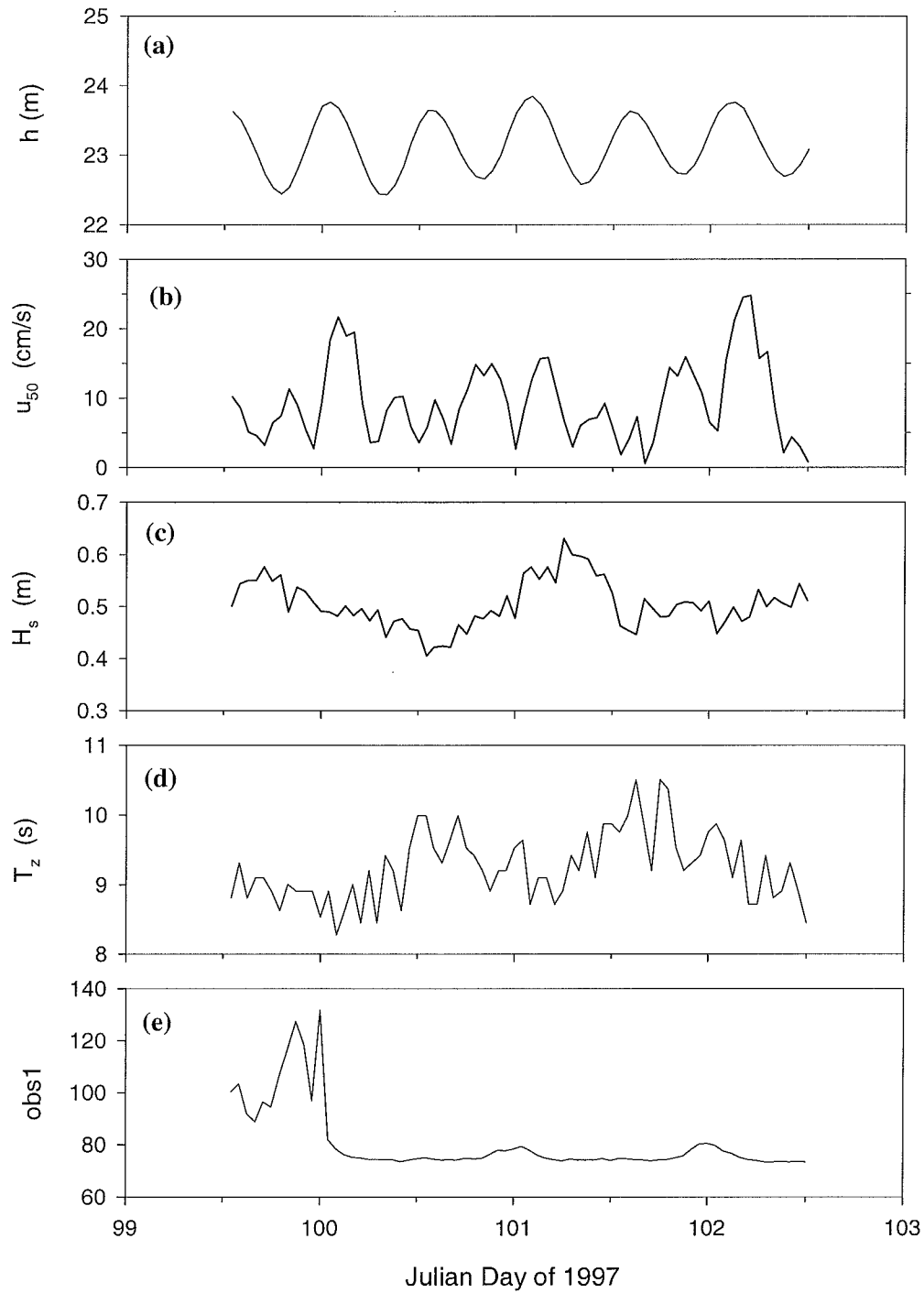


Fig. 21 Time series plots of water depth h , mean velocity u_{50} , significant wave height H_s , mean wave period T_z and obs1 reading for the SI97b Ralph deployment.

0.6 m and wave effects were weak (Fig. 21c). The time series plot of the obs1 data (Fig. 21e) only shows one weak resuspension event at the beginning of the deployment. This probably corresponded to the first peak of the mean current around day 100.

The time series of burst-averaged mean velocity u_{50} , its direction C_{dir} , and the maximum instantaneous velocity u_{max} are plotted in Fig. 22 for the SI97b Ralph data. As shown in Fig. 21, the peaks of the mean current ranged from 10 to 25 cm/s and they were dominantly to the NE and SW. Though there was no storm event in this deployment, Fig. 22d shows that the peaks of the maximum instantaneous velocity u_{max} reached about 50 cm/s, suggesting that wave orbital velocity was still roughly equivalent to the mean current speed.

Ralph sediment trap data were not available.

5.3.2 Bedform and Bed Elevation Change

The time series of the roll and pitch data for the SI97b Ralph deployment is plotted in Fig. 10c. As found in previous data sets, Fig. 10c shows nearly constant roll and pitch of Ralph for the entire duration and indicates stability of the Ralph frame throughout this short deployment. The ABS data of the SI97a Ralph deployment are plotted in Fig. 23. Due to the absence of any storm event in the SI97b deployment, all 4 ABS sensors show steady seabed elevation around 130 cm from the sensors and only small (1-2 cm) variations of seabed elevation were recorded. These were most likely caused by the migration of small ripples on the seabed. Indeed, the digital DULCE seabed photos showed that the seabed was covered by current-dominant or combined wave-current (Li and Amos, 1998) ripples for most time of the deployment duration. These ripples on average were about 10 to 15 cm in wavelength and mobile (in bedload transport) corresponding to the moderate mean current and wave oscillations.

Because of the low-energy condition in the SI97b deployment, the Imagenex sonar images were generally featureless. The profiler images did show small-scale bedforms, but these were too small to determine the bedform heights. Given our current focus on large-scale bedforms and mobile layer depth in storms, these images were not further analysed in this report.

5.4 Predictions By SEDTRANS96

The bottom sediment at the SI97b site was fine sand of a mean grain size $D = 0.23$ mm. This value, the wave and current data given in Appendix 5, and the values of the mean ripple height, ripple wavelength, bed slope, sediment and flow density as defined in section 3.4 were used in SEDTRANS96 to predict the bottom boundary layer and sediment transport parameters for this deployment. Appendix 6A lists the

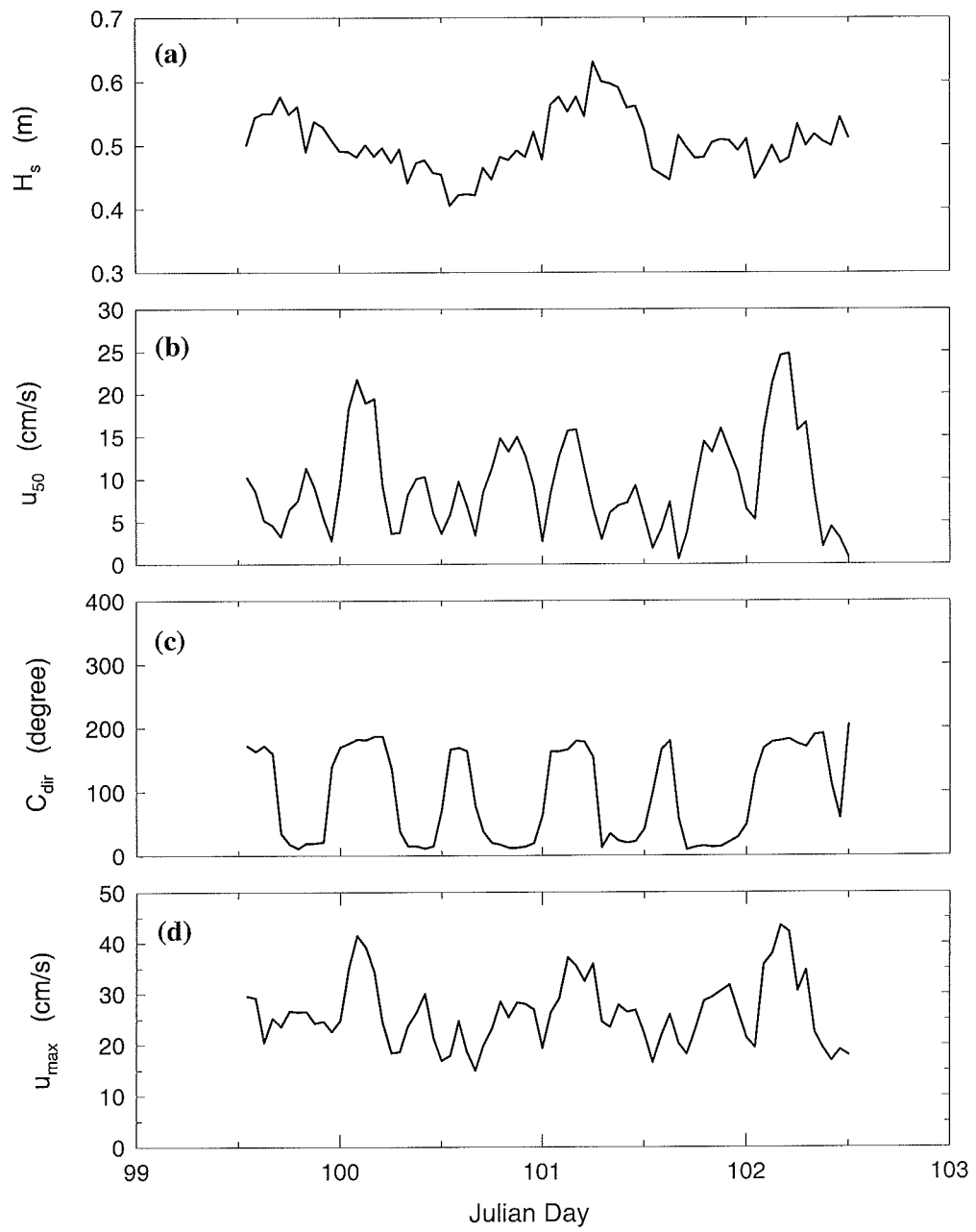


Fig. 22 Time series plots of significant wave height H_s , mean current velocity u_{50} , mean current direction C_{dir} and maximum instantaneous velocity u_{max} (at 50 cm above the seabed) for SI97b Ralph deployment.

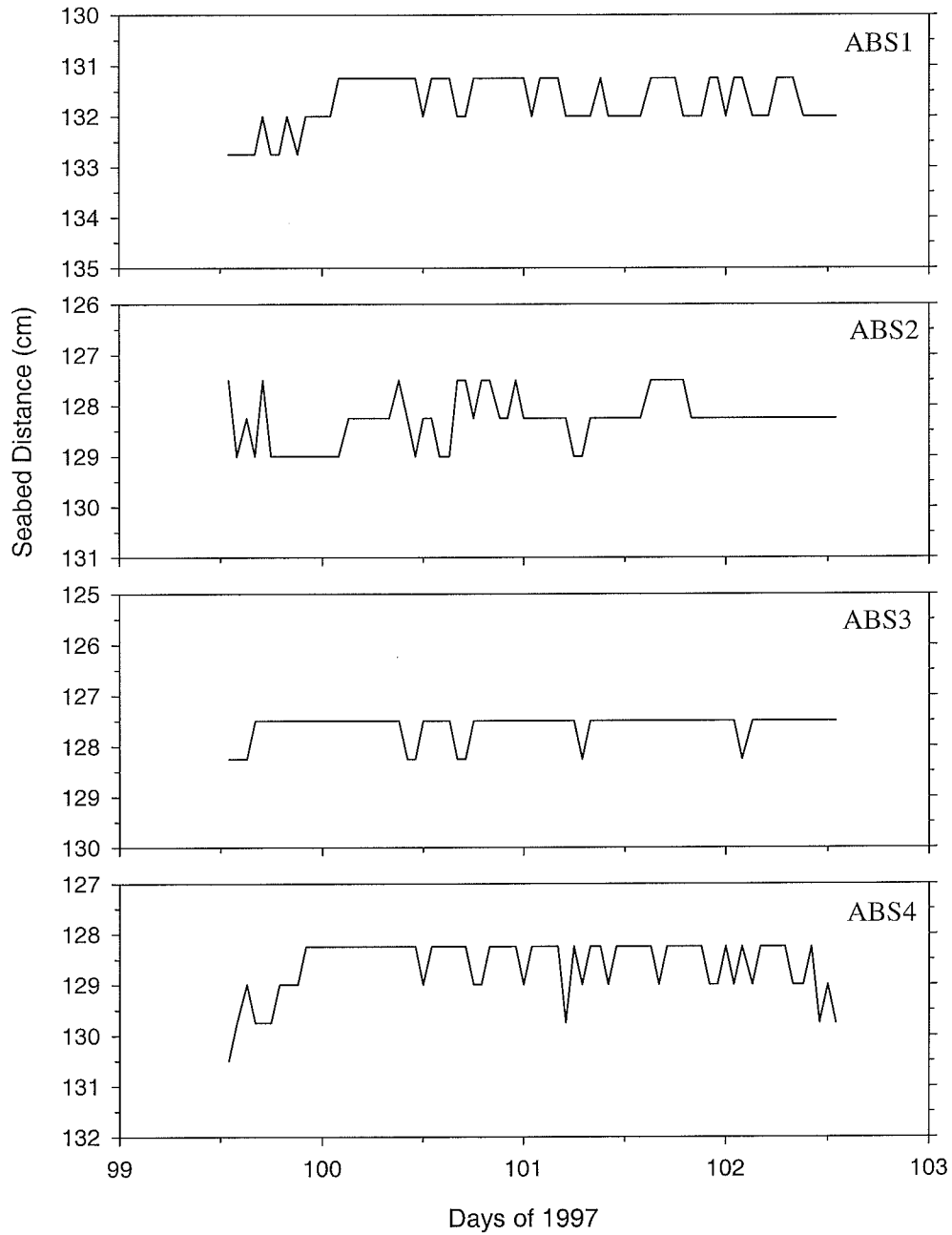


Fig. 23 The seabed elevation changes recorded by ABS sensors in SI97b Ralph deployment.

predicted bottom boundary layer parameters and Appendix 6B gives the predicted ripple height, ripple wavelength, and the magnitude and direction of predicted sediment transport. Appendix 6B shows that due to the low energy conditions in the SI97b deployment, the peak values of the predicted bedload transport rates were only about $0.0003 \text{ kg m}^{-1} \text{ s}^{-1}$ and were dominantly to the N, NE or S, SW. Sand suspension only occurred once toward the end of the deployment. Because of the finer grain size of the bottom sediment, the maximum predicted suspended load transport rates reached $0.008 \text{ kg m}^{-1} \text{ s}^{-1}$, which was more than 1 order of magnitude higher than the peak bedload transport rate.

6. DATA FROM SI97C DEPLOYMENT

6.1 General Description of Deployment

At the end of the Hudson 97001cruise, Ralph and the two S4 wave-current meters were redeployed (12 April, 1997) at a site about 34 km to the west-southwest of Sable Island (Fig. 1). Ralph was deployed at $43^{\circ} 56.03'N$, $60^{\circ} 37.77'W$ in 42 m water depth in a trough of sand ridges. The first S4 meter (S4A) was deployed at $43^{\circ} 56.56'N$, $60^{\circ} 35.01'W$ in 28 m water depth on the upper lee flank of the sand ridge, and the second S4 meter (S4B) was deployed at $43^{\circ} 56.28'N$, $60^{\circ} 35.58'W$ in 31 m water depth on the brink of the lee flank. All three instruments were recovered on 29 May 1997.

No bottom sediment samples were collected at the Ralph and S4 sites of this deployment. Sediment trap samples on Ralph, as listed in Table 8, show that the bottom sediment was probably composed of moderately sorted fine sand. The first layer of suspended sediment (from 0 - 4 cm height of the sediment trap sample) had an average mean grain size of 0.23 mm and an average sorting coefficient of 0.72ϕ . These were taken as the characteristics of the bottom sediment at the SI97c Ralph deployment site.

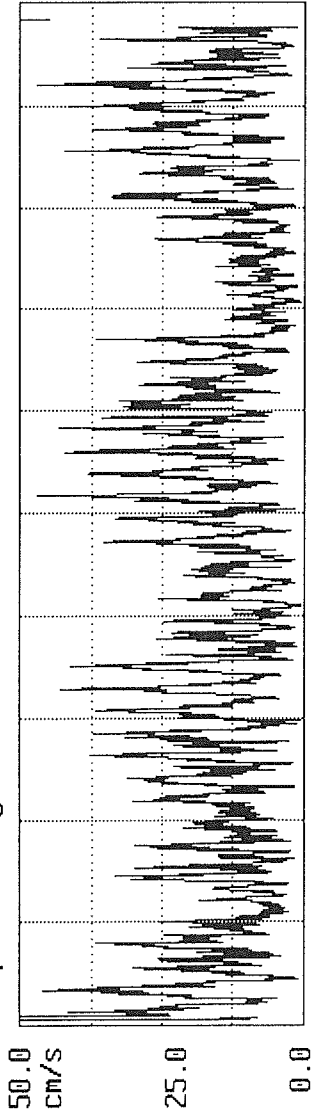
6.2 S4 Wave-Current Meter Data

The two S4 wave-current meters were programmed to burst sample for 3 minute durations every 2 hours at a frequency of 1 Hz. A single OBS sensor was attached to the deeper water S4 meter (S4B) at 20 cm above the seabed to continuously record 16-s average of suspended sediment concentration. S4A recorded data from hour 13:19 of 12 April to hour 15:21 of 29 May 1997 for 566 data bursts. S4B recorded data from 13:26 of 9 April to 13:28 of 29 May 1997 for 564 data bursts. The 30 s average mean velocity, direction of this mean flow, and water depth are plotted in Fig. 24 for the S4A meter and in Fig. 25 for the S4B meter. The depth data from both S4 meters demonstrate the occurrence of three neap and three spring tides. The peak mean current speed reached about 45 cm/s at the S4A meter and the directions were dominantly to the

Fig. 24 Time-series plots of (a) mean current and its direction, and (b) mean water depth (lower panel) for the S4A meter of SI97c deployment.

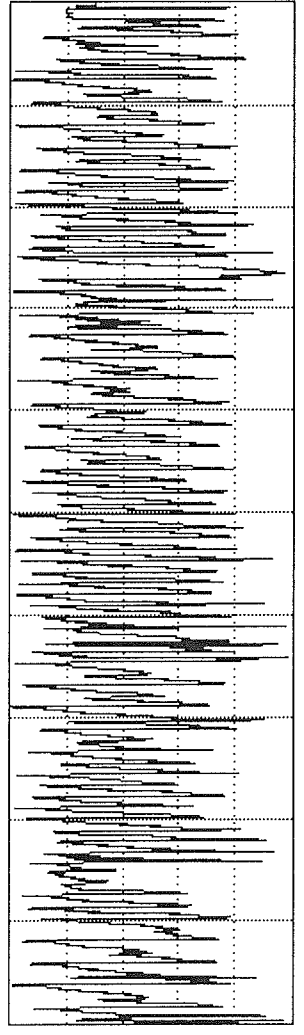


InterOcean Systems, Inc. Model S4 Current Meter #01002196
SAB97-4 File : SAB97-4.S4B
Xoffset: +0.00 cm/s Yoffset: +0.00 cm/s Mag.Var.: 0 deg
Samples averaged : 30 Mean : 17.82



S
p
e
e
d

Mean Direction : 344.3

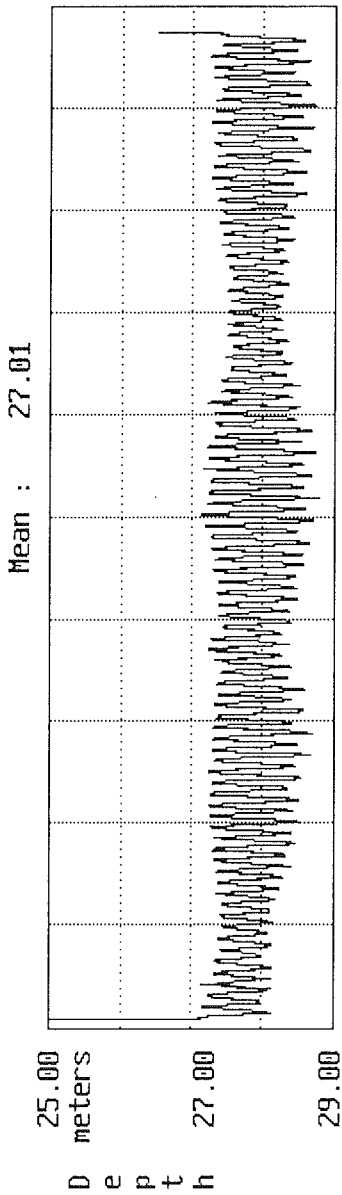
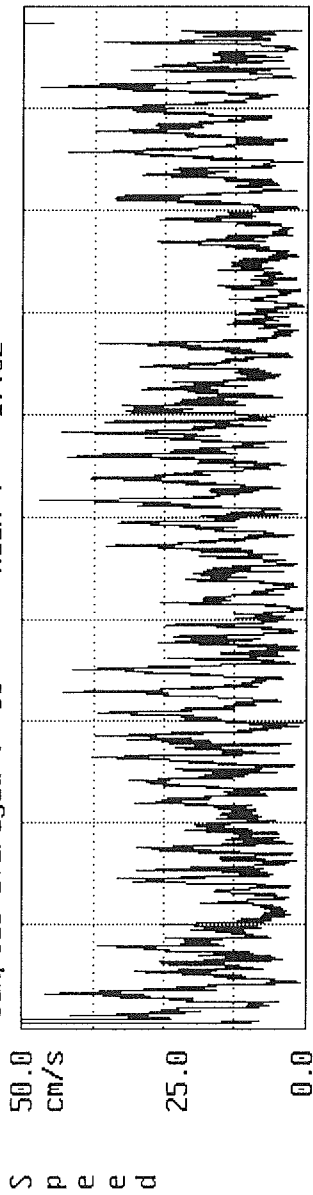


D
i
r
e
c
t
i
o
n

1 4/12/97 13:19:00 Samples 101879 5/29/97 15:21:58



InterOcean Systems, Inc. Model S4 Current Meter #01002196
SAB97-4 File : SAB97-4.S4B
Xoffset: +0.00 cm/s Yoffset: +0.00 cm/s Mag.Var.: 0 deg
Samples averaged : 30 Mean : 17.82



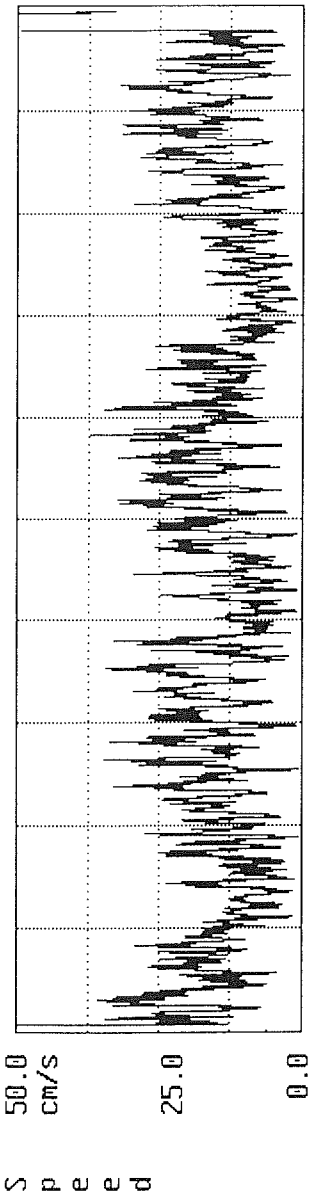
1 4/12/97 13:19:00 Samples 101879 5/29/97 15:21:58

Fig. 25 Time-series plots of (a) mean current and its direction, and (b) mean water depth (lower panel) for the S4B meter of SI97c deployment.

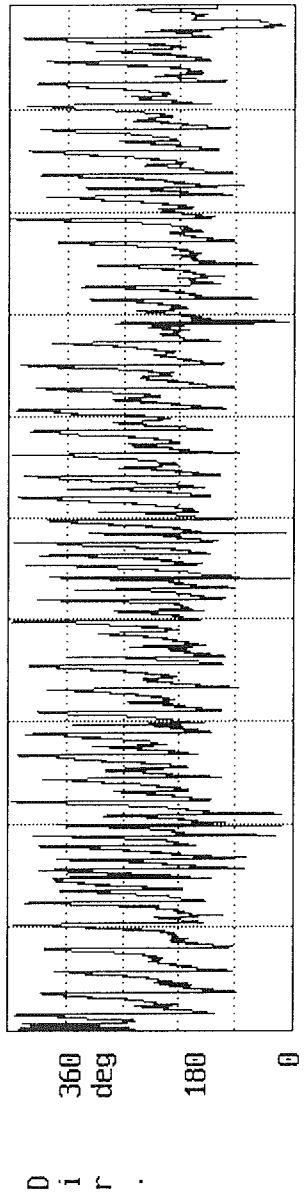


InterOcean Systems, Inc. Model S4 Current Meter #07801668
SAB97-3 File : SAB97-3.S4B

Xoffset: +0.00 cm/s Yoffset: +0.00 cm/s Mag.Var.: 0 deg
Samples averaged : 30 Mean : 16.84



Mean Direction : 185.3



1 4/12/97 13:26:00

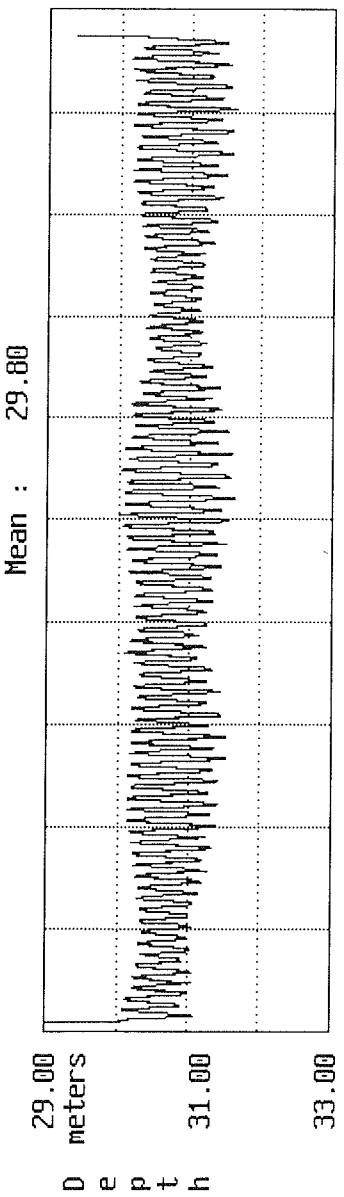
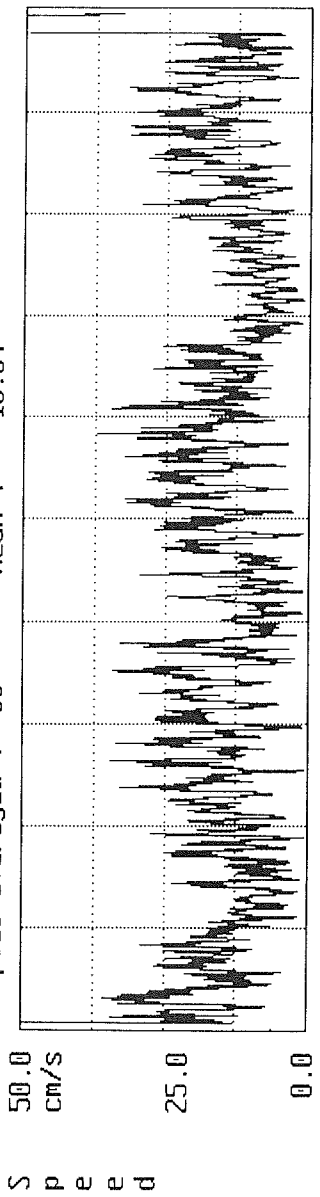
Samples 101699
5/29/97 13:28:58

A



InterOcean Systems, Inc. Model S4 Current Meter #078001668
SAB97-3 File : SAB97-3.S4B

Xoffset: +0.00 cm/s Yoffset: +0.00 cm/s Mag.Var.: 0 deg
Samples averaged : 30 Mean : 16.84



1 4/12/97 13:26:00 Samples 101699 5/29/97 13:28:58

B

N and NE. The peak mean current speeds at S4B were slightly smaller, reaching about 35 cm/s and the directions were generally to the NE, SW. The OBS data were not available.

Sediment traps were again attached to the two S4 meters. The sediment samples recovered from these traps have not been analysed yet.

6.3 Ralph Data

6.3.1 Hydrodynamics and Sediment Suspension

Ralph was deployed in the trough of sand ridges from 12 April to May 29 of 1997. The pressure, velocity, and OBS data were again logged for a 15 minute duration every hour at a frequency of 5 Hz. Corresponding to each data burst, the four ABS logged data for 1 minute duration at 1 Hz every hour. Similarly, the Imagenex profiler and sonar scanned the seabed for 3 minutes at the beginning of each data burst. The DULCE digital camera took a seabed photograph every 20 minutes. Ralph recorded good data from 20GMT on 12 April to 20GMT on 27 April 1997 for a total of 361 data bursts.

The Ralph data were processed following the same procedures and programs as described in section 3.3.1. The burst-averaged data of h , u_{50} , C_{dir} , H_s , T_z , W_{dir} and obs2 of the SI97c Ralph deployment are listed in Appendix 7. The time series of h , u_{50} , H_s , T_z , and obs2 are plotted in Fig. 26. Similar to the S4 data in Figs. 24 and 25, the depth data recorded by Ralph show semi-diurnal tidal oscillation of 1 m range (Fig. 26a). The maximum peak mean current was about 35 cm/s (Fig. 26b), comparable to that of the S4 current meter data. Three storm events occurred (Figs. 26c and 26d). The significant wave height ranged from 1 to 2 m and the wave periods were from 10 to 12 s during these storms. The time series plot of the obs2 data (Fig. 26e; obs1 malfunctioned) shows correlations with the peaks of u_{50} and H_s only to some degree and the response to the passage of the first storm was very weak.

The time series of burst-averaged mean velocity u_{50} , its direction C_{dir} , and the maximum instantaneous velocity u_{max} are plotted in Fig. 27 for SI97c Ralph data. As shown in Fig. 26, the peaks of the mean current ranged from 10 to 35 cm/s and they were dominantly to the N, NE and S, SW. The mean velocity seemed to have been suppressed during the storms (e.g., on days 104 - 105 and 110). Fig. 27d shows that the peaks of the maximum instantaneous velocity u_{max} reached about 80 cm/s during the storms. These are 2-3 times higher than the mean current. The durations, peak values of u_{max} and their directions for the storms in the SI97a data set are listed below:

storm 1, D104H04-D105H06, $u_{max} = 81$ cm/s, direction is to 206°

storm 2, D109H10-D111H06, $u_{max} = 80$ cm/s, direction is to 24°

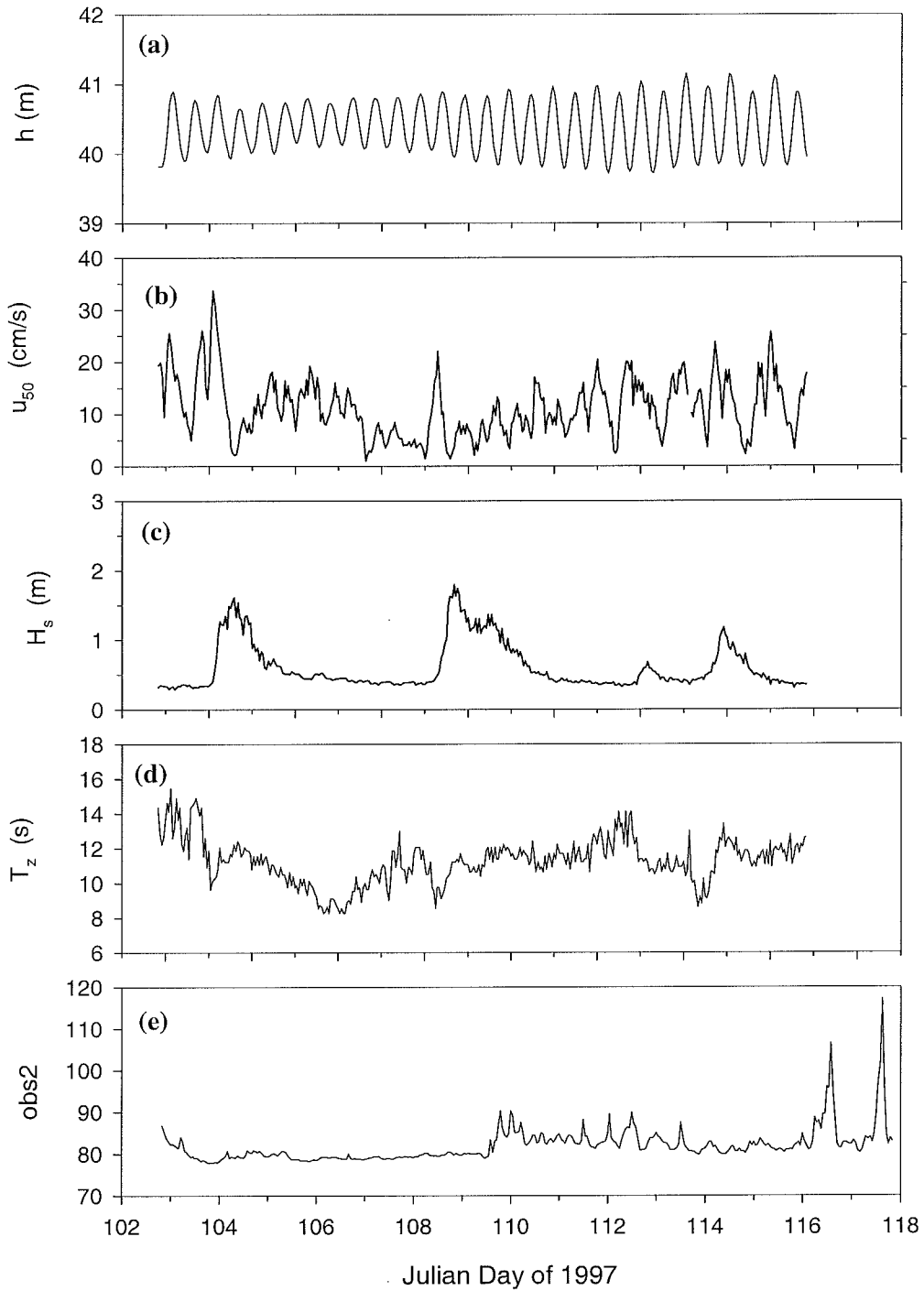


Fig. 26 Time series plots of water depth h , mean velocity u_{50} , significant wave height H_s , mean wave period T_z and obs2 reading for the SI97c Ralph deployment.

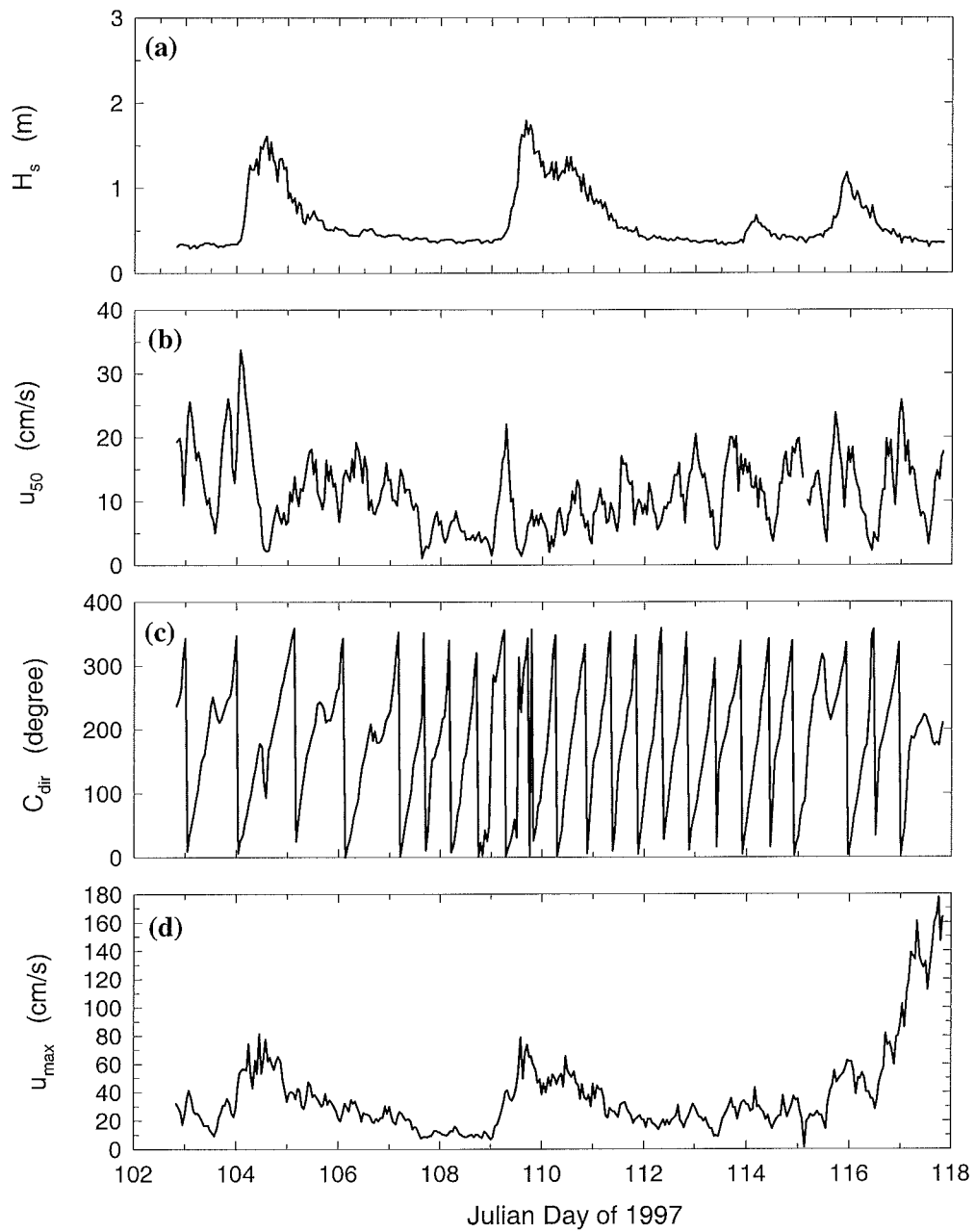


Fig. 27 Time series plots of significant wave height H_s , mean current velocity u_{50} , mean current direction C_{dir} and maximum instantaneous velocity u_{max} (at 50 cm above the seabed) for SI97c Ralph deployment.

storm 3, D115H19-D116H04, $u_{\max} = 63$ cm/s, direction is to 38°

As found in SI96a and SI97a deployments, the comparison of Figs. 24, 25 and 27 suggests that the mean current speed in the trough (measured by Ralph) again did not differ significantly from that at the upper lee flank of the sand ridge for the SI97c deployment (35 to 45 cm/s) and that they were generally to the N, NE or S, SW.

The Ralph sediment traps were at the heights: 0.30 m, 0.48 m, 0.60 m and 1.00 m above the bottom. Only the suspended sediment collected by the lowest trap has been processed. The total length of the sediment trap sample was 18 cm, indicating that significant resuspension had occurred during this deployment. The mean grain size D (in mm) and sorting coefficient (in ϕ) at different heights of the sediment trap sample are listed in Table 8. The height again is upward from the bottom of the sediment trap. Three layers of suspended sediment can be defined corresponding to the three storms shown in Fig. 26c: the first layer from 0 to 4 cm, the second layer from 5 to 12 cm and the third layer from 14 cm to 18 cm. The first layer demonstrates an upward-fining trend in sediment mean grain size. The second layer shows a complete resuspension cycle due to a storm passage: The mean grain size of suspended sediment was initially finer

Table 8 Mean grain size D and sorting coefficient of SI97c Ralph sediment trap sample.

Sediment trap sample at 0.3 m height; total length 18 cm.		
Height (cm)	D (mm)	Sorting (ϕ)
0.5	0.24	0.47
2.5	0.22	0.69
3.5	0.22	0.99
5.5	0.22	0.98
7.5	0.24	0.66
8.5	0.26	0.81
9.5	0.24	0.82
11.5	0.25	0.63
14.5	0.23	0.78
17.5	0.25	0.68
average:	0.24	0.75

corresponding with the start of the storm (0.22 mm to 0.24 mm at 5.5 and 7.5 cm heights), reached the maximum roughly at the middle of the layer (0.26 mm at 8.5 cm height) corresponding to the peak of the storm, and then decreased again as the storm waned (0.24 mm at 9.5 cm height). During the passage of the third storm, the sediment trap was completely filled up. Thus the last layer of the sediment trap sample recorded only the build up (mean grain size of 0.23 mm at 14.5 cm height) and the peak of the storm (0.25 mm at 17.5 cm height).

6.3.2 Bedform and Bed Elevation Change

The time series of the roll and pitch data of the SI97c Ralph deployment is plotted in Fig. 10d. Similar to previous data sets, Fig. 10d shows steady roll and pitch of Ralph with only a drift of less than half a degree for the entire duration. This indicates a stable Ralph frame in this deployment. The ABS data of the SI97c Ralph deployment, plotted in Fig. 28, show significant bed elevation changes corresponding to the passage of several storms. At the early stage of the deployment (days 103 to 104), the seabed was covered by small active ripples of 2-3 cm height. As the first storm approached, data from ABS1, ABS2 and ABS3 show that the seabed was first raised about 14 cm, dropped slightly after the peak of the storm and stayed roughly constant after that. ABS4 data show that seabed was raised only about 10 cm in the first storm. These changes of 10 to 14 cm probably were caused by the migration of large-scale bedforms of 10-15 cm height. Seabed responses to the second storm (around day 109.5) were complex. The bed elevation under ABS1 and ABS4 first dropped about 10 cm and 4 cm respectively. The seabed then rose about 12 cm and stayed roughly steady after that. In contrast, the data from ABS2 and ABS3 show that seabed first dropped about 10 cm and then quickly recovered from drop before another 10 cm fall which was followed by approximately steady seabed elevations. The seabed responses to the third storm were variable with ABS2 and ABS3 showing a 5 cm rise and ABS 1 showing a drop of about 8 cm. The seabed generally experienced secondary bed elevation changes of about 4 cm and 2 cm during the fair weather periods between storms (days 105-109 and days 111 - 115).

The Imagenex profiler and sonar both worked well in this deployment. Example profiler and sonar images are shown in Fig. 29. Again, the height of the profiler image in Fig. 29a is about 130 cm and the diameter of the sonar image in Fig. 29b is 40 m with the top of the image pointing about 3° from magnetic North. Fig. 29a shows a maximum bedform height of 18 cm, while Fig. 29b depicts dominant bedforms of about 1m wavelength oriented 120° from the magnetic North. Bed elevation changes and bedform parameters derived from the Imagenex profiler and sonar data are listed in Table 9 for each of the 3 storms recorded by Ralph in SI97a deployment. The peak significant wave height in storm 1 was 1.6 m. Large wave ripples developed with average wavelength of 0.88 m. The maximum bedform height was measured at 0.22 m, though the seabed elevation over bedform crests (E_c) did not change much. Thus the estimated maximum mobile layer depth is about 0.11 m. The peak significant wave height in Storm 2 was slightly higher, reaching 1.8 m (Table 9). The largest bedforms again developed during the decay of the storm (D109H20, H_s of 1.4 m): maximum ripple height reached 0.19 m and wavelength reached 1.02 m. The maximum bed elevation change was only 3 cm. So the estimated maximum mobile layer depth is about 0.1 m. The third storm had a significant wave height of 1.2 m. The maximum measured bedform height was 0.11 m and the

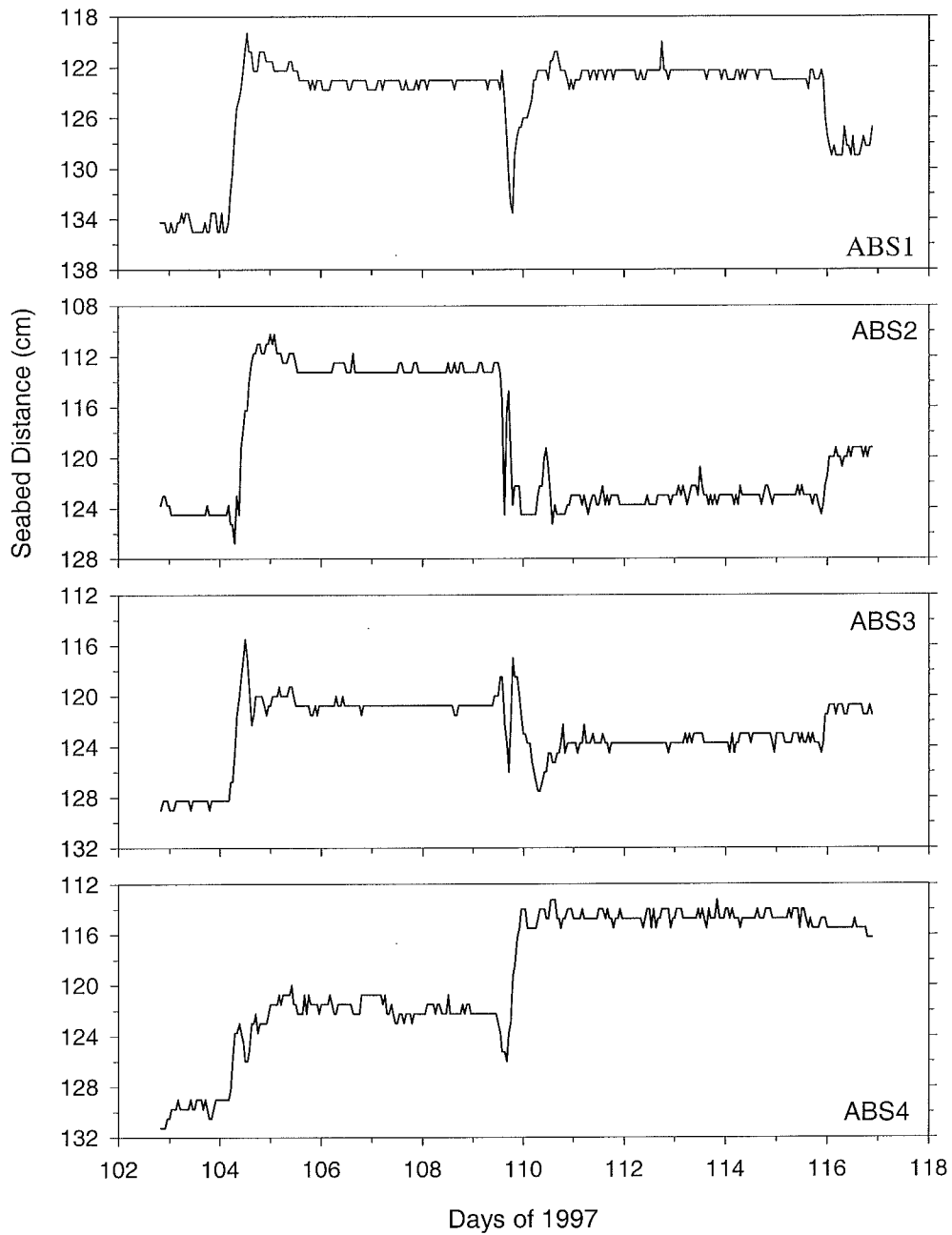


Fig. 28 The seabed elevation changes recorded by ABS sensors in SI97c Ralph deployment.

Fig. 29 Examples of the Imagenex (a) profiler and (b) sonar images collected in SI97c Ralph deployment.

19-APR-1997 16:04:14 IP109A16.81B

A

19-APR-1997 16:01:50 II109A16.81B

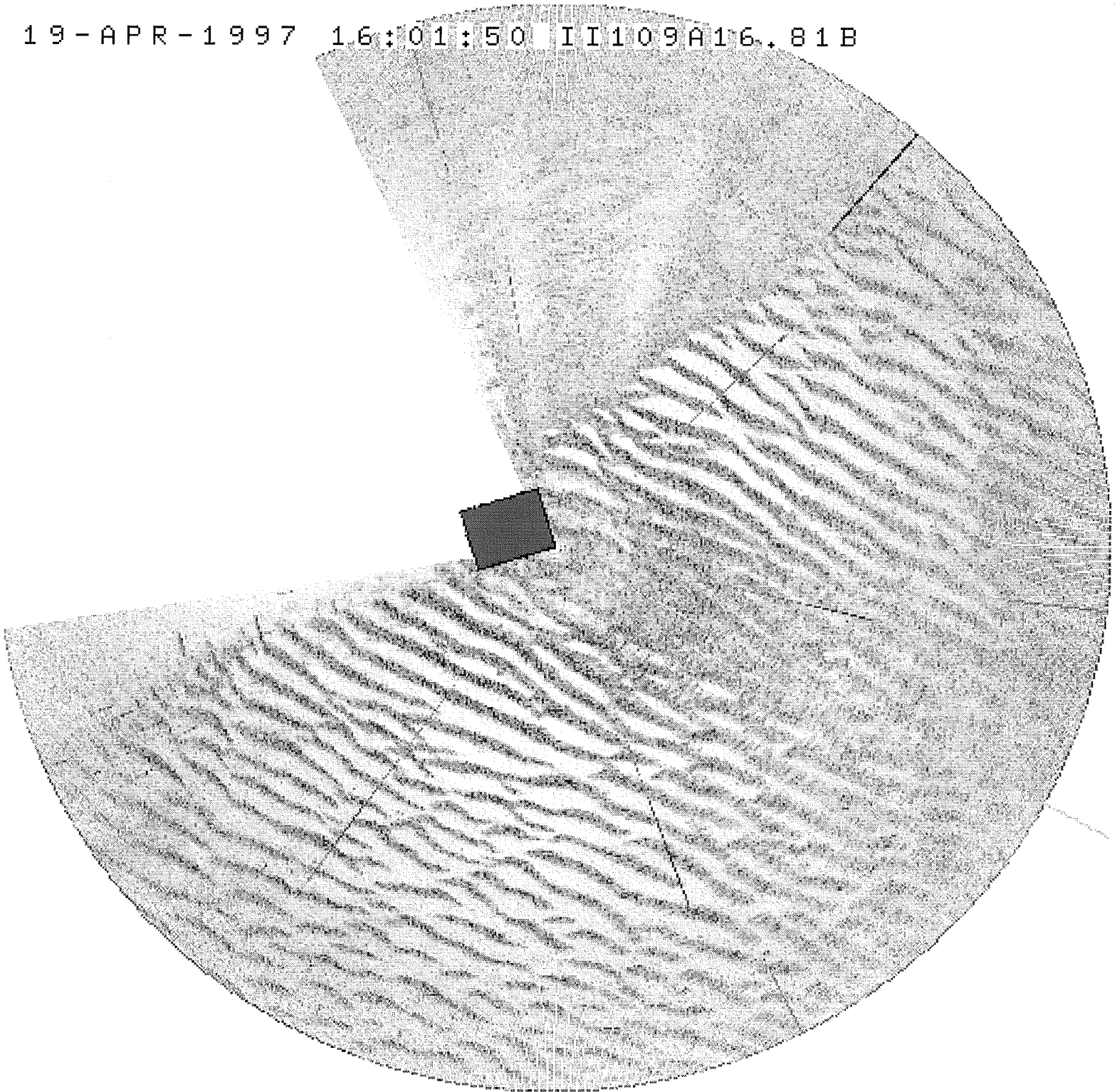


Table 9 Estimated bed-elevation changes and bedform parameters in the storms of SI97c Ralph deployment.

DayHour	H_s (m)	η_{\max} (m)	λ (m)	E (m)	E_c (m)
storm 1					
D104H12	1.5	0.20	0.74		1.05
D104H14	1.6	0.21	0.74		1.04
D104H17	1.4	0.22	0.88		1.04
storm 2					
D109H14	1.6	0.17	0.97	1.13	1.07
D109H16	1.8	0.18	0.88	1.12	1.06
D109H19	1.7	0.17	1.00	1.15	1.09
D109H20	1.4	0.19	1.02	1.15	1.09
storm 3					
D115H20	1.0	0.11	0.97	1.07	1.12
D115H22	1.2	0.10	0.94	1.07	1.12
D116H00	1.0	0.10	0.94	1.08	1.12

maximum average wavelength was 0.97 m. Bed elevation did not show any change. The estimated maximum mobile layer depth will be 0.06 m.

6.4 Predictions By SEDTRANS96

The mean grain size D was 0.23 mm at the SI97c site. This value, the parameters of mean ripple height, ripple wavelength, bed slope, sediment and flow densities as defined in section 3.4 and the wave and current data listed in Appendix 7 were used to run the sediment transport model SEDTRANS96. The model outputs are again divided into two parts: Appendix 8A lists the predicted bottom boundary layer parameters and Appendix 8B gives the predicted ripple height, ripple wavelength, and the magnitude and direction of predicted sediment transport. Definitions of the parameters in Appendices 8A and 8B are the same as that in section 3.4 for SI96a predictions. Appendix 8B shows that using the Einstein-Brown bedload formula, the peak values of the predicted bedload transport rates during storms were about $0.0007 \text{ kg m}^{-1} \text{ s}^{-1}$ and were generally to the N, NE or S, SW. The maximum predicted suspended load transport rates, however, reached as high as $0.02 \text{ kg m}^{-1} \text{ s}^{-1}$ for the fine sand sediment at this site. This is almost two orders of magnitude higher than the predicted bedload transport rates.

7. PREDICTIONS OF MOBILE LAYER DEPTH DURING STORMS

A total of 9 storms were recorded in the four Ralph/S4 deployments in 1996 and 1997. Seabed elevation changes, maximum bedform heights and wavelengths were measured for these storms. These data can be used for a preliminary evaluation of mobile layer depth as function of storm intensity which is of

interest to Mobil as well as to the design and safe operation of other offshore installations. Table 10 lists the estimated maximum mobile layer depth as well as the hydrodynamics parameters of the 9 storms recorded in the four deployments. Water depth h is in m, mean grain size D is in mm, mean velocity u_{50} and nearbed wave orbital velocity u_b are both in cm/s, significant wave height H_s is in m, mobile layer depth d_M is in cm, M is the dimensionless wave mobility number defined as $\rho u_b^2 / (\rho_s - \rho) g D$, $\tau_{cws} = \rho u_{*cws}^2$ is the skin-friction combined bed shear stress in N/m^2 , $\theta_{cws} = \tau_{cws} / (\rho_s - \rho) g D$ is the dimensionless Shields parameter, and d_M/D is the normalized mobile layer depth.

Table 10 Summary of hydrodynamic parameters and estimated maximum mobile layer depths for the storms recorded in all the 1996/97 deployments.

Storm	h	D	u_{50}	H_s	u_b	M	τ_{cws}	θ_{cws}	d_M	d_M/D
D333H04	19.8	0.39	20.0	1.93	44.8	33.1	1.51	0.240	14	359
D029H04	30.2	0.40	7.8	1.54	27.7	12.3	0.56	0.087	11	275
D032H10	30.8	0.40	1.2	2.89	60.0	57.9	1.73	0.272	17	425
D037H10	30.7	0.40	37.9	1.70	34.0	18.6	1.40	0.219	8	200
D041H06	30.6	0.40	32.5	1.80	37.4	22.5	1.38	0.217	8	200
D047H00	31.1	0.40	25.6	1.95	37.3	22.4	1.15	0.181	14	350
D104H14	40.3	0.23	2.2	1.61	25.2	17.8	0.34	0.093	11	478
D109H16	40.0	0.23	3.9	1.79	25.4	18.1	0.36	0.099	10	435
D115H22	40.3	0.23	14.3	1.18	20.3	11.5	0.31	0.086	6	261
C_{r1}				0.83	0.78	0.79	0.51	0.51		
C_{r2}				0.40	0.15	0.37	-0.23	-0.14		

Table 10 shows that H_s of the recorded storms ranged from 1.2 m to 2.9 m in water depths from 20 m to 40 m. The measured mobile layer depth ranged from 6 cm to 14 cm over fine sand ($D = 0.23$ mm) and medium sand ($D = 0.39$ and 0.40 mm) bottom sediments. As an initial step, two correlation coefficients were calculated and listed in the last two rows in Table 10: C_{r1} is the correlation coefficient between various hydrodynamic parameters and the mobile layer depth d_M , and C_{r2} is the correlation coefficient between the hydrodynamic parameters and the normalized mobile layer depth d_M/D . Firstly, the significant wave height H_s gives the highest correlation coefficient with d_M (at 0.83). The values of C_{r1} for the nearbed wave orbital velocity u_b and wave mobility number M are slightly lower, respectively at 0.78 and 0.79. Since H_s only represents wave height, and u_b and M both include the effect of water depth, this seems to suggest that water depth is not critical in affecting the mobile layer depth during storms (at least for the storm conditions in our deployments). Secondly, the skin-friction combined shear stress τ_{cws} and Shields parameter θ_{cws} both incorporate the effect of wave-current interaction under combined flow conditions. Their correlation coefficients with d_M are substantially lower than that of H_s , u_b , or M which only represent the wave energy level. This may indicate that due to the predominance of waves over steady currents during storms, effects

of wave-current interaction are not relevant to the estimation of mobile layer depth. C_{r2} values in the last row of Table 10 are the correlation coefficients between various hydrodynamic parameters and d_M/D , the mobile layer depth normalized by sediment grain size. These values are much lower than those with just the mobile layer depth and seem to suggest that bottom sediment grain size is also not significant in affecting the mobile layer depth during storms.

The significant wave height and the mobile layer depth data given in Table 10 are plotted in Fig. 30. Though there is some scatter in the data, Fig. 30 clearly shows a trend of increasing mobile layer depth with the increase of H_s . The least-square linear regression of the data in Fig. 30 gave the following empirical relationship:

$$d_M = 0.061H_s \quad (r^2 = 0.64) \quad (1)$$

where H_s and d_M both are in metres. The peak significant wave height during typical winter storms on SIB can reach about 8 m. For this, equation 1 predicts a maximum mobile layer depth of about 0.5 m which is in general agreement with the estimates from IKU grab core peels (Hudson Cruise 96-029 report and Amos, et al., 1999) and cone penetrometer data (Forsythe, 1998). Nevertheless equation 1 is only based on limited data and needs to be calibrated with more data from stronger storms over wider range of water depths.

8. SUMMARY

In this GSCA-Mobil joint project, the upgraded Ralph platform and S4 wave-current meters were deployed at four locations on Sable Island Bank in 1996/97 to study the stability of large scale bedforms, seabed scouring and mobile layer depth during storms. The four deployments are respectively SI96a from 26 November to 6 December of 1996, SI97a from 28 January to 24 March of 1997, SI97b from 9 April to 12 April of 1997, and SI97c from 12 April to 29 May of 1997. The water depths of these deployments ranged from 20 m to as deep as 55 m, and the bottom sediments were mostly fine sand (mean grain size of 0.23 mm) and medium sand (mean grain size of 0.39 - 0.40 mm). A total of 9 storms were recorded in these deployments. The peak significant wave height ranged from 1.2 to 2.9 m and the mean wave periods were generally from 9 s to 13 s during these storms.

The mean current data from these deployments show that depending on the relative direction between tidal and wind-driven currents, storms can significantly enhance or suppress the mean flow velocity on SIB. When the wind-driven current is roughly parallel with the tidal current, the mean current speed u_{50} can be increased from 25 - 30 cm/s during non-storm periods to 40 - 50 cm/s during storms. In contrast to the mean

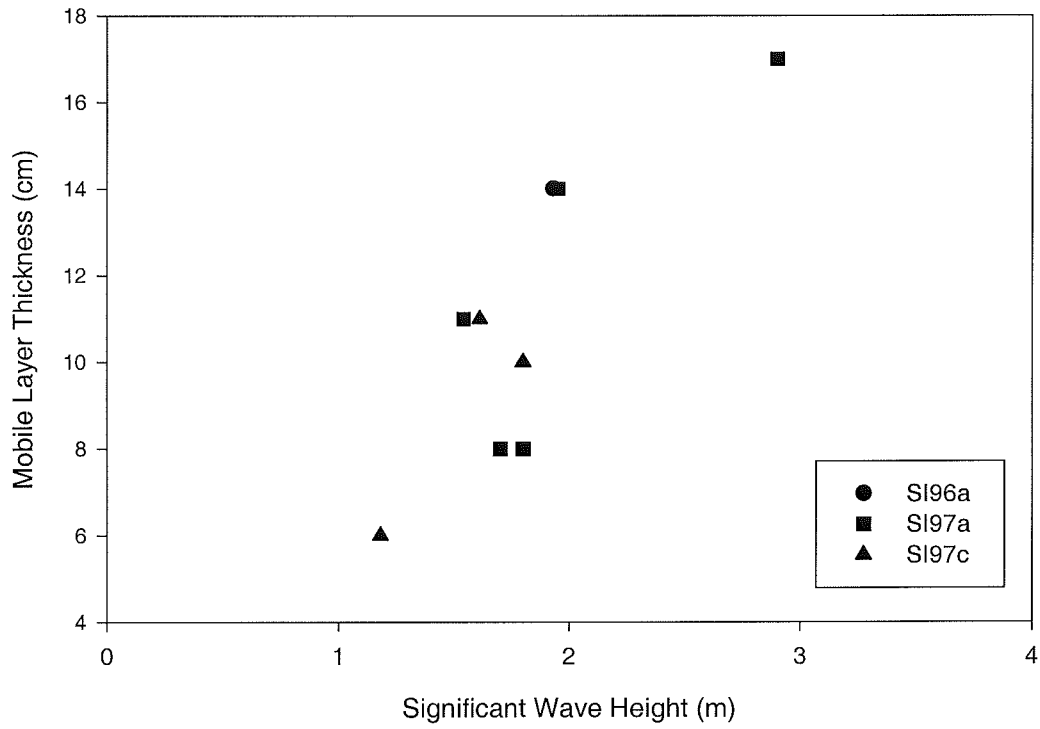


Fig. 30 Scatter plot of mobile layer depth versus significant wave height for all storms recorded in 1996/97 deployments.

currents, the instantaneous nearbed velocity often reached 80 to 130 cm/s during the storms recorded in these deployments. These values are 2 to 4 times higher than that of the mean current. The impact force on offshore installations and the effect on sediment transport by these strong instantaneous flows need to be evaluated. Ralph and S4 meters in SI96a, SI97a and SI97c deployments were strategically placed at different locations across a sand ridge in order to evaluate flow dynamics across sand ridges on SIB. These simultaneous data seem to suggest that the magnitude and direction of the peak mean current did not change significantly from the ridge crests to the upper and lower lee flank of sand ridges, though the nearbed maximum instantaneous velocity in the ridge trough (lower lee flank) was generally lower than that at the crest or upper lee flank of a sand ridge.

The qualitative OBS data from Ralph and S4 meters indicate that there was a general agreement between the resuspension events and the peaks of wave height or mean current speed. However, the response of sand resuspension to a storm at different sites and that to different storms at the same site can be variable. Water depth, morphological location on sand ridges, bedform development as well as bottom sediment grain size distribution can be speculated as possible causes. But further studies are needed to resolve these issues. Catchment sediment traps attached on Ralph and S4 meters proved to be an effective way to collect composite resuspension sediment samples and record resuspension events during storms. Analyses of these sediment trap samples show that the amount and mean grain size of the resuspended sediment decreased with the increase of the sediment trap height above the sea floor. The sorting of these resuspended sediment increased as well. The maximum height reached by the resuspension events was less than 1.5 m above the seabed for the storm conditions recorded in these deployments. Layers in the sediment trap samples, defined by grain size variations, reflect resuspension events during storms. Each layer generally shows finer grain size at the bottom corresponding to the onset of the storm, then reaching the maximum grain size formed at the peak of the storm, and finally a decrease of grain size resulted from the decay of the storm.

The newly-added Imagenex profiler and sonar performed very well during these deployments. Seabed profiles and images recorded by these sensors, together with the seabed elevation changes recorded by the ABS sensors, proved to be powerful *in situ* methods to monitor seabed scour and estimate mobile layer depth during storms on SIB, issues of critical interest to Mobil and SOEP. Analyses of Ralph roll and pitch data show that the Ralph frame was stable during storms and the vertical error caused by the tilt and/or sink of Ralph was generally less than 5 cm. Bedform heights derived from the Imagenex profiler data were in general agreement with those obtained from ABS data. This confirms the applicability of these sensors to *in situ* monitoring/measurements of seabed scour and bedform height in otherwise hostile continental shelf environments. The combined ABS, Imagenex profiler and sonar data indicate that the maximum seabed

elevation change reached 25 cm and medium scale bedforms were generated with maximum height of about 30 cm and wavelength of 2 m for the storm conditions recorded in these deployments (maximum significant wave height 2.9 m). The data also showed that the largest bedforms tend to develop during the decay periods of storms, not at the peaks of storms. The estimated maximum mobile layer depths ranged from 6 cm to 17 cm for the 9 storms in which significant wave height varied from 1.2 m to 2.9 m. Correlation coefficients between various hydrodynamic parameters and mobile layer depth indicate that significant wave height best correlates with the estimated mobile layer depth and that water depth, sediment grain size and interaction between waves and current are less significant. An empirical relationship was derived between maximum mobile layer depth and peak significant wave height during storms. Though based on limited data, this relationship predicts maximum mobile layer depth of 0.5 m for typical annual winter storms on SIB. This is in reasonable agreement with estimates from sediment cores and cone penetrometer data.

Acknowledgements

We would like to thank Roger Ingersoll, Jim Suggett, and Hugh Steward of Mobil/SOEP for their support and corporation in this joint project. The effort of crews of CSS Hudson and CCGS Cornwallis was appreciated. Thanks also goes to Gary Grant for drafting support and Don Clattenburg for sediment grain size analyses. The reviews of the draft of this report by Gary Sonnichsen and Don Forbes have improved this Open File Report. This project was jointly funded by Mobil/SOEP and the Panel on Energy Research and Development (PERD) of the Federal Government of Canada through the East Coast Offshore Geotechnics Program 532208.

References

- Amos, C.L. and Judge, J.T., 1991. Sediment transport on the eastern Canadian continental shelf. *Cont. Shelf Res.*, 11: 1073-1068.
- Amos, C.L., Bowen, A.J., Huntley, D.A. and Lewis, C.F.M., 1988. Ripple generation under the combined influences of waves and currents on the Canadian continental shelf. *Continental Shelf Research*, 8: 1129-1153.
- Amos, C.L., Bentham, K., Choung, K., Currie, R., Muschenheim, K., Sutherland, T., and Zevenhuizen, J., 1994a. C.S.S. Hudson cruise 93016 Sable Island Bank, Scotian Shelf: A multi-disciplinary survey of the Cohasset development region. GSC Open File Report 2897.
- Amos, C.L., Christian, H.A., Heffler, D.E., and MacKinnon, W., 1994b. Instrumentation for *in situ* monitoring of marine sediment geodynamics. *Bedford Institute of Oceanography Science Review 1992&'93*, p. 55-59.
- Amos, C.L., Li, M.Z. and Choung, K-S., 1996. Storm-generated, hummocky stratification on the outer-Scotian Shelf. *Geo-Marine Letters*, 16: 85-94.
- Amos, C.L., Heffler, D.E., Li, M.Z., Robertson, A.G., Cloutier, D. and the participants of the cruise, 1999. CSS Hudson Cruise 98-001: Sable Island Bank and Scotian Shelf. Gsca Internal Cruise Report, 25p.
- Cacchione, D.A. and Drake, D.E., 1990. Shelf sediment transport: an overview with applications to the Northern California continental shelf. In: *The Sea*, Vol.9, B. Le Mehaute and D.M. Hanes, eds., Wiley-Interscience, pp. 729-773.
- Downing, J.P., 1983. An optical instrument for monitoring suspended particulates in ocean and laboratory. in: *Proceedings of Oceans'83*: 199-202.
- Forsythe, A., 1998. Analysis of geotechnical data for offshore pipeline design: Sable Offshore Energy Project. CE 1404 Civil Engineering Project report, Dalhousie University, 32p.
- Grant, W.D. and Madsen, O.S., 1979. Combined wave and current interaction with a rough bottom. *J. Geophys. Res.*, 84: 1797-1808.
- Grant, W.D. and O.S.Madsen, 1986. The continental shelf bottom boundary layer. *Annual Review of Fluid Mechanics*, 18: 265-305.
- Hammond, T.M. and Collins, M.B., 1979. On the threshold of transport of sand-sized sediment under the combined influence of unidirectional and oscillatory flow. *Sedimentology*, 26: 795-812.
- Heffler, D.E., 1984. RALPH - An instrument to monitor seabed sediments. *Current Research Part B, Geological Survey of Canada Paper 84-1b*, p. 47-52.
- Heffler, D.E., 1996. RALPH - A dynamic instrument for sediment dynamics. *Proc. Oceans'96, IEEE, Ft. Lauderdale, Florida, USA, September 1996*, p. 728-732.
- Hodgins, D.O. and Sayao, O.J., 1986. Field measurements of sediment transport on the Scotian Shelf. Vol. II Boundary layer measurements and sand transport prediction. *Environmental Studies Revolving Funds, Report 041, Ottawa*, 114 pp.
- Hudson Cruise 96-029: Sable Island Bank and Laurentian Fan. The participants of the Cruise, 1996. GSCA Internal Cruise Report, 25p.
- Li, M.Z., 1994. Direct skin friction measurements and stress partitioning over movable sand ripples. *Journal of Geophysical Research*, 99: 791-799.
- Li, M.Z. and Amos, C.L., 1995. SEDTRANS92: A sediment transport model for continental shelves. *Computers and Geosciences*, 21(4): 533-554.
- Li, M.Z. and Amos, C.L., 1997. SEDTRANS96: Upgrade and Calibration of the GSC Sediment Transport Model. GSCA Open File Report 3512.
- Li, M.Z. and Amos, C.L., 1998. Predicting ripple geometry and bed roughness under combined waves and currents in a continental shelf environment. *Continental Shelf Research*, 18: 941-970.
- Li, M.Z. and Amos, C.L., (in press^a) Sheet flow and large wave ripples under combined waves and currents:

Their field observation, model prediction and effects on boundary layer dynamics.
Continental Shelf Research.

- Li, M.Z. and Amos, C.L., (in press^b) Field observations of bedforms and sediment transport thresholds of fine sand under combined waves and currents. *Marine Geology*.
- Li, M.Z., Amos, C.L., Zevenhuizen, J., Heffler, D.E., Wile, B., and Drapeau, G., 1994. Hydrodynamics and Seabed Stability Observations on Sable Island Bank - AGC/LASMO Joint Program: A Summary of the Data for 1993/94. Geological Survey of Canada Open File Report 2949.
- Li, M.Z., Wright, L.D. and Amos, C.L., 1996a. Predicting ripple roughness and sand resuspension under combined flows in a shoreface environment. *Marine Geology*, 130: 139-161.
- Li, M.Z., Amos, C.L., Zevenhuizen, J., Heffler, D.E., and Wile, B., 1996b. Hydrodynamics and Seabed Stability Observations on Sable Island Bank: A Summary of the Data for 1994/95. Geological Survey of Canada Open File Report 3311.
- Li, M.Z., Amos, C.L. and Heffler, D.E., 1997. Boundary layer dynamics and sediment transport under storm and non-storm conditions on the Scotian shelf. *Marine Geology*, 141: 157-181.
- Li, M.Z., Heffler, D.E. and Gatchalian, K., (in preparation) Theories and operation of Matlab programs for the preliminary processing of Ralph data. GSCA Open File Report.
- Osborne, P.D. and Vincent, C.E., 1993. Dynamics of large and small scale bedforms on a macrotidal shoreface under shoaling and breaking waves. *Marine Geology*, 115: 207-226.
- Smith, J.D., 1977. Modelling of sediment transport on continental shelves. In: *The Sea*, Vol. 6, E.D. Goldberg et al., eds., Wiley-Interscience, New York, pp. 539-577.
- Vincent, C.E., Hanes, D.M. and Bowen, A.J., 1991. Acoustic measurements of suspended sand on the shoreface and the control of concentration by bed roughness. *Marine Geology*, 96: 1-18.
- Wiberg, P.L. and Nelson, J.M., 1992. Unidirectional flow over asymmetric and symmetric ripples. *Journal of Geophysical Research*, 97: 12,745-12,761.
- Zevenhuizen, J. and Li, M.Z., 1994. Seabed stability monitoring at the Cohasset-Panuke Development Region, Sable Island Bank, Scotian Shelf: Field activities during 1993 and 1994. Geological Survey of Canada, Internal Report.

Appendix 1

The burst-averaged data of wave, current and sediment suspension for the SI96a Ralph deployment: burst number BT, Julian Day (JD) and Hour, water depth (m), mean current speed u_{50} (cm/s), direction of mean current C_{dir} (degree), significant wave height H_s (m), mean wave period T_z (s), wave propagation direction W_{dir} (degree), and relative concentration of suspended sediment (obs1 readings).

BT	JD	Hour	depth	u ₅₀	C _{dir}	H _s	T _z	W _{dir}	obs l
1	331	15	19.82	27.8	128	0.32	13.9	4	596
2	331	16	19.49	25.6	157	0.40	12.4	352	596
3	331	17	19.25	25.1	171	0.43	12.2	350	596
4	331	18	19.10	20.8	185	0.39	11.5	356	595
5	331	19	19.05	13.9	203	0.45	11.5	352	594
6	331	20	19.10	11.1	255	0.48	9.4	4	594
7	331	21	19.37	11.7	297	0.53	9.3	14	594
8	331	22	19.70	10.2	316	0.55	9.3	12	594
9	331	23	19.99	6.2	303	0.53	9.3	8	594
10	332	0	20.22	7.1	197	0.54	9.6	4	595
11	332	1	20.20	12.7	195	0.57	10.2	356	596
12	332	2	20.01	24.5	208	0.61	9.4	4	594
13	332	3	19.76	30.6	217	0.56	10.2	360	593
14	332	4	19.48	28.0	224	0.72	8.9	360	593
15	332	5	19.23	24.7	247	0.91	8.5	16	594
16	332	6	19.05	22.9	264	1.19	8.6	18	594
17	332	7	19.05	20.4	293	1.07	8.9	22	594
18	332	8	19.14	22.3	317	1.16	8.6	22	595
19	332	9	19.44	27.7	342	1.12	8.8	22	596
20	332	10	19.73	38.7	356	1.02	8.4	24	597
21	332	11	20.08	41.5	4	1.15	9.2	26	599
22	332	12	20.35	27.0	16	1.11	8.8	20	600
23	332	13	20.44	11.2	34	1.13	9.2	26	603
24	332	14	20.32	4.8	110	1.26	9.3	30	604
25	332	15	20.06	13.9	176	1.32	9.1	24	600
26	332	16	19.72	23.6	189	1.32	9.3	20	598
27	332	17	19.48	24.1	206	1.41	9.3	24	597
28	332	18	19.25	21.5	236	1.38	9.3	24	597
29	332	19	19.17	20.9	259	1.63	9.6	26	596
30	332	20	19.12	19.9	277	1.51	9.3	26	596
31	332	21	19.31	18.7	308	1.75	9.3	210	596
32	332	22	19.49	18.8	313	1.89	9.2	212	597
33	332	23	19.87	15.0	318	1.40	9.2	202	597
34	333	0	20.22	10.4	314	1.67	9.1	204	595
35	333	1	20.35	7.2	289	1.63	9.2	208	595
36	333	2	20.33	13.9	233	1.50	8.8	210	595
37	333	3	20.08	14.1	235	1.62	8.8	208	595
38	333	4	19.84	20.0	233	1.93	8.9	216	595
39	333	5	19.59	15.9	259	1.81	9.1	212	596
40	333	6	19.44	12.8	280	1.78	9.4	210	595
41	333	7	19.32	15.2	311	1.48	8.7	224	594
42	333	8	19.34	18.4	322	1.57	8.8	216	595
43	333	9	19.46	19.4	338	1.27	9.0	218	595
44	333	10	19.70	22.6	355	1.34	9.0	212	595
45	333	11	20.02	33.5	5	1.41	9.3	216	596
46	333	12	20.26	32.7	13	1.35	9.4	222	596

BT	JD	Hour	depth	u ₅₀	C _{dir}	H _s	T _z	W _{dir}	obs1
47	333	13	20.54	21.8	26	1.29	9.4	228	597
48	333	14	20.51	16.8	58	1.38	9.2	234	599
49	333	15	20.32	9.8	102	1.32	9.3	234	600
50	333	16	20.06	15.8	138	1.23	8.9	232	600
51	333	17	19.78	16.2	156	1.24	9.5	228	600
52	333	18	19.54	18.9	168	1.16	9.0	224	597
53	333	19	19.35	15.7	184	1.27	8.9	230	596
54	333	20	19.29	10.5	196	1.18	9.0	214	596
55	333	21	19.32	5.5	257	1.11	9.3	234	596
56	333	22	19.49	6.3	308	1.03	9.0	224	596
57	333	23	19.75	7.2	342	1.00	9.2	230	596
58	334	0	20.06	4.5	356	1.00	8.8	234	597
59	334	1	20.24	1.1	104	1.17	9.0	238	597
60	334	2	20.31	10.4	172	1.00	8.8	234	597
61	334	3	20.23	23.4	185	1.01	8.6	226	596
62	334	4	19.99	26.1	197	1.15	8.9	236	598
63	334	5	19.76	24.7	214	1.08	8.9	238	596
64	334	6	19.53	16.8	228	0.97	9.0	232	595
65	334	7	19.39	15.7	247	0.88	8.7	232	596
66	334	8	19.40	14.7	288	0.87	8.8	228	596
67	334	9	19.39	12.9	325	0.78	8.7	230	597
68	334	10	19.55	20.3	343	0.70	8.9	212	597
69	334	11	19.79	30.6	358	0.65	8.9	214	598
70	334	12	20.05	36.7	11	0.62	8.9	226	597
71	334	13	20.34	27.1	21	0.66	8.7	224	598
72	334	14	20.48	19.1	42	0.60	9.0	228	598
73	334	15	20.48	15.9	78	0.60	9.0	234	597
74	334	16	20.27	15.0	124	0.57	8.6	224	599
75	334	17	20.01	21.2	148	0.57	9.1	218	598
76	334	18	19.77	23.4	167	0.49	9.0	224	594
77	334	19	19.56	23.2	183	0.58	8.4	226	594
78	334	20	19.43	15.6	207	0.59	8.6	226	593
79	334	21	19.39	13.0	237	0.53	8.6	246	594
80	334	22	19.46	15.5	264	0.48	8.4	244	596
81	334	23	19.61	15.0	296	0.46	8.9	224	596
82	335	0	19.86	14.6	318	0.39	9.8	232	597
83	335	1	20.12	11.1	323	0.43	8.4	224	597
84	335	2	20.31	7.0	285	0.40	9.5	236	596
85	335	3	20.36	6.6	244	0.34	10.9	240	596
86	335	4	20.21	11.8	204	0.37	9.3	222	595
87	335	5	20.01	11.2	231	0.37	10.5	246	596
88	335	6	19.82	13.0	261	0.31	11.7	234	598
89	335	7	19.65	16.2	291	0.34	12.2	232	600
90	335	8	19.55	17.0	312	0.36	10.8	226	601
91	335	9	19.51	19.6	333	0.33	12.4	224	600
92	335	10	19.58	28.7	351	0.35	14.4	202	594

BT	JD	Hour	depth	u ₅₀	C _{dir}	H _s	T _z	W _{dir}	obs1
93	335	11	19.72	37.6	2	0.33	12.6	204	593
94	335	12	19.93	41.1	12	0.39	11.7	210	592
95	335	13	20.23	40.3	25	0.35	14.4	222	593
96	335	14	20.40	39.8	36	0.32	12.0	214	596
97	335	15	20.47	31.9	58	0.31	14.6	266	596
98	335	16	20.38	23.8	77	0.39	13.9	246	597

Appendix 2

Predictions by SEDTRANS96 for SI96a Ralph deployment: (a) bottom boundary layer dynamics parameters and (b) sediment transport parameters. bt# is the burst number. The boundary layer dynamics parameters include near-bed wave orbital velocity (u_b , m/s), near-bed wave orbital amplitude (A_b , m), combined wave-current friction factor (f_{cws}), skin friction current shear velocity (u_{*cs} , cm/s), skin friction wave shear velocity (u_{*ws} , cm/s), skin friction combined wave-current shear velocity (u_{*cws} , cm/s), ripple-enhanced combined wave-current shear velocity (u_{*cwe} , cm/s), bedload-enhanced combined wave-current shear velocity (u_{*cwb} , cm/s), total current shear velocity (u_{*c} , cm/s), total wave shear velocity (u_{*w} , cm/s), total combined wave-current shear velocity (u_{*cw} , cm/s), thickness of the wave-current boundary layer (δ_{cw} , cm), inner-layer bottom roughness (z_o , cm), apparent bottom roughness above the wave boundary layer (z_{oc} , cm). The sediment transport parameters include predicted ripple height (η_p , cm), predicted ripple wavelength (λ_p , cm), mean sediment transport rate of Einstein-Brown bedload method (Q_b , kg m⁻¹ s⁻¹), mean suspended load sediment transport rate (Q_s , kg m⁻¹ s⁻¹), and direction of bedload sediment transport (Q_{b-dir}).

bt#	u_b	A_b	f_{cws}	u^*_{cs}	u^*_{ws}	u^*_{cws}	u^*_{cwe}	u^*_{cwb}	u^*_c	u^*_w	u^*_{cw}	δ_{cw}	Z_0	Z_{0c}
1	0.097	0.214	0.0123	1.33	1.11	1.63	2.62	1.95	2.29	2.31	3.06	5.41	0.16	0.39
2	0.118	0.232	0.0122	1.33	1.31	1.85	2.97	2.61	2.43	2.96	3.81	6.02	0.22	0.73
3	0.127	0.246	0.0122	1.33	1.37	1.91	3.06	2.77	2.45	3.17	4.01	6.23	0.23	0.84
4	0.112	0.206	0.0131	1.11	1.23	1.65	2.65	2.06	1.93	2.66	3.28	4.81	0.17	0.67
5	0.130	0.238	0.0137	0.82	1.26	1.48	2.27	1.48	1.41	2.78	3.08	4.52	0.16	0.98
6	0.122	0.182	0.0159	0.66	1.16	1.24	1.90	1.24	1.12	2.66	2.75	3.29	0.15	0.93
7	0.131	0.194	0.0157	0.69	1.23	1.30	1.98	1.30	1.18	2.82	2.90	3.43	0.15	0.96
8	0.134	0.198	0.0154	0.64	1.27	1.37	2.09	1.37	1.08	2.90	3.02	3.58	0.15	1.16
9	0.127	0.189	0.0161	0.43	1.18	1.22	1.86	1.22	0.71	2.73	2.77	3.28	0.15	1.49
10	0.132	0.202	0.0153	0.50	1.24	1.34	2.04	1.34	0.81	2.84	2.95	3.60	0.15	1.51
11	0.146	0.237	0.0139	0.79	1.40	1.60	3.02	1.84	1.48	3.58	3.86	5.01	0.27	1.63
12	0.148	0.221	0.0131	1.33	1.56	2.03	3.83	3.12	2.77	4.38	5.14	6.15	0.43	1.46
13	0.146	0.238	0.0124	1.57	1.58	2.17	3.49	3.43	3.06	3.91	4.84	6.29	0.30	0.91
14	0.170	0.241	0.0130	1.50	1.74	2.21	4.18	3.60	3.23	5.07	5.83	6.61	0.49	1.56
15	0.208	0.281	0.0130	1.40	1.97	2.31	3.89	3.94	2.90	5.44	5.95	6.44	0.39	1.65
16	0.278	0.380	0.0124	1.40	2.38	2.59	3.42	4.79	2.56	5.51	5.79	6.34	0.21	1.40
17	0.259	0.366	0.0130	1.22	2.14	2.20	3.85	3.83	2.60	6.17	6.23	7.06	0.42	2.17
18	0.270	0.369	0.0125	1.37	2.32	2.53	3.48	4.63	2.55	5.56	5.84	6.40	0.23	1.51
19	0.262	0.367	0.0119	1.64	2.39	2.82	3.33	5.25	2.84	5.05	5.67	6.35	0.16	1.01
20	0.224	0.299	0.0118	2.08	2.28	3.04	3.29	5.65	3.53	4.64	5.75	6.15	0.15	0.62
21	0.272	0.399	0.0109	2.30	2.64	3.47	3.47	6.74	4.02	5.48	6.74	7.89	0.17	0.81
22	0.248	0.347	0.0119	1.62	2.33	2.83	3.35	5.24	2.79	4.92	5.66	6.34	0.16	1.04
23	0.263	0.385	0.0125	0.85	2.22	2.38	3.66	4.23	1.60	5.78	5.99	7.02	0.31	3.06
24	0.298	0.441	0.0124	0.46	2.36	2.37	3.54	4.33	0.81	6.06	6.07	7.18	0.29	4.68
25	0.310	0.449	0.0119	1.04	2.56	2.74	3.27	5.21	1.75	5.46	5.70	6.61	0.16	2.10
26	0.321	0.476	0.0112	1.56	2.76	3.16	3.16	6.18	2.63	5.61	6.18	7.32	0.14	1.38
27	0.347	0.514	0.0110	1.62	2.94	3.35	3.35	6.71	2.79	6.10	6.71	7.94	0.16	1.58
28	0.344	0.509	0.0112	1.47	2.85	3.17	3.17	6.27	2.48	5.83	6.27	7.43	0.15	1.57
29	0.418	0.639	0.0107	1.50	3.27	3.49	3.49	7.23	2.64	6.91	7.23	8.84	0.17	2.11
30	0.378	0.560	0.0113	1.38	2.97	3.10	3.10	6.23	2.34	6.06	6.23	7.38	0.14	1.66
31	0.434	0.643	0.0110	1.37	3.28	3.34	3.34	7.00	2.38	6.92	7.00	8.29	0.16	2.17
32	0.461	0.675	0.0108	1.41	3.46	3.54	3.54	7.55	2.49	7.44	7.55	8.84	0.18	2.44
33	0.335	0.491	0.0118	1.10	2.68	2.79	3.18	5.40	1.84	5.57	5.71	6.69	0.14	1.93
34	0.389	0.563	0.0114	0.89	2.99	3.04	3.04	6.17	1.45	6.11	6.17	7.15	0.13	2.82
35	0.381	0.558	0.0116	0.67	2.91	2.93	3.02	5.88	1.07	5.89	5.90	6.91	0.13	3.36
36	0.336	0.470	0.0117	1.06	2.74	2.93	3.11	5.75	1.74	5.57	5.81	6.51	0.13	2.03
37	0.367	0.514	0.0115	1.10	2.95	3.13	3.13	6.31	1.83	6.07	6.31	7.07	0.14	2.28
38	0.448	0.635	0.0106	1.51	3.54	3.84	3.84	8.23	2.72	7.79	8.23	9.33	0.21	2.65
39	0.435	0.630	0.0109	1.26	3.36	3.52	3.52	7.43	2.19	7.20	7.43	8.61	0.18	2.74
40	0.443	0.663	0.0109	1.07	3.33	3.40	3.40	7.15	1.84	7.06	7.15	8.56	0.17	3.10
41	0.345	0.477	0.0121	1.10	2.71	2.74	3.15	5.37	1.85	5.70	5.73	6.35	0.14	1.86
42	0.370	0.518	0.0116	1.30	2.92	3.02	3.02	6.07	2.16	5.94	6.07	6.80	0.13	1.67
43	0.304	0.435	0.0120	1.29	2.52	2.71	3.29	5.12	2.24	5.47	5.72	6.55	0.17	1.56
44	0.317	0.454	0.0115	1.48	2.69	3.02	3.13	5.86	2.48	5.44	5.89	6.75	0.13	1.30
45	0.338	0.501	0.0108	2.03	2.96	3.53	3.53	7.10	3.59	6.24	7.10	8.41	0.18	1.20
46	0.323	0.484	0.0108	1.98	2.86	3.42	3.42	6.79	3.45	5.94	6.79	8.12	0.17	1.13

bt#	u _b	A _b	f _{cws}	U* _{cs}	U* _{ws}	U* _{cws}	U* _{cwe}	U* _{cwb}	U* _c	U* _w	U* _{cw}	δ _{cw}	Z ₀	Z _{0c}
47	0.305	0.456	0.0114	1.44	2.61	2.97	3.19	5.68	2.41	5.28	5.77	6.91	0.14	1.34
48	0.320	0.469	0.0115	1.21	2.67	2.93	3.16	5.67	2.00	5.41	5.77	6.76	0.13	1.74
49	0.312	0.462	0.0120	0.80	2.51	2.59	3.35	4.88	1.38	5.68	5.80	6.86	0.19	2.93
50	0.282	0.400	0.0127	1.06	2.29	2.33	3.61	4.22	2.08	6.06	6.11	6.92	0.32	2.41
51	0.307	0.464	0.0120	1.12	2.47	2.57	3.39	4.78	2.03	5.69	5.82	7.04	0.21	2.06
52	0.276	0.396	0.0123	1.23	2.35	2.55	3.47	4.67	2.27	5.55	5.83	6.68	0.23	1.79
53	0.302	0.428	0.0121	1.11	2.51	2.69	3.30	5.08	1.92	5.49	5.73	6.49	0.17	1.91
54	0.285	0.408	0.0123	0.82	2.36	2.50	3.48	4.58	1.48	5.71	5.89	6.75	0.24	2.92
55	0.275	0.408	0.0126	0.50	2.24	2.29	3.70	4.07	0.92	6.07	6.14	7.27	0.35	4.61
56	0.246	0.352	0.0133	0.53	2.02	2.03	3.83	3.39	1.03	6.06	6.07	6.95	0.45	4.37
57	0.241	0.352	0.0132	0.58	1.99	2.03	3.83	3.36	1.15	5.93	5.97	7.00	0.45	4.12
58	0.227	0.318	0.0137	0.40	1.90	1.92	3.64	3.09	0.74	5.62	5.65	6.33	0.42	4.42
59	0.269	0.386	0.0130	0.13	2.17	2.17	3.82	3.82	0.22	6.31	6.32	7.24	0.42	6.56
60	0.224	0.314	0.0135	0.75	1.92	1.99	3.76	3.24	1.51	5.68	5.78	6.47	0.44	3.19
61	0.221	0.303	0.0127	1.38	2.06	2.42	3.73	4.23	2.72	5.36	5.88	6.44	0.32	1.61
62	0.265	0.375	0.0119	1.57	2.39	2.79	3.35	5.18	2.74	5.10	5.67	6.42	0.17	1.10
63	0.252	0.357	0.0120	1.50	2.31	2.73	3.41	5.01	2.66	5.06	5.68	6.43	0.18	1.22
64	0.231	0.331	0.0126	1.11	2.08	2.35	3.77	4.10	2.18	5.54	5.95	6.82	0.35	2.30
65	0.204	0.283	0.0133	1.01	1.88	2.13	4.03	3.53	2.12	5.58	5.96	6.60	0.47	2.59
66	0.204	0.286	0.0137	0.94	1.81	1.95	3.69	3.09	1.93	5.29	5.48	6.14	0.42	2.38
67	0.181	0.251	0.0147	0.80	1.59	1.63	3.09	2.07	1.55	4.35	4.40	4.87	0.29	1.81
68	0.165	0.234	0.0137	1.15	1.61	1.90	3.58	2.85	2.36	4.55	4.97	5.63	0.39	1.59
69	0.151	0.214	0.0129	1.59	1.65	2.23	3.58	3.59	3.11	4.19	5.10	5.78	0.31	0.97
70	0.142	0.202	0.0126	1.83	1.65	2.40	4.03	3.96	3.76	4.40	5.65	6.40	0.39	1.00
71	0.146	0.202	0.0133	1.44	1.59	2.12	4.01	3.35	3.04	4.55	5.43	6.02	0.46	1.42
72	0.136	0.195	0.0140	1.08	1.43	1.79	3.38	2.52	2.14	3.91	4.45	5.10	0.35	1.41
73	0.136	0.195	0.0145	0.93	1.38	1.65	3.12	2.08	1.78	3.67	4.05	4.64	0.30	1.39
74	0.125	0.171	0.0162	0.82	1.21	1.31	2.00	1.31	1.41	2.80	2.90	3.17	0.15	0.72
75	0.134	0.194	0.0146	1.10	1.35	1.58	2.99	1.70	2.10	3.43	3.73	4.32	0.25	0.87
76	0.115	0.165	0.0145	1.18	1.26	1.62	2.60	1.94	2.04	2.79	3.26	3.74	0.16	0.51
77	0.128	0.172	0.0144	1.22	1.39	1.79	3.38	2.51	2.44	3.83	4.41	4.72	0.35	1.12
78	0.135	0.185	0.0147	0.91	1.38	1.65	3.11	2.07	1.74	3.68	4.06	4.44	0.30	1.39
79	0.122	0.166	0.0154	0.78	1.25	1.47	2.25	1.47	1.31	2.86	3.14	3.44	0.16	0.95
80	0.107	0.143	0.0157	0.86	1.17	1.44	2.20	1.44	1.47	2.65	3.02	3.23	0.16	0.74
81	0.108	0.153	0.0163	0.80	1.10	1.24	1.89	1.24	1.37	2.51	2.67	3.02	0.15	0.64
82	0.099	0.154	0.0167	0.75	0.98	1.07	1.63	1.07	1.29	2.23	2.31	2.88	0.14	0.53
83	0.092	0.123	0.0183	0.61	0.94	1.01	1.57	1.01	1.04	2.26	2.33	2.49	0.15	0.71
84	0.097	0.146	0.0171	0.45	0.96	1.03	1.57	1.03	0.73	2.20	2.28	2.76	0.14	1.06
85	0.091	0.157	0.0164	0.43	0.91	1.00	1.57	1.00	0.70	2.10	2.21	3.07	0.15	1.18
86	0.088	0.130	0.0164	0.67	0.96	1.17	1.78	1.17	1.12	2.17	2.43	2.88	0.14	0.73
87	0.098	0.163	0.0154	0.66	1.02	1.21	1.84	1.21	1.10	2.26	2.51	3.35	0.15	0.85
88	0.088	0.163	0.0149	0.72	0.94	1.17	1.79	1.17	1.21	2.06	2.36	3.52	0.14	0.68
89	0.099	0.191	0.0143	0.85	1.02	1.24	1.89	1.24	1.45	2.21	2.50	3.88	0.15	0.58
90	0.098	0.169	0.0157	0.84	0.99	1.11	1.70	1.11	1.45	2.19	2.32	3.19	0.14	0.46
91	0.097	0.191	0.0141	0.97	1.01	1.26	1.93	1.26	1.66	2.19	2.50	3.95	0.15	0.45
92	0.108	0.248	0.0116	1.43	1.23	1.85	2.97	2.58	2.60	2.73	3.71	6.80	0.22	0.61

bt#	u_b	A_b	f_{cws}	u^*_{cs}	u^*_{ws}	u^*_{cws}	u^*_{cwe}	u^*_{cwb}	u^*_c	u^*_w	u^*_{cw}	δ_{cw}	z_0	z_{0c}
93	0.097	0.194	0.0115	1.79	1.26	2.17	3.48	3.29	3.42	2.97	4.49	7.20	0.29	0.62
94	0.110	0.204	0.0114	1.97	1.41	2.41	4.19	3.84	4.10	3.68	5.47	8.15	0.43	0.90
95	0.106	0.242	0.0107	1.92	1.34	2.34	4.35	3.65	4.12	3.54	5.40	9.91	0.49	1.00
96	0.090	0.171	0.0115	1.87	1.24	2.25	3.60	3.45	3.62	2.95	4.67	7.14	0.30	0.62
97	0.093	0.217	0.0114	1.54	1.16	1.90	3.04	2.66	2.81	2.56	3.75	6.97	0.23	0.53
98	0.116	0.257	0.0119	1.25	1.26	1.77	2.84	2.39	2.24	2.77	3.55	6.29	0.20	0.71

bt#	η_p	λ_p	Q_b	Q_s	Q_{b-dir}
1	1.3	11.0	0.000489	0.000000	133
2	1.7	14.1	0.000628	0.000000	162
3	1.8	14.7	0.000694	0.000000	171
4	1.4	11.5	0.000351	0.000000	181
5	1.5	14.0	0.000149	0.000000	184
6	1.4	12.9	0.000042	0.000000	229
7	1.5	13.2	0.000049	0.000000	313
8	1.5	13.5	0.000063	0.000000	341
9	1.4	12.8	0.000021	0.000000	333
10	1.5	13.3	0.000055	0.000000	189
11	1.9	12.5	0.000428	0.000000	185
12	2.7	18.3	0.001881	0.000000	199
13	2.1	17.8	0.001357	0.000000	208
14	3.1	20.4	0.002961	0.000000	210
15	2.7	20.7	0.001204	0.000000	227
16	1.6	20.7	0.000858	0.001603	241
17	2.8	20.7	0.000754	0.000000	294
18	1.8	20.7	0.000838	0.001992	340
19	1.0	20.7	0.001466	0.001062	2
20	0.5	20.7	0.002447	0.001290	8
21	0.0	0.0	0.004794	0.000228	14
22	1.0	20.7	0.001598	0.001025	18
23	2.3	20.7	0.000607	0.001373	29
24	2.2	20.7	0.000082	0.000327	95
25	1.1	20.7	0.000761	0.000425	193
26	0.0	0.0	0.002112	0.000044	196
27	0.0	0.0	0.002956	0.000084	205
28	0.0	0.0	0.001866	0.000041	217
29	0.0	0.0	0.002525	0.000112	231
30	0.0	0.0	0.001020	0.000032	252
31	0.0	0.0	0.001179	0.000068	322
32	0.0	0.0	0.001615	0.000117	331
33	0.8	20.7	0.000574	0.000397	346
34	0.0	0.0	0.000421	0.000010	341
35	0.2	20.7	0.000175	0.000110	273
36	0.4	20.7	0.000914	0.000290	218
37	0.0	0.0	0.001208	0.000021	218
38	0.0	0.0	0.005087	0.000246	222
39	0.0	0.0	0.002132	0.000084	232
40	0.0	0.0	0.000961	0.000045	253
41	0.9	20.7	0.000402	0.000412	306
42	0.0	0.0	0.000773	0.000021	346
43	1.2	20.7	0.000788	0.000778	4
44	0.2	20.7	0.001503	0.000613	16
45	0.0	0.0	0.004621	0.000224	22
46	0.0	0.0	0.003852	0.000155	29

bt#	η_p	λ_p	Q_b	Q_s	Q_{b-dir}
47	0.5	20.7	0.001490	0.000584	39
48	0.5	20.7	0.001181	0.000397	55
49	1.5	20.7	0.000389	0.000415	76
50	2.3	20.7	0.000445	0.002609	132
51	1.6	20.7	0.000514	0.001041	178
52	1.8	20.7	0.000770	0.001489	193
53	1.2	20.7	0.000723	0.000599	209
54	1.9	20.7	0.000529	0.000710	207
55	2.5	20.7	0.000234	0.000000	243
56	2.9	19.5	0.000237	0.000000	300
57	2.9	19.3	0.000353	0.000000	5
58	2.7	18.1	0.000171	0.000000	21
59	2.8	20.7	0.000015	0.000000	80
60	2.8	18.8	0.000582	0.000000	195
61	2.3	20.7	0.001139	0.003769	204
62	1.1	20.7	0.001369	0.001060	217
63	1.3	20.7	0.001348	0.001219	227
64	2.5	20.7	0.000962	0.000000	230
65	3.0	20.1	0.001691	0.000000	239
66	2.7	18.1	0.000845	0.000000	267
67	2.0	13.6	0.000313	0.000000	330
68	2.6	17.0	0.001144	0.000000	0
69	2.2	18.5	0.001487	0.000000	8
70	2.7	20.7	0.002147	0.000000	20
71	2.9	19.3	0.002473	0.000000	29
72	2.3	15.6	0.000946	0.000000	45
73	2.0	13.6	0.000575	0.000000	67
74	1.5	13.2	0.000071	0.000000	113
75	1.8	11.9	0.000598	0.000000	158
76	1.3	11.0	0.000371	0.000000	176
77	2.3	15.5	0.001054	0.000000	196
78	2.0	13.5	0.000567	0.000000	216
79	1.5	13.9	0.000147	0.000000	243
80	1.5	13.8	0.000144	0.000000	252
81	1.4	12.9	0.000060	0.000000	272
82	1.3	12.2	0.000020	0.000000	288
83	1.4	12.2	0.000000	0.000000	0
84	1.3	12.0	0.000004	0.000000	244
85	1.4	12.2	0.000000	0.000000	0
86	1.4	12.6	0.000051	0.000000	216
87	1.4	12.7	0.000060	0.000000	241
88	1.4	12.6	0.000053	0.000000	245
89	1.4	12.9	0.000076	0.000000	259
90	1.4	12.3	0.000040	0.000000	302
91	1.4	13.0	0.000098	0.000000	349
92	1.7	13.9	0.000733	0.000000	356

bt#	η_p	λ_p	Q_b	Q_s	Q_{b-dir}
93	2.1	17.2	0.001772	0.000000	5
94	2.8	20.7	0.002865	0.000000	15
95	3.0	20.7	0.003106	0.000000	27
96	2.2	17.9	0.002163	0.000000	36
97	1.7	14.3	0.000908	0.000000	62
98	1.6	13.0	0.000499	0.000000	73

Appendix 3

The burst-averaged data of wave, current and sediment suspension for the SI97a Ralph deployment. The parameters are as defined in Appendix 1.

BT	JD	Hour	depth	u ₅₀	C _{dir}	H _s	T _z	W _{dir}	obs l
1	28	10	31.03	21.5	46	0.42	10.8	60	703
2	28	12	30.85	18.6	87	0.39	12.6	62	697
3	28	14	30.34	15.7	141	0.40	10.9	354	695
4	28	16	30.02	6.3	176	0.46	9.8	338	692
5	28	18	30.05	9.5	319	0.52	9.0	332	690
6	28	20	30.52	21.5	1	0.62	8.5	10	690
7	28	22	30.96	23.2	31	0.94	9.1	34	693
8	29	0	30.91	17.1	86	1.43	9.6	28	694
9	29	2	30.50	13.0	144	1.49	10.1	24	693
10	29	4	30.15	7.8	186	1.54	10.5	12	693
11	29	6	30.12	7.1	192	1.51	10.1	10	694
12	29	8	30.44	6.3	212	1.29	10.1	20	693
13	29	10	30.89	9.0	165	1.33	10.1	36	694
14	29	12	30.97	23.9	166	1.18	10.0	50	694
15	29	14	30.55	27.9	183	1.15	10.6	36	690
16	29	16	30.12	21.3	216	1.12	9.8	40	688
17	29	18	30.11	12.7	257	1.04	10.1	48	688
18	29	20	30.44	13.8	315	0.99	9.5	56	688
19	29	22	30.95	12.5	6	0.95	9.5	62	691
20	30	0	31.12	11.1	90	0.98	9.3	56	691
21	30	2	30.83	20.2	160	0.83	10.0	54	692
22	30	4	30.43	19.8	186	0.82	9.8	52	691
23	30	6	30.27	18.2	216	0.75	9.6	48	692
24	30	8	30.47	12.1	251	0.71	9.1	62	693
25	30	10	31.00	8.2	252	0.64	9.2	58	695
26	30	12	31.15	13.3	215	0.61	9.1	52	695
27	30	14	30.91	18.6	214	0.55	9.1	54	697
28	30	16	30.54	28.4	234	0.49	9.9	56	712
29	30	18	30.33	22.0	271	0.47	9.2	62	732
30	30	20	30.47	27.3	319	0.43	9.4	338	731
31	30	22	30.93	22.0	340	0.42	10.0	348	708
32	31	0	31.24	11.3	26	0.39	10.0	280	715
33	31	2	31.07	10.5	96	0.41	10.6	6	726
34	31	4	30.72	12.9	89	0.41	10.0	4	730
35	31	6	30.42	7.5	102	0.39	10.0	4	727
36	31	8	30.45	5.7	50	0.38	10.2	14	725
37	31	10	30.82	11.6	33	0.39	10.1	352	722
38	31	12	31.13	11.5	61	0.37	10.5	44	725
39	31	14	31.03	9.1	143	0.42	9.3	334	702
40	31	16	30.70	17.8	195	0.45	8.7	318	708
41	31	18	30.42	29.1	235	0.60	8.2	278	699
42	31	20	30.46	36.0	254	0.85	8.2	262	705
43	31	22	30.77	39.9	282	1.38	9.4	342	697
44	32	0	31.27	31.6	295	2.13	10.5	340	694
45	32	2	31.43	14.2	293	1.68	11.2	350	694
46	32	4	30.98	11.0	293	2.22	11.7	350	692

BT	JD	Hour	depth	u ₅₀	C _{dir}	H _s	T _z	W _{dir}	obs l
47	32	6	30.71	2.4	242	2.85	13.2	346	698
48	32	8	30.64	3.8	336	2.31	13.0	348	699
49	32	10	30.82	1.2	120	2.89	12.6	340	703
50	32	12	31.21	3.7	96	1.97	11.9	338	701
51	32	14	31.26	6.0	157	2.21	12.0	346	704
52	32	16	31.04	12.2	181	2.06	11.9	354	698
53	32	18	30.73	14.6	219	1.77	10.9	352	697
54	32	20	30.52	14.4	259	1.40	11.2	4	696
55	32	22	30.71	22.4	312	1.24	10.8	360	696
56	33	0	31.17	16.5	353	1.13	10.5	10	697
57	33	2	31.37	10.5	42	0.96	10.8	12	699
58	33	4	31.28	13.8	72	0.97	10.9	10	702
59	33	6	30.93	9.9	107	1.08	10.6	4	702
60	33	8	30.68	2.9	131	0.84	10.6	360	703
61	33	10	30.71	1.6	0	0.93	10.0	12	712
62	33	12	31.07	2.4	65	0.79	10.0	12	714
63	33	14	31.30	6.5	151	0.77	10.2	12	715
64	33	16	31.24	6.3	172	0.68	10.0	8	715
65	33	18	30.98	13.7	210	0.73	10.0	22	708
66	33	20	30.62	15.8	241	0.72	9.4	30	701
67	33	22	30.58	16.7	292	0.66	9.4	20	702
68	34	0	30.95	19.5	338	0.64	9.1	14	701
69	34	2	31.39	17.1	21	0.57	8.9	24	704
70	34	4	31.44	19.1	56	0.64	8.9	32	709
71	34	6	31.16	19.8	85	0.58	9.5	28	703
72	34	8	30.76	12.4	107	0.53	8.6	20	704
73	34	10	30.51	4.4	110	0.56	9.0	38	706
74	34	12	30.73	4.9	75	0.56	8.6	26	705
75	34	14	31.15	9.2	121	0.55	9.2	26	706
76	34	16	31.29	17.1	154	0.51	9.4	358	709
77	34	18	31.08	20.6	168	0.51	8.9	350	707
78	34	20	30.73	29.4	221	0.52	9.2	28	702
79	34	22	30.48	30.0	250	0.50	8.3	36	702
80	35	0	30.71	24.0	303	0.49	7.8	316	702
81	35	2	31.20	24.4	339	0.47	8.3	344	702
82	35	4	31.56	20.4	18	0.48	8.6	344	708
83	35	6	31.40	18.3	66	0.46	8.7	62	708
84	35	8	30.98	13.1	115	0.48	7.5	4	709
85	35	10	30.50	11.6	171	0.47	7.9	358	708
86	35	12	30.54	9.6	231	0.50	7.6	202	707
87	35	14	30.98	8.0	266	0.47	7.4	192	707
88	35	16	31.36	8.1	234	0.44	8.0	218	709
89	35	18	31.42	16.9	219	0.46	9.4	228	715
90	35	20	31.03	25.1	221	0.48	8.6	56	714
91	35	22	30.50	26.0	245	0.44	8.0	79	714
92	36	0	30.45	25.6	310	0.44	6.9	322	717

BT	JD	Hour	depth	u ₅₀	C _{dir}	H _s	T _z	W _{dir}	obs I
93	36	2	30.93	30.4	342	0.43	8.2	344	714
94	36	4	31.56	26.1	18	0.43	7.6	350	708
95	36	6	31.67	24.1	59	0.43	8.7	56	722
96	36	8	31.26	23.0	100	0.41	9.4	84	716
97	36	10	30.61	19.1	143	0.44	8.2	342	712
98	36	12	30.32	11.0	173	0.43	8.0	334	712
99	36	14	30.56	3.7	264	0.40	8.3	338	713
100	36	16	31.26	3.8	13	0.39	9.4	332	714
101	36	18	31.47	8.2	133	0.44	8.8	322	716
102	36	20	31.13	14.3	165	0.47	8.2	326	716
103	36	22	30.62	12.6	199	0.55	8.3	152	715
104	37	0	30.23	9.4	317	0.79	7.7	360	722
105	37	2	30.47	23.1	8	0.90	8.6	14	709
106	37	4	31.20	24.5	31	1.25	9.3	16	712
107	37	6	31.64	36.4	71	1.37	9.9	16	710
108	37	8	31.39	35.3	118	1.46	10.6	10	707
109	37	10	30.67	37.9	157	1.80	11.2	4	706
110	37	12	30.09	25.3	192	1.64	10.8	14	709
111	37	14	30.20	25.9	246	1.51	10.6	14	710
112	37	16	30.89	21.5	273	1.39	10.5	12	712
113	37	18	31.48	13.5	264	1.26	10.9	28	707
114	37	20	31.39	19.4	232	1.13	10.6	360	714
115	37	22	30.80	21.2	240	1.21	10.9	2	706
116	38	0	30.21	22.3	266	0.98	10.1	16	705
117	38	2	30.19	31.0	319	1.07	10.6	356	709
118	38	4	30.82	34.3	344	1.09	10.4	356	716
119	38	6	31.58	16.2	20	0.83	10.5	8	715
120	38	8	31.71	22.8	86	0.81	10.5	12	712
121	38	10	31.12	24.0	148	0.80	10.4	360	715
122	38	12	30.33	25.9	185	0.77	10.0	4	712
123	38	14	30.10	24.9	235	0.71	9.8	22	716
124	38	16	30.59	20.1	282	0.69	9.5	2	716
125	38	18	31.41	15.8	287	0.58	10.0	336	714
126	38	20	31.60	11.8	226	0.57	9.5	8	715
127	38	22	31.09	14.5	205	0.58	9.4	8	716
128	39	0	30.39	29.9	230	0.60	10.1	356	709
129	39	2	30.01	25.4	268	0.55	9.2	344	726
130	39	4	30.44	31.9	329	0.52	9.5	336	722
131	39	6	31.35	35.5	7	0.46	10.2	352	716
132	39	8	31.74	23.5	50	0.52	9.3	32	713
133	39	10	31.35	13.9	118	0.48	10.1	352	732
134	39	12	30.55	21.7	152	0.46	9.6	336	728
135	39	14	30.00	23.1	203	0.46	9.4	344	724
136	39	16	30.18	15.7	267	0.44	9.6	342	725
137	39	18	31.06	12.0	308	0.44	9.4	338	728
138	39	20	31.64	9.0	192	0.43	10.0	2	731

BT	JD	Hour	depth	u ₅₀	C _{dir}	H _s	T _z	W _{dir}	obs1
139	39	22	31.36	24.5	197	0.39	10.9	26	735
140	40	0	30.69	35.1	224	0.40	9.6	28	709
141	40	2	30.09	34.4	249	0.40	9.6	62	713
142	40	4	30.13	37.1	310	0.40	9.8	306	719
143	40	6	30.93	41.1	343	0.38	10.6	352	718
144	40	8	31.70	29.1	21	0.37	10.6	356	723
145	40	10	31.62	24.3	77	0.37	10.9	252	725
146	40	12	30.93	20.2	141	0.39	9.2	342	727
147	40	14	30.27	18.5	182	0.37	10.8	338	728
148	40	16	30.05	17.7	248	0.38	10.1	56	730
149	40	18	30.72	24.7	311	0.38	9.3	322	733
150	40	20	31.59	13.2	330	0.42	8.4	300	730
151	40	22	31.68	8.0	179	0.47	8.8	312	732
152	41	0	31.06	23.0	212	0.52	9.2	328	730
153	41	2	30.38	24.7	239	0.67	9.9	334	726
154	41	4	30.14	22.2	280	0.90	11.7	354	721
155	41	6	30.60	32.5	334	1.79	12.6	360	718
156	41	8	31.43	29.3	14	1.24	12.4	360	717
157	41	10	31.72	22.5	77	1.16	12.2	12	717
158	41	12	31.18	19.1	139	1.00	12.0	14	719
159	41	14	30.45	20.2	169	0.89	12.0	360	719
160	41	16	30.10	17.0	210	0.80	11.4	20	717
161	41	18	30.45	12.5	293	0.70	10.8	358	717
162	41	20	31.29	9.5	359	0.57	10.8	352	718
163	41	22	31.68	9.6	145	0.54	11.2	6	718
164	42	0	31.35	19.3	164	0.52	10.6	2	719
165	42	2	30.71	28.1	210	0.53	10.4	18	721
166	42	4	30.25	25.7	245	0.51	9.9	38	715
167	42	6	30.37	24.1	302	0.46	10.5	350	716
168	42	8	31.13	29.8	344	0.48	9.9	344	721
169	42	10	31.66	20.6	42	0.46	10.4	62	717
170	42	12	31.38	10.9	122	0.41	11.4	342	719
171	42	14	30.76	12.2	169	0.41	10.4	344	723
172	42	16	30.35	17.6	226	0.42	10.1	10	719
173	42	18	30.35	21.4	282	0.41	9.6	4	720
174	42	20	30.96	28.5	331	0.43	9.1	336	719
175	42	22	31.65	16.9	5	0.45	8.7	22	719
176	43	0	31.57	2.2	113	0.45	8.0	46	719
177	43	2	31.03	14.6	202	0.50	8.4	48	720
178	43	4	30.51	17.8	230	0.49	8.7	60	719
179	43	6	30.36	15.0	267	0.52	8.4	284	720
180	43	8	30.79	21.8	328	0.51	9.3	322	718
181	43	10	31.45	17.1	9	0.56	9.6	312	716
182	43	12	31.51	9.6	103	0.63	11.1	314	716
183	43	14	30.97	10.9	168	0.79	10.5	320	718
184	43	16	30.49	8.1	200	0.82	11.5	324	720

BT	JD	Hour	depth	u ₅₀	C _{dir}	H _s	T _z	W _{dir}	obs l
185	43	18	30.31	2.9	272	0.88	11.9	340	720
186	43	20	30.68	10.6	351	1.02	10.8	342	719
187	43	22	31.35	15.0	20	0.83	10.4	338	716
188	44	0	31.57	17.0	72	0.86	10.5	338	716
189	44	2	31.14	13.1	122	0.79	11.1	340	716
190	44	4	30.71	9.5	147	0.75	10.1	324	718
191	44	6	30.47	5.4	174	0.73	10.5	330	719
192	44	8	30.60	3.9	348	0.58	10.5	334	722
193	44	10	31.21	6.1	21	0.59	10.1	302	720
194	44	12	31.50	8.4	130	0.54	11.1	324	718
195	44	14	31.20	16.1	175	0.57	10.2	330	719
196	44	16	30.80	28.4	202	0.72	8.8	328	717
197	44	18	30.58	27.8	228	0.80	8.4	174	716
198	44	20	30.61	25.6	256	0.71	8.9	178	716
199	44	22	31.16	21.8	312	0.67	8.2	176	718
200	45	0	31.66	8.3	353	0.69	8.7	176	719
201	45	2	31.46	3.0	136	0.52	9.4	266	720
202	45	4	31.08	4.5	105	0.53	9.6	250	718
203	45	6	30.78	0.4	184	0.53	10.0	264	721
204	45	8	30.61	3.7	348	0.53	10.9	66	724
205	45	10	30.92	12.8	18	0.55	9.3	88	722
206	45	12	31.35	12.5	57	0.51	10.0	70	717
207	45	14	31.34	12.2	134	0.48	9.9	82	719
208	45	16	31.00	18.4	166	0.53	9.6	120	719
209	45	18	30.71	17.1	196	0.56	10.0	86	718
210	45	20	30.56	12.0	230	0.56	9.6	70	720
211	45	22	30.85	17.3	318	0.54	9.5	124	718
212	46	0	31.41	18.3	18	0.45	10.0	106	718
213	46	2	31.51	20.7	59	0.47	10.0	56	718
214	46	4	31.21	23.5	85	0.45	10.4	84	719
215	46	6	30.88	24.7	96	1.01	9.1	28	719
216	46	8	30.60	17.3	110	1.25	9.8	26	719
217	46	10	30.61	10.2	112	1.41	10.5	32	724
218	46	12	31.09	9.3	120	1.54	10.8	34	725
219	46	14	31.20	10.1	158	1.58	11.4	4	723
220	46	16	31.03	28.0	172	1.82	11.4	338	721
221	46	18	30.78	27.2	218	1.94	11.1	348	728
222	46	20	30.58	19.9	248	1.92	11.4	356	722
223	46	22	30.65	23.8	287	1.86	10.6	334	725
224	47	0	31.07	25.6	316	1.95	11.5	360	724
225	47	2	31.41	13.5	330	1.84	11.7	348	721
226	47	4	31.38	6.4	3	1.50	12.2	122	719
227	47	6	31.03	6.8	89	1.36	11.4	128	720
228	47	8	30.71	5.9	253	1.52	11.7	128	720
229	47	10	30.56	11.2	227	1.77	12.0	130	721
230	47	12	30.86	6.0	287	1.33	11.4	132	722

BT	JD	Hour	depth	u ₅₀	C _{dir}	H _s	T _z	W _{dir}	obs l
231	47	14	31.28	14.0	241	1.26	12.0	128	722
232	47	16	31.28	16.5	236	1.14	11.5	116	721
233	47	18	31.08	26.3	243	1.23	11.1	108	717
234	47	20	30.85	24.3	247	0.98	11.4	104	720
235	47	22	30.67	19.7	273	1.04	11.4	108	718
236	48	0	30.87	29.9	303	0.87	11.1	342	715
237	48	2	31.32	22.2	304	0.82	10.9	346	718
238	48	4	31.54	16.6	56	0.70	10.4	356	720
239	48	6	31.37	19.7	105	0.72	10.6	22	720

Appendix 4

Predictions by SEDTRANS96 for SI97a Ralph deployment: (a) bottom boundary layer dynamics parameters; (b) sediment transport parameters. Listed parameters are as defined in Appendix 2.

bt#	u_b	A_b	f_{cws}	u^*_{cs}	u^*_{ws}	u^*_{cws}	u^*_{cwe}	u^*_{cwb}	u^*_c	u^*_w	u^*_{cw}	δ_{cw}	Z_0	Z_{0c}
1	0.076	0.130	0.0144	1.07	0.96	1.43	2.19	1.43	1.84	2.08	2.76	3.80	0.16	0.46
2	0.081	0.162	0.0139	0.95	0.95	1.33	2.03	1.33	1.63	2.03	2.57	4.13	0.16	0.52
3	0.074	0.129	0.0155	0.81	0.88	1.17	1.79	1.17	1.37	1.92	2.31	3.21	0.15	0.52
4	0.076	0.119	0.0182	0.40	0.81	0.89	1.40	0.89	0.65	1.91	2.01	2.51	0.15	1.02
5	0.075	0.108	0.0179	0.55	0.85	1.00	1.57	1.00	0.91	1.97	2.17	2.49	0.15	0.77
6	0.078	0.106	0.0156	1.08	1.01	1.48	2.26	1.48	1.85	2.26	2.91	3.15	0.16	0.48
7	0.133	0.192	0.0137	1.26	1.45	1.92	3.63	2.83	2.57	4.03	4.78	5.54	0.40	1.35
8	0.221	0.338	0.0129	1.08	1.94	2.12	4.01	3.50	2.30	5.71	5.97	7.30	0.48	2.56
9	0.252	0.405	0.0125	0.92	2.10	2.21	4.05	3.76	1.93	6.10	6.26	8.05	0.47	3.36
10	0.277	0.462	0.0121	0.66	2.24	2.33	3.81	4.10	1.27	6.01	6.14	8.21	0.37	4.32
11	0.259	0.416	0.0125	0.60	2.13	2.21	4.01	3.79	1.20	6.16	6.28	8.07	0.46	4.68
12	0.219	0.351	0.0132	0.52	1.84	1.91	3.62	2.97	1.00	5.27	5.36	6.90	0.41	4.07
13	0.222	0.356	0.0131	0.68	1.87	1.95	3.69	3.07	1.36	5.37	5.48	7.05	0.42	3.52
14	0.193	0.308	0.0128	1.32	1.79	2.07	3.91	3.28	2.84	5.11	5.53	7.04	0.45	1.72
15	0.206	0.347	0.0118	1.57	1.98	2.48	3.89	4.23	3.16	5.03	5.84	7.88	0.35	1.46
16	0.185	0.288	0.0127	1.26	1.79	2.19	4.14	3.56	2.69	5.18	5.83	7.28	0.49	2.10
17	0.179	0.287	0.0135	0.83	1.63	1.81	3.42	2.61	1.65	4.49	4.75	6.11	0.37	2.30
18	0.154	0.233	0.0149	0.81	1.40	1.48	2.26	1.48	1.42	3.22	3.31	4.00	0.16	1.01
19	0.145	0.218	0.0148	0.77	1.37	1.50	2.29	1.50	1.31	3.12	3.28	3.97	0.16	1.11
20	0.143	0.212	0.0149	0.71	1.37	1.52	2.32	1.52	1.20	3.13	3.32	3.93	0.16	1.24
21	0.137	0.218	0.0144	1.06	1.33	1.53	2.34	1.53	1.86	3.00	3.24	4.12	0.17	0.65
22	0.134	0.208	0.0140	1.08	1.37	1.68	3.17	2.14	2.11	3.60	4.05	5.05	0.31	1.18
23	0.119	0.182	0.0143	1.01	1.28	1.63	3.08	1.93	1.92	3.30	3.81	4.66	0.28	1.13
24	0.103	0.149	0.0160	0.71	1.09	1.30	1.99	1.30	1.19	2.48	2.75	3.18	0.15	0.86
25	0.092	0.135	0.0172	0.51	0.96	1.09	1.66	1.09	0.83	2.20	2.35	2.75	0.14	0.97
26	0.086	0.124	0.0165	0.73	0.97	1.21	1.85	1.21	1.23	2.18	2.50	2.89	0.15	0.67
27	0.078	0.113	0.0158	0.95	0.96	1.34	2.05	1.34	1.62	2.15	2.67	3.09	0.16	0.51
28	0.081	0.127	0.0137	1.38	1.08	1.75	2.81	2.31	2.44	2.42	3.44	4.34	0.19	0.48
29	0.070	0.102	0.0155	1.07	0.92	1.40	2.13	1.40	1.83	2.04	2.70	3.16	0.16	0.41
30	0.066	0.098	0.0145	1.30	0.94	1.59	2.56	1.69	2.16	1.96	2.89	3.46	0.14	0.32
31	0.069	0.110	0.0149	1.08	0.92	1.42	2.17	1.42	1.85	2.00	2.72	3.47	0.16	0.43
32	0.063	0.101	0.0187	0.57	0.71	0.82	1.28	0.82	0.99	1.68	1.79	2.28	0.15	0.51
33	0.072	0.122	0.0186	0.54	0.74	0.79	1.23	0.79	0.94	1.77	1.81	2.44	0.15	0.57
34	0.068	0.108	0.0185	0.63	0.74	0.84	1.31	0.84	1.10	1.75	1.84	2.34	0.15	0.46
35	0.065	0.104	0.0198	0.42	0.69	0.72	1.13	0.72	0.71	1.68	1.71	2.18	0.15	0.72
36	0.065	0.106	0.0191	0.35	0.70	0.77	1.21	0.77	0.57	1.69	1.77	2.29	0.15	0.95
37	0.065	0.105	0.0175	0.62	0.76	0.95	1.48	0.95	1.04	1.75	1.99	2.55	0.15	0.58
38	0.064	0.107	0.0170	0.62	0.76	0.97	1.52	0.97	1.04	1.73	2.01	2.69	0.15	0.61
39	0.062	0.091	0.0187	0.51	0.72	0.88	1.38	0.88	0.85	1.71	1.90	2.25	0.15	0.68
40	0.059	0.082	0.0177	0.85	0.77	1.08	1.65	1.08	1.43	1.73	2.11	2.34	0.14	0.35
41	0.070	0.092	0.0152	1.36	1.00	1.63	2.62	1.91	2.32	2.17	3.06	3.20	0.16	0.33
42	0.099	0.129	0.0135	1.74	1.34	2.19	3.52	3.40	3.35	3.35	4.73	4.94	0.30	0.68
43	0.208	0.311	0.0119	2.02	2.08	2.70	3.67	4.74	3.80	4.80	5.72	6.84	0.24	0.75
44	0.368	0.614	0.0104	1.97	3.06	3.52	3.52	7.05	3.48	6.36	7.05	9.43	0.18	1.33
45	0.310	0.552	0.0114	1.04	2.46	2.59	3.52	4.74	1.92	5.69	5.87	8.37	0.23	2.60
46	0.433	0.805	0.0103	0.98	3.19	3.27	3.27	6.60	1.65	6.49	6.60	9.84	0.16	3.49

bt#	u_b	A_b	f_{cws}	u^*_{cs}	u^*_{ws}	u^*_{cws}	u^*_{cwe}	u^*_{cwb}	u^*_c	u^*_w	u^*_{cw}	δ_{cw}	Z_0	Z_{0c}
47	0.612	1.286	0.0092	0.36	4.15	4.15	4.15	9.02	0.64	9.02	9.02	15.17	0.24	11.28
48	0.492	1.019	0.0097	0.48	3.47	3.50	3.50	7.19	0.80	7.15	7.19	11.91	0.18	7.46
49	0.600	1.203	0.0093	0.20	4.10	4.11	4.11	8.94	0.34	8.94	8.94	14.35	0.23	12.26
50	0.387	0.733	0.0107	0.42	2.85	2.86	3.20	5.54	0.67	5.75	5.77	8.75	0.14	5.43
51	0.436	0.833	0.0102	0.64	3.19	3.25	3.25	6.54	1.05	6.45	6.54	9.98	0.15	5.10
52	0.407	0.770	0.0103	1.05	3.08	3.25	3.25	6.45	1.76	6.21	6.45	9.77	0.15	3.14
53	0.325	0.563	0.0112	1.09	2.58	2.74	3.37	5.14	1.89	5.54	5.76	8.00	0.18	2.28
54	0.266	0.474	0.0120	0.99	2.14	2.22	4.04	3.78	2.11	6.11	6.23	8.88	0.47	3.27
55	0.225	0.387	0.0120	1.34	2.01	2.33	4.02	3.94	2.81	5.49	6.00	8.24	0.42	2.06
56	0.196	0.327	0.0126	1.05	1.79	2.07	3.91	3.28	2.19	5.09	5.53	7.39	0.45	2.45
57	0.171	0.293	0.0135	0.72	1.53	1.67	3.16	2.16	1.36	4.05	4.25	5.84	0.31	2.28
58	0.175	0.303	0.0134	0.86	1.55	1.68	3.18	2.20	1.68	4.12	4.30	5.96	0.32	1.89
59	0.191	0.322	0.0137	0.68	1.62	1.66	3.14	2.14	1.31	4.33	4.39	5.92	0.31	2.45
60	0.150	0.253	0.0149	0.26	1.31	1.33	2.03	1.33	0.39	2.99	3.01	4.06	0.15	2.65
61	0.154	0.245	0.0151	0.16	1.35	1.36	2.07	1.36	0.23	3.11	3.12	3.97	0.16	3.13
62	0.129	0.205	0.0160	0.21	1.17	1.18	1.80	1.18	0.32	2.69	2.70	3.44	0.15	2.38
63	0.128	0.208	0.0155	0.46	1.19	1.26	1.92	1.26	0.75	2.71	2.79	3.62	0.15	1.55
64	0.110	0.176	0.0162	0.43	1.07	1.15	1.76	1.15	0.70	2.44	2.53	3.22	0.15	1.37
65	0.120	0.190	0.0147	0.81	1.23	1.47	2.24	1.47	1.38	2.75	3.07	3.91	0.16	0.94
66	0.109	0.163	0.0152	0.88	1.17	1.44	2.20	1.44	1.50	2.63	2.99	3.58	0.16	0.75
67	0.100	0.150	0.0168	0.83	1.02	1.12	1.71	1.12	1.44	2.31	2.41	2.88	0.14	0.48
68	0.091	0.131	0.0154	1.00	1.06	1.43	2.18	1.43	1.72	2.38	2.87	3.32	0.16	0.54
69	0.076	0.107	0.0162	0.89	0.94	1.29	1.97	1.29	1.50	2.10	2.58	2.92	0.15	0.52
70	0.085	0.120	0.0156	0.98	1.03	1.41	2.15	1.41	1.68	2.30	2.82	3.19	0.16	0.53
71	0.087	0.132	0.0156	0.99	1.01	1.32	2.02	1.32	1.69	2.25	2.65	3.21	0.15	0.46
72	0.068	0.093	0.0199	0.61	0.75	0.83	1.30	0.83	1.06	1.81	1.88	2.06	0.15	0.47
73	0.079	0.113	0.0196	0.29	0.80	0.82	1.29	0.82	0.47	1.98	2.00	2.29	0.15	1.20
74	0.072	0.098	0.0202	0.32	0.76	0.81	1.26	0.81	0.51	1.88	1.93	2.11	0.15	1.05
75	0.079	0.115	0.0191	0.50	0.81	0.85	1.33	0.85	0.87	1.96	2.00	2.34	0.15	0.71
76	0.075	0.112	0.0160	0.88	0.92	1.26	1.92	1.26	1.49	2.04	2.50	3.00	0.15	0.51
77	0.069	0.097	0.0158	1.02	0.92	1.37	2.10	1.37	1.74	2.03	2.68	3.03	0.16	0.44
78	0.076	0.111	0.0141	1.41	1.06	1.76	2.82	2.31	2.50	2.38	3.44	4.03	0.20	0.45
79	0.060	0.079	0.0151	1.38	0.92	1.63	2.62	1.91	2.35	1.99	3.02	3.19	0.16	0.31
80	0.049	0.061	0.0167	1.12	0.79	1.37	2.09	1.37	1.91	1.75	2.58	2.56	0.16	0.32
81	0.054	0.072	0.0160	1.15	0.83	1.42	2.17	1.42	1.96	1.83	2.69	2.84	0.16	0.35
82	0.059	0.081	0.0167	0.98	0.82	1.25	1.91	1.25	1.66	1.82	2.41	2.64	0.15	0.37
83	0.058	0.081	0.0168	0.90	0.80	1.21	1.85	1.21	1.52	1.79	2.35	2.60	0.15	0.41
84	0.042	0.050	0.0220	0.61	0.58	0.77	1.20	0.77	1.05	1.41	1.61	1.54	0.15	0.34
85	0.050	0.063	0.0200	0.60	0.67	0.90	1.40	0.90	1.00	1.58	1.87	1.88	0.15	0.49
86	0.047	0.057	0.0216	0.50	0.62	0.79	1.23	0.79	0.84	1.51	1.71	1.66	0.15	0.51
87	0.040	0.047	0.0254	0.40	0.51	0.58	0.91	0.58	0.68	1.31	1.38	1.30	0.15	0.45
88	0.046	0.058	0.0219	0.44	0.59	0.73	1.14	0.73	0.72	1.45	1.61	1.64	0.15	0.57
89	0.067	0.101	0.0162	0.86	0.86	1.21	1.86	1.21	1.45	1.90	2.39	2.86	0.15	0.48
90	0.061	0.083	0.0155	1.19	0.89	1.48	2.26	1.48	2.04	1.96	2.82	3.09	0.16	0.37
91	0.048	0.061	0.0162	1.20	0.79	1.43	2.19	1.43	2.05	1.74	2.68	2.73	0.16	0.31
92	0.030	0.033	0.0181	1.14	0.61	1.29	1.97	1.29	1.92	1.35	2.34	2.06	0.15	0.24

bt#	u_b	A_b	f_{cws}	u^*_{cs}	u^*_{ws}	u^*_{cws}	u^*_{cwe}	u^*_{cwb}	u^*_c	u^*_w	u^*_{cw}	δ_{cw}	Z_0	Z_{0c}
93	0.049	0.064	0.0153	1.39	0.83	1.62	2.60	1.85	2.35	1.78	2.95	3.08	0.15	0.28
94	0.038	0.046	0.0170	1.18	0.69	1.35	2.06	1.35	1.99	1.52	2.47	2.39	0.16	0.26
95	0.054	0.075	0.0158	1.14	0.82	1.40	2.14	1.40	1.94	1.80	2.65	2.93	0.16	0.35
96	0.061	0.091	0.0154	1.10	0.86	1.39	2.13	1.39	1.88	1.88	2.65	3.17	0.16	0.38
97	0.051	0.066	0.0174	0.92	0.75	1.18	1.80	1.18	1.54	1.67	2.25	2.35	0.15	0.35
98	0.048	0.061	0.0204	0.57	0.64	0.85	1.32	0.85	0.95	1.52	1.78	1.81	0.15	0.48
99	0.048	0.063	0.0245	0.23	0.54	0.56	0.88	0.56	0.36	1.42	1.43	1.52	0.15	0.85
100	0.058	0.086	0.0212	0.25	0.63	0.66	1.04	0.66	0.39	1.57	1.61	1.92	0.15	1.03
101	0.057	0.080	0.0198	0.46	0.68	0.82	1.28	0.82	0.76	1.64	1.80	2.02	0.15	0.68
102	0.053	0.069	0.0187	0.72	0.72	1.01	1.58	1.01	1.21	1.66	2.04	2.13	0.15	0.44
103	0.065	0.086	0.0188	0.65	0.79	0.98	1.54	0.98	1.11	1.85	2.09	2.21	0.15	0.53
104	0.079	0.097	0.0192	0.54	0.88	1.01	1.57	1.01	0.90	2.12	2.26	2.21	0.15	0.76
105	0.117	0.160	0.0143	1.22	1.34	1.81	2.91	2.53	2.21	3.16	3.86	4.22	0.21	0.76
106	0.182	0.269	0.0127	1.40	1.82	2.28	4.16	3.78	2.97	5.19	5.96	7.06	0.47	1.84
107	0.216	0.340	0.0117	1.91	2.10	2.68	3.67	4.70	3.60	4.87	5.74	7.23	0.25	0.87
108	0.254	0.428	0.0115	1.87	2.26	2.65	3.64	4.70	3.55	5.22	5.78	7.80	0.25	0.94
109	0.340	0.606	0.0101	2.25	2.98	3.69	3.69	7.32	4.03	6.21	7.32	10.44	0.19	1.16
110	0.304	0.523	0.0108	1.63	2.63	3.09	3.23	5.87	2.74	5.23	5.91	8.12	0.14	1.25
111	0.274	0.462	0.0114	1.56	2.37	2.71	3.51	4.93	2.84	5.25	5.76	7.77	0.21	1.30
112	0.243	0.406	0.0124	1.26	2.03	2.16	4.08	3.60	2.78	5.94	6.11	8.17	0.49	2.27
113	0.225	0.391	0.0125	0.92	1.91	2.04	3.86	3.28	1.91	5.45	5.65	7.84	0.45	2.98
114	0.196	0.331	0.0126	1.16	1.78	2.03	3.84	3.20	2.44	5.04	5.42	7.32	0.44	2.07
115	0.221	0.384	0.0122	1.26	1.95	2.20	4.16	3.63	2.75	5.62	6.01	8.34	0.50	2.29
116	0.168	0.269	0.0135	1.20	1.58	1.81	3.42	2.58	2.47	4.31	4.63	5.95	0.36	1.34
117	0.194	0.327	0.0117	1.68	1.92	2.49	3.92	4.22	3.38	4.88	5.80	7.83	0.35	1.28
118	0.189	0.313	0.0115	1.85	1.96	2.69	3.72	4.66	3.47	4.53	5.70	7.54	0.26	0.96
119	0.142	0.237	0.0136	0.96	1.41	1.70	3.21	2.22	1.86	3.70	4.14	5.53	0.32	1.53
120	0.138	0.230	0.0139	1.16	1.36	1.60	2.57	1.77	2.00	2.90	3.20	4.28	0.14	0.52
121	0.137	0.227	0.0131	1.29	1.45	1.90	3.60	2.77	2.63	3.94	4.66	6.17	0.39	1.30
122	0.129	0.206	0.0130	1.37	1.44	1.99	3.19	2.97	2.57	3.47	4.31	5.49	0.26	0.89
123	0.117	0.183	0.0136	1.29	1.32	1.81	2.90	2.50	2.33	3.06	3.77	4.70	0.21	0.69
124	0.107	0.161	0.0157	0.99	1.11	1.30	1.99	1.30	1.72	2.49	2.71	3.28	0.15	0.47
125	0.094	0.149	0.0156	0.84	1.02	1.26	1.93	1.26	1.43	2.27	2.59	3.29	0.15	0.60
126	0.084	0.128	0.0168	0.66	0.93	1.11	1.69	1.11	1.10	2.09	2.32	2.80	0.14	0.68
127	0.086	0.129	0.0160	0.79	0.98	1.25	1.92	1.25	1.33	2.20	2.56	3.07	0.15	0.64
128	0.102	0.164	0.0135	1.43	1.22	1.78	2.86	2.39	2.58	2.77	3.57	4.59	0.20	0.48
129	0.083	0.121	0.0156	1.17	1.00	1.37	2.09	1.37	2.01	2.21	2.66	3.11	0.16	0.32
130	0.081	0.122	0.0135	1.53	1.12	1.89	3.04	2.66	2.79	2.61	3.81	4.61	0.23	0.51
131	0.076	0.124	0.0129	1.67	1.11	1.99	3.20	2.87	3.09	2.58	4.01	5.21	0.25	0.50
132	0.074	0.109	0.0150	1.15	0.98	1.50	2.30	1.50	1.98	2.16	2.91	3.45	0.16	0.43
133	0.079	0.126	0.0166	0.73	0.88	1.08	1.65	1.08	1.23	1.96	2.21	2.84	0.14	0.54
134	0.072	0.111	0.0150	1.08	0.95	1.44	2.19	1.44	1.84	2.08	2.78	3.40	0.16	0.45
135	0.072	0.107	0.0152	1.12	0.94	1.42	2.17	1.42	1.91	2.07	2.74	3.27	0.16	0.40
136	0.070	0.107	0.0176	0.76	0.81	0.99	1.54	0.99	1.31	1.85	2.06	2.51	0.15	0.42
137	0.066	0.098	0.0177	0.64	0.78	0.99	1.55	0.99	1.08	1.80	2.07	2.48	0.15	0.58
138	0.069	0.109	0.0177	0.51	0.78	0.93	1.45	0.93	0.86	1.80	1.99	2.54	0.15	0.75

bt#	u_b	A_b	f_{cws}	u^*_{cs}	u^*_{ws}	u^*_{cws}	u^*_{cwe}	u^*_{cwb}	u^*_c	u^*_w	u^*_{cw}	δ_{cw}	Z_0	Z_{0c}
139	0.070	0.122	0.0140	1.19	0.94	1.52	2.32	1.52	2.04	2.03	2.88	3.99	0.16	0.41
140	0.063	0.096	0.0135	1.62	0.98	1.89	3.03	2.61	2.93	2.26	3.68	4.50	0.23	0.42
141	0.064	0.098	0.0135	1.59	0.99	1.88	3.01	2.59	2.89	2.28	3.68	4.49	0.22	0.43
142	0.066	0.103	0.0131	1.71	1.03	2.00	3.21	2.87	3.17	2.41	3.98	4.97	0.25	0.46
143	0.067	0.113	0.0124	1.88	1.07	2.16	3.47	3.22	3.57	2.53	4.37	5.90	0.29	0.50
144	0.064	0.107	0.0138	1.36	0.93	1.63	2.62	1.90	2.31	1.95	2.99	4.04	0.16	0.33
145	0.066	0.114	0.0141	1.17	0.91	1.48	2.26	1.48	2.01	1.95	2.80	3.89	0.16	0.40
146	0.056	0.082	0.0162	0.98	0.80	1.25	1.91	1.25	1.65	1.75	2.38	2.79	0.15	0.37
147	0.068	0.117	0.0152	0.93	0.86	1.25	1.91	1.25	1.57	1.87	2.42	3.33	0.15	0.45
148	0.065	0.105	0.0157	0.89	0.84	1.22	1.87	1.22	1.50	1.84	2.37	3.05	0.15	0.45
149	0.056	0.083	0.0152	1.17	0.84	1.44	2.19	1.44	1.99	1.84	2.70	3.20	0.16	0.35
150	0.049	0.065	0.0192	0.66	0.66	0.92	1.44	0.92	1.11	1.55	1.88	2.01	0.15	0.43
151	0.060	0.084	0.0201	0.45	0.69	0.80	1.24	0.80	0.75	1.68	1.80	2.01	0.15	0.69
152	0.075	0.109	0.0158	1.08	0.94	1.32	2.02	1.32	1.85	2.07	2.56	3.00	0.15	0.35
153	0.111	0.175	0.0150	1.16	1.16	1.41	2.16	1.41	2.03	2.58	2.85	3.60	0.16	0.39
154	0.180	0.335	0.0127	1.21	1.62	1.82	3.45	2.61	2.50	4.35	4.63	6.90	0.37	1.42
155	0.374	0.750	0.0097	2.06	3.09	3.67	3.67	7.29	3.69	6.38	7.29	11.70	0.19	1.47
156	0.250	0.494	0.0106	1.73	2.28	2.85	3.52	5.12	3.08	4.79	5.68	8.96	0.19	1.11
157	0.229	0.445	0.0117	1.32	1.96	2.20	4.16	3.61	2.89	5.56	5.94	9.23	0.50	2.23
158	0.198	0.378	0.0122	1.14	1.75	1.99	3.76	3.07	2.40	4.84	5.21	7.96	0.43	2.07
159	0.180	0.344	0.0120	1.20	1.70	2.08	3.93	3.25	2.53	4.70	5.33	8.14	0.45	2.06
160	0.157	0.284	0.0128	1.02	1.51	1.82	3.44	2.57	2.04	4.04	4.52	6.55	0.36	1.78
161	0.128	0.221	0.0148	0.74	1.21	1.33	2.03	1.33	1.26	2.72	2.86	3.94	0.16	0.95
162	0.102	0.175	0.0155	0.59	1.03	1.18	1.81	1.18	0.97	2.30	2.49	3.43	0.15	1.01
163	0.099	0.176	0.0156	0.58	0.99	1.12	1.71	1.12	0.96	2.20	2.36	3.37	0.14	0.93
164	0.091	0.153	0.0144	1.01	1.06	1.45	2.21	1.45	1.73	2.31	2.87	3.87	0.16	0.57
165	0.092	0.153	0.0133	1.39	1.17	1.81	2.90	2.47	2.50	2.65	3.63	4.81	0.21	0.56
166	0.085	0.134	0.0141	1.26	1.08	1.64	2.63	1.95	2.17	2.33	3.14	3.95	0.16	0.43
167	0.082	0.137	0.0143	1.17	1.01	1.48	2.26	1.48	2.01	2.20	2.85	3.81	0.16	0.41
168	0.077	0.122	0.0136	1.43	1.07	1.78	2.86	2.39	2.55	2.40	3.51	4.42	0.20	0.47
169	0.077	0.128	0.0147	1.04	0.97	1.41	2.15	1.41	1.77	2.11	2.73	3.62	0.16	0.48
170	0.077	0.140	0.0162	0.60	0.83	1.00	1.57	1.00	1.02	1.89	2.10	3.05	0.15	0.71
171	0.071	0.118	0.0165	0.66	0.83	1.06	1.62	1.06	1.10	1.84	2.14	2.84	0.14	0.60
172	0.071	0.115	0.0158	0.89	0.88	1.22	1.86	1.22	1.50	1.93	2.39	3.07	0.15	0.46
173	0.065	0.099	0.0168	0.96	0.81	1.10	1.68	1.10	1.64	1.78	2.10	2.57	0.14	0.27
174	0.061	0.088	0.0146	1.34	0.92	1.62	2.61	1.87	2.27	1.96	3.00	3.47	0.15	0.33
175	0.056	0.078	0.0173	0.84	0.77	1.13	1.73	1.13	1.40	1.71	2.20	2.44	0.15	0.40
176	0.046	0.059	0.0254	0.15	0.53	0.54	0.84	0.54	0.23	1.40	1.41	1.44	0.15	1.00
177	0.060	0.080	0.0181	0.74	0.78	1.06	1.62	1.06	1.24	1.75	2.12	2.27	0.14	0.45
178	0.065	0.090	0.0167	0.89	0.86	1.24	1.89	1.24	1.51	1.91	2.43	2.69	0.15	0.45
179	0.064	0.086	0.0176	0.77	0.82	1.12	1.72	1.12	1.29	1.86	2.25	2.41	0.14	0.48
180	0.075	0.112	0.0151	1.09	0.98	1.46	2.24	1.46	1.86	2.16	2.85	3.38	0.16	0.46
181	0.085	0.130	0.0161	0.87	0.96	1.22	1.86	1.22	1.48	2.15	2.47	3.02	0.15	0.50
182	0.115	0.203	0.0150	0.60	1.12	1.25	1.91	1.25	1.01	2.49	2.66	3.77	0.15	1.11
183	0.138	0.230	0.0144	0.70	1.31	1.47	2.24	1.47	1.18	2.94	3.15	4.21	0.16	1.24
184	0.160	0.292	0.0139	0.57	1.40	1.47	2.24	1.47	0.96	3.14	3.23	4.72	0.16	1.73

bt#	u_b	A_b	f_{cws}	u^*_{cs}	u^*_{ws}	u^*_{cws}	u^*_{cwe}	u^*_{cwb}	u^*_c	u^*_w	u^*_{cw}	δ_{cw}	Z_0	Z_{0c}
185	0.178	0.336	0.0136	0.27	1.48	1.48	2.27	1.48	0.43	3.33	3.34	5.06	0.16	3.27
186	0.186	0.319	0.0131	0.74	1.65	1.81	3.41	2.60	1.45	4.51	4.73	6.51	0.37	2.69
187	0.141	0.234	0.0140	0.89	1.37	1.58	3.00	1.59	1.64	3.39	3.69	4.89	0.24	1.29
188	0.147	0.245	0.0146	0.92	1.34	1.42	2.18	1.42	1.62	3.02	3.11	4.16	0.16	0.76
189	0.146	0.257	0.0137	0.81	1.37	1.56	2.38	1.56	1.39	3.06	3.31	4.67	0.17	1.15
190	0.126	0.202	0.0150	0.62	1.22	1.37	2.09	1.37	1.03	2.76	2.94	3.79	0.16	1.24
191	0.130	0.217	0.0153	0.40	1.19	1.25	1.91	1.25	0.65	2.71	2.78	3.72	0.15	1.77
192	0.103	0.171	0.0167	0.29	0.98	1.02	1.56	1.02	0.46	2.23	2.28	3.04	0.14	1.64
193	0.097	0.156	0.0175	0.40	0.93	0.95	1.49	0.95	0.66	2.21	2.24	2.88	0.15	1.21
194	0.098	0.174	0.0157	0.53	0.99	1.12	1.70	1.12	0.87	2.20	2.37	3.34	0.14	1.05
195	0.095	0.154	0.0150	0.87	1.06	1.35	2.07	1.35	1.49	2.34	2.75	3.57	0.16	0.66
196	0.096	0.135	0.0145	1.36	1.18	1.71	2.74	2.18	2.40	2.66	3.39	3.80	0.18	0.44
197	0.098	0.131	0.0148	1.34	1.20	1.70	2.73	2.17	2.36	2.71	3.40	3.63	0.18	0.45
198	0.098	0.139	0.0155	1.20	1.11	1.44	2.20	1.44	2.08	2.49	2.87	3.26	0.16	0.37
199	0.075	0.098	0.0163	1.06	0.97	1.39	2.12	1.39	1.82	2.17	2.73	2.85	0.16	0.41
200	0.086	0.120	0.0178	0.51	0.93	1.06	1.61	1.06	0.83	2.14	2.29	2.54	0.14	0.90
201	0.076	0.114	0.0196	0.22	0.77	0.79	1.24	0.79	0.34	1.90	1.92	2.30	0.15	1.42
202	0.082	0.125	0.0185	0.31	0.83	0.87	1.37	0.87	0.49	1.99	2.04	2.50	0.15	1.27
203	0.088	0.139	0.0185	0.04	0.84	0.84	1.32	0.84	0.05	2.05	2.05	2.61	0.15	2.43
204	0.098	0.169	0.0171	0.27	0.91	0.92	1.44	0.92	0.43	2.17	2.18	3.02	0.15	1.66
205	0.081	0.120	0.0177	0.67	0.87	1.00	1.57	1.00	1.15	2.04	2.19	2.59	0.15	0.58
206	0.082	0.131	0.0162	0.69	0.92	1.15	1.76	1.15	1.16	2.06	2.36	3.01	0.15	0.68
207	0.077	0.121	0.0171	0.65	0.85	1.02	1.56	1.02	1.09	1.91	2.12	2.67	0.14	0.58
208	0.082	0.125	0.0157	0.93	0.97	1.29	1.97	1.29	1.59	2.14	2.57	3.14	0.15	0.48
209	0.093	0.148	0.0159	0.86	0.99	1.20	1.83	1.20	1.48	2.22	2.46	3.13	0.15	0.50
210	0.088	0.134	0.0163	0.68	0.97	1.17	1.79	1.17	1.14	2.17	2.44	2.98	0.15	0.73
211	0.083	0.125	0.0156	0.91	0.98	1.33	2.04	1.33	1.54	2.19	2.67	3.23	0.16	0.56
212	0.073	0.115	0.0172	0.84	0.82	1.00	1.56	1.00	1.46	1.86	2.04	2.59	0.15	0.34
213	0.076	0.120	0.0149	1.04	0.96	1.42	2.16	1.42	1.78	2.10	2.75	3.51	0.16	0.48
214	0.077	0.127	0.0142	1.16	1.00	1.53	2.34	1.53	2.00	2.17	2.95	3.91	0.17	0.46
215	0.143	0.208	0.0142	1.27	1.46	1.76	3.33	2.41	2.56	3.96	4.37	5.06	0.34	1.05
216	0.202	0.315	0.0136	1.02	1.74	1.82	3.44	2.68	2.11	4.90	4.98	6.22	0.37	1.89
217	0.249	0.416	0.0127	0.76	2.01	2.05	3.87	3.37	1.57	5.89	5.93	7.93	0.46	3.73
218	0.276	0.475	0.0122	0.73	2.17	2.19	4.01	3.77	1.52	6.31	6.33	8.70	0.47	4.32
219	0.299	0.542	0.0114	0.82	2.38	2.50	3.63	4.50	1.53	5.77	5.95	8.63	0.28	3.57
220	0.346	0.627	0.0103	1.81	2.91	3.42	3.42	6.70	3.16	5.92	6.70	9.72	0.17	1.44
221	0.362	0.639	0.0105	1.75	2.94	3.29	3.29	6.47	3.03	5.95	6.47	9.15	0.16	1.37
222	0.370	0.671	0.0108	1.38	2.84	2.97	3.18	5.76	2.33	5.66	5.84	8.48	0.14	1.64
223	0.332	0.560	0.0109	1.55	2.73	3.05	3.19	5.86	2.62	5.45	5.90	7.96	0.14	1.32
224	0.373	0.683	0.0103	1.70	2.99	3.35	3.35	6.61	2.95	6.08	6.61	9.68	0.16	1.56
225	0.354	0.659	0.0107	1.07	2.76	2.96	3.23	5.66	1.79	5.53	5.79	8.63	0.14	2.43
226	0.299	0.581	0.0114	0.59	2.30	2.34	3.82	4.10	1.13	6.07	6.12	9.50	0.37	5.22
227	0.258	0.469	0.0121	0.58	2.07	2.14	4.04	3.57	1.19	6.01	6.10	8.86	0.49	5.04
228	0.299	0.556	0.0116	0.55	2.31	2.35	3.78	4.15	1.05	6.07	6.12	9.12	0.36	5.25
229	0.357	0.681	0.0109	0.91	2.66	2.69	3.36	5.07	1.60	5.76	5.79	8.85	0.18	3.04
230	0.254	0.461	0.0122	0.53	2.04	2.10	3.98	3.48	1.06	5.90	5.99	8.69	0.48	5.19

bt#	u_b	A_b	f_{cws}	u^*_{cs}	u^*_{ws}	u^*_{cws}	u^*_{cwe}	u^*_{cwb}	u^*_c	u^*_w	u^*_{cw}	δ_{cw}	z_0	z_{0c}
231	0.249	0.475	0.0119	0.96	2.02	2.12	4.02	3.50	2.05	5.77	5.93	9.06	0.48	3.27
232	0.217	0.397	0.0123	1.04	1.85	2.02	3.82	3.19	2.20	5.22	5.47	8.01	0.44	2.49
233	0.227	0.402	0.0116	1.52	2.07	2.48	3.85	4.26	3.04	5.22	5.87	8.29	0.34	1.58
234	0.187	0.340	0.0120	1.38	1.78	2.20	4.16	3.54	2.98	5.03	5.73	8.31	0.49	1.91
235	0.200	0.363	0.0120	1.21	1.84	2.19	4.15	3.56	2.59	5.22	5.81	8.43	0.49	2.38
236	0.162	0.286	0.0120	1.57	1.67	2.23	3.58	3.56	3.09	4.14	5.03	7.10	0.31	1.04
237	0.148	0.256	0.0130	1.21	1.48	1.85	3.51	2.66	2.47	3.99	4.57	6.34	0.38	1.38
238	0.118	0.196	0.0147	0.90	1.19	1.40	2.14	1.40	1.56	2.66	2.92	3.87	0.16	0.70
239	0.125	0.211	0.0147	1.00	1.21	1.37	2.09	1.37	1.75	2.71	2.88	3.88	0.16	0.55

bt#	η_p	λ_p	Q_b	Q_s	Q_{b-dir}
1	1.6	14.1	0.000174	0.000000	51
2	1.5	13.6	0.000116	0.000000	77
3	1.4	12.9	0.000057	0.000000	158
4	1.4	12.2	0.000000	0.000000	0
5	1.4	12.2	0.000000	0.000000	0
6	1.6	14.2	0.000192	0.000000	4
7	2.6	17.3	0.001454	0.000000	32
8	3.1	20.3	0.001420	0.000000	64
9	3.1	21.2	0.000615	0.000000	169
10	2.6	21.2	0.000446	0.000000	190
11	3.0	21.2	0.000435	0.000000	191
12	2.7	17.9	0.000405	0.000000	205
13	2.8	18.4	0.000518	0.000000	188
14	2.9	19.3	0.001793	0.000000	182
15	2.5	21.2	0.001578	0.000000	197
16	3.1	20.6	0.002429	0.000000	218
17	2.4	16.3	0.000667	0.000000	242
18	1.6	14.3	0.000096	0.000000	304
19	1.6	14.3	0.000105	0.000000	28
20	1.6	14.4	0.000115	0.000000	72
21	1.6	14.5	0.000214	0.000000	167
22	2.1	14.1	0.000707	0.000000	200
23	2.0	13.2	0.000633	0.000000	222
24	1.5	13.5	0.000086	0.000000	245
25	1.4	12.5	0.000025	0.000000	241
26	1.4	13.1	0.000064	0.000000	225
27	1.5	13.7	0.000121	0.000000	223
28	1.6	12.9	0.000575	0.000000	234
29	1.5	13.9	0.000161	0.000000	262
30	1.2	10.0	0.000415	0.000000	322
31	1.5	14.0	0.000171	0.000000	343
32	1.4	12.2	0.000000	0.000000	0
33	1.4	12.2	0.000000	0.000000	0
34	1.4	12.2	0.000000	0.000000	0
35	1.4	12.2	0.000000	0.000000	0
36	1.4	12.2	0.000000	0.000000	0
37	1.4	12.2	0.000000	0.000000	0
38	1.4	12.2	0.000000	0.000000	0
39	1.4	12.2	0.000000	0.000000	0
40	1.4	12.5	0.000031	0.000000	170
41	1.3	11.0	0.000513	0.000000	239
42	2.2	18.0	0.001679	0.000000	255
43	1.8	21.2	0.002150	0.003513	295
44	0.0	0.0	0.004064	0.000178	318
45	1.8	21.2	0.000606	0.000986	320
46	0.0	0.0	0.000857	0.000022	323

Appendix 4b page 2

bt#	η_p	λ_p	Q_b	Q_s	Q_{b-dir}
47	0.0	0.0	0.000223	0.000019	219
48	0.0	0.0	0.000457	0.000009	344
49	0.0	0.0	0.000127	0.000005	144
50	0.7	21.2	0.000104	0.000044	125
51	0.0	0.0	0.000588	0.000008	163
52	0.0	0.0	0.001383	0.000022	176
53	1.3	21.2	0.000738	0.000537	194
54	3.1	21.2	0.000586	0.000000	241
55	2.8	21.2	0.001255	0.000000	333
56	2.9	19.4	0.001537	0.000000	2
57	2.1	14.2	0.000405	0.000000	27
58	2.2	14.4	0.000444	0.000000	53
59	2.1	14.1	0.000238	0.000000	121
60	1.5	13.6	0.000011	0.000000	155
61	1.5	13.7	0.000006	0.000000	7
62	1.4	12.9	0.000006	0.000000	33
63	1.5	13.3	0.000036	0.000000	177
64	1.4	12.8	0.000040	0.000000	186
65	1.6	14.2	0.000147	0.000000	205
66	1.6	14.1	0.000142	0.000000	223
67	1.4	12.7	0.000041	0.000000	297
68	1.5	14.0	0.000155	0.000000	354
69	1.5	13.4	0.000098	0.000000	22
70	1.5	13.9	0.000146	0.000000	46
71	1.5	13.6	0.000116	0.000000	61
72	1.4	12.2	0.000000	0.000000	0
73	1.4	12.2	0.000000	0.000000	0
74	1.4	12.2	0.000000	0.000000	0
75	1.4	12.2	0.000000	0.000000	0
76	1.5	13.3	0.000087	0.000000	165
77	1.5	13.8	0.000143	0.000000	169
78	1.6	12.9	0.000617	0.000000	219
79	1.3	11.0	0.000539	0.000000	248
80	1.5	13.8	0.000171	0.000000	306
81	1.5	14.0	0.000196	0.000000	340
82	1.5	13.2	0.000099	0.000000	7
83	1.4	13.0	0.000077	0.000000	64
84	1.4	12.2	0.000000	0.000000	0
85	1.4	12.2	0.000000	0.000000	0
86	1.4	12.2	0.000000	0.000000	0
87	1.4	12.2	0.000000	0.000000	0
88	1.4	12.2	0.000000	0.000000	0
89	1.4	13.1	0.000074	0.000000	223
90	1.6	14.3	0.000233	0.000000	224
91	1.6	14.1	0.000229	0.000000	247
92	1.5	13.4	0.000174	0.000000	311

bt#	η_p	λ_p	Q_b	Q_s	Q_{b-dir}
93	1.3	10.8	0.000541	0.000000	342
94	1.5	13.7	0.000206	0.000000	15
95	1.5	13.9	0.000186	0.000000	58
96	1.5	13.9	0.000170	0.000000	96
97	1.4	12.9	0.000070	0.000000	150
98	1.4	12.2	0.000000	0.000000	0
99	1.4	12.2	0.000000	0.000000	0
100	1.4	12.2	0.000000	0.000000	0
101	1.4	12.2	0.000000	0.000000	0
102	1.4	12.2	0.000000	0.000000	0
103	1.4	12.2	0.000000	0.000000	0
104	1.4	12.2	0.000000	0.000000	0
105	1.7	13.9	0.000526	0.000000	11
106	3.1	21.2	0.001594	0.000000	24
107	1.8	21.2	0.001903	0.003360	56
108	1.8	21.2	0.001714	0.003434	132
109	0.0	0.0	0.006237	0.000342	171
110	0.3	21.2	0.002031	0.000701	193
111	1.5	21.2	0.001287	0.001584	224
112	3.1	20.8	0.001733	0.000000	263
113	2.9	19.3	0.000960	0.000000	241
114	2.8	19.0	0.001430	0.000000	213
115	3.1	20.9	0.002085	0.000000	220
116	2.4	16.1	0.000996	0.000000	253
117	2.5	21.2	0.001748	0.000000	333
118	1.9	21.2	0.001948	0.003158	349
119	2.2	14.5	0.000674	0.000000	14
120	1.3	10.4	0.000348	0.000000	79
121	2.6	17.0	0.001405	0.000000	159
122	1.9	16.0	0.000824	0.000000	185
123	1.7	13.8	0.000551	0.000000	223
124	1.5	13.5	0.000121	0.000000	288
125	1.5	13.3	0.000082	0.000000	314
126	1.4	12.6	0.000033	0.000000	201
127	1.5	13.3	0.000079	0.000000	195
128	1.6	13.3	0.000684	0.000000	224
129	1.5	13.8	0.000239	0.000000	270
130	1.7	14.5	0.000888	0.000000	330
131	1.9	15.5	0.001226	0.000000	6
132	1.6	14.4	0.000223	0.000000	45
133	1.4	12.5	0.000026	0.000000	150
134	1.6	14.1	0.000176	0.000000	153
135	1.5	14.0	0.000181	0.000000	192
136	1.4	12.2	0.000000	0.000000	0
137	1.4	12.2	0.000000	0.000000	0
138	1.4	12.2	0.000000	0.000000	0

bt#	η_p	λ_p	Q_b	Q_s	Q_{b-dir}
139	1.6	14.4	0.000243	0.000000	199
140	1.7	14.3	0.001030	0.000000	223
141	1.7	14.2	0.000981	0.000000	249
142	1.9	15.5	0.001337	0.000000	310
143	2.1	17.1	0.002030	0.000000	344
144	1.3	11.0	0.000514	0.000000	19
145	1.6	14.3	0.000224	0.000000	76
146	1.5	13.2	0.000098	0.000000	148
147	1.5	13.2	0.000091	0.000000	172
148	1.4	13.1	0.000079	0.000000	243
149	1.6	14.1	0.000208	0.000000	313
150	1.4	12.2	0.000000	0.000000	0
151	1.4	12.2	0.000000	0.000000	0
152	1.5	13.5	0.000162	0.000000	203
153	1.5	14.0	0.000249	0.000000	238
154	2.4	16.3	0.001017	0.000000	291
155	0.0	0.0	0.005615	0.000275	349
156	1.3	21.2	0.001850	0.001413	7
157	3.1	20.9	0.002158	0.000000	59
158	2.8	18.4	0.001282	0.000000	158
159	2.9	19.2	0.001861	0.000000	175
160	2.4	16.1	0.000924	0.000000	205
161	1.5	13.6	0.000066	0.000000	317
162	1.4	12.9	0.000051	0.000000	354
163	1.4	12.6	0.000034	0.000000	175
164	1.6	14.1	0.000165	0.000000	172
165	1.6	13.6	0.000628	0.000000	207
166	1.3	11.2	0.000409	0.000000	238
167	1.6	14.2	0.000223	0.000000	314
168	1.6	13.2	0.000659	0.000000	344
169	1.5	13.9	0.000156	0.000000	49
170	1.4	12.2	0.000000	0.000000	0
171	1.4	12.4	0.000019	0.000000	166
172	1.4	13.1	0.000076	0.000000	210
173	1.4	12.6	0.000046	0.000000	312
174	1.3	10.9	0.000478	0.000000	332
175	1.4	12.7	0.000049	0.000000	12
176	1.4	12.2	0.000000	0.000000	0
177	1.4	12.4	0.000020	0.000000	215
178	1.5	13.2	0.000083	0.000000	234
179	1.4	12.7	0.000043	0.000000	276
180	1.6	14.2	0.000188	0.000000	326
181	1.4	13.1	0.000071	0.000000	340
182	1.5	13.2	0.000068	0.000000	126
183	1.6	14.2	0.000109	0.000000	152
184	1.6	14.2	0.000059	0.000000	177

bt#	η_p	λ_p	Q_b	Q_s	Q_{b-dir}
185	1.6	14.3	0.000012	0.000000	292
186	2.4	16.2	0.000592	0.000000	346
187	1.7	11.6	0.000438	0.000000	3
188	1.5	14.0	0.000120	0.000000	75
189	1.6	14.6	0.000147	0.000000	141
190	1.5	13.8	0.000090	0.000000	145
191	1.5	13.2	0.000033	0.000000	158
192	1.3	12.2	0.000000	0.000000	0
193	1.4	12.2	0.000000	0.000000	0
194	1.4	12.6	0.000033	0.000000	141
195	1.5	13.7	0.000114	0.000000	162
196	1.5	12.3	0.000558	0.000000	196
197	1.5	12.2	0.000533	0.000000	222
198	1.6	14.1	0.000270	0.000000	253
199	1.5	13.8	0.000154	0.000000	327
200	1.4	12.4	0.000015	0.000000	355
201	1.4	12.2	0.000000	0.000000	0
202	1.4	12.2	0.000000	0.000000	0
203	1.4	12.2	0.000000	0.000000	0
204	1.4	12.2	0.000000	0.000000	0
205	1.4	12.2	0.000000	0.000000	0
206	1.4	12.8	0.000047	0.000000	65
207	1.3	12.2	0.000000	0.000000	0
208	1.5	13.4	0.000099	0.000000	145
209	1.4	13.0	0.000063	0.000000	234
210	1.4	12.9	0.000052	0.000000	243
211	1.5	13.6	0.000112	0.000000	311
212	1.4	12.2	0.000000	0.000000	0
213	1.5	14.0	0.000161	0.000000	58
214	1.6	14.5	0.000238	0.000000	85
215	2.3	15.4	0.001041	0.000000	85
216	2.5	16.6	0.000694	0.000000	104
217	3.0	19.8	0.000516	0.000000	99
218	3.1	21.2	0.000282	0.000000	114
219	2.1	21.2	0.000558	0.000870	174
220	0.0	0.0	0.003543	0.000107	164
221	0.0	0.0	0.002455	0.000074	193
222	0.4	21.2	0.000886	0.000506	224
223	0.3	21.2	0.001554	0.000637	312
224	0.0	0.0	0.002674	0.000082	340
225	0.6	21.2	0.001003	0.000302	342
226	2.6	21.2	0.000225	0.000000	336
227	3.1	20.7	0.000611	0.000000	110
228	2.6	21.2	0.000215	0.000000	280
229	1.4	21.2	0.000308	0.000434	239
230	3.0	20.3	0.000542	0.000000	301

bt#	η_p	λ_p	Q_b	Q_s	Q_{b-dir}
231	3.1	20.3	0.001059	0.000000	262
232	2.8	19.0	0.001123	0.000000	257
233	2.4	21.2	0.001415	0.000000	262
234	3.1	20.5	0.002602	0.000000	262
235	3.1	20.6	0.002306	0.000000	281
236	2.2	18.7	0.001455	0.000000	314
237	2.5	16.5	0.001169	0.000000	318
238	1.5	13.9	0.000114	0.000000	34
239	1.5	13.8	0.000141	0.000000	101

Appendix 5

The burst-averaged data of wave, current and sediment suspension for the SI97b Ralph deployment. Listed parameters are as defined in Appendix 1.

BT	JD	Hour	depth	u ₅₀	C _{dir}	H _s	T _z	W _{dir}	obs1
1	99	13	23.62	10.22	172	0.50	8.8	119	100
2	99	14	23.50	8.61	163	0.54	9.3	111	103
3	99	15	23.27	5.15	172	0.55	8.8	117	92
4	99	16	23.01	4.58	160	0.55	9.1	295	89
5	99	17	22.72	3.25	34	0.58	9.1	119	96
6	99	18	22.53	6.44	18	0.55	8.9	121	95
7	99	19	22.44	7.48	11	0.56	8.6	119	107
8	99	20	22.54	11.31	19	0.49	9.0	301	117
9	99	21	22.81	9.01	19	0.54	8.9	295	127
10	99	22	23.12	5.51	21	0.53	8.9	119	118
11	99	23	23.44	2.77	140	0.51	8.9	131	97
12	100	0	23.70	9.39	170	0.49	8.5	137	132
13	100	1	23.77	18.36	176	0.49	8.9	137	82
14	100	2	23.67	21.71	182	0.48	8.3	143	78
15	100	3	23.47	18.97	181	0.50	8.6	143	76
16	100	4	23.18	19.47	187	0.48	9.0	153	75
17	100	5	22.88	9.35	187	0.50	8.4	133	75
18	100	6	22.61	3.63	136	0.47	9.2	303	74
19	100	7	22.44	3.77	38	0.49	8.4	125	74
20	100	8	22.43	8.23	15	0.44	9.4	313	74
21	100	9	22.57	10.07	15	0.47	9.2	325	74
22	100	10	22.84	10.28	11	0.48	8.6	321	74
23	100	11	23.19	5.97	15	0.46	9.5	319	74
24	100	12	23.47	3.61	71	0.45	10.0	5	75
25	100	13	23.65	5.86	166	0.41	10.0	329	75
26	100	14	23.63	9.76	169	0.42	9.5	335	75
27	100	15	23.51	6.94	164	0.42	9.3	3	74
28	100	16	23.30	3.43	77	0.42	9.6	329	74
29	100	17	23.04	8.50	37	0.47	10.0	105	74
30	100	18	22.83	11.28	20	0.45	9.5	39	75
31	100	19	22.69	14.82	17	0.48	9.4	85	75
32	100	20	22.66	13.26	12	0.48	9.2	111	75
33	100	21	22.77	14.95	12	0.49	8.9	15	76
34	100	22	23.00	12.77	14	0.48	9.2	329	78
35	100	23	23.31	9.26	19	0.52	9.2	3	78
36	101	0	23.61	2.69	63	0.48	9.5	93	78
37	101	1	23.79	8.40	163	0.56	9.6	357	79
38	101	2	23.85	12.70	163	0.58	8.7	327	78
39	101	3	23.73	15.70	166	0.55	9.1	339	76
40	101	4	23.53	15.83	180	0.58	9.1	339	75
41	101	5	23.22	11.19	178	0.55	8.7	341	74
42	101	6	22.95	6.64	154	0.63	8.9	9	74
43	101	7	22.72	2.95	13	0.60	9.4	351	75
44	101	8	22.58	6.07	34	0.60	9.2	343	74
45	101	9	22.61	6.89	23	0.59	9.8	17	74
46	101	10	22.77	7.23	20	0.56	9.1	353	74

BT	JD	Hour	depth	u ₅₀	C _{dir}	H _s	T _z	W _{dir}	obs1
47	101	11	23.01	9.26	22	0.56	9.9	19	75
48	101	12	23.29	5.60	41	0.53	9.9	13	74
49	101	13	23.51	1.89	100	0.46	9.8	13	75
50	101	14	23.63	4.10	166	0.45	10.0	1	75
51	101	15	23.59	7.33	180	0.45	10.5	11	74
52	101	16	23.45	0.64	58	0.52	9.9	25	74
53	101	17	23.25	3.60	9	0.50	9.2	355	74
54	101	18	23.03	9.13	13	0.48	10.5	25	74
55	101	19	22.84	14.41	15	0.48	10.4	33	74
56	101	20	22.74	13.19	13	0.50	9.5	21	75
57	101	21	22.73	15.94	14	0.51	9.2	11	76
58	101	22	22.86	13.30	21	0.51	9.3	355	78
59	101	23	23.09	10.75	29	0.49	9.4	13	80
60	102	0	23.37	6.47	49	0.51	9.8	1	81
61	102	1	23.62	5.29	127	0.45	9.9	349	80
62	102	2	23.73	15.48	168	0.47	9.6	9	78
63	102	3	23.76	21.28	178	0.50	9.1	5	77
64	102	4	23.67	24.52	180	0.47	9.6	3	75
65	102	5	23.46	24.75	182	0.48	8.7	7	74
66	102	6	23.19	15.73	175	0.53	8.7	343	74
67	102	7	22.97	16.66	170	0.50	9.4	353	73
68	102	8	22.79	8.39	189	0.52	8.8	301	73
69	102	9	22.69	2.11	191	0.51	8.9	107	74
70	102	10	22.74	4.38	112	0.50	9.3	299	73
71	102	11	22.87	3.02	59	0.54	8.9	111	74
72	102	12	23.08	0.80	205	0.51	8.4	317	73

Appendix 6

Predictions by SEDTRANS96 for SI97b Ralph deployment: (a) bottom boundary layer dynamics parameters; (b) sediment transport parameters. Listed parameters are as defined in Appendix 2.

bt#	u _b	A _b	f _{cws}	u* _{cs}	u* _{ws}	u* _{cws}	u* _{cwe}	u* _{cwb}	u* _c	u* _w	u* _{cw}	δ _{cw}	z ₀	z _{0c}
1	0.095	0.133	0.0143	0.56	0.90	1.02	1.55	1.02	0.91	1.98	2.11	2.36	0.09	0.57
2	0.110	0.163	0.0137	0.51	0.99	1.08	1.65	1.08	0.83	2.17	2.27	2.69	0.09	0.77
3	0.106	0.149	0.0145	0.34	0.94	0.98	1.50	0.98	0.54	2.09	2.13	2.39	0.08	1.03
4	0.112	0.162	0.0141	0.32	0.98	1.02	1.55	1.02	0.49	2.16	2.20	2.55	0.09	1.20
5	0.120	0.173	0.0142	0.24	1.01	1.01	1.55	1.01	0.37	2.25	2.26	2.62	0.09	1.50
6	0.112	0.158	0.0144	0.40	0.97	1.00	1.52	1.00	0.64	2.16	2.19	2.48	0.08	0.92
7	0.109	0.150	0.0145	0.45	0.97	1.01	1.54	1.01	0.73	2.16	2.20	2.41	0.09	0.80
8	0.101	0.144	0.0143	0.59	0.92	0.99	1.51	0.99	0.98	2.02	2.09	2.40	0.08	0.50
9	0.108	0.153	0.0145	0.51	0.95	0.98	1.50	0.98	0.83	2.11	2.14	2.42	0.08	0.66
10	0.105	0.148	0.0148	0.35	0.91	0.93	1.42	0.93	0.55	2.04	2.05	2.32	0.08	0.94
11	0.099	0.140	0.0149	0.21	0.88	0.90	1.38	0.90	0.31	1.96	1.98	2.25	0.08	1.34
12	0.088	0.119	0.0146	0.52	0.87	1.00	1.52	1.00	0.84	1.90	2.05	2.22	0.08	0.58
13	0.094	0.133	0.0130	0.90	0.99	1.30	1.99	1.30	1.51	2.12	2.53	2.87	0.10	0.38
14	0.083	0.110	0.0131	1.02	0.96	1.36	2.18	1.54	1.67	1.98	2.52	2.66	0.09	0.28
15	0.093	0.127	0.0131	0.93	0.99	1.32	2.02	1.32	1.55	2.13	2.57	2.81	0.10	0.37
16	0.096	0.137	0.0127	0.96	1.02	1.37	2.20	1.61	1.58	2.13	2.60	2.98	0.09	0.36
17	0.092	0.123	0.0148	0.52	0.88	0.98	1.50	0.98	0.84	1.95	2.06	2.20	0.08	0.58
18	0.099	0.145	0.0147	0.26	0.88	0.92	1.40	0.92	0.39	1.95	1.98	2.32	0.08	1.21
19	0.093	0.124	0.0158	0.26	0.83	0.83	1.30	0.83	0.43	2.24	2.24	2.40	0.15	1.42
20	0.095	0.143	0.0144	0.47	0.87	0.94	1.44	0.94	0.76	1.91	1.99	2.38	0.08	0.66
21	0.099	0.145	0.0139	0.56	0.93	1.05	1.60	1.05	0.92	2.02	2.16	2.53	0.09	0.61
22	0.092	0.126	0.0145	0.56	0.89	1.01	1.54	1.01	0.91	1.95	2.09	2.29	0.09	0.55
23	0.098	0.147	0.0144	0.38	0.87	0.92	1.41	0.92	0.59	1.92	1.97	2.39	0.08	0.87
24	0.099	0.158	0.0145	0.25	0.86	0.88	1.34	0.88	0.39	1.89	1.91	2.43	0.08	1.22
25	0.090	0.143	0.0143	0.37	0.83	0.90	1.38	0.90	0.58	1.79	1.88	2.40	0.08	0.85
26	0.087	0.132	0.0139	0.55	0.86	1.02	1.55	1.02	0.88	1.85	2.04	2.47	0.09	0.58
27	0.086	0.127	0.0146	0.41	0.82	0.91	1.39	0.91	0.65	1.78	1.89	2.24	0.08	0.72
28	0.090	0.137	0.0152	0.24	0.79	0.80	1.26	0.80	0.39	2.11	2.12	2.59	0.15	1.53
29	0.105	0.168	0.0138	0.49	0.93	0.99	1.52	0.99	0.80	2.03	2.09	2.67	0.08	0.71
30	0.097	0.147	0.0134	0.62	0.94	1.12	1.72	1.12	1.02	2.03	2.26	2.73	0.09	0.59
31	0.103	0.154	0.0134	0.74	0.97	1.12	1.72	1.12	1.24	2.10	2.28	2.72	0.09	0.42
32	0.101	0.147	0.0141	0.67	0.92	1.01	1.55	1.01	1.11	2.02	2.11	2.47	0.09	0.42
33	0.098	0.139	0.0131	0.78	1.01	1.28	1.95	1.28	1.29	2.16	2.52	2.85	0.09	0.50
34	0.099	0.145	0.0135	0.68	0.96	1.14	1.74	1.14	1.12	2.07	2.29	2.69	0.09	0.51
35	0.106	0.155	0.0135	0.55	0.99	1.13	1.72	1.13	0.88	2.15	2.32	2.72	0.09	0.74
36	0.100	0.151	0.0146	0.20	0.87	0.89	1.37	0.89	0.30	1.93	1.95	2.36	0.08	1.40
37	0.117	0.179	0.0131	0.52	1.05	1.17	1.79	1.17	0.83	2.28	2.43	2.97	0.09	0.89
38	0.107	0.148	0.0133	0.70	1.05	1.25	1.91	1.25	1.15	2.27	2.53	2.81	0.09	0.60
39	0.108	0.157	0.0126	0.83	1.08	1.37	2.58	1.60	1.51	2.65	3.05	3.53	0.16	0.77
40	0.115	0.167	0.0125	0.84	1.13	1.40	2.64	1.76	1.55	2.82	3.20	3.71	0.17	0.85
41	0.105	0.145	0.0136	0.63	1.01	1.19	1.81	1.19	1.03	2.20	2.42	2.68	0.09	0.64
42	0.125	0.178	0.0135	0.43	1.10	1.17	1.78	1.17	0.69	2.42	2.50	2.83	0.09	1.09
43	0.128	0.192	0.0135	0.23	1.08	1.10	1.68	1.10	0.35	2.38	2.41	2.88	0.09	1.75
44	0.126	0.185	0.0135	0.41	1.08	1.14	1.73	1.14	0.65	2.39	2.45	2.87	0.09	1.15
45	0.132	0.206	0.0128	0.46	1.14	1.23	1.88	1.23	0.74	2.48	2.58	3.22	0.09	1.17
46	0.115	0.167	0.0136	0.46	1.03	1.12	1.71	1.12	0.73	2.26	2.37	2.74	0.09	0.96

bt#	u_b	A_b	f_{cws}	u^*_{cs}	u^*_{ws}	u^*_{cws}	u^*_{cwe}	u^*_{cwb}	u^*_c	u^*_w	u^*_{cw}	δ_{cw}	z_0	z_{0c}
47	0.125	0.196	0.0127	0.57	1.11	1.25	1.91	1.25	0.93	2.40	2.57	3.24	0.09	0.90
48	0.117	0.184	0.0134	0.38	1.01	1.07	1.64	1.07	0.59	2.20	2.27	2.87	0.09	1.15
49	0.099	0.155	0.0147	0.15	0.85	0.85	1.33	0.85	0.24	2.25	2.25	2.81	0.15	2.06
50	0.098	0.157	0.0142	0.29	0.87	0.92	1.40	0.92	0.44	1.90	1.95	2.49	0.08	1.16
51	0.103	0.172	0.0133	0.45	0.93	1.03	1.58	1.03	0.72	2.00	2.12	2.84	0.09	0.87
52	0.114	0.179	0.0140	0.06	0.95	0.95	1.46	0.95	0.08	2.11	2.11	2.66	0.08	2.33
53	0.102	0.149	0.0145	0.26	0.90	0.94	1.43	0.94	0.39	2.00	2.03	2.38	0.08	1.25
54	0.112	0.187	0.0128	0.55	1.02	1.15	1.76	1.15	0.89	2.17	2.34	3.13	0.09	0.82
55	0.112	0.186	0.0122	0.78	1.08	1.32	2.02	1.32	1.29	2.28	2.61	3.45	0.10	0.58
56	0.108	0.163	0.0128	0.72	1.05	1.27	1.94	1.27	1.19	2.25	2.54	3.07	0.09	0.60
57	0.107	0.156	0.0126	0.84	1.07	1.36	2.57	1.58	1.51	2.61	3.02	3.54	0.16	0.75
58	0.107	0.159	0.0129	0.72	1.04	1.25	1.91	1.25	1.19	2.23	2.51	2.97	0.09	0.58
59	0.103	0.154	0.0133	0.61	0.98	1.15	1.76	1.15	0.99	2.12	2.33	2.79	0.09	0.65
60	0.111	0.173	0.0137	0.41	0.97	1.03	1.58	1.03	0.66	2.12	2.19	2.73	0.09	0.97
61	0.098	0.154	0.0142	0.34	0.87	0.92	1.41	0.92	0.54	1.90	1.96	2.47	0.08	0.97
62	0.098	0.150	0.0127	0.80	1.00	1.27	1.94	1.27	1.33	2.13	2.49	3.04	0.09	0.48
63	0.098	0.142	0.0122	1.05	1.07	1.50	2.41	2.05	1.81	2.37	2.98	3.45	0.12	0.45
64	0.099	0.151	0.0117	1.18	1.10	1.61	2.59	2.33	2.09	2.49	3.25	3.97	0.14	0.46
65	0.090	0.125	0.0122	1.18	1.06	1.58	2.54	2.24	2.07	2.38	3.15	3.49	0.13	0.41
66	0.101	0.140	0.0130	0.82	1.04	1.32	2.01	1.32	1.36	2.23	2.61	2.89	0.10	0.49
67	0.106	0.158	0.0124	0.87	1.07	1.38	2.61	1.68	1.59	2.63	3.08	3.68	0.17	0.75
68	0.103	0.144	0.0145	0.48	0.93	0.99	1.51	0.99	0.78	2.06	2.12	2.38	0.08	0.69
69	0.103	0.146	0.0150	0.17	0.89	0.89	1.37	0.89	0.24	2.00	2.00	2.27	0.08	1.52
70	0.106	0.156	0.0142	0.31	0.94	0.98	1.50	0.98	0.47	2.06	2.11	2.50	0.08	1.18
71	0.108	0.153	0.0146	0.23	0.94	0.96	1.46	0.96	0.34	2.09	2.11	2.39	0.08	1.40
72	0.093	0.125	0.0158	0.07	0.83	0.83	1.30	0.83	0.10	2.25	2.25	2.41	0.15	2.12

bt#	η_p	λ_p	Q_b	Q_s	Q_{b-dir}
1	0.8	7.5	0.000029	0.000000	134
2	0.8	7.7	0.000027	0.000000	133
3	0.8	7.4	0.000012	0.000000	134
4	0.8	7.5	0.000012	0.000000	131
5	0.8	7.5	0.000003	0.000000	44
6	0.8	7.4	0.000009	0.000000	353
7	0.8	7.5	0.000013	0.000000	341
8	0.8	7.4	0.000018	0.000000	353
9	0.8	7.4	0.000012	0.000000	5
10	0.8	7.2	0.000005	0.000000	347
11	0.8	7.2	0.000010	0.000000	132
12	0.8	7.4	0.000026	0.000000	146
13	0.9	8.4	0.000109	0.000000	159
14	0.7	6.1	0.000184	0.000000	171
15	0.9	8.4	0.000118	0.000000	165
16	0.8	6.3	0.000169	0.000000	173
17	0.8	7.4	0.000023	0.000000	147
18	0.8	7.2	0.000012	0.000000	124
19	1.4	12.2	0.000000	0.000000	0
20	0.8	7.3	0.000017	0.000000	326
21	0.8	7.6	0.000033	0.000000	339
22	0.8	7.5	0.000028	0.000000	336
23	0.8	7.2	0.000013	0.000000	327
24	0.8	7.1	0.000001	0.000000	9
25	0.8	7.1	0.000010	0.000000	152
26	0.8	7.5	0.000029	0.000000	159
27	0.8	7.2	0.000012	0.000000	179
28	1.4	12.2	0.000000	0.000000	0
29	0.8	7.4	0.000017	0.000000	76
30	0.9	7.8	0.000049	0.000000	32
31	0.9	7.8	0.000047	0.000000	37
32	0.8	7.5	0.000025	0.000000	357
33	0.9	8.3	0.000091	0.000000	14
34	0.9	7.9	0.000053	0.000000	346
35	0.9	7.8	0.000047	0.000000	7
36	0.8	7.1	0.000008	0.000000	92
37	0.9	8.0	0.000044	0.000000	172
38	0.9	8.2	0.000079	0.000000	153
39	1.1	7.5	0.000309	0.000000	162
40	1.2	8.0	0.000327	0.000000	170
41	0.9	8.0	0.000061	0.000000	167
42	0.9	8.0	0.000028	0.000000	173
43	0.9	7.8	0.000008	0.000000	360
44	0.9	7.9	0.000020	0.000000	9
45	0.9	8.1	0.000039	0.000000	20
46	0.9	7.8	0.000031	0.000000	3

bt#	η_p	λ_p	Q_b	Q_s	Q_{b-dir}
47	0.9	8.2	0.000058	0.000000	20
48	0.8	7.7	0.000020	0.000000	23
49	1.4	12.2	0.000000	0.000000	0
50	0.8	7.2	0.000012	0.000000	180
51	0.8	7.5	0.000030	0.000000	189
52	0.8	7.3	0.000000	0.000000	34
53	0.8	7.2	0.000015	0.000000	356
54	0.9	7.9	0.000052	0.000000	22
55	0.9	8.4	0.000102	0.000000	26
56	0.9	8.3	0.000086	0.000000	18
57	1.1	7.4	0.000307	0.000000	12
58	0.9	8.2	0.000080	0.000000	5
59	0.9	7.9	0.000054	0.000000	18
60	0.8	7.5	0.000019	0.000000	18
61	0.8	7.2	0.000013	0.000000	164
62	0.9	8.3	0.000091	0.000000	179
63	0.9	7.7	0.000254	0.005929	181
64	1.0	8.6	0.000378	0.007949	181
65	1.0	8.4	0.000352	0.007501	184
66	0.9	8.4	0.000105	0.000000	169
67	1.2	7.7	0.000335	0.000000	172
68	0.8	7.4	0.000016	0.000000	149
69	0.8	7.1	0.000001	0.000000	141
70	0.8	7.4	0.000017	0.000000	118
71	0.8	7.3	0.000005	0.000000	96
72	1.4	12.2	0.000000	0.000000	0

Appendix 7

The burst-averaged data of wave, current and sediment suspension for the SI97c Ralph deployment. Listed parameters are as defined in Appendix 1.

BT	JD	Hour	depth	u ₅₀	C _{dir}	H _s	T _z	W _{dir}	obs2
1	102	20	39.82	19.38	237	0.32	14.4	55	86.8
2	102	21	39.82	19.89	249	0.35	12.8	57	85.0
3	102	22	39.83	17.42	264	0.35	12.2	79	83.8
4	102	23	39.93	9.50	315	0.34	12.6	7	83.0
5	103	0	40.14	16.55	343	0.33	13.7	343	82.2
6	103	1	40.42	23.34	10	0.33	14.6	323	82.4
7	103	2	40.71	25.55	33	0.30	14.1	25	82.0
8	103	3	40.86	22.81	52	0.32	15.5	29	81.6
9	103	4	40.90	19.05	69	0.33	12.6	245	81.4
10	103	5	40.76	16.52	89	0.30	13.2	263	84.0
11	103	6	40.50	17.78	105	0.32	14.9	277	82.9
12	103	7	40.30	16.35	132	0.34	13.7	35	80.7
13	103	8	40.10	14.15	151	0.34	14.4	343	80.4
14	103	9	39.96	11.16	161	0.36	12.2	355	79.8
15	103	10	39.90	9.57	183	0.36	11.9	237	79.2
16	103	11	39.91	10.49	207	0.36	12.8	283	79.4
17	103	12	40.04	7.90	235	0.34	13.2	51	78.9
18	103	13	40.26	7.08	251	0.36	11.4	267	79.1
19	103	14	40.52	5.07	237	0.33	14.4	69	78.7
20	103	15	40.72	8.70	217	0.31	14.5	29	78.2
21	103	16	40.78	13.50	211	0.33	14.6	69	78.5
22	103	17	40.72	17.92	216	0.32	14.9	63	78.3
23	103	18	40.58	21.44	227	0.32	14.4	37	78.0
24	103	19	40.41	23.12	237	0.34	13.9	51	77.8
25	103	20	40.24	26.03	247	0.34	14.4	245	77.9
26	103	21	40.10	23.50	252	0.34	11.5	253	77.9
27	103	22	40.04	15.21	270	0.34	12.6	61	78.1
28	103	23	40.02	12.95	309	0.34	10.9	355	77.9
29	104	0	40.14	17.98	347	0.34	11.9	341	78.2
30	104	1	40.33	27.61	6	0.37	9.6	3	78.7
31	104	2	40.56	33.68	25	0.39	10.1	3	79.0
32	104	3	40.75	30.85	34	0.57	10.2	9	79.5
33	104	4	40.84	26.77	53	0.76	10.4	25	80.7
34	104	5	40.83	24.09	67	1.07	10.8	31	79.0
35	104	6	40.65	21.28	86	1.27	12.0	33	79.3
36	104	7	40.48	18.33	98	1.22	11.2	35	79.2
37	104	8	40.31	15.12	122	1.22	11.4	35	79.0
38	104	9	40.17	12.47	140	1.34	11.2	33	79.6
39	104	10	40.05	9.82	161	1.16	11.2	33	79.3
40	104	11	39.95	9.06	178	1.49	11.2	31	79.1
41	104	12	39.93	3.66	173	1.46	11.7	41	79.1
42	104	13	40.08	2.55	119	1.56	11.5	39	79.6
43	104	14	40.30	2.19	93	1.61	12.2	33	80.8
44	104	15	40.54	2.33	168	1.34	11.9	37	80.3
45	104	16	40.63	4.08	176	1.54	12.4	55	80.2
46	104	17	40.65	6.50	194	1.33	12.2	47	80.8

BT	JD	Hour	depth	u ₅₀	C _{dir}	H _s	T _z	W _{dir}	obs2
47	104	18	40.62	7.92	208	1.29	11.5	47	80.6
48	104	19	40.47	9.33	223	1.08	11.7	49	80.3
49	104	20	40.33	7.87	238	1.34	12.0	41	80.7
50	104	21	40.18	6.56	263	1.35	11.9	37	80.2
51	104	22	40.09	8.26	275	1.23	11.9	43	79.5
52	104	23	40.02	6.41	295	1.25	11.7	37	79.4
53	105	0	40.03	6.80	307	0.89	10.8	43	79.4
54	105	1	40.09	11.46	323	0.94	11.5	37	79.5
55	105	2	40.21	9.99	343	0.84	11.1	37	79.9
56	105	3	40.49	13.84	359	0.89	11.5	51	80.1
57	105	4	40.66	11.04	25	0.71	11.1	45	79.9
58	105	5	40.73	9.31	55	0.83	11.7	47	79.6
59	105	6	40.72	12.01	82	0.81	11.1	49	80.1
60	105	7	40.63	11.70	109	0.61	11.4	51	80.6
61	105	8	40.51	13.62	133	0.58	11.5	41	80.6
62	105	9	40.34	15.98	159	0.69	11.1	39	80.3
63	105	10	40.20	17.76	171	0.63	10.5	27	79.5
64	105	11	40.04	18.15	186	0.68	11.1	33	79.1
65	105	12	40.00	14.29	196	0.73	11.1	37	78.6
66	105	13	40.05	16.53	210	0.67	10.8	45	78.6
67	105	14	40.19	11.28	239	0.63	10.5	47	78.6
68	105	15	40.40	10.19	243	0.63	10.4	45	78.8
69	105	16	40.56	8.80	239	0.61	10.9	55	78.4
70	105	17	40.69	10.43	232	0.53	10.5	49	78.4
71	105	18	40.74	16.44	212	0.52	10.5	59	78.4
72	105	19	40.71	13.24	215	0.51	10.2	47	78.4
73	105	20	40.62	15.49	214	0.52	9.8	47	78.3
74	105	21	40.52	12.37	228	0.51	10.6	49	78.3
75	105	22	40.39	12.86	244	0.54	9.9	51	78.5
76	105	23	40.25	9.86	260	0.53	10.4	47	78.6
77	106	0	40.16	6.83	265	0.51	9.8	43	78.5
78	106	1	40.16	9.61	324	0.51	9.9	37	78.6
79	106	2	40.26	13.73	343	0.51	9.4	29	79.0
80	106	3	40.40	14.85	0	0.49	10.2	33	79.3
81	106	4	40.59	13.90	16	0.46	9.9	43	79.2
82	106	5	40.74	13.16	26	0.45	10.2	41	79.3
83	106	6	40.79	16.65	42	0.45	9.6	27	79.1
84	106	7	40.79	13.81	61	0.44	9.3	53	79.1
85	106	8	40.72	19.20	75	0.45	10.1	61	79.2
86	106	9	40.60	17.93	88	0.44	9.9	61	79.3
87	106	10	40.45	15.88	121	0.48	9.8	51	79.2
88	106	11	40.29	12.95	142	0.51	9.4	47	79.0
89	106	12	40.15	17.00	153	0.52	9.2	43	79.0
90	106	13	40.10	15.07	171	0.50	8.5	63	78.8
91	106	14	40.13	8.70	189	0.51	8.7	59	78.8
92	106	15	40.23	10.24	208	0.53	8.6	55	78.8

BT	JD	Hour	depth	u ₅₀	C _{dir}	H _s	T _z	W _{dir}	obs2
93	106	16	40.40	8.18	183	0.49	8.3	57	80.0
94	106	17	40.57	8.02	197	0.46	8.4	65	78.9
95	106	18	40.70	9.19	180	0.45	8.6	71	78.8
96	106	19	40.73	10.02	180	0.45	8.3	67	78.9
97	106	20	40.72	11.66	183	0.44	9.1	61	78.8
98	106	21	40.64	12.76	194	0.43	9.1	61	78.8
99	106	22	40.54	15.99	213	0.43	9.0	69	78.7
100	106	23	40.35	13.28	220	0.45	8.7	63	78.6
101	107	0	40.26	13.42	228	0.44	8.5	55	78.7
102	107	1	40.15	10.19	253	0.45	8.3	57	78.8
103	107	2	40.12	10.29	277	0.45	8.5	49	79.0
104	107	3	40.20	9.33	329	0.45	8.3	17	79.1
105	107	4	40.35	12.38	352	0.45	8.3	21	79.2
106	107	5	40.54	14.98	1	0.42	8.9	15	79.4
107	107	6	40.70	13.97	20	0.40	9.0	51	79.3
108	107	7	40.78	11.47	43	0.42	8.8	65	79.4
109	107	8	40.81	11.92	62	0.42	9.5	71	79.0
110	107	9	40.75	11.80	83	0.40	9.5	65	78.8
111	107	10	40.61	9.48	104	0.39	10.4	61	78.8
112	107	11	40.48	8.74	143	0.40	9.6	47	78.9
113	107	12	40.31	9.67	160	0.42	9.8	51	78.9
114	107	13	40.16	9.14	171	0.41	8.9	337	78.8
115	107	14	40.07	5.38	190	0.40	9.8	43	78.8
116	107	15	40.09	1.11	217	0.41	10.0	63	79.1
117	107	16	40.22	2.17	351	0.42	9.6	31	79.2
118	107	17	40.41	3.02	11	0.41	9.6	45	79.3
119	107	18	40.61	2.73	42	0.38	10.4	17	79.2
120	107	19	40.75	3.64	105	0.37	10.8	51	79.2
121	107	20	40.80	5.67	152	0.38	10.4	37	79.4
122	107	21	40.78	7.68	157	0.38	10.5	29	79.2
123	107	22	40.70	8.35	171	0.36	10.2	15	79.3
124	107	23	40.55	6.28	178	0.37	10.0	33	79.3
125	108	0	40.41	6.93	195	0.39	10.8	65	79.1
126	108	1	40.23	4.71	216	0.40	11.1	47	79.4
127	108	2	40.09	3.59	220	0.40	10.9	59	79.3
128	108	3	40.10	4.47	270	0.40	9.6	57	79.7
129	108	4	40.16	5.92	340	0.40	9.0	303	79.8
130	108	5	40.36	6.97	8	0.39	10.0	15	80.0
131	108	6	40.55	7.04	18	0.38	11.9	5	80.2
132	108	7	40.71	8.45	37	0.35	11.9	29	80.1
133	108	8	40.81	6.89	68	0.37	10.9	251	79.7
134	108	9	40.81	5.55	85	0.37	11.7	253	79.6
135	108	10	40.73	5.25	123	0.36	13.0	273	79.5
136	108	11	40.62	5.34	153	0.36	10.9	37	79.6
137	108	12	40.42	3.99	160	0.38	10.8	37	79.4
138	108	13	40.20	4.16	181	0.39	10.8	59	79.4

BT	JD	Hour	depth	u ₅₀	C _{dir}	H _s	T _z	W _{dir}	obs2
139	108	14	40.10	4.04	209	0.39	10.0	59	79.7
140	108	15	40.02	4.69	246	0.39	10.9	49	79.7
141	108	16	40.07	3.87	294	0.39	10.8	63	80.0
142	108	17	40.23	4.47	320	0.40	10.5	41	80.4
143	108	18	40.47	5.15	1	0.39	11.7	69	80.4
144	108	19	40.66	3.58	23	0.36	12.0	351	80.1
145	108	20	40.79	4.00	3	0.37	12.0	271	79.7
146	108	21	40.86	4.43	42	0.38	12.0	51	80.1
147	108	22	40.82	3.91	25	0.38	11.4	11	79.8
148	108	23	40.71	2.91	48	0.36	11.9	307	79.7
149	109	0	40.54	1.52	201	0.36	11.2	257	79.7
150	109	1	40.33	3.09	285	0.39	10.5	245	80.1
151	109	2	40.14	7.61	275	0.40	10.5	257	80.0
152	109	3	40.05	10.02	301	0.40	11.2	249	80.1
153	109	4	40.08	12.04	319	0.40	9.8	1	80.0
154	109	5	40.16	16.35	343	0.42	9.5	337	80.0
155	109	6	40.35	17.31	356	0.46	8.5	359	80.0
156	109	7	40.57	22.03	2	0.49	9.8	31	79.9
157	109	8	40.79	17.05	12	0.54	9.8	13	80.2
158	109	9	40.89	9.96	25	0.75	9.1	49	79.9
159	109	10	40.88	10.42	38	0.80	9.3	69	79.4
160	109	11	40.77	5.06	59	0.94	9.6	57	78.9
161	109	12	40.60	2.64	31	1.02	10.2	23	79.2
162	109	13	40.38	2.27	313	1.48	10.4	9	79.5
163	109	14	40.15	1.48	228	1.62	10.5	11	83.4
164	109	15	39.98	2.78	294	1.60	11.2	9	80.4
165	109	16	39.95	3.85	310	1.79	11.2	5	83.1
166	109	17	40.01	6.42	343	1.63	11.2	355	83.4
167	109	18	40.22	6.92	2	1.74	11.4	3	86.9
168	109	19	40.46	8.62	357	1.67	11.2	5	90.3
169	109	20	40.69	6.15	26	1.41	11.7	9	86.3
170	109	21	40.80	7.76	47	1.43	11.2	359	84.4
171	109	22	40.85	6.28	80	1.43	11.1	1	84.0
172	109	23	40.74	8.07	88	1.26	11.1	15	84.7
173	110	0	40.56	6.96	123	1.32	11.1	7	90.3
174	110	1	40.34	6.44	145	1.13	10.6	1	89.3
175	110	2	40.09	5.41	163	1.16	10.6	3	85.1
176	110	3	39.91	2.07	208	1.18	10.9	13	85.1
177	110	4	39.88	4.51	264	1.31	10.6	3	85.4
178	110	5	39.94	2.94	323	1.10	10.6	15	87.5
179	110	6	40.07	5.13	348	1.30	11.1	9	85.5
180	110	7	40.30	8.17	2	1.10	10.4	13	82.5
181	110	8	40.56	8.92	21	1.15	11.1	1	82.0
182	110	9	40.74	6.46	42	1.20	10.9	19	82.6
183	110	10	40.83	4.71	86	1.18	11.9	9	83.3
184	110	11	40.78	5.30	114	1.36	12.0	17	84.4

BT	JD	Hour	depth	u ₅₀	C _{dir}	H _s	T _z	W _{dir}	obs2
185	110	12	40.62	7.89	139	1.21	11.4	23	84.4
186	110	13	40.36	8.58	169	1.36	12.0	19	82.6
187	110	14	40.12	11.56	191	1.21	11.2	33	82.8
188	110	15	39.95	9.73	214	1.24	12.0	21	85.0
189	110	16	39.84	13.22	249	1.14	11.4	37	84.8
190	110	17	39.84	12.45	262	1.13	11.4	41	82.6
191	110	18	40.00	7.82	294	0.96	12.0	39	82.3
192	110	19	40.26	7.91	307	1.16	11.7	27	83.2
193	110	20	40.54	5.88	333	0.95	12.2	23	83.6
194	110	21	40.78	6.84	6	0.85	11.9	23	82.8
195	110	22	40.92	4.15	52	1.02	12.0	23	83.3
196	110	23	40.91	3.40	103	0.87	11.9	41	84.3
197	111	0	40.77	8.18	149	0.81	11.5	47	84.8
198	111	1	40.54	8.54	163	0.87	11.7	29	83.6
199	111	2	40.26	10.25	175	0.82	11.4	29	83.1
200	111	3	40.02	11.98	194	0.86	11.4	35	82.5
201	111	4	39.90	9.49	230	0.76	11.5	43	83.9
202	111	5	39.85	9.93	246	0.83	12.0	41	84.4
203	111	6	39.93	6.63	276	0.75	11.5	33	84.3
204	111	7	40.14	6.92	330	0.63	11.9	31	83.6
205	111	8	40.42	9.72	353	0.70	11.7	27	82.5
206	111	9	40.65	8.56	10	0.61	11.5	23	82.4
207	111	10	40.82	6.48	41	0.62	11.1	45	82.2
208	111	11	40.85	5.35	100	0.53	11.2	43	83.1
209	111	12	40.77	7.76	145	0.53	12.4	21	88.2
210	111	13	40.55	17.07	167	0.54	11.7	19	84.1
211	111	14	40.29	15.82	185	0.52	10.6	43	84.3
212	111	15	40.02	15.95	202	0.54	11.2	45	82.1
213	111	16	39.85	13.25	231	0.50	10.8	51	81.6
214	111	17	39.80	12.61	243	0.51	10.9	45	81.6
215	111	18	39.89	13.09	257	0.49	10.6	43	81.3
216	111	19	40.09	6.39	314	0.50	11.5	27	82.0
217	111	20	40.37	8.71	348	0.54	10.8	7	82.4
218	111	21	40.68	10.23	5	0.43	11.7	21	82.7
219	111	22	40.88	9.62	34	0.44	11.4	23	82.8
220	111	23	40.97	7.99	60	0.43	10.9	33	83.0
221	112	0	40.86	9.47	92	0.41	11.7	39	84.9
222	112	1	40.68	7.93	124	0.39	11.4	51	89.5
223	112	2	40.43	12.80	149	0.40	12.2	21	83.8
224	112	3	40.11	11.12	170	0.42	11.7	351	82.9
225	112	4	39.91	8.44	185	0.44	11.7	23	82.7
226	112	5	39.79	7.85	225	0.42	11.7	43	81.8
227	112	6	39.80	5.57	257	0.41	11.4	33	81.3
228	112	7	39.96	6.14	335	0.43	11.1	11	83.0
229	112	8	40.22	6.98	359	0.40	11.7	13	84.6
230	112	9	40.50	9.11	28	0.41	10.8	9	86.0

BT	JD	Hour	depth	u ₅₀	C _{dir}	H _s	T _z	W _{dir}	obs2
231	112	10	40.75	8.82	55	0.39	11.5	19	86.3
232	112	11	40.87	9.78	79	0.39	12.4	51	86.1
233	112	12	40.86	9.69	113	0.40	11.2	23	89.9
234	112	13	40.69	11.98	146	0.39	11.7	27	87.4
235	112	14	40.45	14.08	168	0.39	12.0	3	86.5
236	112	15	40.15	13.98	185	0.42	11.2	49	83.4
237	112	16	39.93	16.00	207	0.40	11.2	35	80.9
238	112	17	39.77	10.74	242	0.40	11.4	47	80.9
239	112	18	39.79	11.00	265	0.39	11.4	47	81.0
240	112	19	39.91	6.57	313	0.39	12.2	25	81.3
241	112	20	40.17	11.13	352	0.41	10.6	7	82.6
242	112	21	40.52	14.30	11	0.37	12.2	353	83.8
243	112	22	40.81	14.94	42	0.37	12.8	39	83.7
244	112	23	40.97	17.88	59	0.38	12.6	35	84.2
245	113	0	40.98	20.46	72	0.37	12.2	69	85.0
246	113	1	40.85	16.83	90	0.36	12.8	253	84.2
247	113	2	40.58	15.17	116	0.36	13.2	7	83.8
248	113	3	40.30	13.67	141	0.37	12.4	343	82.9
249	113	4	39.99	14.27	161	0.38	11.5	351	82.6
250	113	5	39.78	12.15	181	0.38	11.4	49	82.5
251	113	6	39.72	10.24	202	0.37	13.0	69	82.0
252	113	7	39.81	7.49	240	0.37	12.4	47	80.9
253	113	8	40.00	8.56	262	0.37	12.0	63	81.0
254	113	9	40.32	2.88	311	0.39	11.5	45	81.0
255	113	10	40.61	2.42	16	0.34	13.7	1	81.4
256	113	11	40.80	3.18	145	0.35	13.0	7	82.3
257	113	12	40.88	8.42	163	0.37	14.1	11	87.5
258	113	13	40.80	12.89	177	0.34	13.2	173	84.3
259	113	14	40.59	15.42	187	0.33	13.4	227	82.0
260	113	15	40.32	17.66	207	0.36	12.2	193	81.3
261	113	16	40.00	20.03	235	0.35	14.1	49	80.6
262	113	17	39.79	19.94	244	0.35	12.0	49	80.6
263	113	18	39.74	18.36	254	0.35	13.9	63	80.5
264	113	19	39.80	20.10	272	0.35	14.1	37	80.4
265	113	20	40.02	11.56	293	0.37	12.8	53	80.0
266	113	21	40.32	17.23	338	0.39	12.2	355	79.8
267	113	22	40.64	14.18	5	0.36	12.6	11	80.7
268	113	23	40.91	16.45	33	0.48	11.2	17	81.1
269	114	0	41.04	14.38	57	0.51	11.4	15	81.3
270	114	1	40.97	15.88	83	0.55	11.4	25	81.9
271	114	2	40.77	12.22	108	0.59	11.2	13	82.8
272	114	3	40.49	12.05	138	0.60	11.4	15	82.9
273	114	4	40.17	13.85	163	0.68	11.2	19	81.6
274	114	5	39.91	9.04	181	0.59	10.6	19	81.9
275	114	6	39.74	13.44	209	0.59	10.8	5	81.1
276	114	7	39.72	11.52	249	0.54	10.8	23	80.3

BT	JD	Hour	depth	u ₅₀	C _{dir}	H _s	T _z	W _{dir}	obs2
277	114	8	39.82	11.30	267	0.54	10.5	21	80.0
278	114	9	40.10	6.98	307	0.50	10.8	17	79.9
279	114	10	40.42	7.35	342	0.49	11.2	1	79.9
280	114	11	40.70	4.93	16	0.43	11.4	3	80.3
281	114	12	40.89	3.76	83	0.46	10.6	11	80.8
282	114	13	40.89	6.25	151	0.45	11.1	3	81.6
283	114	14	40.72	7.97	170	0.40	10.8	357	81.8
284	114	15	40.50	12.84	185	0.39	11.7	359	80.6
285	114	16	40.20	12.74	213	0.44	10.9	5	80.6
286	114	17	39.95	16.57	245	0.45	10.6	35	81.2
287	114	18	39.79	17.63	255	0.42	10.6	47	80.5
288	114	19	39.82	14.09	281	0.42	10.9	27	80.6
289	114	20	39.92	13.81	309	0.43	11.5	1	80.2
290	114	21	40.14	18.38	339	0.42	10.9	1	81.2
291	114	22	40.48	17.51	3	0.40	10.9	349	82.9
292	114	23	40.81	19.49	22	0.38	10.9	17	82.0
293	115	0	41.04	19.82	31	0.42	11.2	349	82.8
294	115	1	41.15	16.54	61	0.42	10.4	259	81.9
295	115	2	41.02	13.69	80	0.40	10.6	41	82.1
296	115	3	40.68		88	0.36	13.0	73	83.6
297	115	4	40.44	10.16	152	0.39	10.2	343	83.0
298	115	5	40.18	9.36	197	0.42	10.0	35	82.3
299	115	6	39.92	11.96	216	0.41	10.1	27	81.8
300	115	7	39.84	12.26	251	0.42	9.3	67	82.2
301	115	8	39.82	14.24	260	0.44	8.6	61	81.8
302	115	9	40.00	14.64	277	0.44	9.2	65	81.2
303	115	10	40.28	11.64	302	0.45	8.8	67	81.1
304	115	11	40.63	8.98	318	0.42	10.2	343	80.7
305	115	12	40.90	5.66	309	0.49	9.2	281	80.9
306	115	13	40.96	3.65	249	0.49	9.1	315	81.2
307	115	14	40.93	10.61	229	0.52	9.5	29	80.8
308	115	15	40.70	16.39	215	0.53	10.6	9	80.4
309	115	16	40.40	19.04	228	0.66	10.6	19	81.0
310	115	17	40.13	23.78	240	0.64	10.5	31	80.9
311	115	18	39.94	21.34	252	0.70	11.9	43	81.2
312	115	19	39.85	17.75	266	0.81	11.7	37	81.0
313	115	20	39.87	15.37	289	1.04	12.6	27	81.9
314	115	21	40.00	9.02	307	1.12	12.4	29	82.4
315	115	22	40.27	14.28	336	1.18	13.4	27	82.8
316	115	23	40.60	18.33	4	1.06	12.0	37	81.9
317	116	0	40.93	16.00	15	1.03	12.4	25	84.8
318	116	1	41.14	18.37	38	0.89	12.6	31	83.1
319	116	2	41.12	14.56	63	0.86	12.4	43	82.0
320	116	3	40.95	12.60	83	0.96	12.2	41	81.0
321	116	4	40.67	11.78	104	0.88	11.9	37	81.3
322	116	5	40.38	8.92	129	0.77	12.6	35	82.9

BT	JD	Hour	depth	u ₅₀	C _{dir}	H _s	T _z	W _{dir}	obs2
323	116	6	40.06	8.19	152	0.75	11.5	33	88.7
324	116	7	39.87	7.78	170	0.78	11.9	33	87.4
325	116	8	39.81	4.39	175	0.74	11.2	39	87.9
326	116	9	39.88	3.26	234	0.65	11.5	45	85.8
327	116	10	40.07	2.27	349	0.79	11.9	31	89.6
328	116	11	40.34	4.98	357	0.67	11.9	31	89.4
329	116	12	40.65	4.10	34	0.58	11.7	37	96.1
330	116	13	40.84	3.69	109	0.56	11.2	45	95.6
331	116	14	40.89	8.17	167	0.52	10.9	55	106.5
332	116	15	40.77	11.72	183	0.49	11.2	51	94.5
333	116	16	40.54	11.77	195	0.51	10.9	51	87.8
334	116	17	40.27	19.74	210	0.50	11.5	47	82.4
335	116	18	40.01	16.93	229	0.48	11.4	49	81.5
336	116	19	39.87	19.48	242	0.45	11.7	51	81.4
337	116	20	39.82	13.97	260	0.51	11.9	47	82.7
338	116	21	39.87	9.44	281	0.46	11.1	49	82.8
339	116	22	40.05	15.87	308	0.42	11.9	49	82.6
340	116	23	40.36	23.05	336	0.46	11.1	41	82.2
341	117	0	40.70	25.74	4	0.35	12.4	55	82.3
342	117	1	40.97	23.30	25	0.41	10.9	57	83.2
343	117	2	41.12	16.25	49	0.42	11.9	61	82.5
344	117	3	41.07	19.40	123	0.40	12.0	57	80.7
345	117	4	40.86	14.11	168	0.42	11.9	55	80.3
346	117	5	40.59	15.30	188	0.36	11.9	51	80.9
347	117	6	40.29	14.74	185	0.40	12.2	45	82.5
348	117	7	40.03	12.00	191	0.39	11.7	43	84.0
349	117	8	39.88	9.95	203	0.37	11.9	41	83.5
350	117	9	39.83	7.64	210	0.37	11.2	35	84.0
351	117	10	39.92	8.20	215	0.37	12.0	29	82.8
352	117	11	40.15	7.87	223	0.36	12.8	25	85.0
353	117	12	40.44	5.69	220	0.37	11.1	27	89.2
354	117	13	40.70	3.23	210	0.31	11.5	29	97.1
355	117	14	40.88	6.06	200	0.35	12.0	47	101.3
356	117	15	40.88	9.35	180	0.37	12.2	57	117.2
357	117	16	40.77	13.45	175	0.35	11.7	71	95.9
358	117	17	40.58	14.70	180	0.36	12.2	75	84.7
359	117	18	40.32	13.38	175	0.36	12.0	69	82.3
360	117	19	40.07	16.87	195	0.36	12.6	259	83.7
361	117	20	39.95	17.71	210	0.36	12.6	67	83.0

Appendix 8

Predictions by SEDTRANS96 for SI97c Ralph deployment: (a) bottom boundary layer dynamics parameters; (b) sediment transport parameters. Listed parameters are as defined in Appendix 2.

bt#	u_b	A_b	f_{cws}	u^*_{cs}	u^*_{ws}	u^*_{cws}	u^*_{cwe}	u^*_{cwb}	u^*_c	u^*_w	u^*_{cw}	δ_{cw}	z_0	z_{0c}
1	0.059	0.134	0.0114	0.90	0.71	1.14	1.75	1.14	1.47	1.42	2.05	3.74	0.09	0.26
2	0.058	0.119	0.0118	0.91	0.72	1.16	1.77	1.16	1.50	1.46	2.09	3.40	0.09	0.25
3	0.056	0.108	0.0124	0.81	0.68	1.06	1.62	1.06	1.32	1.38	1.91	2.98	0.09	0.26
4	0.056	0.111	0.0143	0.47	0.58	0.71	1.11	0.71	0.85	1.45	1.62	2.59	0.15	0.58
5	0.058	0.125	0.0120	0.78	0.68	1.04	1.59	1.04	1.28	1.37	1.88	3.26	0.09	0.28
6	0.060	0.141	0.0111	1.03	0.74	1.22	1.86	1.22	1.70	1.47	2.15	4.01	0.09	0.21
7	0.053	0.120	0.0109	1.13	0.73	1.34	2.16	1.43	1.82	1.38	2.28	4.10	0.08	0.18
8	0.060	0.148	0.0108	1.03	0.75	1.26	1.92	1.26	1.70	1.48	2.23	4.39	0.09	0.23
9	0.053	0.105	0.0121	0.87	0.67	1.10	1.68	1.10	1.42	1.36	1.96	3.15	0.09	0.24
10	0.050	0.106	0.0124	0.76	0.62	0.99	1.51	0.99	1.24	1.26	1.77	2.97	0.08	0.24
11	0.059	0.140	0.0115	0.83	0.70	1.09	1.66	1.09	1.36	1.39	1.95	3.69	0.09	0.27
12	0.059	0.129	0.0132	0.70	0.63	0.82	1.28	0.82	1.29	1.50	1.72	2.99	0.15	0.32
13	0.062	0.142	0.0121	0.69	0.68	0.97	1.48	0.97	1.12	1.38	1.77	3.25	0.08	0.32
14	0.057	0.111	0.0136	0.56	0.63	0.84	1.31	0.84	1.00	1.53	1.82	2.84	0.15	0.57
15	0.055	0.104	0.0147	0.47	0.58	0.71	1.11	0.71	0.86	1.46	1.63	2.46	0.15	0.56
16	0.060	0.122	0.0144	0.50	0.59	0.69	1.08	0.69	0.92	1.50	1.60	2.61	0.15	0.51
17	0.058	0.122	0.0139	0.42	0.59	0.73	1.14	0.73	0.75	1.48	1.66	2.79	0.15	0.74
18	0.052	0.094	0.0153	0.38	0.55	0.66	1.04	0.66	0.67	1.41	1.56	2.26	0.15	0.71
19	0.060	0.136	0.0142	0.30	0.57	0.64	1.00	0.64	0.52	1.44	1.53	2.80	0.15	1.03
20	0.056	0.129	0.0134	0.45	0.58	0.74	1.15	0.74	0.81	1.42	1.63	3.02	0.15	0.68
21	0.060	0.140	0.0124	0.65	0.65	0.89	1.36	0.89	1.05	1.31	1.64	3.05	0.08	0.30
22	0.059	0.140	0.0116	0.83	0.69	1.07	1.63	1.07	1.36	1.38	1.91	3.62	0.09	0.26
23	0.058	0.132	0.0112	0.97	0.72	1.21	1.85	1.21	1.60	1.44	2.15	3.94	0.09	0.24
24	0.060	0.132	0.0111	1.05	0.76	1.29	1.97	1.29	1.73	1.52	2.30	4.07	0.10	0.24
25	0.062	0.141	0.0106	1.17	0.80	1.41	2.27	1.74	1.94	1.59	2.51	4.60	0.10	0.24
26	0.050	0.092	0.0119	1.04	0.70	1.25	1.91	1.25	1.72	1.41	2.22	3.27	0.09	0.21
27	0.055	0.111	0.0128	0.71	0.65	0.95	1.45	0.95	1.16	1.32	1.73	2.78	0.08	0.26
28	0.046	0.080	0.0146	0.60	0.56	0.79	1.23	0.79	1.08	1.38	1.68	2.34	0.15	0.40
29	0.052	0.098	0.0126	0.83	0.66	1.06	1.61	1.06	1.35	1.34	1.90	2.87	0.09	0.24
30	0.039	0.061	0.0124	1.18	0.65	1.35	2.16	1.46	1.90	1.27	2.29	2.81	0.08	0.15
31	0.046	0.073	0.0115	1.43	0.74	1.60	2.57	2.21	2.49	1.61	2.95	3.79	0.13	0.22
32	0.068	0.110	0.0114	1.37	0.91	1.62	2.61	2.29	2.41	2.01	3.10	4.04	0.14	0.29
33	0.092	0.152	0.0113	1.25	1.06	1.61	2.59	2.31	2.21	2.35	3.18	4.20	0.14	0.39
34	0.139	0.238	0.0108	1.21	1.34	1.77	3.03	2.74	2.38	3.41	4.07	5.59	0.23	0.87
35	0.194	0.372	0.0102	1.16	1.62	1.90	2.92	3.12	2.20	3.84	4.25	6.52	0.19	1.03
36	0.170	0.304	0.0110	0.99	1.43	1.63	3.03	2.46	2.02	3.89	4.17	5.95	0.27	1.33
37	0.175	0.316	0.0114	0.83	1.38	1.43	2.71	1.92	1.60	3.48	3.54	5.13	0.19	1.15
38	0.189	0.337	0.0112	0.76	1.48	1.56	2.95	2.34	1.48	3.90	4.00	5.71	0.22	1.72
39	0.164	0.293	0.0115	0.63	1.33	1.43	2.70	1.91	1.16	3.37	3.50	4.99	0.19	1.69
40	0.211	0.378	0.0107	0.65	1.65	1.75	2.90	2.85	1.20	4.20	4.34	6.20	0.21	2.44
41	0.219	0.408	0.0108	0.33	1.63	1.65	2.93	2.63	0.60	4.36	4.38	6.53	0.24	4.17
42	0.229	0.421	0.0108	0.25	1.68	1.69	2.89	2.74	0.44	4.42	4.43	6.50	0.23	4.66
43	0.252	0.491	0.0103	0.23	1.81	1.82	2.83	3.09	0.38	4.42	4.43	6.89	0.18	5.04
44	0.201	0.380	0.0110	0.22	1.51	1.52	2.87	2.24	0.38	3.94	3.95	5.97	0.22	4.35
45	0.243	0.480	0.0103	0.37	1.76	1.78	2.86	2.98	0.66	4.37	4.40	6.95	0.20	4.09
46	0.206	0.402	0.0106	0.50	1.57	1.64	2.97	2.55	0.95	4.21	4.30	6.69	0.26	3.25

bt#	u_b	A_b	f_{cws}	u^*_{cs}	u^*_{ws}	u^*_{cws}	u^*_{cwe}	u^*_{cwb}	u^*_c	u^*_w	u^*_{cw}	δ_{cw}	z_0	z_{0c}
47	0.187	0.343	0.0110	0.56	1.48	1.58	2.98	2.37	1.05	3.87	4.00	5.88	0.23	2.50
48	0.160	0.297	0.0113	0.61	1.32	1.45	2.75	1.98	1.12	3.32	3.50	5.22	0.19	1.82
49	0.206	0.395	0.0106	0.58	1.59	1.69	2.95	2.68	1.10	4.15	4.29	6.58	0.24	2.81
50	0.205	0.387	0.0108	0.50	1.56	1.62	2.98	2.51	0.96	4.24	4.32	6.52	0.26	3.19
51	0.187	0.354	0.0110	0.58	1.46	1.53	2.90	2.25	1.08	3.78	3.88	5.86	0.22	2.33
52	0.187	0.349	0.0113	0.47	1.43	1.45	2.73	1.99	0.86	3.65	3.67	5.47	0.19	2.51
53	0.119	0.204	0.0133	0.43	0.99	1.00	1.53	1.00	0.69	2.14	2.16	2.97	0.09	0.96
54	0.138	0.254	0.0121	0.66	1.14	1.22	1.86	1.22	1.10	2.44	2.53	3.72	0.09	0.75
55	0.116	0.204	0.0126	0.58	1.02	1.12	1.72	1.12	0.95	2.17	2.30	3.24	0.09	0.74
56	0.129	0.237	0.0118	0.76	1.14	1.31	2.00	1.31	1.27	2.40	2.63	3.86	0.10	0.65
57	0.097	0.170	0.0127	0.61	0.92	1.10	1.68	1.10	1.00	1.94	2.17	3.06	0.09	0.60
58	0.122	0.227	0.0120	0.57	1.07	1.21	1.85	1.21	0.93	2.26	2.44	3.64	0.09	0.90
59	0.110	0.194	0.0123	0.67	1.02	1.20	1.83	1.20	1.10	2.15	2.38	3.36	0.09	0.64
60	0.087	0.157	0.0133	0.61	0.82	0.96	1.47	0.96	0.99	1.74	1.91	2.76	0.08	0.45
61	0.084	0.155	0.0138	0.64	0.77	0.86	1.31	0.86	1.06	1.64	1.72	2.53	0.08	0.30
62	0.095	0.167	0.0126	0.79	0.92	1.13	1.73	1.13	1.31	1.94	2.20	3.10	0.09	0.38
63	0.080	0.134	0.0126	0.86	0.87	1.19	1.82	1.19	1.42	1.82	2.25	3.01	0.09	0.33
64	0.094	0.166	0.0119	0.91	0.98	1.32	2.01	1.32	1.51	2.04	2.50	3.53	0.10	0.40
65	0.101	0.179	0.0122	0.76	0.99	1.24	1.89	1.24	1.25	2.08	2.41	3.40	0.09	0.52
66	0.089	0.153	0.0123	0.83	0.93	1.25	1.90	1.25	1.38	1.95	2.38	3.27	0.09	0.42
67	0.080	0.134	0.0134	0.60	0.81	1.01	1.54	1.01	0.97	1.72	1.97	2.63	0.09	0.48
68	0.078	0.128	0.0138	0.55	0.78	0.95	1.45	0.95	0.89	1.66	1.88	2.48	0.08	0.50
69	0.082	0.142	0.0136	0.50	0.79	0.93	1.43	0.93	0.79	1.68	1.86	2.59	0.08	0.59
70	0.066	0.111	0.0141	0.54	0.70	0.89	1.35	0.89	0.87	1.48	1.72	2.30	0.08	0.42
71	0.065	0.108	0.0131	0.78	0.75	1.07	1.63	1.07	1.28	1.56	1.99	2.66	0.09	0.30
72	0.061	0.099	0.0139	0.65	0.69	0.95	1.44	0.95	1.05	1.45	1.79	2.33	0.08	0.33
73	0.056	0.087	0.0139	0.73	0.68	1.00	1.53	1.00	1.19	1.43	1.86	2.31	0.09	0.28
74	0.066	0.111	0.0137	0.63	0.72	0.95	1.45	0.95	1.01	1.50	1.81	2.46	0.08	0.37
75	0.060	0.095	0.0142	0.64	0.69	0.93	1.43	0.93	1.03	1.45	1.78	2.23	0.08	0.33
76	0.066	0.108	0.0145	0.51	0.68	0.84	1.31	0.84	0.92	1.73	1.93	2.55	0.15	0.66
77	0.056	0.087	0.0163	0.37	0.58	0.67	1.05	0.67	0.64	1.54	1.65	2.04	0.15	0.74
78	0.058	0.090	0.0161	0.47	0.59	0.68	1.07	0.68	0.85	1.56	1.66	2.08	0.15	0.54
79	0.052	0.077	0.0150	0.64	0.62	0.85	1.33	0.85	1.15	1.54	1.85	2.22	0.15	0.42
80	0.059	0.096	0.0138	0.70	0.69	0.96	1.47	0.96	1.14	1.43	1.80	2.34	0.08	0.28
81	0.051	0.080	0.0144	0.66	0.62	0.89	1.36	0.89	1.06	1.30	1.66	2.08	0.08	0.26
82	0.054	0.087	0.0142	0.64	0.63	0.89	1.37	0.89	1.03	1.33	1.67	2.18	0.08	0.29
83	0.047	0.072	0.0140	0.76	0.62	0.98	1.50	0.98	1.24	1.29	1.78	2.19	0.08	0.23
84	0.042	0.063	0.0151	0.64	0.56	0.85	1.32	0.85	1.14	1.39	1.79	2.13	0.15	0.39
85	0.052	0.084	0.0131	0.87	0.68	1.11	1.69	1.11	1.43	1.42	2.01	2.58	0.09	0.23
86	0.049	0.077	0.0137	0.81	0.64	1.02	1.56	1.02	1.32	1.33	1.85	2.32	0.09	0.22
87	0.052	0.081	0.0148	0.70	0.62	0.85	1.32	0.85	1.27	1.53	1.81	2.25	0.15	0.34
88	0.052	0.077	0.0163	0.57	0.57	0.69	1.08	0.69	1.04	1.48	1.59	1.90	0.15	0.36
89	0.050	0.073	0.0150	0.74	0.61	0.87	1.33	0.87	1.20	1.29	1.60	1.87	0.08	0.17
90	0.039	0.052	0.0165	0.65	0.51	0.75	1.17	0.75	1.17	1.30	1.57	1.71	0.15	0.28
91	0.042	0.059	0.0177	0.42	0.49	0.62	0.97	0.62	0.75	1.33	1.47	1.63	0.15	0.48
92	0.042	0.058	0.0168	0.49	0.52	0.70	1.10	0.70	0.87	1.36	1.60	1.75	0.15	0.46

bt#	u_b	A_b	f_{cws}	u^*_{cs}	u^*_{ws}	u^*_{cws}	u^*_{cwe}	u^*_{cwb}	u^*_c	u^*_w	u^*_{cw}	δ_{cw}	z_0	z_{0c}
93	0.034	0.044	0.0192	0.38	0.42	0.54	0.84	0.54	0.69	1.16	1.29	1.36	0.15	0.42
94	0.032	0.043	0.0192	0.38	0.41	0.53	0.83	0.53	0.67	1.13	1.27	1.35	0.15	0.42
95	0.035	0.048	0.0189	0.41	0.43	0.54	0.84	0.54	0.75	1.16	1.27	1.40	0.15	0.38
96	0.030	0.040	0.0191	0.44	0.40	0.55	0.85	0.55	0.80	1.09	1.24	1.31	0.15	0.33
97	0.040	0.058	0.0167	0.53	0.50	0.68	1.06	0.68	0.95	1.29	1.51	1.75	0.15	0.37
98	0.039	0.057	0.0161	0.58	0.51	0.74	1.16	0.74	1.04	1.30	1.60	1.85	0.15	0.36
99	0.038	0.055	0.0151	0.71	0.54	0.87	1.33	0.87	1.14	1.12	1.56	1.79	0.08	0.19
100	0.037	0.051	0.0160	0.61	0.51	0.78	1.22	0.78	1.08	1.28	1.66	1.84	0.15	0.36
101	0.034	0.046	0.0162	0.61	0.48	0.78	1.21	0.78	1.08	1.23	1.63	1.77	0.15	0.35
102	0.031	0.041	0.0178	0.47	0.43	0.64	1.00	0.64	0.84	1.14	1.41	1.49	0.15	0.38
103	0.035	0.047	0.0178	0.47	0.45	0.62	0.98	0.62	0.84	1.20	1.41	1.53	0.15	0.38
104	0.031	0.041	0.0187	0.43	0.41	0.57	0.89	0.57	0.76	1.12	1.30	1.37	0.15	0.38
105	0.031	0.041	0.0171	0.56	0.45	0.70	1.10	0.70	0.99	1.16	1.50	1.58	0.15	0.33
106	0.036	0.051	0.0153	0.67	0.52	0.85	1.32	0.85	1.20	1.29	1.75	1.99	0.15	0.34
107	0.035	0.051	0.0158	0.63	0.50	0.79	1.23	0.79	1.12	1.24	1.64	1.88	0.15	0.34
108	0.035	0.049	0.0167	0.53	0.47	0.70	1.10	0.70	0.94	1.21	1.52	1.71	0.15	0.38
109	0.043	0.065	0.0154	0.56	0.54	0.78	1.22	0.78	1.00	1.37	1.69	2.05	0.15	0.44
110	0.041	0.062	0.0156	0.55	0.52	0.76	1.18	0.76	0.99	1.32	1.64	1.99	0.15	0.42
111	0.048	0.079	0.0157	0.46	0.54	0.69	1.07	0.69	0.83	1.39	1.57	2.08	0.15	0.52
112	0.042	0.065	0.0181	0.40	0.46	0.53	0.82	0.53	0.73	1.26	1.32	1.62	0.15	0.43
113	0.046	0.071	0.0169	0.45	0.51	0.62	0.96	0.62	0.82	1.35	1.46	1.82	0.15	0.45
114	0.036	0.051	0.0174	0.44	0.46	0.63	0.99	0.63	0.77	1.21	1.43	1.62	0.15	0.45
115	0.044	0.069	0.0177	0.29	0.48	0.55	0.86	0.55	0.51	1.30	1.39	1.72	0.15	0.71
116	0.048	0.076	0.0187	0.08	0.47	0.47	0.74	0.47	0.12	1.33	1.34	1.70	0.15	1.36
117	0.045	0.069	0.0190	0.14	0.45	0.47	0.74	0.47	0.23	1.30	1.31	1.61	0.15	1.07
118	0.044	0.067	0.0189	0.18	0.45	0.48	0.75	0.48	0.30	1.28	1.31	1.60	0.15	0.93
119	0.047	0.077	0.0180	0.17	0.47	0.50	0.77	0.50	0.28	1.31	1.33	1.76	0.15	1.05
120	0.048	0.083	0.0175	0.21	0.48	0.51	0.80	0.51	0.36	1.32	1.35	1.86	0.15	0.95
121	0.046	0.076	0.0176	0.30	0.48	0.53	0.82	0.53	0.53	1.31	1.36	1.80	0.15	0.68
122	0.047	0.079	0.0164	0.39	0.51	0.61	0.95	0.61	0.69	1.35	1.47	1.96	0.15	0.58
123	0.043	0.070	0.0163	0.41	0.50	0.64	1.00	0.64	0.73	1.30	1.48	1.93	0.15	0.54
124	0.042	0.067	0.0174	0.33	0.47	0.56	0.88	0.56	0.57	1.26	1.37	1.74	0.15	0.62
125	0.051	0.088	0.0161	0.36	0.53	0.62	0.97	0.62	0.64	1.41	1.51	2.07	0.15	0.68
126	0.055	0.097	0.0160	0.28	0.55	0.62	0.96	0.62	0.47	1.46	1.54	2.17	0.15	0.95
127	0.054	0.094	0.0165	0.22	0.53	0.58	0.90	0.58	0.37	1.44	1.49	2.07	0.15	1.07
128	0.043	0.066	0.0183	0.25	0.46	0.52	0.81	0.52	0.43	1.28	1.34	1.64	0.15	0.76
129	0.036	0.052	0.0190	0.30	0.42	0.51	0.79	0.51	0.53	1.17	1.26	1.45	0.15	0.56
130	0.045	0.071	0.0166	0.36	0.50	0.62	0.97	0.62	0.64	1.33	1.48	1.88	0.15	0.63
131	0.057	0.108	0.0148	0.38	0.58	0.70	1.09	0.70	0.67	1.49	1.64	2.47	0.15	0.78
132	0.052	0.099	0.0146	0.44	0.57	0.72	1.12	0.72	0.78	1.43	1.63	2.46	0.15	0.64
133	0.049	0.085	0.0158	0.37	0.53	0.64	1.01	0.64	0.64	1.38	1.52	2.12	0.15	0.69
134	0.054	0.101	0.0155	0.32	0.55	0.63	0.99	0.63	0.55	1.43	1.53	2.28	0.15	0.86
135	0.059	0.123	0.0147	0.31	0.57	0.64	1.00	0.64	0.54	1.47	1.56	2.58	0.15	0.97
136	0.048	0.084	0.0171	0.29	0.49	0.53	0.83	0.53	0.50	1.32	1.37	1.91	0.15	0.75
137	0.050	0.086	0.0173	0.23	0.50	0.53	0.83	0.53	0.40	1.36	1.39	1.91	0.15	0.92
138	0.052	0.089	0.0170	0.24	0.51	0.54	0.85	0.54	0.42	1.39	1.43	1.96	0.15	0.92

bt#	u_b	A_b	f_{cws}	u^*_{cs}	u^*_{ws}	u^*_{cws}	u^*_{cwe}	u^*_{cwb}	u^*_c	u^*_w	u^*_{cw}	δ_{cw}	z_0	z_{0c}
139	0.045	0.072	0.0180	0.23	0.47	0.52	0.81	0.52	0.39	1.30	1.36	1.72	0.15	0.85
140	0.053	0.092	0.0163	0.27	0.54	0.60	0.94	0.60	0.47	1.43	1.50	2.09	0.15	0.92
141	0.052	0.089	0.0170	0.23	0.51	0.55	0.85	0.55	0.40	1.40	1.43	1.97	0.15	0.97
142	0.051	0.085	0.0177	0.25	0.49	0.51	0.80	0.51	0.44	1.38	1.39	1.86	0.15	0.84
143	0.058	0.107	0.0160	0.29	0.55	0.58	0.91	0.58	0.51	1.47	1.51	2.24	0.15	0.90
144	0.055	0.105	0.0160	0.22	0.53	0.57	0.89	0.57	0.38	1.41	1.45	2.23	0.15	1.11
145	0.056	0.108	0.0165	0.23	0.52	0.52	0.82	0.52	0.41	1.42	1.42	2.18	0.15	1.01
146	0.058	0.111	0.0154	0.27	0.56	0.62	0.97	0.62	0.45	1.47	1.54	2.36	0.15	1.04
147	0.054	0.097	0.0162	0.24	0.53	0.58	0.90	0.58	0.40	1.41	1.47	2.13	0.15	1.03
148	0.054	0.102	0.0168	0.18	0.50	0.51	0.80	0.51	0.31	1.38	1.39	2.10	0.15	1.17
149	0.050	0.090	0.0176	0.11	0.48	0.48	0.76	0.48	0.17	1.34	1.34	1.92	0.15	1.40
150	0.049	0.082	0.0176	0.19	0.49	0.52	0.81	0.52	0.32	1.36	1.38	1.85	0.15	1.04
151	0.051	0.085	0.0157	0.40	0.55	0.68	1.06	0.68	0.70	1.43	1.59	2.13	0.15	0.66
152	0.057	0.101	0.0148	0.49	0.60	0.74	1.15	0.74	0.89	1.52	1.69	2.42	0.15	0.56
153	0.044	0.069	0.0155	0.56	0.54	0.75	1.17	0.75	1.00	1.37	1.65	2.04	0.15	0.42
154	0.044	0.067	0.0142	0.75	0.59	0.95	1.46	0.95	1.21	1.24	1.73	2.10	0.08	0.22
155	0.035	0.048	0.0150	0.76	0.53	0.93	1.42	0.93	1.23	1.12	1.66	1.81	0.08	0.18
156	0.053	0.082	0.0129	0.98	0.71	1.20	1.83	1.20	1.61	1.48	2.15	2.67	0.09	0.21
157	0.058	0.090	0.0135	0.80	0.71	1.08	1.64	1.08	1.31	1.49	1.99	2.47	0.09	0.27
158	0.068	0.098	0.0150	0.52	0.72	0.88	1.34	0.88	0.84	1.55	1.75	2.02	0.08	0.43
159	0.077	0.113	0.0144	0.55	0.78	0.94	1.44	0.94	0.89	1.69	1.88	2.23	0.08	0.47
160	0.098	0.151	0.0142	0.34	0.89	0.95	1.45	0.95	0.52	1.94	2.01	2.46	0.08	1.02
161	0.122	0.199	0.0134	0.21	1.02	1.04	1.59	1.04	0.31	2.23	2.25	2.93	0.09	1.80
162	0.182	0.301	0.0119	0.21	1.41	1.42	2.69	1.92	0.35	3.66	3.67	4.85	0.19	3.56
163	0.206	0.344	0.0114	0.16	1.56	1.57	2.96	2.41	0.25	4.21	4.21	5.63	0.23	4.65
164	0.227	0.405	0.0109	0.27	1.68	1.68	2.89	2.73	0.46	4.43	4.43	6.33	0.23	4.47
165	0.254	0.454	0.0105	0.35	1.86	1.88	2.79	3.25	0.60	4.43	4.46	6.37	0.17	3.91
166	0.231	0.412	0.0106	0.51	1.75	1.82	2.85	3.06	0.91	4.30	4.40	6.28	0.19	3.03
167	0.250	0.452	0.0103	0.56	1.87	1.95	2.80	3.39	0.96	4.32	4.42	6.41	0.15	2.84
168	0.233	0.417	0.0104	0.64	1.79	1.90	2.83	3.24	1.14	4.24	4.39	6.27	0.17	2.45
169	0.207	0.386	0.0108	0.48	1.59	1.65	2.95	2.60	0.90	4.23	4.32	6.44	0.25	3.28
170	0.198	0.353	0.0110	0.56	1.54	1.61	2.98	2.48	1.08	4.23	4.32	6.17	0.27	2.81
171	0.194	0.341	0.0114	0.47	1.48	1.50	2.83	2.17	0.86	3.87	3.89	5.49	0.21	2.67
172	0.171	0.301	0.0117	0.54	1.35	1.39	2.62	1.74	0.98	3.37	3.42	4.82	0.17	1.85
173	0.180	0.318	0.0115	0.50	1.41	1.45	2.74	2.01	0.91	3.62	3.68	5.18	0.20	2.30
174	0.146	0.247	0.0122	0.45	1.20	1.27	1.94	1.27	0.71	2.60	2.68	3.63	0.09	1.38
175	0.151	0.256	0.0122	0.40	1.23	1.29	1.98	1.29	0.63	2.67	2.74	3.71	0.10	1.60
176	0.161	0.280	0.0121	0.19	1.27	1.28	1.96	1.28	0.29	2.75	2.77	3.85	0.09	2.63
177	0.172	0.291	0.0120	0.35	1.34	1.35	2.55	1.50	0.60	3.29	3.30	4.47	0.15	2.43
178	0.144	0.244	0.0126	0.24	1.16	1.17	1.79	1.17	0.36	2.52	2.54	3.44	0.09	2.05
179	0.180	0.318	0.0115	0.40	1.41	1.47	2.77	2.06	0.71	3.65	3.71	5.24	0.20	2.81
180	0.136	0.224	0.0123	0.53	1.17	1.28	1.96	1.28	0.86	2.52	2.66	3.51	0.09	1.09
181	0.157	0.277	0.0116	0.59	1.30	1.42	2.69	1.88	1.06	3.28	3.44	4.85	0.19	1.76
182	0.160	0.277	0.0118	0.46	1.30	1.37	2.59	1.66	0.81	3.21	3.30	4.59	0.17	2.03
183	0.176	0.332	0.0115	0.37	1.35	1.36	2.57	1.60	0.64	3.30	3.31	5.01	0.16	2.59
184	0.207	0.397	0.0109	0.42	1.54	1.55	2.92	2.32	0.78	4.03	4.05	6.21	0.22	3.27

bt#	u_b	A_b	f_{cws}	u_{*cs}	u_{*ws}	u_{*cws}	u_{*cwe}	u_{*cwb}	u_{*c}	u_{*w}	u_{*cw}	δ_{cw}	Z_0	Z_{0c}
185	0.172	0.311	0.0115	0.54	1.35	1.41	2.66	1.83	0.98	3.40	3.47	5.02	0.18	1.97
186	0.209	0.401	0.0105	0.62	1.61	1.72	2.93	2.74	1.17	4.16	4.30	6.60	0.23	2.64
187	0.171	0.305	0.0111	0.73	1.42	1.59	3.00	2.37	1.40	3.71	3.95	5.64	0.23	1.81
188	0.193	0.370	0.0106	0.66	1.53	1.67	2.98	2.59	1.28	4.04	4.24	6.50	0.25	2.43
189	0.166	0.300	0.0110	0.80	1.40	1.58	2.99	2.35	1.53	3.62	3.89	5.63	0.23	1.59
190	0.164	0.297	0.0112	0.75	1.37	1.53	2.89	2.20	1.43	3.51	3.74	5.42	0.21	1.57
191	0.149	0.286	0.0119	0.51	1.18	1.22	1.86	1.22	0.83	2.53	2.58	3.95	0.09	1.18
192	0.173	0.321	0.0115	0.53	1.34	1.36	2.58	1.61	0.96	3.28	3.31	4.93	0.16	1.84
193	0.148	0.288	0.0118	0.42	1.18	1.23	1.88	1.23	0.67	2.52	2.58	4.02	0.09	1.50
194	0.127	0.240	0.0122	0.45	1.07	1.16	1.77	1.16	0.73	2.28	2.38	3.60	0.09	1.18
195	0.155	0.296	0.0117	0.33	1.22	1.26	1.92	1.26	0.51	2.61	2.66	4.07	0.09	1.98
196	0.129	0.245	0.0126	0.27	1.04	1.06	1.62	1.06	0.41	2.24	2.26	3.42	0.09	1.77
197	0.117	0.214	0.0129	0.49	0.97	1.01	1.55	1.01	0.80	2.09	2.14	3.14	0.09	0.82
198	0.128	0.239	0.0122	0.53	1.09	1.18	1.80	1.18	0.86	2.31	2.43	3.61	0.09	0.98
199	0.118	0.213	0.0123	0.60	1.04	1.18	1.81	1.18	0.98	2.21	2.39	3.47	0.09	0.78
200	0.124	0.225	0.0118	0.69	1.12	1.30	1.99	1.30	1.14	2.36	2.61	3.78	0.10	0.75
201	0.112	0.206	0.0123	0.57	1.01	1.16	1.77	1.16	0.92	2.13	2.32	3.41	0.09	0.81
202	0.129	0.248	0.0117	0.60	1.12	1.26	1.92	1.26	0.99	2.36	2.54	3.90	0.09	0.91
203	0.111	0.203	0.0131	0.42	0.94	0.99	1.51	0.99	0.67	2.02	2.07	3.04	0.08	0.96
204	0.096	0.181	0.0134	0.41	0.84	0.89	1.36	0.89	0.66	1.79	1.85	2.80	0.08	0.79
205	0.104	0.193	0.0126	0.56	0.94	1.08	1.64	1.08	0.91	1.98	2.16	3.21	0.09	0.70
206	0.088	0.162	0.0132	0.49	0.83	0.96	1.47	0.96	0.79	1.75	1.92	2.82	0.08	0.66
207	0.084	0.148	0.0139	0.39	0.78	0.88	1.34	0.88	0.62	1.67	1.78	2.52	0.08	0.76
208	0.073	0.131	0.0149	0.32	0.67	0.72	1.13	0.72	0.56	1.76	1.82	2.59	0.15	1.07
209	0.083	0.165	0.0135	0.44	0.76	0.84	1.31	0.84	0.79	1.90	2.00	3.15	0.15	0.95
210	0.080	0.148	0.0122	0.83	0.85	1.17	1.79	1.17	1.37	1.76	2.19	3.27	0.09	0.35
211	0.067	0.114	0.0132	0.75	0.75	1.04	1.58	1.04	1.24	1.57	1.94	2.63	0.09	0.30
212	0.077	0.137	0.0125	0.79	0.83	1.13	1.73	1.13	1.29	1.72	2.13	3.04	0.09	0.36
213	0.067	0.115	0.0134	0.67	0.74	0.99	1.52	0.99	1.08	1.54	1.88	2.58	0.08	0.36
214	0.070	0.121	0.0134	0.64	0.75	0.98	1.49	0.98	1.04	1.56	1.87	2.59	0.08	0.39
215	0.064	0.109	0.0138	0.64	0.71	0.93	1.43	0.93	1.04	1.48	1.77	2.40	0.08	0.33
216	0.073	0.135	0.0149	0.36	0.67	0.71	1.11	0.71	0.64	1.75	1.79	2.63	0.15	0.94
217	0.071	0.122	0.0142	0.48	0.72	0.85	1.33	0.85	0.84	1.80	1.98	2.71	0.15	0.79
218	0.063	0.118	0.0138	0.53	0.67	0.85	1.32	0.85	0.94	1.64	1.89	2.81	0.15	0.65
219	0.062	0.112	0.0141	0.50	0.65	0.82	1.29	0.82	0.89	1.63	1.85	2.69	0.15	0.67
220	0.057	0.099	0.0151	0.42	0.60	0.72	1.13	0.72	0.75	1.53	1.69	2.35	0.15	0.69
221	0.060	0.112	0.0145	0.48	0.61	0.74	1.16	0.74	0.86	1.56	1.71	2.55	0.15	0.61
222	0.055	0.100	0.0158	0.40	0.55	0.62	0.96	0.62	0.72	1.45	1.52	2.20	0.15	0.62
223	0.062	0.122	0.0135	0.62	0.66	0.86	1.31	0.86	1.00	1.37	1.62	2.52	0.08	0.30
224	0.063	0.117	0.0136	0.57	0.67	0.88	1.35	0.88	0.91	1.40	1.67	2.49	0.08	0.38
225	0.066	0.123	0.0141	0.46	0.67	0.80	1.26	0.80	0.81	1.67	1.85	2.75	0.15	0.77
226	0.063	0.118	0.0143	0.43	0.64	0.77	1.21	0.77	0.76	1.62	1.79	2.67	0.15	0.79
227	0.060	0.108	0.0155	0.32	0.58	0.65	1.01	0.65	0.56	1.53	1.60	2.32	0.15	0.90
228	0.060	0.105	0.0154	0.34	0.59	0.67	1.05	0.67	0.60	1.55	1.65	2.32	0.15	0.86
229	0.060	0.111	0.0147	0.39	0.60	0.71	1.12	0.71	0.68	1.54	1.68	2.51	0.15	0.81
230	0.054	0.092	0.0149	0.47	0.59	0.75	1.17	0.75	0.83	1.50	1.70	2.34	0.15	0.61

bt#	u_b	A_b	f_{cws}	u^*_{cs}	u^*_{ws}	u^*_{cws}	u^*_{cwe}	u^*_{cwb}	u^*_c	u^*_w	u^*_{cw}	δ_{cw}	z_0	z_{0c}
231	0.056	0.103	0.0147	0.45	0.59	0.73	1.14	0.73	0.81	1.50	1.68	2.46	0.15	0.64
232	0.061	0.121	0.0137	0.50	0.64	0.80	1.25	0.80	0.90	1.58	1.80	2.84	0.15	0.65
233	0.055	0.099	0.0161	0.45	0.54	0.60	0.94	0.60	0.83	1.44	1.48	2.12	0.15	0.48
234	0.057	0.107	0.0142	0.57	0.61	0.78	1.21	0.78	1.03	1.53	1.73	2.58	0.15	0.47
235	0.060	0.115	0.0130	0.68	0.68	0.96	1.47	0.96	1.11	1.40	1.78	2.73	0.08	0.31
236	0.059	0.106	0.0136	0.66	0.67	0.91	1.38	0.91	1.08	1.38	1.69	2.42	0.08	0.28
237	0.057	0.101	0.0130	0.76	0.68	1.02	1.55	1.02	1.23	1.41	1.87	2.67	0.09	0.28
238	0.058	0.105	0.0140	0.54	0.64	0.83	1.30	0.83	0.96	1.58	1.84	2.67	0.15	0.59
239	0.057	0.103	0.0142	0.54	0.62	0.80	1.25	0.80	0.97	1.54	1.78	2.58	0.15	0.55
240	0.062	0.120	0.0152	0.35	0.58	0.63	0.98	0.63	0.64	1.53	1.58	2.46	0.15	0.79
241	0.053	0.090	0.0145	0.55	0.61	0.82	1.28	0.82	0.98	1.52	1.80	2.44	0.15	0.54
242	0.058	0.112	0.0130	0.69	0.66	0.95	1.45	0.95	1.11	1.36	1.75	2.72	0.08	0.29
243	0.060	0.122	0.0125	0.72	0.69	0.99	1.52	0.99	1.17	1.40	1.82	2.97	0.08	0.30
244	0.060	0.121	0.0122	0.83	0.72	1.09	1.66	1.09	1.37	1.45	1.97	3.17	0.09	0.27
245	0.057	0.111	0.0119	0.94	0.72	1.18	1.81	1.18	1.54	1.46	2.12	3.31	0.09	0.24
246	0.058	0.119	0.0123	0.79	0.69	1.04	1.59	1.04	1.29	1.40	1.89	3.09	0.09	0.27
247	0.061	0.127	0.0131	0.68	0.65	0.85	1.33	0.85	1.25	1.55	1.81	3.04	0.15	0.38
248	0.059	0.116	0.0130	0.66	0.66	0.93	1.42	0.93	1.08	1.36	1.72	2.72	0.08	0.31
249	0.056	0.103	0.0133	0.69	0.66	0.95	1.45	0.95	1.11	1.35	1.75	2.57	0.08	0.29
250	0.055	0.100	0.0142	0.58	0.61	0.81	1.26	0.81	1.05	1.52	1.78	2.57	0.15	0.48
251	0.063	0.130	0.0136	0.52	0.64	0.79	1.23	0.79	0.93	1.57	1.77	2.92	0.15	0.61
252	0.060	0.118	0.0143	0.41	0.61	0.73	1.14	0.73	0.72	1.53	1.68	2.66	0.15	0.78
253	0.057	0.110	0.0143	0.45	0.60	0.75	1.17	0.75	0.80	1.51	1.70	2.61	0.15	0.68
254	0.057	0.105	0.0167	0.19	0.52	0.53	0.83	0.53	0.31	1.45	1.45	2.13	0.15	1.21
255	0.059	0.128	0.0152	0.17	0.54	0.56	0.88	0.56	0.27	1.42	1.45	2.51	0.15	1.48
256	0.058	0.119	0.0155	0.21	0.54	0.57	0.88	0.57	0.35	1.42	1.46	2.41	0.15	1.24
257	0.065	0.147	0.0133	0.45	0.64	0.78	1.21	0.78	0.81	1.58	1.75	3.15	0.15	0.78
258	0.057	0.120	0.0129	0.63	0.64	0.90	1.37	0.90	1.02	1.30	1.65	2.78	0.08	0.32
259	0.056	0.120	0.0126	0.72	0.65	0.94	1.43	0.94	1.17	1.31	1.70	2.91	0.08	0.25
260	0.056	0.110	0.0124	0.82	0.69	1.07	1.63	1.07	1.34	1.40	1.93	3.01	0.09	0.26
261	0.063	0.142	0.0113	0.93	0.75	1.20	1.83	1.20	1.53	1.51	2.15	3.86	0.09	0.27
262	0.055	0.105	0.0122	0.91	0.70	1.14	1.74	1.14	1.49	1.42	2.04	3.14	0.09	0.24
263	0.063	0.138	0.0116	0.86	0.73	1.13	1.73	1.13	1.42	1.48	2.04	3.61	0.09	0.28
264	0.063	0.142	0.0117	0.90	0.73	1.09	1.67	1.09	1.48	1.45	1.95	3.51	0.09	0.22
265	0.061	0.125	0.0137	0.56	0.63	0.79	1.23	0.79	1.02	1.55	1.75	2.85	0.15	0.52
266	0.061	0.119	0.0124	0.81	0.72	1.08	1.65	1.08	1.33	1.47	1.97	3.06	0.09	0.28
267	0.058	0.116	0.0128	0.69	0.66	0.95	1.46	0.95	1.11	1.35	1.75	2.81	0.08	0.30
268	0.066	0.118	0.0127	0.79	0.76	1.09	1.67	1.09	1.30	1.57	2.02	2.89	0.09	0.31
269	0.072	0.129	0.0131	0.70	0.76	1.00	1.53	1.00	1.15	1.58	1.89	2.75	0.09	0.33
270	0.077	0.140	0.0129	0.76	0.80	1.03	1.57	1.03	1.25	1.66	1.96	2.83	0.09	0.31
271	0.082	0.146	0.0141	0.59	0.76	0.83	1.30	0.83	1.09	1.91	1.99	2.84	0.15	0.57
272	0.085	0.155	0.0132	0.62	0.82	0.97	1.48	0.97	1.02	1.73	1.91	2.77	0.08	0.43
273	0.096	0.171	0.0124	0.73	0.93	1.16	1.77	1.16	1.20	1.96	2.25	3.22	0.09	0.48
274	0.077	0.131	0.0139	0.50	0.76	0.91	1.39	0.91	0.80	1.63	1.80	2.44	0.08	0.55
275	0.079	0.136	0.0130	0.69	0.82	1.06	1.62	1.06	1.12	1.73	2.04	2.80	0.09	0.42
276	0.073	0.125	0.0138	0.58	0.74	0.91	1.39	0.91	0.95	1.56	1.77	2.43	0.08	0.40

bt#	u _b	A _b	f _{cws}	u* _{cs}	u* _{ws}	u* _{cws}	u* _{cwe}	u* _{cwb}	u* _c	u* _w	u* _{cw}	δ _{cw}	z ₀	z _{0c}
277	0.069	0.116	0.0145	0.56	0.70	0.82	1.28	0.82	1.01	1.77	1.91	2.56	0.15	0.57
278	0.067	0.114	0.0155	0.38	0.63	0.69	1.07	0.69	0.68	1.67	1.73	2.37	0.15	0.80
279	0.069	0.122	0.0144	0.41	0.68	0.79	1.23	0.79	0.72	1.72	1.86	2.65	0.15	0.87
280	0.061	0.110	0.0154	0.29	0.59	0.66	1.03	0.66	0.50	1.55	1.63	2.36	0.15	1.01
281	0.058	0.099	0.0168	0.23	0.55	0.57	0.89	0.57	0.39	1.51	1.53	2.08	0.15	1.06
282	0.061	0.107	0.0153	0.35	0.61	0.69	1.08	0.69	0.62	1.58	1.68	2.36	0.15	0.85
283	0.052	0.089	0.0153	0.42	0.57	0.70	1.10	0.70	0.74	1.45	1.63	2.24	0.15	0.66
284	0.058	0.107	0.0134	0.63	0.65	0.91	1.38	0.91	1.01	1.35	1.69	2.52	0.08	0.32
285	0.060	0.103	0.0138	0.62	0.67	0.90	1.37	0.90	1.01	1.39	1.69	2.35	0.08	0.32
286	0.059	0.100	0.0133	0.78	0.70	1.03	1.57	1.03	1.27	1.46	1.90	2.57	0.09	0.27
287	0.055	0.094	0.0132	0.81	0.68	1.05	1.60	1.05	1.32	1.41	1.91	2.58	0.09	0.24
288	0.058	0.100	0.0145	0.63	0.62	0.80	1.24	0.80	1.16	1.56	1.75	2.44	0.15	0.39
289	0.063	0.117	0.0135	0.66	0.69	0.90	1.37	0.90	1.07	1.42	1.70	2.49	0.08	0.29
290	0.057	0.099	0.0128	0.85	0.71	1.09	1.67	1.09	1.39	1.45	1.99	2.77	0.09	0.25
291	0.054	0.093	0.0130	0.81	0.67	1.05	1.60	1.05	1.32	1.39	1.91	2.65	0.09	0.25
292	0.050	0.088	0.0128	0.88	0.67	1.11	1.69	1.11	1.45	1.37	1.99	2.77	0.09	0.23
293	0.058	0.103	0.0126	0.89	0.71	1.10	1.69	1.10	1.46	1.46	2.00	2.85	0.09	0.22
294	0.050	0.083	0.0136	0.76	0.64	0.99	1.51	0.99	1.24	1.33	1.80	2.38	0.08	0.24
295	0.051	0.086	0.0142	0.64	0.60	0.85	1.33	0.85	1.15	1.48	1.83	2.47	0.15	0.42
296	0.060	0.123	0.0130	0.60	0.65	0.88	1.34	0.88	0.96	1.33	1.64	2.71	0.08	0.34
297	0.047	0.076	0.0153	0.50	0.55	0.74	1.16	0.74	0.89	1.40	1.66	2.16	0.15	0.51
298	0.049	0.077	0.0156	0.47	0.56	0.72	1.13	0.72	0.83	1.43	1.65	2.10	0.15	0.55
299	0.049	0.079	0.0147	0.58	0.59	0.82	1.29	0.82	1.03	1.47	1.79	2.31	0.15	0.48
300	0.042	0.062	0.0155	0.58	0.54	0.79	1.24	0.79	1.03	1.37	1.71	2.03	0.15	0.42
301	0.036	0.049	0.0158	0.64	0.51	0.81	1.27	0.81	1.14	1.28	1.70	1.87	0.15	0.34
302	0.043	0.062	0.0151	0.66	0.56	0.85	1.33	0.85	1.19	1.40	1.80	2.11	0.15	0.37
303	0.038	0.053	0.0170	0.52	0.49	0.67	1.05	0.67	0.94	1.26	1.49	1.68	0.15	0.37
304	0.050	0.082	0.0155	0.45	0.56	0.71	1.12	0.71	0.81	1.44	1.64	2.14	0.15	0.58
305	0.045	0.067	0.0178	0.31	0.50	0.58	0.90	0.58	0.53	1.36	1.45	1.70	0.15	0.69
306	0.044	0.064	0.0194	0.21	0.46	0.48	0.75	0.48	0.36	1.31	1.33	1.54	0.15	0.82
307	0.053	0.080	0.0153	0.53	0.61	0.80	1.24	0.80	0.94	1.54	1.79	2.17	0.15	0.54
308	0.068	0.115	0.0130	0.79	0.77	1.09	1.66	1.09	1.29	1.60	2.03	2.75	0.09	0.31
309	0.085	0.144	0.0122	0.92	0.92	1.28	1.96	1.28	1.53	1.92	2.42	3.28	0.09	0.35
310	0.081	0.136	0.0118	1.11	0.95	1.43	2.30	1.83	1.87	1.99	2.69	3.59	0.11	0.31
311	0.107	0.202	0.0111	1.05	1.09	1.49	2.39	2.02	1.82	2.34	2.92	4.41	0.12	0.46
312	0.122	0.227	0.0115	0.91	1.13	1.39	2.63	1.71	1.69	2.72	3.09	4.60	0.17	0.76
313	0.170	0.341	0.0111	0.85	1.34	1.42	2.69	1.88	1.62	3.33	3.42	5.49	0.18	1.11
314	0.180	0.355	0.0112	0.59	1.37	1.40	2.65	1.81	1.09	3.41	3.44	5.44	0.18	1.84
315	0.203	0.434	0.0101	0.88	1.59	1.75	2.96	2.79	1.71	3.98	4.22	7.21	0.22	1.77
316	0.162	0.311	0.0105	1.01	1.42	1.71	3.02	2.64	2.00	3.66	4.11	6.30	0.25	1.30
317	0.161	0.319	0.0105	0.92	1.40	1.67	3.04	2.55	1.83	3.66	4.09	6.46	0.26	1.53
318	0.141	0.283	0.0106	1.00	1.29	1.63	3.09	2.41	1.95	3.27	3.81	6.11	0.23	1.15
319	0.134	0.265	0.0111	0.82	1.20	1.44	2.73	1.91	1.53	2.94	3.30	5.21	0.19	1.11
320	0.148	0.288	0.0112	0.74	1.25	1.42	2.68	1.84	1.38	3.07	3.31	5.15	0.18	1.28
321	0.132	0.249	0.0120	0.67	1.11	1.21	1.85	1.21	1.11	2.36	2.48	3.75	0.09	0.71
322	0.124	0.249	0.0124	0.52	1.01	1.03	1.58	1.03	0.86	2.14	2.17	3.48	0.09	0.80

bt#	u_b	A_b	f_{cws}	u^*_{cs}	u^*_{ws}	u^*_{cws}	u^*_{cwe}	u^*_{cwb}	u^*_c	u^*_w	u^*_{cw}	δ_{cw}	z_0	z_{0c}
323	0.110	0.202	0.0129	0.49	0.95	1.02	1.56	1.02	0.79	2.03	2.11	3.10	0.09	0.80
324	0.119	0.226	0.0124	0.49	1.02	1.11	1.69	1.11	0.79	2.17	2.27	3.44	0.09	0.96
325	0.105	0.188	0.0134	0.31	0.90	0.94	1.43	0.94	0.47	1.94	1.99	2.84	0.08	1.22
326	0.096	0.176	0.0137	0.24	0.83	0.86	1.32	0.86	0.36	1.79	1.82	2.68	0.08	1.33
327	0.120	0.227	0.0129	0.19	0.98	0.99	1.52	0.99	0.28	2.11	2.12	3.21	0.08	1.97
328	0.101	0.191	0.0132	0.34	0.87	0.93	1.42	0.93	0.52	1.87	1.93	2.91	0.08	1.10
329	0.085	0.159	0.0140	0.28	0.76	0.81	1.26	0.81	0.47	1.94	2.00	2.98	0.15	1.48
330	0.077	0.138	0.0150	0.24	0.69	0.71	1.11	0.71	0.41	1.82	1.84	2.63	0.15	1.39
331	0.069	0.120	0.0150	0.43	0.66	0.73	1.14	0.73	0.78	1.71	1.79	2.49	0.15	0.74
332	0.068	0.121	0.0138	0.58	0.70	0.87	1.34	0.87	0.95	1.47	1.69	2.41	0.08	0.36
333	0.068	0.119	0.0138	0.60	0.72	0.91	1.39	0.91	0.97	1.51	1.75	2.44	0.08	0.38
334	0.073	0.134	0.0120	0.93	0.84	1.25	1.91	1.25	1.55	1.73	2.30	3.39	0.09	0.31
335	0.069	0.126	0.0125	0.82	0.79	1.14	1.73	1.14	1.34	1.63	2.11	3.05	0.09	0.32
336	0.068	0.126	0.0120	0.92	0.80	1.21	1.85	1.21	1.51	1.63	2.22	3.31	0.09	0.29
337	0.078	0.148	0.0126	0.70	0.81	1.05	1.60	1.05	1.15	1.67	2.00	3.02	0.09	0.39
338	0.064	0.113	0.0146	0.48	0.65	0.77	1.21	0.77	0.87	1.65	1.80	2.54	0.15	0.65
339	0.064	0.121	0.0136	0.71	0.67	0.86	1.31	0.86	1.16	1.39	1.60	2.41	0.08	0.20
340	0.063	0.111	0.0125	1.00	0.76	1.16	1.77	1.16	1.65	1.56	2.08	2.93	0.09	0.19
341	0.055	0.109	0.0116	1.11	0.73	1.27	1.94	1.27	1.83	1.47	2.24	3.53	0.09	0.18
342	0.054	0.094	0.0122	1.03	0.72	1.24	1.89	1.24	1.70	1.48	2.21	3.07	0.09	0.21
343	0.062	0.117	0.0126	0.78	0.72	1.06	1.62	1.06	1.27	1.48	1.95	2.94	0.09	0.30
344	0.060	0.116	0.0127	0.85	0.70	1.01	1.55	1.01	1.40	1.42	1.83	2.80	0.09	0.19
345	0.063	0.118	0.0137	0.65	0.66	0.85	1.33	0.85	1.19	1.62	1.85	2.80	0.15	0.43
346	0.054	0.102	0.0133	0.71	0.64	0.92	1.40	0.92	1.15	1.30	1.68	2.53	0.08	0.24
347	0.063	0.122	0.0129	0.70	0.69	0.96	1.46	0.96	1.14	1.43	1.77	2.76	0.08	0.29
348	0.058	0.109	0.0137	0.59	0.64	0.86	1.31	0.86	0.95	1.33	1.61	2.40	0.08	0.32
349	0.057	0.107	0.0141	0.50	0.61	0.79	1.23	0.79	0.90	1.52	1.76	2.66	0.15	0.61
350	0.053	0.094	0.0152	0.40	0.56	0.69	1.08	0.69	0.71	1.44	1.61	2.30	0.15	0.69
351	0.058	0.110	0.0143	0.44	0.60	0.74	1.16	0.74	0.77	1.51	1.70	2.60	0.15	0.71
352	0.059	0.121	0.0141	0.42	0.60	0.73	1.15	0.73	0.75	1.51	1.68	2.74	0.15	0.75
353	0.051	0.089	0.0160	0.32	0.53	0.61	0.96	0.61	0.55	1.39	1.49	2.10	0.15	0.80
354	0.045	0.082	0.0173	0.19	0.45	0.49	0.77	0.49	0.33	1.24	1.28	1.87	0.15	0.98
355	0.053	0.102	0.0153	0.34	0.54	0.63	0.98	0.63	0.59	1.40	1.51	2.32	0.15	0.80
356	0.057	0.111	0.0146	0.46	0.59	0.70	1.10	0.70	0.84	1.48	1.63	2.53	0.15	0.59
357	0.051	0.096	0.0146	0.60	0.57	0.73	1.14	0.73	1.09	1.41	1.60	2.38	0.15	0.36
358	0.056	0.109	0.0139	0.65	0.61	0.80	1.24	0.80	1.19	1.49	1.71	2.66	0.15	0.36
359	0.055	0.106	0.0142	0.60	0.60	0.76	1.18	0.76	1.10	1.47	1.66	2.55	0.15	0.39
360	0.059	0.117	0.0129	0.76	0.66	0.93	1.41	0.93	1.23	1.34	1.68	2.70	0.08	0.21
361	0.059	0.118	0.0124	0.82	0.69	1.04	1.59	1.04	1.33	1.41	1.89	3.03	0.09	0.25

bt#	η_p	λ_p	Q_b	Q_s	Q_{b-dir}
1	0.9	7.9	0.000075	0.000000	236
2	0.9	7.9	0.000081	0.000000	246
3	0.8	7.6	0.000049	0.000000	262
4	1.4	12.2	0.000000	0.000000	0
5	0.8	7.6	0.000044	0.000000	343
6	0.9	8.1	0.000140	0.000000	8
7	0.7	5.8	0.000242	0.000000	32
8	0.9	8.2	0.000128	0.000000	48
9	0.9	7.7	0.000063	0.000000	68
10	0.8	7.4	0.000034	0.000000	87
11	0.9	7.7	0.000056	0.000000	102
12	1.4	12.2	0.000000	0.000000	0
13	0.8	7.4	0.000027	0.000000	157
14	1.4	12.2	0.000000	0.000000	0
15	1.4	12.2	0.000000	0.000000	0
16	1.4	12.2	0.000000	0.000000	0
17	1.4	12.2	0.000000	0.000000	0
18	1.4	12.2	0.000000	0.000000	0
19	1.4	12.2	0.000000	0.000000	0
20	1.4	12.2	0.000000	0.000000	0
21	0.8	7.1	0.000010	0.000000	230
22	0.8	7.6	0.000052	0.000000	225
23	0.9	8.1	0.000102	0.000000	225
24	0.9	8.3	0.000139	0.000000	236
25	0.8	6.8	0.000282	0.000000	247
26	0.9	8.2	0.000132	0.000000	252
27	0.8	7.3	0.000024	0.000000	258
28	1.4	12.2	0.000000	0.000000	0
29	0.8	7.6	0.000051	0.000000	345
30	0.7	5.9	0.000276	0.000000	6
31	1.0	8.2	0.000619	0.009209	24
32	1.0	8.5	0.000544	0.009570	32
33	1.0	8.6	0.000430	0.008688	48
34	1.6	12.2	0.000473	0.021604	55
35	1.4	12.2	0.000403	0.012500	66
36	1.8	12.2	0.000309	0.024404	80
37	1.3	8.5	0.000279	0.000000	119
38	1.5	9.8	0.000299	0.011763	156
39	1.3	8.5	0.000194	0.000000	183
40	1.5	12.2	0.000174	0.004475	196
41	1.7	12.2	0.000046	0.001458	197
42	1.6	12.2	0.000016	0.000672	105
43	1.4	12.2	0.000018	0.000336	66
44	1.4	9.5	0.000035	0.000728	191
45	1.5	12.2	0.000046	0.001151	202
46	1.7	12.2	0.000119	0.004254	212

bt#	η_p	λ_p	Q_b	Q_s	Q_{b-dir}
47	1.5	9.9	0.000280	0.005172	219
48	1.3	8.7	0.000249	0.000000	226
49	1.7	12.2	0.000164	0.004620	228
50	1.8	12.2	0.000107	0.004664	240
51	1.4	9.5	0.000210	0.006122	252
52	1.3	8.7	0.000087	0.000000	281
53	0.8	7.5	0.000009	0.000000	295
54	0.9	8.1	0.000043	0.000000	338
55	0.9	7.8	0.000035	0.000000	10
56	0.9	8.4	0.000079	0.000000	19
57	0.9	7.7	0.000044	0.000000	38
58	0.9	8.1	0.000056	0.000000	50
59	0.9	8.0	0.000064	0.000000	61
60	0.8	7.3	0.000022	0.000000	72
61	0.8	7.0	0.000000	0.000000	0
62	0.9	7.8	0.000057	0.000000	190
63	0.9	8.0	0.000078	0.000000	186
64	0.9	8.4	0.000114	0.000000	198
65	0.9	8.2	0.000079	0.000000	208
66	0.9	8.2	0.000088	0.000000	217
67	0.8	7.5	0.000030	0.000000	232
68	0.8	7.3	0.000020	0.000000	231
69	0.8	7.2	0.000017	0.000000	236
70	0.8	7.1	0.000007	0.000000	230
71	0.8	7.6	0.000048	0.000000	223
72	0.8	7.3	0.000022	0.000000	221
73	0.8	7.4	0.000034	0.000000	219
74	0.8	7.3	0.000022	0.000000	229
75	0.8	7.2	0.000019	0.000000	237
76	1.4	12.2	0.000000	0.000000	0
77	1.4	12.2	0.000000	0.000000	0
78	1.4	12.2	0.000000	0.000000	0
79	1.4	12.2	0.000000	0.000000	0
80	0.8	7.3	0.000026	0.000000	15
81	0.8	7.1	0.000010	0.000000	29
82	0.8	7.1	0.000011	0.000000	33
83	0.8	7.4	0.000033	0.000000	37
84	1.4	12.2	0.000000	0.000000	0
85	0.9	7.8	0.000065	0.000000	71
86	0.8	7.5	0.000043	0.000000	79
87	1.4	12.2	0.000000	0.000000	0
88	1.4	12.2	0.000000	0.000000	0
89	0.8	7.0	0.000000	0.000000	0
90	1.4	12.2	0.000000	0.000000	0
91	1.4	12.2	0.000000	0.000000	0
92	1.4	12.2	0.000000	0.000000	0

bt#	η_p	λ_p	Q_b	Q_s	Q_{b-dir}
93	1.4	12.2	0.000000	0.000000	0
94	1.4	12.2	0.000000	0.000000	0
95	1.4	12.2	0.000000	0.000000	0
96	1.4	12.2	0.000000	0.000000	0
97	1.4	12.2	0.000000	0.000000	0
98	1.4	12.2	0.000000	0.000000	0
99	0.8	7.0	0.000000	0.000000	0
100	1.4	12.2	0.000000	0.000000	0
101	1.4	12.2	0.000000	0.000000	0
102	1.4	12.2	0.000000	0.000000	0
103	1.4	12.2	0.000000	0.000000	0
104	1.4	12.2	0.000000	0.000000	0
105	1.4	12.2	0.000000	0.000000	0
106	1.4	12.2	0.000000	0.000000	0
107	1.4	12.2	0.000000	0.000000	0
108	1.4	12.2	0.000000	0.000000	0
109	1.4	12.2	0.000000	0.000000	0
110	1.4	12.2	0.000000	0.000000	0
111	1.4	12.2	0.000000	0.000000	0
112	1.4	12.2	0.000000	0.000000	0
113	1.4	12.2	0.000000	0.000000	0
114	1.4	12.2	0.000000	0.000000	0
115	1.4	12.2	0.000000	0.000000	0
116	1.4	12.2	0.000000	0.000000	0
117	1.4	12.2	0.000000	0.000000	0
118	1.4	12.2	0.000000	0.000000	0
119	1.4	12.2	0.000000	0.000000	0
120	1.4	12.2	0.000000	0.000000	0
121	1.4	12.2	0.000000	0.000000	0
122	1.4	12.2	0.000000	0.000000	0
123	1.4	12.2	0.000000	0.000000	0
124	1.4	12.2	0.000000	0.000000	0
125	1.4	12.2	0.000000	0.000000	0
126	1.4	12.2	0.000000	0.000000	0
127	1.4	12.2	0.000000	0.000000	0
128	1.4	12.2	0.000000	0.000000	0
129	1.4	12.2	0.000000	0.000000	0
130	1.4	12.2	0.000000	0.000000	0
131	1.4	12.2	0.000000	0.000000	0
132	1.4	12.2	0.000000	0.000000	0
133	1.4	12.2	0.000000	0.000000	0
134	1.4	12.2	0.000000	0.000000	0
135	1.4	12.2	0.000000	0.000000	0
136	1.4	12.2	0.000000	0.000000	0
137	1.4	12.2	0.000000	0.000000	0
138	1.4	12.2	0.000000	0.000000	0

bt#	η_p	λ_p	Q_b	Q_s	Q_{b-dir}
139	1.4	12.2	0.000000	0.000000	0
140	1.4	12.2	0.000000	0.000000	0
141	1.4	12.2	0.000000	0.000000	0
142	1.4	12.2	0.000000	0.000000	0
143	1.4	12.2	0.000000	0.000000	0
144	1.4	12.2	0.000000	0.000000	0
145	1.4	12.2	0.000000	0.000000	0
146	1.4	12.2	0.000000	0.000000	0
147	1.4	12.2	0.000000	0.000000	0
148	1.4	12.2	0.000000	0.000000	0
149	1.4	12.2	0.000000	0.000000	0
150	1.4	12.2	0.000000	0.000000	0
151	1.4	12.2	0.000000	0.000000	0
152	1.4	12.2	0.000000	0.000000	0
153	1.4	12.2	0.000000	0.000000	0
154	0.8	7.3	0.000027	0.000000	341
155	0.8	7.2	0.000024	0.000000	357
156	0.9	8.0	0.000102	0.000000	8
157	0.8	7.7	0.000052	0.000000	12
158	0.8	7.1	0.000004	0.000000	41
159	0.8	7.3	0.000018	0.000000	58
160	0.8	7.3	0.000017	0.000000	57
161	0.8	7.6	0.000007	0.000000	26
162	1.3	8.5	0.000024	0.000000	337
163	1.5	10.0	0.000022	0.000289	208
164	1.6	12.2	0.000019	0.000754	313
165	1.3	12.2	0.000043	0.000665	337
166	1.4	12.2	0.000128	0.001952	350
167	1.2	12.2	0.000152	0.001510	3
168	1.3	12.2	0.000192	0.002508	2
169	1.7	12.2	0.000118	0.003417	16
170	1.8	12.2	0.000128	0.006251	23
171	1.4	9.3	0.000094	0.004369	67
172	1.2	7.9	0.000108	0.000000	71
173	1.3	8.8	0.000118	0.005670	145
174	0.9	8.3	0.000034	0.000000	163
175	0.9	8.3	0.000032	0.000000	174
176	0.9	8.3	0.000008	0.000000	200
177	1.1	7.2	0.000039	0.000000	253
178	0.9	8.0	0.000008	0.000000	346
179	1.3	8.9	0.000122	0.003064	360
180	0.9	8.3	0.000053	0.000000	8
181	1.3	8.4	0.000211	0.000000	10
182	1.2	7.7	0.000127	0.000000	30
183	1.1	7.5	0.000046	0.000000	71
184	1.5	9.7	0.000081	0.003146	123

bt#	η_p	λ_p	Q_b	Q_s	Q_{b-dir}
185	1.2	8.2	0.000123	0.000000	160
186	1.6	12.2	0.000169	0.004892	186
187	1.5	9.9	0.000423	0.008972	203
188	1.7	12.2	0.000210	0.007165	206
189	1.5	9.8	0.000451	0.010962	233
190	1.4	9.4	0.000350	0.010586	243
191	0.9	8.1	0.000026	0.000000	278
192	1.1	7.5	0.000093	0.000000	318
193	0.9	8.2	0.000025	0.000000	355
194	0.9	7.9	0.000033	0.000000	16
195	0.9	8.2	0.000020	0.000000	37
196	0.8	7.6	0.000006	0.000000	75
197	0.8	7.5	0.000014	0.000000	171
198	0.9	8.0	0.000036	0.000000	186
199	0.9	8.0	0.000051	0.000000	196
200	0.9	8.4	0.000084	0.000000	206
201	0.9	7.9	0.000053	0.000000	225
202	0.9	8.2	0.000061	0.000000	232
203	0.8	7.4	0.000014	0.000000	236
204	0.8	7.1	0.000008	0.000000	20
205	0.8	7.7	0.000038	0.000000	17
206	0.8	7.3	0.000021	0.000000	19
207	0.8	7.1	0.000002	0.000000	44
208	1.4	12.2	0.000000	0.000000	0
209	1.4	12.2	0.000000	0.000000	0
210	0.9	8.0	0.000070	0.000000	181
211	0.8	7.6	0.000040	0.000000	202
212	0.9	7.8	0.000060	0.000000	212
213	0.8	7.4	0.000030	0.000000	231
214	0.8	7.4	0.000026	0.000000	233
215	0.8	7.2	0.000019	0.000000	239
216	1.4	12.2	0.000000	0.000000	0
217	1.4	12.2	0.000000	0.000000	0
218	1.4	12.2	0.000000	0.000000	0
219	1.4	12.2	0.000000	0.000000	0
220	1.4	12.2	0.000000	0.000000	0
221	1.4	12.2	0.000000	0.000000	0
222	1.4	12.2	0.000000	0.000000	0
223	0.8	7.0	0.000000	0.000000	0
224	0.8	7.1	0.000005	0.000000	171
225	1.4	12.2	0.000000	0.000000	0
226	1.4	12.2	0.000000	0.000000	0
227	1.4	12.2	0.000000	0.000000	0
228	1.4	12.2	0.000000	0.000000	0
229	1.4	12.2	0.000000	0.000000	0
230	1.4	12.2	0.000000	0.000000	0

bt#	η_p	λ_p	Q_b	Q_s	Q_{b-dir}
231	1.4	12.2	0.000000	0.000000	0
232	1.4	12.2	0.000000	0.000000	0
233	1.4	12.2	0.000000	0.000000	0
234	1.4	12.2	0.000000	0.000000	0
235	0.8	7.3	0.000025	0.000000	175
236	0.8	7.2	0.000013	0.000000	207
237	0.8	7.5	0.000038	0.000000	210
238	1.4	12.2	0.000000	0.000000	0
239	1.4	12.2	0.000000	0.000000	0
240	1.4	12.2	0.000000	0.000000	0
241	1.4	12.2	0.000000	0.000000	0
242	0.8	7.3	0.000023	0.000000	3
243	0.8	7.4	0.000032	0.000000	41
244	0.9	7.7	0.000057	0.000000	51
245	0.9	8.0	0.000089	0.000000	71
246	0.8	7.6	0.000045	0.000000	84
247	1.4	12.2	0.000000	0.000000	0
248	0.8	7.2	0.000019	0.000000	152
249	0.8	7.3	0.000023	0.000000	166
250	1.4	12.2	0.000000	0.000000	0
251	1.4	12.2	0.000000	0.000000	0
252	1.4	12.2	0.000000	0.000000	0
253	1.4	12.2	0.000000	0.000000	0
254	1.4	12.2	0.000000	0.000000	0
255	1.4	12.2	0.000000	0.000000	0
256	1.4	12.2	0.000000	0.000000	0
257	1.4	12.2	0.000000	0.000000	0
258	0.8	7.1	0.000012	0.000000	175
259	0.8	7.2	0.000022	0.000000	204
260	0.8	7.7	0.000052	0.000000	202
261	0.9	8.0	0.000090	0.000000	233
262	0.9	7.9	0.000076	0.000000	240
263	0.9	7.8	0.000068	0.000000	250
264	0.9	7.7	0.000067	0.000000	257
265	1.4	12.2	0.000000	0.000000	0
266	0.8	7.7	0.000053	0.000000	344
267	0.8	7.3	0.000024	0.000000	8
268	0.9	7.7	0.000053	0.000000	27
269	0.8	7.4	0.000032	0.000000	36
270	0.8	7.5	0.000038	0.000000	55
271	1.4	12.2	0.000000	0.000000	0
272	0.8	7.4	0.000023	0.000000	174
273	0.9	7.9	0.000059	0.000000	183
274	0.8	7.2	0.000012	0.000000	194
275	0.8	7.6	0.000041	0.000000	196
276	0.8	7.2	0.000012	0.000000	221

bt#	η_p	λ_p	Q_b	Q_s	Q_{b-dir}
277	1.4	12.2	0.000000	0.000000	0
278	1.4	12.2	0.000000	0.000000	0
279	1.4	12.2	0.000000	0.000000	0
280	1.4	12.2	0.000000	0.000000	0
281	1.4	12.2	0.000000	0.000000	0
282	1.4	12.2	0.000000	0.000000	0
283	1.4	12.2	0.000000	0.000000	0
284	0.8	7.2	0.000013	0.000000	182
285	0.8	7.1	0.000011	0.000000	198
286	0.8	7.5	0.000041	0.000000	233
287	0.8	7.6	0.000047	0.000000	245
288	1.4	12.2	0.000000	0.000000	0
289	0.8	7.1	0.000012	0.000000	336
290	0.9	7.7	0.000059	0.000000	346
291	0.8	7.6	0.000048	0.000000	358
292	0.9	7.8	0.000067	0.000000	21
293	0.9	7.8	0.000067	0.000000	19
294	0.8	7.4	0.000034	0.000000	68
295	1.4	12.2	0.000000	0.000000	0
296	0.8	7.1	0.000004	0.000000	80
297	1.4	12.2	0.000000	0.000000	0
298	1.4	12.2	0.000000	0.000000	0
299	1.4	12.2	0.000000	0.000000	0
300	1.4	12.2	0.000000	0.000000	0
301	1.4	12.2	0.000000	0.000000	0
302	1.4	12.2	0.000000	0.000000	0
303	1.4	12.2	0.000000	0.000000	0
304	1.4	12.2	0.000000	0.000000	0
305	1.4	12.2	0.000000	0.000000	0
306	1.4	12.2	0.000000	0.000000	0
307	1.4	12.2	0.000000	0.000000	0
308	0.9	7.7	0.000052	0.000000	204
309	0.9	8.3	0.000107	0.000000	217
310	0.8	7.0	0.000247	0.000000	233
311	0.9	7.6	0.000251	0.006011	241
312	1.2	7.8	0.000338	0.000000	252
313	1.3	8.4	0.000282	0.000000	282
314	1.2	8.1	0.000122	0.000000	316
315	1.6	12.2	0.000259	0.010627	359
316	1.7	12.2	0.000364	0.017168	19
317	1.7	12.2	0.000345	0.015738	20
318	1.5	10.0	0.000706	0.016670	35
319	1.3	8.5	0.000354	0.000000	53
320	1.2	8.2	0.000265	0.000000	65
321	0.9	8.1	0.000046	0.000000	85
322	0.8	7.5	0.000016	0.000000	136

bt#	η_p	λ_p	Q_b	Q_s	Q_{b-dir}
323	0.8	7.5	0.000020	0.000000	189
324	0.9	7.8	0.000029	0.000000	195
325	0.8	7.2	0.000015	0.000000	215
326	0.8	7.0	0.000000	0.000000	0
327	0.8	7.4	0.000004	0.000000	17
328	0.8	7.2	0.000014	0.000000	27
329	1.4	12.2	0.000000	0.000000	0
330	1.4	12.2	0.000000	0.000000	0
331	1.4	12.2	0.000000	0.000000	0
332	0.8	7.0	0.000000	0.000000	0
333	0.8	7.2	0.000013	0.000000	216
334	0.9	8.2	0.000102	0.000000	216
335	0.9	7.9	0.000063	0.000000	229
336	0.9	8.1	0.000091	0.000000	238
337	0.8	7.6	0.000040	0.000000	243
338	1.4	12.2	0.000000	0.000000	0
339	0.8	7.0	0.000000	0.000000	0
340	0.9	7.9	0.000125	0.000000	338
341	0.9	8.3	0.000179	0.000000	6
342	0.9	8.2	0.000128	0.000000	30
343	0.8	7.6	0.000047	0.000000	54
344	0.8	7.5	0.000046	0.000000	103
345	1.4	12.2	0.000000	0.000000	0
346	0.8	7.2	0.000017	0.000000	206
347	0.8	7.3	0.000025	0.000000	204
348	0.8	7.0	0.000000	0.000000	0
349	1.4	12.2	0.000000	0.000000	0
350	1.4	12.2	0.000000	0.000000	0
351	1.4	12.2	0.000000	0.000000	0
352	1.4	12.2	0.000000	0.000000	0
353	1.4	12.2	0.000000	0.000000	0
354	1.4	12.2	0.000000	0.000000	0
355	1.4	12.2	0.000000	0.000000	0
356	1.4	12.2	0.000000	0.000000	0
357	1.4	12.2	0.000000	0.000000	0
358	1.4	12.2	0.000000	0.000000	0
359	1.4	12.2	0.000000	0.000000	0
360	0.8	7.2	0.000021	0.000000	221
361	0.8	7.6	0.000047	0.000000	223